

THE GEOLOGICAL SETTING OF DIAMONDIFEROUS DEPOSITS ON THE
INNER SHELF BETWEEN THE ORANGE RIVER AND WRECK POINT,
NAMAQUALAND

R.H. DE DECKER

Thesis submitted in fulfilment of the
requirements for the degree of
Master of Science in the
Faculty of Science at the
University of Cape Town

April, 1986

The University of Cape Town hereby gives
the author permission to publish this thesis in whole
or in part. Copyright is held by the author.

The copyright of this thesis vests in the author. No quotation from it or information derived from it is to be published without full acknowledgement of the source. The thesis is to be used for private study or non-commercial research purposes only.

Published by the University of Cape Town (UCT) in terms of the non-exclusive license granted to UCT by the author.

ABSTRACT

This project presents the geology of the inner shelf between the Orange River and Wreck Point, placing it in the context of the occurrence and distribution of diamondiferous deposits along the west coast of southern Africa. The interpretation is based on high-resolution seismic profiles and complete sonograph coverage obtained by surveying along closely-spaced (100 m to 400 m apart), coast-parallel lines between the breaker zone and approximately 50 m water depth.

The inner shelf is an exposed, rocky region with a steep shoreface to -20 m, which lies mostly between the -20 m and the -30 m isobaths. It extends between 2 and 10 km offshore to the inner-shelf slope. Within the study area the Orange Delta covers most of the inner shelf between the Orange River and Homewood Harbour, 15 km southward, leaving only the shoreface, Tripp Shoal and Peacock Bank as exposed bedrock areas. Farther southward the inner shelf consists mainly of exposed bedrock, interrupted by 0,2 to 2 km wide sediment-filled embayments extending across the inner shelf to the inner-shelf slope. The inner-shelf slope dips seaward at 1° to 2° to eventually disappear beneath an onlapping Holocene terrigenous mudbelt at between -50 m and -70 m. The shoreward edge of the mudbelt defines the boundary between the inner and middle shelves.

Large, sediment-filled channels extend SSW from the embayments south of Homewood Harbour, across the inner shelf. The channels also continue shoreward through the embayments. They are also found beneath the sediment in Buchu Bay, as well as between the outcrops of Tripp Shoal and beneath the delta just

south of the present Orange River mouth. Many of these channels have onshore extensions in the form of palaeo-fluvial channels. These channels would have been conduits for diamondiferous sediment eroded from onland deposits and are therefore important targets for exploration.

Bedrock isobaths show terraces cut into the inner shelf at depths between -10 m and -60 m. The most extensively developed terrace lies at -40 to -45 m and reaches over a kilometre in width. Below -45 m there are subhorizontal bedrock gradients at -50 and -60 m, although these are not very distinctive. Well-developed terraces occur at -30 m and at -22 m to -25 m. The latter is associated with a prominent wave-cut cliff, its base between -20 m and -24 m. Smaller terraces are present at -18 m to -20 m, -14 m to -16 m and at -10 m. These terraces are generally bounded by steeper than average bedrock gradients on their shoreward side. These terraces and cliffs formed during previous sea-level stands below the present and are probably of Quaternary age. Onland exploration of raised terraces has shown that diamondiferous deposits are likely to occur along the base of these wave-cut cliffs.

The average sediment thickness on the inner shelf is 6 m, but increases up to 14 m over buried channels. Seaward, the sediment cover increases rapidly, reaching up to 25 m thickness on the seaward edge of the inner shelf. Within the sedimentary embayments the sediment has discontinuous, lobate, or seaward-dipping ($0,6^{\circ}$), internal reflectors, interpreted as beach deposits. These reflectors invariably lie in water-depths shallower than 20 m. Seaward of the shoreface bedrock, subhorizontal and shallow seaward-dipping, continuous internal

reflectors lie mainly below -20 m, but not deeper than -30 m. These are possibly prograding deltaic deposits with storm-lag gravel horizons. Over the inner-shelf slope and farther seaward several en echelon, sub-horizontal southward and seaward dipping horizons represent delta-front and prodeltaic deposits. These reflectors disappear seaward beneath a gas-rich Acoustical Blanking Layer (ABL), that attenuates all seismic signals 2 to 5 m below the seafloor. Off Rietfontein and farther southward the internal reflectors are absent in a facies change from deltaic deposits to deposits forming a homogeneous terrigenous mudbelt.

The microtopography of the exposed bedrock is interpreted on the basis of lineaments traced from sonograph records and the general sonographic "texture" of the seafloor. The lineaments represent bedding planes, gullies eroded along jointing, foliation or fracturing planes, dolerite dykes, or features such as ridges, cliffs or channels. The classification of the lineaments is facilitated by comparing them with similar lineaments drawn on aerial photographs from the bedrock exposed onshore by wave-action along rocky coastlines and through mining activity. Changes in the sonographic textural pattern are ascribed to lithological changes in the bedrock.

Ninety-nine grab samples of surficial sediment were compositionally and texturally analysed. The dominant grain size is fine sand (mode 2,5 phi) and the sediments have a definite seaward-fining equilibrium profile, showing that they are wave-dominated. There is a preponderance of deltaic terrigenous detritus north of Homewood Harbour, whereas southward the abundance of biogenic fragments in the sediment increases. Samples from bedrock outcrop areas with a sediment veneer and

areas covered by megaripples have an average grain size of coarse sand and are generally fine-skewed. The conclusion is that the inner shelf sediments are mainly terrigenous detritus, chiefly introduced by the Orange River in the north, a marine biogenic fraction that becomes more prevalent southward as terrigenous dilution decreases and which contains up to 10% benthic foraminifera, and a lag deposit consisting of gravelly, shelly, coarse sand in the central part of the area.

Sedimentary bedforms, classified as megaripples (amplitude <1,5 m and wavelength <3,0 m) infer active sedimentary transport on the inner shelf. Close to the breaker zone, in water depths less than 15 m, the megaripples occur adjacent to bedrock outcrops and in narrow, coast-perpendicular strips, their crestlines parallel to the shore. Wave-induced currents or rip-currents are the probable transport agencies for these sediments. In water depths down to 25 m, megaripples are found in large, continuous fields that maintain a dynamic stability. The occurrence of the megaripples is limited to areas covered with gravelly coarse sand. Modal wave conditions (waveheight 2,25 m and wave-period 14.5 sec) are sufficient to transport granule-size (2-4 mm) sediment on the inner shelf down to depths of at least 30 m below sea level. By inference these wave conditions would be sufficient to transport diamonds of equivalent hydraulic size.

The Palaeogene Orange River supplied the Cape west coast with diamonds, by transporting them from the inland kimberlite pipes to the sea and debouching via the palaeo-Olifants River mouth at Latitude 31°S. Most of these diamonds are locked up in Tertiary deposits on the middle shelf and outer shelf. The

Miocene return of the Orange River to its present course at 28°S ended the supply of diamonds from the interior of South Africa to the coast of Namaqualand. Diamonds mined along the coast today mainly derive from secondary redistribution of Tertiary marine deposits eroded, during subsequent sea-level fluctuations, from the middle and inner shelves, and from the raised marine deposits onshore. Fluvial erosion of the raised deposits during regressions concentrated the diamonds along palaeo-river channels that drained the coastal region of the west coast. Wave-induced currents from south-southwesterly swell and from local storms created a strong longshore drift that transported the diamonds mainly northward from the river mouths. Gullies and depressions eroded into the wave-cut terraces acted as depositional traps for the diamonds, contained within a gravel-lag deposit. Quaternary sea-level changes concentrated the diamonds on wave-cut terraces found mainly below sea-level, possibly in a range between -200 m and +30 m. These diamond-deposits are presently being mined along the Cape west coast, both onshore and on the continental shelf.

ACKNOWLEDGEMENTS

This project was financially supported by the Geological Survey and I am grateful to the Chief Director for permitting the release of the data. Prof. R V Dingle is gratefully acknowledged for his supervision and thanked for the use of the facilities and space at the Marine Geoscience Unit.

I am particularly thankful to Dr J Rogers for standing in as my supervisor during Professor Dingle's sabbatical leave in 1986, and for his thorough reading and constructive criticism of the manuscript.

Guidance in the early stages of the project was freely given by Mr A du Plessis, Dr G F Birch, and later also Dr J M Bremner. I am grateful to them and also for the discussions held with Drs B W Flemming, J Rogers, I L Van Heerden, A K Martin and F Shillington, and Mr M W Woodborne.

Fieldwork was undertaken with the cooperation of the management and personnel at State Alluvial Diggings, Alexander Bay. I would specifically like to thank Mr D Kloppers for his assistance, and Messrs H du Preez and D Gird, the past and present Chief Surveyors of SAD, for arranging the logistical support we required during the cruises. Their support in the field not only extended to supplying the survey vessels and crew, but also to maintain well-located shore stations for navigation. The navigational expertise of Mr F Kidd and excellent helmsmanship of Mr H Venter, both of the Fisheries Development Corporation (FDC), are much appreciated. They contributed substantially to the success of the geophysical survey. Maintaining a constant speed and a straight line in choppy seas

with a 2 m swell is a daunting task, particularly at times when the surf is breaking seaward of the vessel!

Early drafts of the manuscript were read by Dr J Rogers, Mr M W Woodborne, Dr I.L. Van Heerden (Chapters 6,7 and 8) and Dr F Shillington (Chapter 7). Dr J M Bremner read much of the work in the form of internal reports. Their assistance is sincerely appreciated.

Thanks are due to the following persons: Mesdames S N Smith, S Sayers, E van Eck, M Brandstätter, S Baumann and Mr S Tyler, for considerably easing the task of draughting; Mr M Smith, for performing the laboratory work, and Mr G Janari, who kindly ran the sediment samples through the settling tube; Mr J Williams made the photographic plates, whereas the photo-reductions of the maps were undertaken by Mr A Vinnicombe.

I am also grateful to Mr A Vonk of FDC for permission to use the "Waverider" data, and to Mr G Nelson of the Sea Fisheries Research Institute, who discussed his current-meter programme and initial results with me. Mr C Steyl of the Precambrian Research Unit is thanked for his guidance in the analysis of the onshore-offshore lineaments, and for debugging the "FAULTS" computer programme for me.

I sincerely thank Mrs E G Krummeck for the many long hours spent at the word processor, preparing the numerous drafts, and for the determination she put into completing the final copy in time.

Finally, I am indebted to my wife, Carol, and my family without whose moral support the task would neither have been embarked upon nor completed.

CONTENTS

	<u>Page</u>
<u>ABSTRACT</u>	i
<u>ACKNOWLEDGEMENTS</u>	vi
<u>CONTENTS</u>	viii
<u>FIGURES</u>	xii
<u>TABLES</u>	xv
<u>PLATES</u>	xvi
<u>MAPS</u>	xvii
CHAPTER 1 <u>INTRODUCTION</u>	1
1.1 Present investigations	1
1.2 Previous investigations	6
1.3 Regional setting	9
1.3.1 Climate	9
1.3.2 Hydrology	15
1.3.3 Morphology	22
1.4 Geology	25
1.4.1 Precambrian Basement	25
1.4.2 Cretaceous and Tertiary deposits	30
1.4.3 Quaternary deposits	36
CHAPTER 2 <u>BATHYMETRY</u>	39
2.1 Introduction	39
2.2 Morphology of the inner shelf between Orange River and Port Nolloth	42
2.3 Seafloor morphology of the study area	46
2.3.1 Orange River to Cape Voltas	47
2.3.2 Cape Voltas to Rietfontein	51
2.3.3 Rietfontein to Wreck Point	55
2.4 Discussion	58
2.5 Conclusions	61

CHAPTER 3	<u>SUBBOTTOM BEDROCK-MORPHOLOGY</u>	63
3.1	Introduction	63
3.2	Orange River to Cape Voltas	66
3.3	Cape Voltas to Rietfontein	68
3.4	Rietfontein to Wreck Point	71
3.5	Discussion	73
3.6	Conclusions	81
CHAPTER 4	<u>SURFACE STRUCTURE OF THE EXPOSED INNER SHELF BEDROCK</u>	84
4.1	Introduction	84
4.2	Orange River to Cape Voltas	89
4.3	Cape Voltas to Rietfontein	91
4.4	Rietfontein to Wreck Point	95
4.5	Discussion	97
4.6	Conclusions	103
CHAPTER 5	<u>SEISMIC STRATIGRAPHY</u>	105
5.1	Introduction	105
5.2	Sediment isopachs to acoustic basement	108
5.2.1	Orange River to Cape Voltas	108
5.2.2	Cape Voltas to Rietfontein	110
5.2.3	Rietfontein to Wreck Point	112
5.3	Internal reflectors	113
5.3.1	Orange River to Cape Voltas	113
5.3.2	Cape Voltas to Rietfontein	115
5.3.3	Rietfontein to Wreck Point	117
5.4	Discussion	120
5.5	Conclusions	126

CHAPTER 6	<u>SURFICIAL SEDIMENTS</u>	128
6.1	Introduction	128
6.1.1	Sediments in the study area	130
6.2	Composition	132
6.2.1	Quartz and Feldspar	132
6.2.2	Rock fragments	134
6.2.3	Biogenic fragments	136
6.2.4	Micas	141
6.3	Texture	141
6.3.1	Grain size fractions	141
6.3.2	Mean	150
6.3.3	Standard sorting	153
6.3.4	Skewness	153
6.4	Discussion	155
6.5	Conclusions	162
CHAPTER 7	<u>WAVE REGIME AND SEDIMENT TRANSPORT</u>	164
7.1	Introduction	164
7.2	Hydrodynamics	165
7.2.1	Waves and currents off the west coast	169
7.2.2	Waves in the study area	175
7.3	Sedimentary bedforms	180
7.3.1	Distribution	185
7.4	Sediment transport on the inner shelf	192
7.5	Discussion	199
7.6	Conclusions	201

CHAPTER 8	<u>THE EVOLUTION OF THE DIAMONDIFEROUS DEPOSITS</u>	203
8.1	Introduction	203
8.1.1	Present-day distribution	203
8.2	The Tertiary Period	205
8.3	The Quaternary Period	209
8.4	Discussion	213
8.5	Conclusions	215
REFERENCES		217
APPENDIX A	<u>METHODS</u>	231
A.1	Field Work	231
A.2	Equipment	232
A.2.1	Navigational	232
A.2.2	Seismics	233
A.2.3	Side-scan sonar	233
A.2.4	Sediment sampling	235
A.2.5	Wave measurements	235
A.3	Data Reduction	236
A.3.1	Track chart	236
A.3.2	Seismic data	237
A.3.3	Side-scan sonar	239
A.3.4	Sediments	245
A.3.5	Wave data	247
APPENDIX B	<u>TABLES</u>	248
B.1	Explanation of column headings	248

LIST OF FIGURES

<u>Fig.No.</u>	<u>Title</u>	<u>Page</u>
1.1	Diamond Concession Areas.	2
1.2	Locality map.	3
1.3	Schematic diagram of track chart.	5
1.4	Synoptic meteorology and hydrology for south-east Atlantic Ocean.	10
1.5	Wind-roses on the west coast.	12
1.6	Diurnal variation in wind speed and direction, Alexander Bay.	14
1.7	Non-conservative properties of the shelf water off the Orange River.	17
1.8	Bathymetry of the west coast continental shelf.	19
1.9	Effect of longshore drift on sediment composition.	21
1.10	Geology of the coastal region between the Orange River and Wreck Point.	26
1.11	Stereographic plots of poles to foliation and fold-hinges in the Holgat and Oranjemund Suites.	29
1.12	Geology of the West Coast continental shelf.	32
2.1	Typical seismic section across the inner shelf - middle shelf boundary.	41
2.2	Bathymetry of the inner shelf area between the Orange River and Port Nolloth. Fold-out following	42
2.3	Sections across the inner shelf between the Orange River and Port Nolloth.	43
2.4	Sections across the inner shelf between the Orange River and Wreck Point.	49
2.5	Bathymetry of Peacock Bank.	54
3.1	Seismic section across the inner shelf and the Acoustical Blanking Layer.	65
3.2	Histograms of bedrock surface area at 2 m intervals.	75
3.3	Histogram of average surface area for the eight transects examined.	76

3.4	Palaeochannels of the Orange River.	78
4.1	Schematic presentation of variables involved in interpretation of side-scan sonar.	87
4.2	Histograms comparing orientation directions of lineaments traced from orthophotomaps and side-scan sonar.	
	A. Orange River - Alexander Bay area	99
	B. Agate Bay - Peacock Bay area.	99
	C. Gielie's Bay - Wreck Point area.	102
5.1	Seismic sections across Tripp Shoal.	109
5.2	Seismic sections through the Orange Delta-front deposits off Alexander Bay.	111
5.3	Seismic sections across the nearshore zone between Long Beach and Homewood Harbour.	116
5.4	Seismic sections across Gielie's Embayment.	119
6.1A.	Textural distribution of sediments on the continental shelf.	129
	B. Lithofacies on the continental shelf.	129
6.2	Percentage variation in composition and texture across the continental shelf off the Orange River.	131
6.3	Sample locations and sediment texture.	133
6.4	Quartz and Feldspar.	135
6.5	Rock fragments.	135
6.6	Calcium carbonate.	138
6.7	Benthic foraminifera.	138
6.8	Micas	142
6.9	Mud.	142
6.10	Very fine sand.	144
6.11	Fine sand.	144
6.12	Medium sand.	148
6.13	Coarse and very coarse sand.	148
6.14	Gravel.	151
6.15	Mean grain-size for sand fraction.	151

6.16	Standard Sorting of sand fraction.	154
6.17	Skewness of sand fraction.	154
6.18	Skewness vs. Mean.	159
6.19	Mean vs. CaCO_3 .	159
6.20	Skewness vs. Sorting.	161
6.21	Sorting vs. Mean.	161
7.1	Correlation between horizontal orbital velocities at the sea floor, determined from Airy wave theory (U_d , Komar 1976b) and Vocoidal wave theory (U_{bc} , Swart 1981).	167
7.2	Wave-rider site.	172
7.3A.	Wave-directions from VOS and Weathership data.	174
	B. Frequency occurrence of wave directions, summer and winter.	174
7.4	Exceedance curve for wave periods (T_p) at Alexander Bay.	177
7.5A.	Exceedance curve for wave periods (T_z) at Alexander Bay.	178
	B. Exceedance curve for wave periods (T_z) at Oranjemund.	178
7.6A.	Exceedance curve for wave heights (H_g) at Alexander Bay.	179
	B. Exceedance curve for wave heights (H_g) at Oranjemund.	179
7.7	Flow velocity vs. grain size to determine transport modes.	182
7.8	Flow velocity vs. grain size to determine sedimentary bedforms.	182
7.9	Flow velocity vs. flow depth, comparing flume studies with field observations.	184
7.10	Wave height vs. wavelength of bedforms.	184
7.11	Orbital velocity under waves for threshold of sediment motion.	194
7.12A	Frequency of wave heights (H_g) at Alexander Bay.	195
	B. Frequency of wave periods (T_p) at Alexander Bay.	195
8.1	Sea-level curves for the Tertiary and Quaternary.	206
A.1	Flowchart of laboratory procedures for sediment analyses.	246

LIST OF TABLES

<u>Table No.</u>	<u>Title</u>	<u>Page</u>
3.1	Bedrock-terrace depths on the South African continental shelf.	77
6.1	Increase in weight percentage mud off the Orange River	143
7.1	Range of depths for deep, intermediate and shallow water.	169
7.2	Percentage occurrence of wave directions (VOS data).	173
7.3	Median wave period (sec) and wave height (m), winter and summer.	175
7.4	Nomenclature and dimensions of bedforms.	183
7.5	Dimensions of bedforms in study area (m).	185
7.6	Horizontal orbital velocity for 50% exceedance wave conditions.	193
7.7	Horizontal orbital velocity for 5% exceedance wave conditions.	196
7.8	5% Exceedance wave-parameters for storm conditions.	197
7.9	Minimum wave conditions to transport granule-size quartz grains.	198
B1	Sample locations.	250
B2	Percentage component distribution.	252
B3	Percentage distribution of size-fractions, CaCO ₃ and organic carbon.	254
B4	Statistical summary of sand-size fraction.	256
B5	Frequency percentage of wave parameters T _p , T _z and H _s per season.	258

LIST OF PLATES

<u>Plate No.</u>	<u>Title</u>	<u>Page</u>
2.1	Typical seismic section across the inner shelf - middle shelf boundary.	41
3.1	Seismic section across the inner shelf and the Acoustical Blanking Layer.	65
4.1	Sonograph displaying various seafloor features.	104a
4.2	Sonograph image of lineaments in bedrock, interpreted as dolerite dykes.	104a
4.3	Sonograph image of part of Peacock Bank, showing different bedrock reflectors.	104a
4.4	Oblique view of Lower Terrace gullies, Alexander Bay.	104b
4.5	Sonograph showing a bedrock lineament, interpreted as a wave-cut cliff.	104b
7.1	Sonograph showing convex reflectors and megaripple-strips perpendicular to the coastline.	202a
7.2	Photograph showing sharp boundary between muddy water and clear seawater.	202a
7.3	Sonograph showing "washed-out" areas arising from possible rip-current activity.	202a
7.4	Sonograph showing megaripple-field.	202b
7.5	Sonograph showing diffuse sedimentary structures.	202b
7.6	Sonograph showing megaripples and diffuse structures.	202b
7.7	Sonograph showing sea-surface interference patterns.	202b

LIST OF MAPS

Map No.	Title
1.	Track chart, (folded)
2.	Coastal topography and nearshore bedrock isobaths, showing courses of palaeo-channels, (folded)
3.	Bathymetry. A. Orange River to Cape Voltas. B. Cape Voltas to Rietfontein. C. Rietfontein to Wreck Point.
4.	Bedrock isobaths. A. Orange River to Cape Voltas. B. Cape Voltas to Rietfontein. C. Rietfontein to Wreck Point.
5.	Seafloor sonographs. A. Orange River to Cape Voltas. B. Cape Voltas to Rietfontein. C. Rietfontein to Wreck Point.
6.	Sediment isopachs. A. Orange River to Cape Voltas. B. Cape Voltas to Rietfontein. C. Rietfontein to Wreck Point.
7.	Depth to internal reflector. A. Orange River to Cape Voltas. B. Cape Voltas to Rietfontein. C. Rietfontein to Wreck Point.

CHAPTER IINTRODUCTION

The discovery of diamonds along the west coast of southern Africa almost 60 years ago, drew considerable interest to the arid and sparsely populated Namaqualand region. However, it is only in the last 20 years or so that the search for diamonds has shifted the emphasis from the raised beaches on the coastal plain to the littoral and the continental shelf.

The work presented here forms part of an intensive study of the inner shelf along the Cape west coast currently being undertaken by the Geological Survey. Termed the West Coast Project, the study aims at a better understanding of the Quaternary evolution of the inner shelf and the present-day processes along the coast. The initial aim of the project is to obtain saturation coverage by means of side-scan sonar and high-resolution seismic profiling, supplemented by grab sampling. Using data from this first phase, the study describes the nature of the seafloor in terms of the bedrock, the overlying sediments and their internal structure. In addition, the wave regime and its effect on sediment transport on the inner shelf is discussed. The Cainozoic sea-level history of the area is also outlined. This project thus examines the fundamental aspects that need to be studied in the exploration of diamondiferous marine deposits along the west coast. This may ultimately help in understanding the distribution, deposition and origin of the diamonds found in such abundance along the entire west coast of southern Africa.

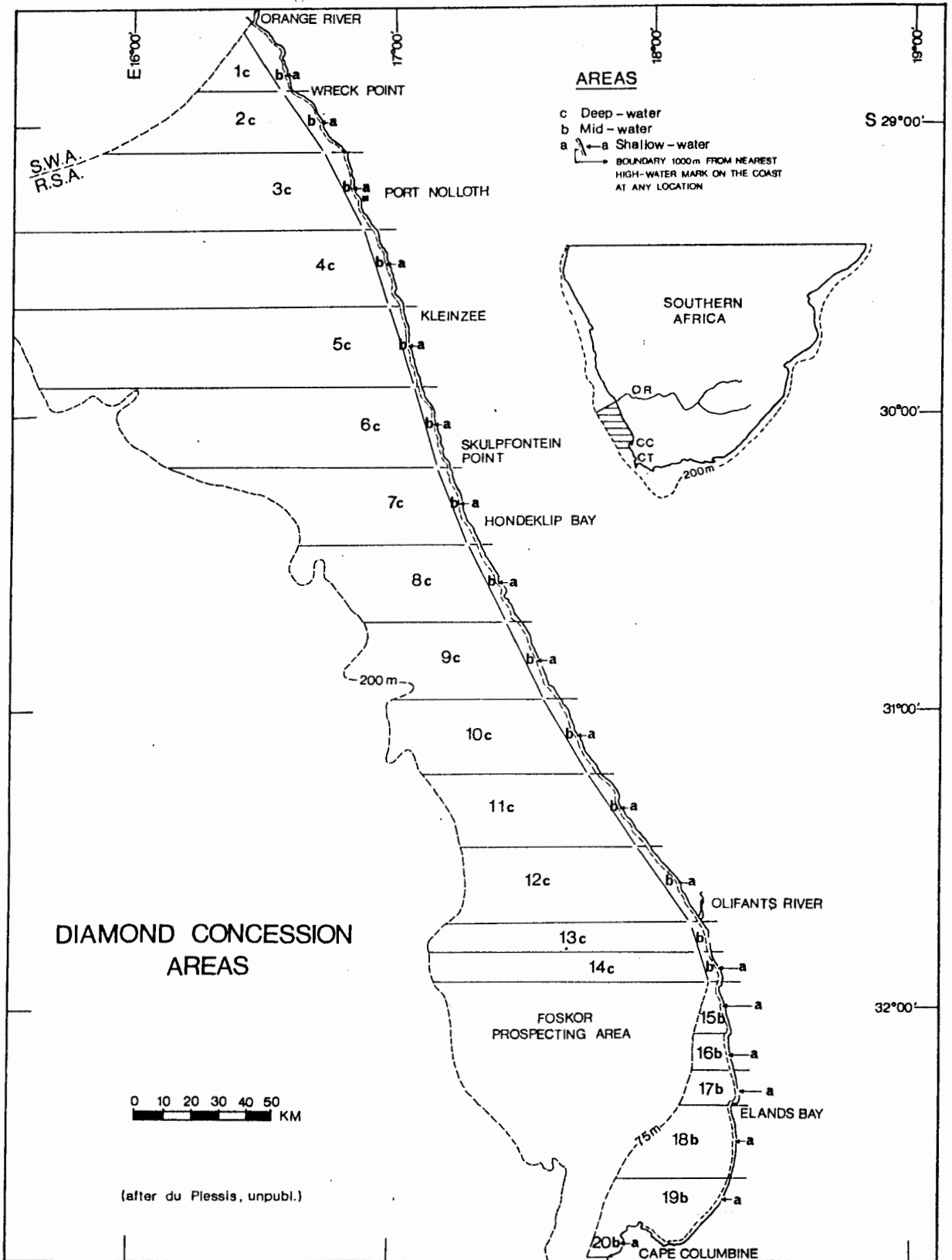


FIGURE 1.1

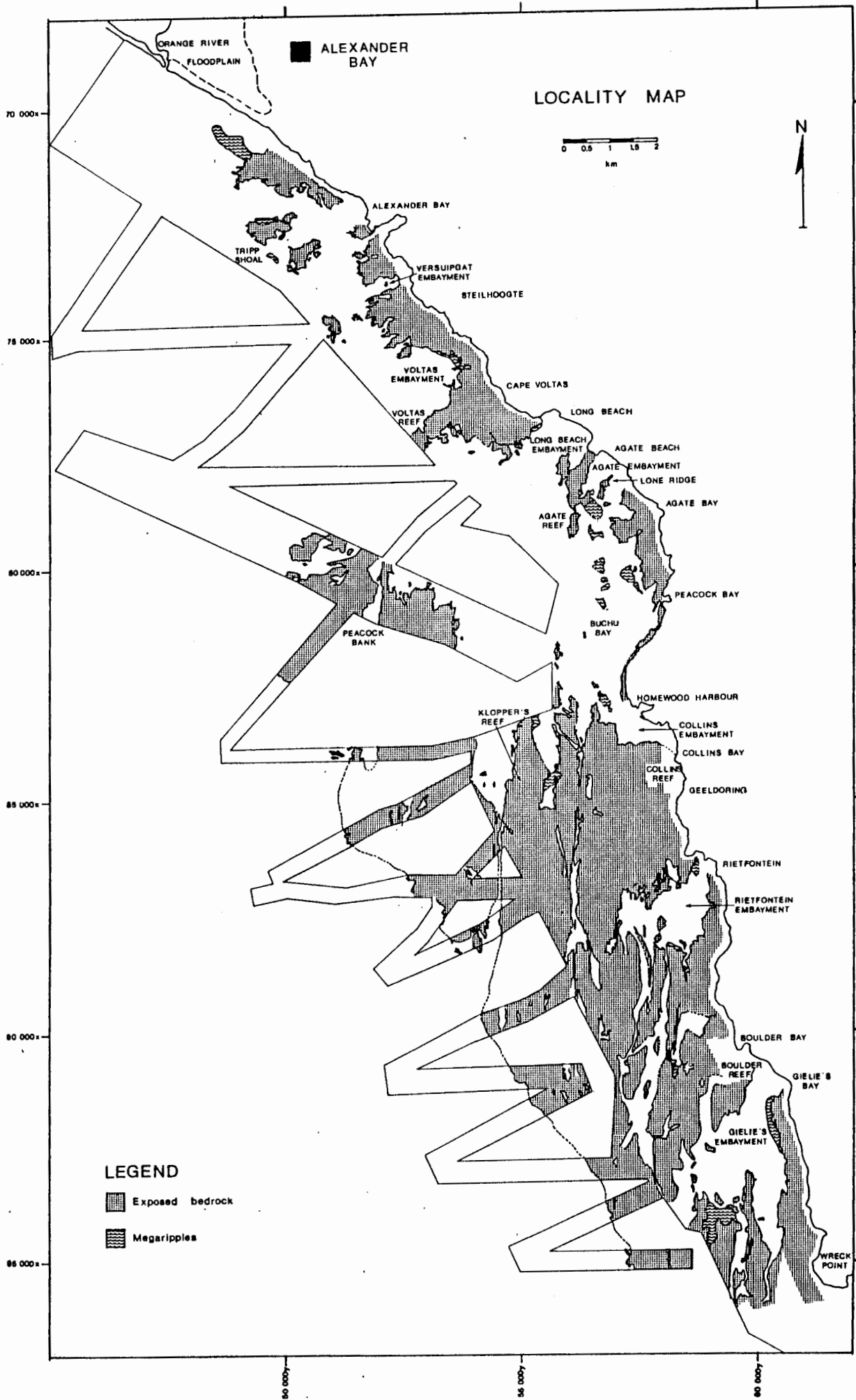


FIGURE 1.2

1.1 Present investigations

The study area is situated off the South African west coast, between the Orange River (Lat. $28^{\circ}30'S$) in the north and Wreck Point (Lat. $28^{\circ}50'S$) in the south (Fig.1.1). It extends from the breaker zone to approximately 50 m water depth and covers Diamond Concession Areas 1a, 1b and part of 1c (Figs.1.1 and 1.2). These diamond concessions, as well as Concessions 3a and 4a are at present being exploited by the State Alluvial Diggings.

The data used in this study were gathered during four cruises between 1980 and 1983 (Du Plessis, 1980 and De Decker, 1983a; 1983b). Coast-parallel survey lines, 100 m to 400 m apart, covered the area up to 2 km seaward of the breaker zone (Fig.1.3). These were supplemented by a set of zig-zag lines extending farther seaward to the inshore edge of a terrigenous mudbelt (Rogers, 1977) that laps onto the inner-shelf slope. Six coast-perpendicular tie-lines were run in selected areas across the densely surveyed area (Fig.1.3 and Map 1). During the surveys side-scan sonar and high-resolution subbottom profiling records were made. The sonographs were recorded at 100 m and 200 m scan range, using an EG-and-G Mark IB and a Klein Hydrosan Model 521 recorder. The seafloor coverage therefore ranged between complete overlap of adjacent lines to 100% coverage, with no overlap, depending on the line-spacing and the scan-range used. The seismic records were run at 125 msec. two-way time, using a 3.5 kHz Edo-Western pinger for all but 4 lines. Ninety-nine surficial sediment samples were collected in water depths between 10 m and 30 m. Details of the survey methods used and of the data reduction are given in the Appendix.

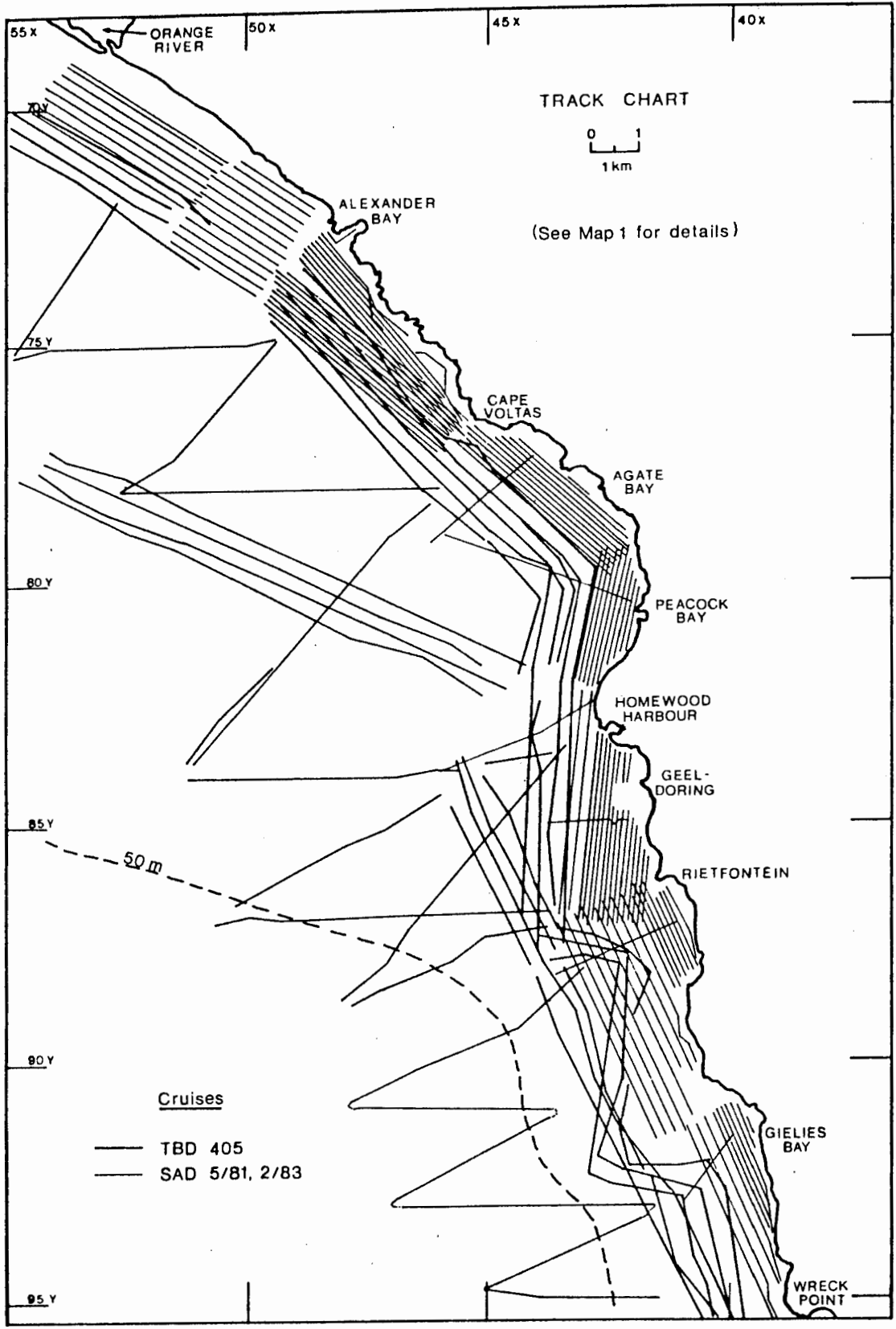


FIGURE 1.3

This study is thus based on data from one of the most intensely surveyed areas along the South African inner shelf. Studies in Saldanha Bay and Langebaan Lagoon (Flemming, 1977; De la Cruz, 1978) used data-sets of comparable density, whereas Woodborne (1985, 1986) obtained similar data coverage in Concession 4a and 4b (Fig.1.1). Records from an equally detailed survey run in Concession 3a and 3b were used in Honours projects by McCrae (1983) and Terhorst (1983).

1.2 Previous investigations

Onshore: The first descriptions of the coastal geology of Namaqualand and southern Namibia (Merensky, 1909; Wagner, 1914), were made soon after the discovery of diamonds in 1908 at Kolmanskop near Luderitz in Namibia. The area south of the Orange River was investigated by Rogers (1915, 1917) before the first Namaqualand diamonds were found at Port Nolloth in 1926. Merensky (1927) documented his own contribution to the discovery of the diamonds at Alexander Bay. The diamondiferous deposits themselves were described by Wagner and Merensky (1928). Contributions on the Cainozoic deposits along the west coast came from Reuning (1931) and Haughton (1931).

The first comprehensive study of Namaqualand geology was presented by De Villiers and Söhnge (1959). Martin (1965) and later Kroner (1974), reinterpreted the Late Precambrian formations in the area. The diamond fields continued to draw interest, with Stocken (1962) describing the deposits in the Sperrgebiet of Namibia just north of the Orange River. This was followed by Hallam's (1964) overview of the coastal geology between the Kunene River (18°S) and St. Helena Bay (32°S). Keyser

(1972) gave a detailed account of the diamondiferous deposits and geology of the coastal lowlands between the Orange River and Port Nolloth, i.e. the immediate hinterland of the study area.

Carrington and Kensley (1969) documented Pleistocene molluscs from the coastal deposits at Hondeklip Bay (Fig.1.1), whereas Davies (1973) gave a detailed description of the Pleistocene beaches along the coast, focussing on Stone Age artefacts and implements found in the deposits. Corvinus and Hendey (1978) gave an account of Miocene fossiliferous deposits at Arrisdrift, 30 km upstream from the Orange River mouth. Fowler (1976, 1982) described both the deposits on fluvial terraces along the lower Orange River and coastal deposits adjacent to the river mouth, emphasising the heavy mineral assemblages. A chronostratigraphic sequence of the raised beaches along the Namibian coast north of Oranjemund, based on Stone Age implements on the raised beach-terraces, was presented by Corvinus (1983).

Offshore: Regional investigations of the continental margin were undertaken by several workers. Simpson and Needham (1967), Simpson and du Plessis (1968), Bryan and Simpson (1971), Simpson (1971), Du Plessis et al. (1972), Dingle (1973a, 1973b, 1973c), Birch (1975), Rogers (1977), Siesser and Dingle (1981), and Dingle and Hendey (1984) are some who have contributed to the present understanding of the morphology, structure, stratigraphy, sedimentology and evolution of the shelf off the Cape west coast. Dingle, Siesser and Newton (1983) give a detailed account of the Mesozoic and Tertiary geological history of the southern African continent and margin in which the development of the west coast since the Palaeozoic era is presented and placed within the regional geological context.

Early studies of the inner shelf were initiated in direct response to the discovery of diamonds offshore. The Marine Diamond Corporation (MDC) (now De Beers Marine) took the lead in 1961 when they began marine prospecting in concession areas they held north of the Orange River (Murray, 1969). In 1965 Consolidated Diamond Mines took over the MDC investigation, extending it to the concessions they held south of the Orange River. At about the same time others, such as Terra Marina Mining Company, started their own marine prospecting work. From data obtained during these investigations, a number of workers have described aspects such as the nature of the seafloor, the distribution and composition of the sediments on and the Quaternary development of the inner shelf in and near the study area (Wright, 1964; Hoyt, Smith and Oostdam, 1965a, 1965b; Maree, 1966; Ahmed, 1968; Hoyt, Oostdam and Smith, 1969; Murray, 1969; Murray et al., 1970; and O'Shea, 1971).

Recent work on the inner shelf includes a geophysical interpretation of the Quaternary sediments along the coast between Cape Point and Baker Bay on the Namibian coast (Birch, in prep.) and a description of the bathymetry between the Orange River and Port Nolloth (De Decker, 1982). Subsequently, De Decker (1985b, 1986) has described the surficial sediments and the wave regime in the study area. Two Honours projects (McCrae, 1983; Terhorst, 1983) deal with the interpretation of sonographs on the inner shelf south of the study area between Cliff Point and Port Nolloth (Diamond Concession 3, Fig.1.1). The bathymetry and seafloor geology of the inner shelf between Kleinzee and White Point, which covers Diamond Concession Area 4, has been described by Woodborne (1985, 1986). Preliminary work on the

first vibrocores retrieved from the inner shelf south of the Orange River has been presented by De Decker (1985a), while Kieser's (1984) Honours project described three vibrocores obtained from an area off Cliff Point (Diamond Concession Area 3) and he compared them with the seismic stratigraphy of the unconsolidated sediment in that area.

1.3 Regional Setting

1.3.1 Climate

The weather on the west coast is predominantly the result of meteorological forces that originate offshore in the Atlantic and Southern Oceans. A subtropical high-pressure region in the South Atlantic forms anticyclonic conditions at about 30°S, whereas cyclonic cells form in the belt of Westerlies, between 35°S and 40°S, (Fig.1.4). These pressure regions move about 3 degrees poleward and equatorward in summer and winter respectively, (Schulze, 1965).

The aridity of the climate along the west coast arises from the presence of cold upwelled water at the coast, the paucity of summer rains that reach the region from the east coast and the presence of a temperature inversion at 600 m to 1800 m (Taljaard and Schumann, 1940, in Brain, 1984). This temperature inversion, which the authors describe for the Walvis Bay area, has the effect of restricting the development of rain-bearing clouds over the coast.

Winds: The cyclonic cells that form in the Southern Ocean migrate eastward at an average speed of over 30 knots (1300 km/day) (Taljaard, 1972). During winter the equatorward shift of

SYNOPTIC METEOROLOGY AND HYDROLOGY

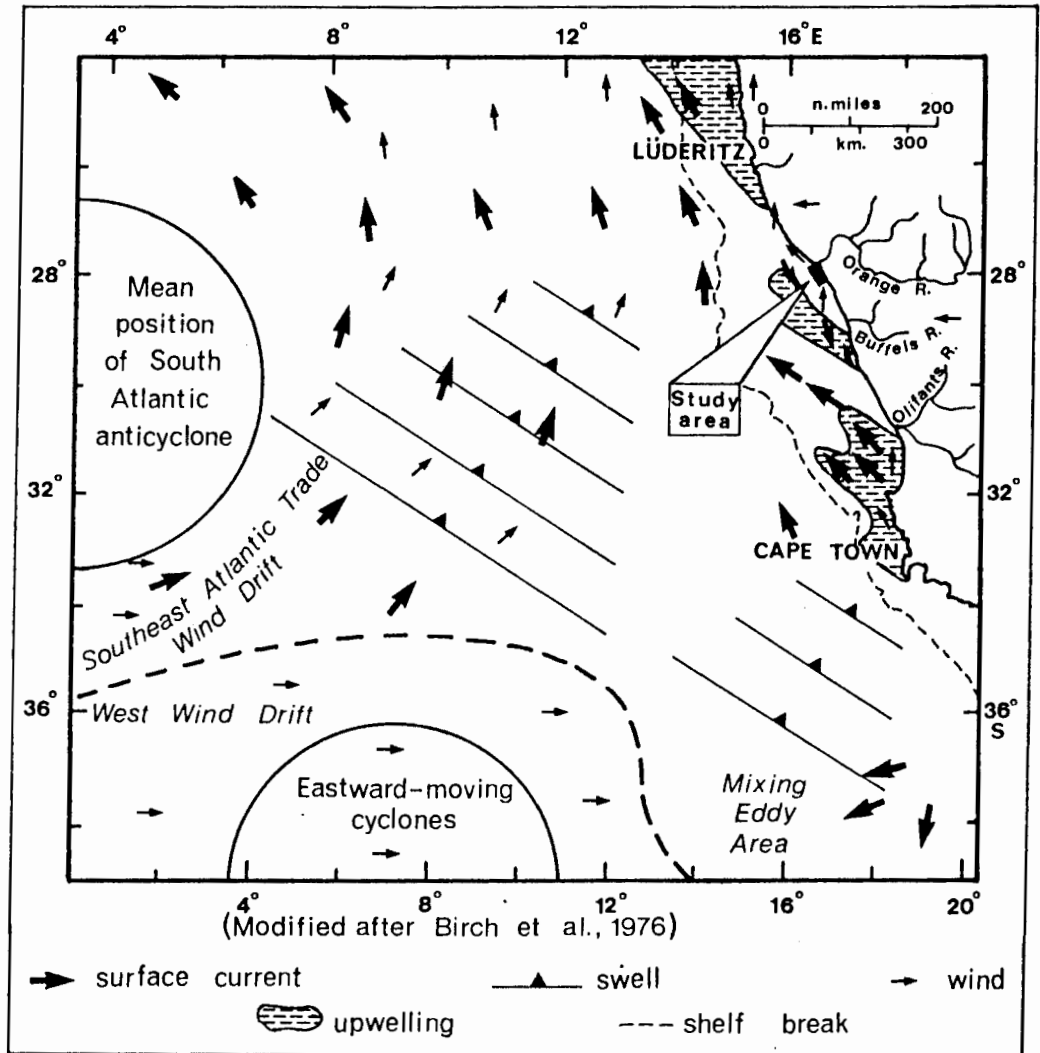


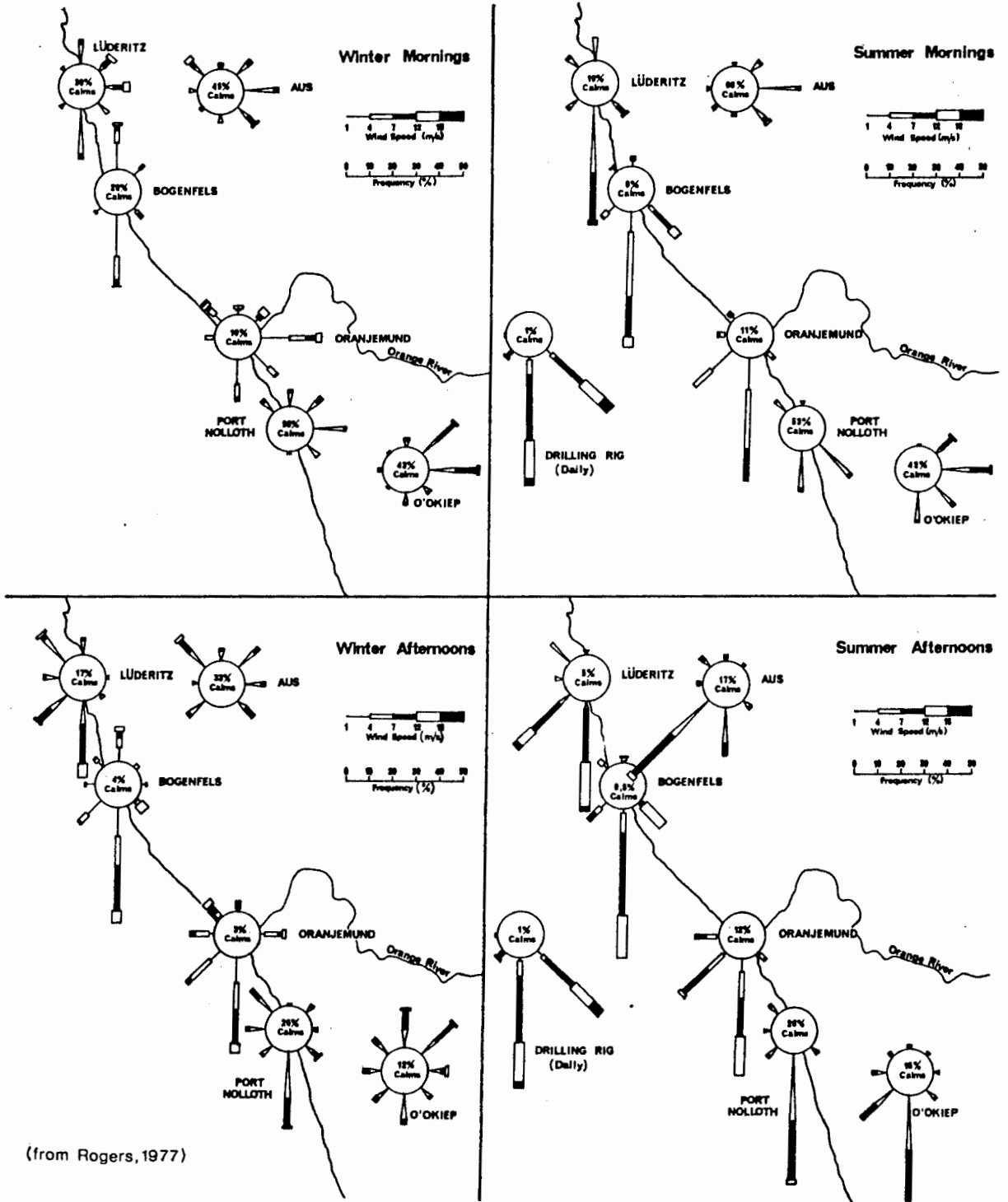
FIGURE 1.4

pressure systems brings the Western Cape into the path of these cyclones, with the result that storm conditions are created along the west coast. Gale-force northwesterly winds that back to southwesterly, usually last for several hours and possess a cyclicity of three to six days (Nelson and Hutchings, 1983).

Nelson and Hutchings (1983) have found that the aridity of the west-coast hinterland acts as a thermal barrier to air flow across the coastline. This results in a curved anticyclonic air flow along the coast (Fig.1.4), which itself is restricted by the continental escarpment (Fig.1.8), and the winds are therefore mostly south to southeasterly, particularly during summer (Fig.1.5).

The west coast is further affected by meso-scale weather patterns in the form of bergwinds and coastal low-pressure cells. Bergwinds occur most commonly during winter, but can develop throughout the year. A high-pressure system over southern Africa results in air moving offshore from the interior, warming in the process and creating hot, dusty conditions along the coast. Shannon and Anderson (1982) remark on the enormous volume of sediment that is transported onto the continental shelf by the bergwinds. They give an estimate of 50×10^6 tonnes for a single event, whereas the average annual output of the Orange River is estimated at 60×10^6 tonnes (Rogers, 1977). Satellite imagery shows that the bergwinds are areally restricted (Shannon and Anderson, 1982) and are locally intensified by coast-perpendicular topographic features such as river valleys. The sediment flux, direction of transport, frequency and extent of bergwinds in the vicinity of Walvis Bay have been described by Whitaker (1984). He concluded that the average dust plume

WIND ROSES



(from Rogers, 1977)

FIGURE 1.5

associated with a bergwind is about 120 km long, extending southwestward halfway across the continental shelf. The direction is determined by the climatic conditions giving rise to bergwinds and the orientation of the dry river beds. These winds are associated with low-pressure cells that originate in the vicinity of Luderitz and migrate as "coastal lows" around the subcontinent, at a speed of about 750 km per day (Taljaard et al., 1961).

As mentioned above, the prevailing winds at Alexander Bay (Fig.1.5) are south to southeasterly during summer. Schulze (1965) notes that the resultant windspeed in January is about 3 m/s in the morning (Fig.1.6), picking up to over 10 m/s in the afternoon, and dropping off again in the evening. In July the resultant windspeed is little more than 1 m/s before noon and generally originates from the southwest. The wind picks up to 2 m/s in the afternoon, but now comes from the south. The wind generally dies down after dark (Fig.1.6).

Rainfall: The low-pressure cells reaching the Western Cape also induce winter-rains along the coast, which occasionally extend as far north as the Orange River (Met. Services, 1944). Tripp (1975) has shown that over a period of 19 years the annual rainfall averaged only 53 mm at Alexander Bay, increasing to 59 mm at Port Nolloth. The monthly average shows a slight increase during the winter months. Low precipitation along the west coast is supplemented by the mist-rain that occurs when thick fog shrouds the coast. The fog forms due to the advection of warm air over the cold upwelled water beside the coast and occurs most frequently towards the end of summer, when upwelling is more frequent. Port Nolloth averages 1400 hours of fog per year (16%

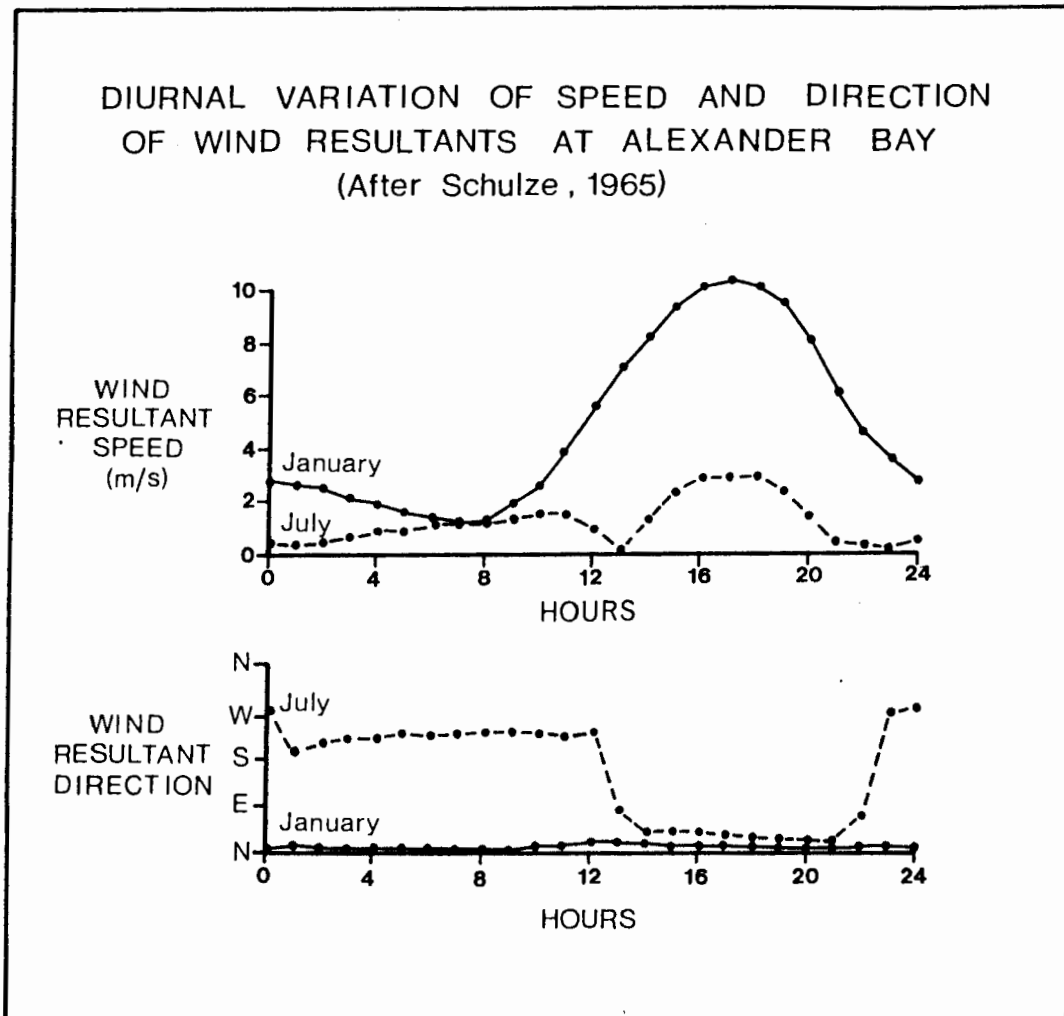


FIGURE 1.6

of the year) (Met. Services, 1944).

The meagre rainfall on this sand-covered coast is not sufficient to maintain any river discharge. There are consequently no perennial rivers between the Orange and the Olifants River, about 300 km farther south (Fig.1.4). Numerous dry river beds, such as the Holgat River entering the sea 15 km south of Wreck Point, bear testimony to much wetter periods during Pleistocene glacial periods, as reported from the Kalahari by Lancaster (1979) and Heine (1982) when most of the rivers would have been perennial (Rogers, 1977, Tankard and Rogers, 1978). This rejuvenation of the rivers would have been enhanced by concomitant sea-level regressions that lowered the base-line of the rivers several times during the Pleistocene (Tankard and Rogers, 1978). The effect of increased runoff and sea-level lowering on the erosion of diamondiferous deposits is discussed in Chapter 8.

1.3.2 Hydrology

The slow northward-flowing Benguela Current, originally defined by Hart and Currie (1960), extends 200 km offshore and forms the eastern boundary of the anticyclonic gyre in the South Atlantic (Fig. 1.4). Bang (1971) placed the western boundary of the Benguela Current at a divergence located over the shelf break. He defined the region shoreward of the divergence as the "weather-dominated Benguela system". Uncertainty about the circulation patterns of the Benguela Current still exists (Nelson and Hutchings, 1983) and these authors prefer to use the term "Benguela upwelling area", since the "current" has no documented core. Shannon (1985) gives a comprehensive review of the

evolution and physical character of what he terms the "Benguela Ecosystem".

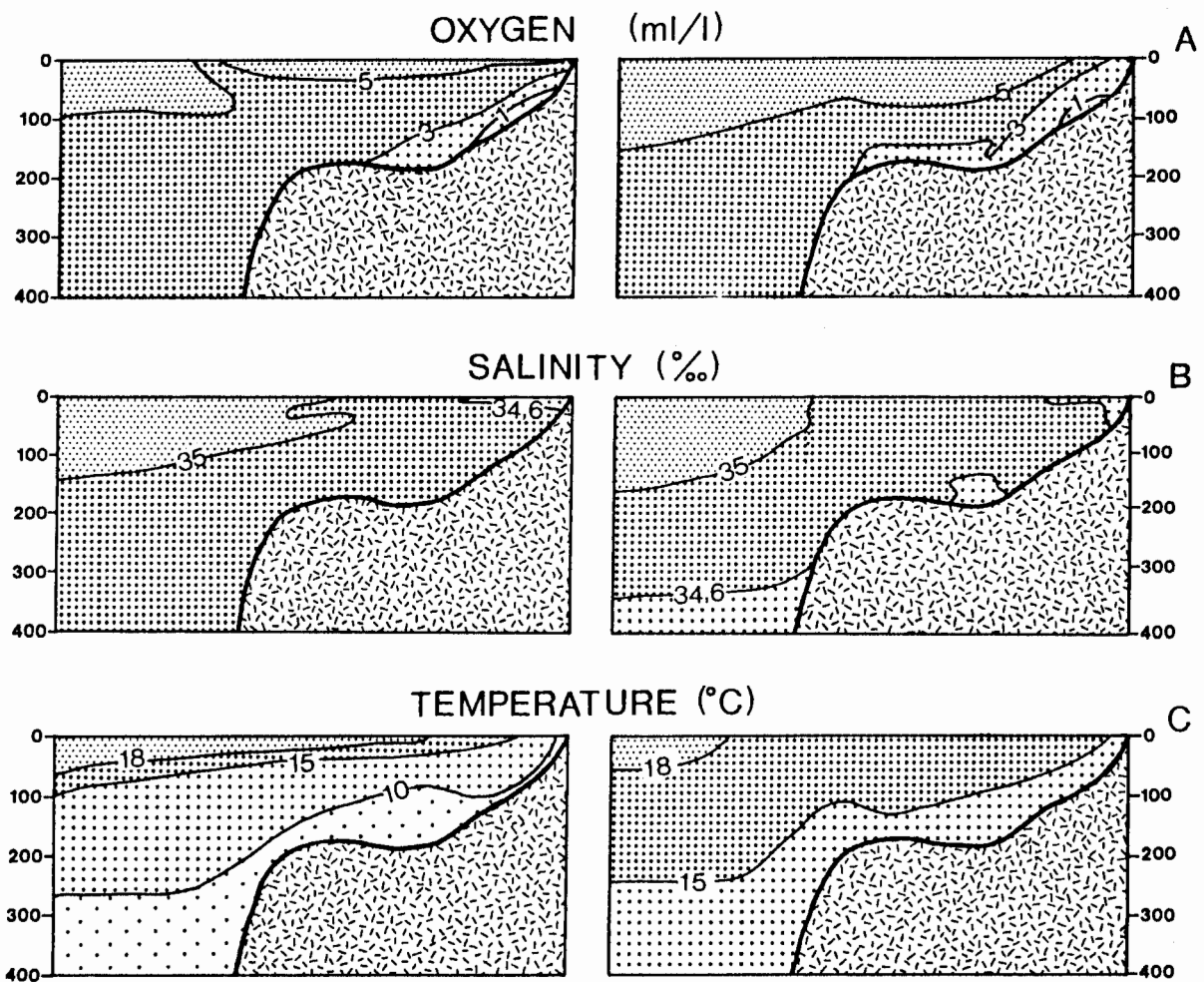
Currents on the continental shelf: Similar paths taken by satellite-tracked buoys on two occasions (Harris and Shannon, 1979, Nelson and Hutchings 1983), followed approximately the 200 m isobath between Cape Town and Luderitz (28°S), thus suggesting a current that is topographically "steered" (Nelson and Hutchings, 1983), with an average velocity of about 17 cm/s (Harris and Shannon, 1979). This compares with the Agulhas Current along the east coast of southern Africa which has a core velocity that at times exceeds 200 cm/sec and is sufficiently strong to produce large-scale bedforms on the continental margin (Flemming, 1978).

Hart and Currie (1960) suggest that bottom currents on the continental shelf are compensation currents, characterised by low oxygen content (<1 ml/l) (Fig.1.7A). The presence of oligoxic (low-oxygen) water on the continental shelf has variously been attributed to upwelling (Nelson and Hutchings, 1983), to the decay of biogenic material (Bailey, 1979), or to a southward compensation current with low oxygen, informally referred to as the De Decker Undercurrent (Bang, 1976; Birch et al., 1976 and Rogers, 1977). The southward compensation current brings oligoxic water from the Namibian shelf as far south as Cape Point (De Decker, 1970). Bailey (1979), concluded from his work off Lüderitz (Fig.1.4) that during autumn a southward moving undercurrent exists between 100 and 150 km offshore, at a depth of 200 m to 400 m. Off the Orange River this current has been identified between -50 m and -100 m (Fig.1.7A; Bailey, 1979). Bang (1976) considers the oligoxic nature of the current to be a special case of a more general undercurrent regime.

NON-CONSERVATIVE PROPERTIES
OFF THE ORANGE RIVER

AUTUMN
weak upwelling

SPRING
strong upwelling



(Modified from Rogers 1977, after Hart and Currie 1960)

FIGURE 1.7

Coastal currents: A review by Harris (1978) of coastal currents reveals that data are scarce for the west coast. Based on wind data (Fig.1.5) he concludes that the predominant coastal currents are most likely northward directed. The sharp change in sediment composition north and south of the Orange River mouth (Fig.1.9) indicates that most of the terrigenous material debouching from the river is transported by northward moving littoral drift. The Sea Fisheries Research Institute has two Aanderaa RCM 4 current meters on an array deployed in 142 m water-depth on the middle shelf (one at -64 m and the other at -122 m) about 48 km southwest of Port Nolloth (Fig.1.8). Preliminary interpretation of the data, which were taken in summer and early autumn between December 1983 and March 1984, indicate a south-southeasterly-moving (138°) bottom current at these depths, with an average current-velocity of 12 cm/sec and ranging up to 25 cm/sec (Nelson pers. commun., 1984). It is this current which is believed to be responsible for the extensive terrigenous mudbelt that continues southward for 500 km along the inner shelf-edge to St Helena Bay (Rogers, 1977). Periodic reversals in current direction, lasting about one week, are tentatively linked to the passage of low-frequency shelf waves such as tidal waves, that propagate northward (Nelson pers. commun., 1984).

Upwelling: Watermass movement along the west coast is principally by way of upwelling. Equatorward wind stress on the sea surface causes Ekman transport of the water which, interacting with Coriolis force, results in offshore movement of the surface water and compensatory upwelling of bottom water. Upwelling occurs along the entire coast (Fig.1.4), but varies both spatially and temporally (Nelson and Hutchings, 1983).

Locally, upwelling intensities are also indirectly affected by the coastal topography in that the winds favouring upwelling are funnelled down river valleys, or become deflected by mountain ranges. The winds are therefore reinforced in certain areas and dissipated elsewhere (Jury 1981, Shannon and Anderson, 1982).

North of Hondeklip Bay (Fig.1.4) upwelling is persistent throughout the year with a maximum in spring and a minimum in autumn (Stander, 1964, Nelson and Hutchings, 1983). Stander (1964) remarks that from the Orange River northward to Luderitz upwelling occurs more frequently and intensely than elsewhere along the coast. The upwelling effect is felt to a depth of 350 m, i.e. on the shelf break. Latun (1962, in Nelson and Hutchings, 1983) estimates the upwelling rate off the Orange River to be 3.5 to 4.7×10^{-4} cm.sec⁻¹. Nelson and Hutchings (1983) consider that both the Luderitz and Hondeklip upwelling cells are influenced by the bathymetry, due to a narrowing of the shelf off Luderitz and the position of Childs Bank off Hondeklip Bay (cf Figs.1.4 and 1.8). This region of the Benguela system has not yet been studied in detail so little is known of the seasonal or long-term trends (Nelson and Hutchings, 1983). Figure 1.7 A to C shows the oxygen, salinity and temperature distributions off the Orange River during periods of reduced and pronounced upwelling. The oligoxic layer (De Decker

BATHYMETRY

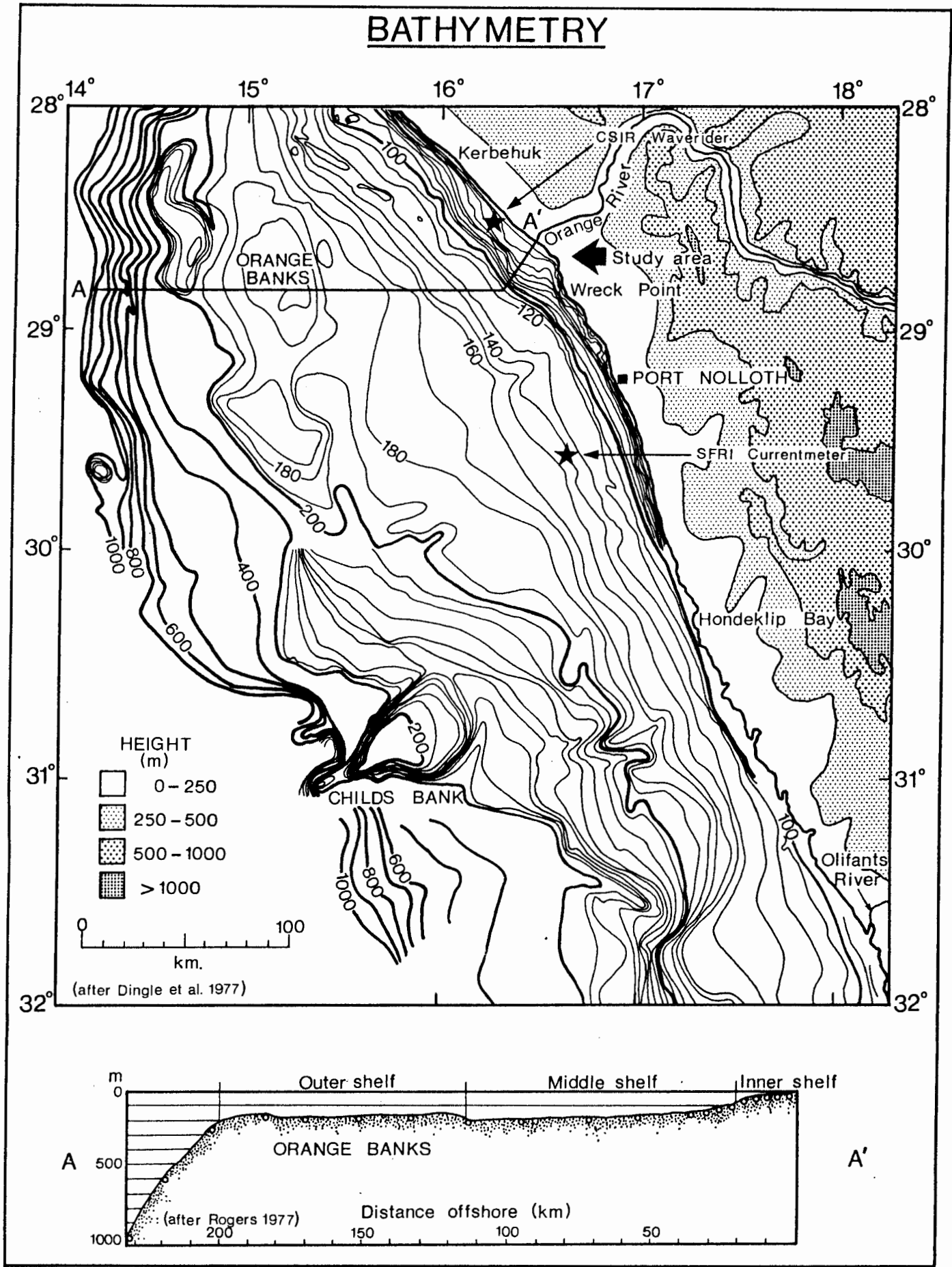


FIGURE 1.8

Undercurrent) at about -100 m and the lower salinity are noteworthy. (The low salinity tongue extending offshore shows the influence of the Orange River input. It is found under weak upwelling conditions as well.)

Water temperature: As a result of removal of warmer surface water offshore through windstress and the concomitant upwelling of colder subsurface water (Fig.1.7C), isotherms are linear and coast-parallel with lowest temperatures close to shore (Shannon, 1966). Boyd (1983) has found a seaward thermal gradient of 3° per 225 km with water cooler than 16°C extending along the coast and up to 225 km offshore in winter and spring. In summer and autumn this area contracts and it lies up to 95 km from the shore, with a resulting temperature gradient of 4° per 225 km (Fig.1.7). Maximum longshore gradients of 1°C per degree of latitude occur during summer and autumn.

Tides and short-term sea-level changes: Davies (1964) classified the west coast as a meso-tidal (tidal range between 2 m and 4 m) wave-dominated region. Heydorn and Tinley (1980), however, noted that the difference between the highest and lowest tidal range on the west coast is 60 cm and that the tidal range at Port Nolloth is 1,6 m. This part of the coast therefore lies in the micro-tidal (<2 m) range and the effect of tidal currents on inner shelf sediment transport is considered to be negligible. Brundrit et al. (1983, 1984) found that extra-tidal variations in sea level correlated well with synoptic air-pressure changes. A lowering of sea level by 10 to 20 cm during the summer months corresponded with the intensity of upwelling (Brundrit et al. 1983). A range of almost 30 cm is associated with the passage of atmospheric disturbances such as coastal lows and could last over

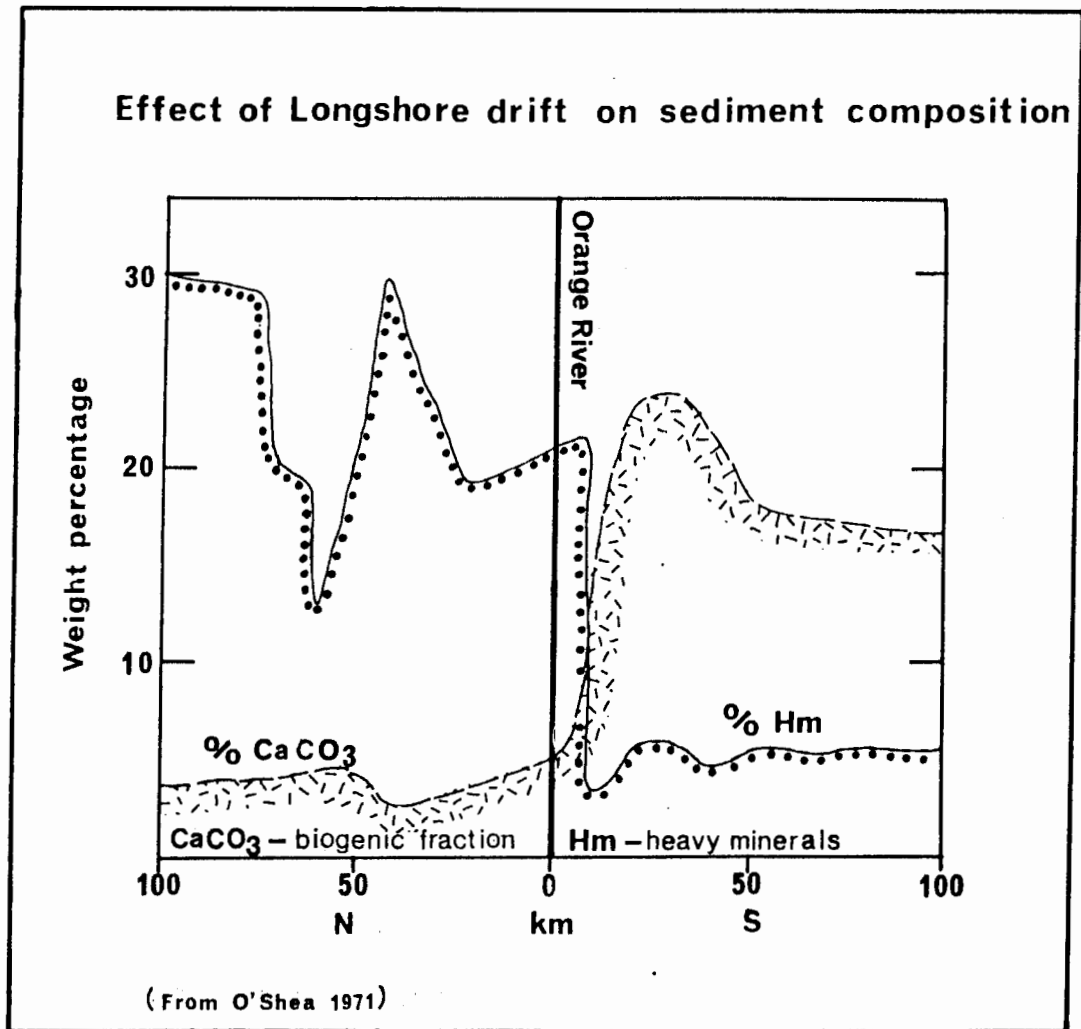


FIGURE 1.9

a period of several days. An inter-annual variation in sea level was also found, with a drop of 20 cm between 1979 and 1982 at Walvis Bay (Brundrit et al., 1984).

Whereas the water-mass movements described above have pronounced effects on the continental margin in general, their influence in the nearshore area will be restricted. On the inner shelf the principal hydrodynamic forces are wave-induced bottom currents and littoral drift. These will be described in detail in Chapter 7.

1.3.3 Morphology

Onshore: The west coast is backed by the "Great Escarpment" that runs 35 to 100 km inland, parallel to the coast and rises to about 700 m (Fig.1.8). It separates the hinterland plateau from the coastal lowlands (Hallam, 1964). Along the Cape west coast the escarpment has been breached in only two places. The Orange River crosses it at latitude 28°S, and the Krom River, a tributary of the Olifants River, at 31°S. Dingle and Hendey (1984) consider the Krom River break to have provided a channel-way for the Orange River during Palaeogene times. This latitudinal shift in the flow of the Orange River will have affected the distribution of diamonds along the west coast - an aspect to be discussed in Chapter 8. Numerous other rivers along the west coast have courses that extend inland only up to the escarpment. The coastline between the Olifants and Orange Rivers is relatively straight and with only a few bays or coastal re-entrants, trends at approximately 335°N (Fig.1.8).

The Buchu Berg Twins (Map 2) act as a pivot for a change in

coastline trend in the study area, from 345° between Wreck Point and Homewood Harbour to 315° north of Homewood Harbour. The coast along the southern part is fringed by beaches or low cliffs rising to a height of 10 m. North of Homewood Harbour steep cliffs, reaching 25 m high, are backed by a coastal plain. The plain extends inland for up to 2 km before the ground rises from about the 30 m contour to form a series of low hills (Map 2). From Buchu Berg southward the 30 m contour extends inland to about 4 km off Wreck Point. Shallow pans, such as Rietfontein Pan and Visagie Pan, are found in this area (Fig.1.10). The pans, which lie between the coast and a series of ridges that rise to over 100 m, have been covered by aeolian sand dunes that give rise to the characteristic contour pattern evident on Map 2.

The unusual topography east of Long Beach and Agate Beach represents man-made hills formed in the process of removing overburden to reach the diamondiferous marine deposits close to bedrock. Another noteworthy feature is the prominent ridge extending northwestward from Namakwa Kop to Spitzkop, coinciding with the regional structural trend in the bedrock. The ridge consists of resistant quartzitic schists of the Holgat Suite (De Villiers and Söhnge, 1959).

The Orange River floodplain extends for more than 2 km southeastward from the present-day mouth, narrowing to the north to form a broad, flat, triangular area. The coastal plain becomes more extensive in this area with the 30 m contour skirting 3 km inland northward of Alexander Bay. The coastal plain contains two prominent wave-cut terraces that are the focus of onland diamond-mining activities. These terraces will be described further in section 1.4.2. Other features that have a

bearing on the diamondiferous deposits include the pronounced valley stretching inland southeastwards from Buchu Berg, past Visagie Pan (Map 2), the valleys that run north-northeast and northeast from Agate Bay and Peacock Bay respectively and the valley extending eastward from Alexander Bay, passed Kolompie se Gat and Jam Pan. These valleys, and others, can be extended seaward across the inner shelf (Map 2). Their effect on the distribution of diamonds eroded from marine deposits on the raised terraces will be discussed in Chapter 3.

Offshore: The continental shelf extends up to 230 km offshore and lies as deep as 500 m below sea level (Rogers 1977, Dingle et al., 1983). This places the shelf amongst the widest and deepest in the world, as the worldwide average is 86 km and 130 m respectively (Shepard, 1963 and Fig.1.8).

Three morphological regions are distinguished on the continental shelf: an inner shelf, a middle shelf and an outer shelf (Rogers, 1977). The inner shelf consists of a narrow, rugged and generally sediment-free rocky platform with an average depth of -30 m. It extends up to 8 km offshore and is marked on the seaward side by a steep ($1,1^{\circ}$ to $1,9^{\circ}$) gradient (Fig.1.8). The inner shelf between Port Nolloth and the Orange River will be described in detail in Chapter 2.

The contact between the inner and middle shelves is usually between 100 and 110 m below sea level (Rogers, 1977) which, in the study area, lies buried beneath a 20 to 30 m-thick succession of Quaternary sediments (Birch, in prep.). The contact is generally not seen on seismic records because of the screening effect of gaseous sediment, the Acoustical Blanking Layer (ABL), within the sediment (O'Shea, 1971 and Fig.2.1). The sudden

change of gradient at the contact is regarded by several workers (Murray et al., 1970, Rogers, 1977 etc.) to have been formed during the major regression (about 18 000y B.P.) that immediately preceded the Flandrian transgression (cf Chapter 8).

The middle shelf is characterised by low relief and a gentle seaward gradient of $0,1^{\circ}$ (Rogers, 1977). The depth varies between 100 m inshore and 190 m where it joins the outer shelf. The latter rises to 160 m off the study area to form the extensive Orange Banks (Rogers, 1977) situated 120 km from the coast (Fig. 1.8). The western margin of the Orange Banks forms the continental shelf-break.

This very broad shelf has been the depositional area for diamonds since early Tertiary times (Du Toit, 1954). Chapter 8 discusses the geological evolution of diamondiferous deposits along the Cape west coast, highlighting the influence of sea-level changes on the distribution of diamonds on the continental shelf.

1.4 Geology

1.4.1 Precambrian Basement

Coastal basement rocks of Precambrian age belong to the Gariep Complex (SACS, 1980, p.439), which is subdivided in the study area into the Holgat, Grootderm and Oranjemund Suites (Fig.1.10). The Swartbank Pluton of the Cape Granite Suite (SACS, 1980) crops out in a few small, scattered localities, 7 to 17 km east of Homewood Harbour (Fig.1.10). The Precambrian Basement which forms the inner shelf continues between 2 km and 10 km offshore (Fig.1.8), and dips beneath gently seaward-dipping Cretaceous beds (Fig.1.12; Dingle, 1973a) at 100m to 110 m below sea level (Rogers, 1977).

GEOLOGY

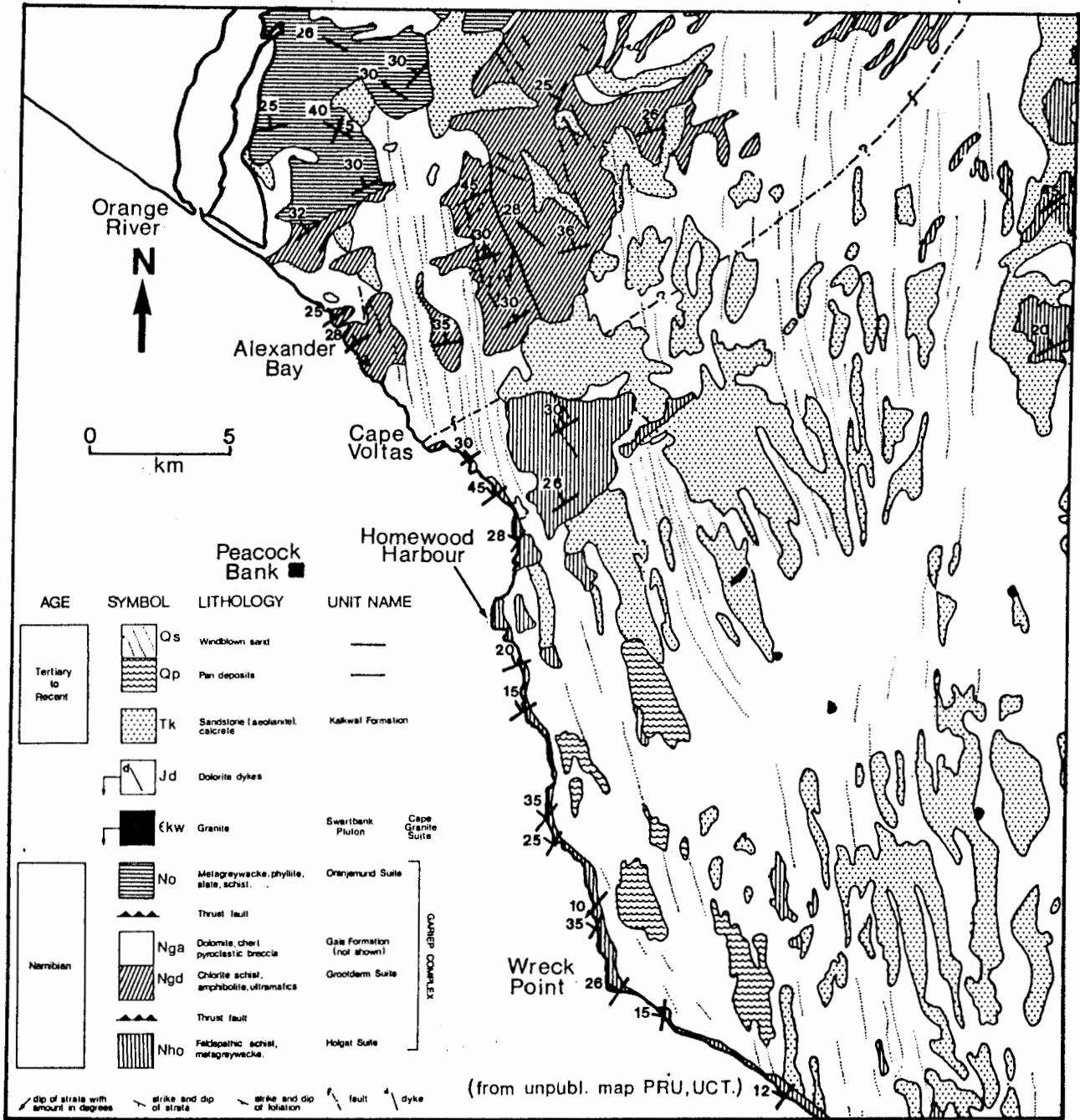


FIGURE 1.10

The Holgat Suite is exposed along a narrow zone on the coast in the south of the study area. It consists of greenish-grey schistose quartzites interspersed with conglomerates of granite-gneiss and quartzite pebbles (Kröner 1974). The schists and schistose greywackes were formed by intense shear deformation that destroyed the original bedding planes. The Holgat Suite lies with a thrust fault contact (exposed at Cape Voltas and at Arris Drift up the Orange River) against the Grootderm Suite (Fig.1.10 and Map 3A). The regional strike of the bedding planes is towards the northeast with a dip towards the northwest, and the well-developed schistosity parallels the original stratification (Fig.1.10). Bedrock exposed on the coastline between Wreck Point and Collins Embayment (Fig.1.2) exhibits rugged topography, with resistant quartzites of the Holgat Suite forming ridges and separated from each other by narrow gullies that trend north-northeast for several hundred metres (cf Maps 3B and C).

The Grootderm Suite (Fig.1.10) consists mainly of basaltic to andesitic volcanics (representing a calc-alkaline suite, Kröner, 1974) and associated volcanic breccia, agglomerates and tuff. Intense shearing has metamorphosed these rocks into greenish, fissile, chlorite schists. The schistosity of the lavas dips toward the north and the west at angles of about 20° (De Villiers and Söhnge, 1959). At Alexander Bay (Fig.1.10) the contact between volcanics of the Grootderm Suite and thinly laminated and tightly folded phyllites, schists and quartzites (De Villiers and Söhnge, 1959), of the Oranjemund Suite lies exposed. The Oranjemund Suite continues northward across the Orange River. The base of this suite consists of dolomites (Kröner, 1974) which, like the other rock-types, are also highly

sheared. Intruded into the country rock before the last phase of the Gariep deformation are small dykes of lamprophyre, sills of altered hornblendite and gabbroic plugs (Kröner, 1974).

Dykes and sills of dolerite, considered to be of post-Karoo age (De Villiers and Söhnge, 1959) are abundant along the coast, particularly between Buchu Berg and Alexander Bay. The dominant strike direction of dykes along the coast is north-northwest, parallel to the regional schistosity. Most of the dykes are only a metre or so wide, but are traceable for up to 4 km in length. It should be possible to detect similar dykes on the inner shelf from sonographs, as the resolution of the side-scan system is about 50 cm close to the transducer (Flemming, 1976b).

The original stratification of all the lithologies has been obliterated by very tight isoclinal slip-folding that produced a penetrative foliation trending northeast with predominantly shallow dips to the northwest (Fig.1.11 and Kröner, 1974). Lineaments arising from this period of deformation have a north-east trend with a near horizontal attitude. The northeast trends are, in addition, parallel to the thrust faulting that is exposed at Cape Voltas (Fig.1.10; Kröner, 1974). De Villiers and Söhnge (1959) have found minor thrust-faulting in the Oranjemund Suite and Hill (pers. comm., 1984) considers that Alexander Bay itself may have been formed along a thrust zone that trends northeastward.

Three phases of folding can be recognized in the Alexander Bay area (Kröner, 1974). The first phase produced the pervasive foliation striking northeastward, described above. The second phase of deformation gave rise to open flexural slip-folds and these trend north-northeast. The last phase of deformation

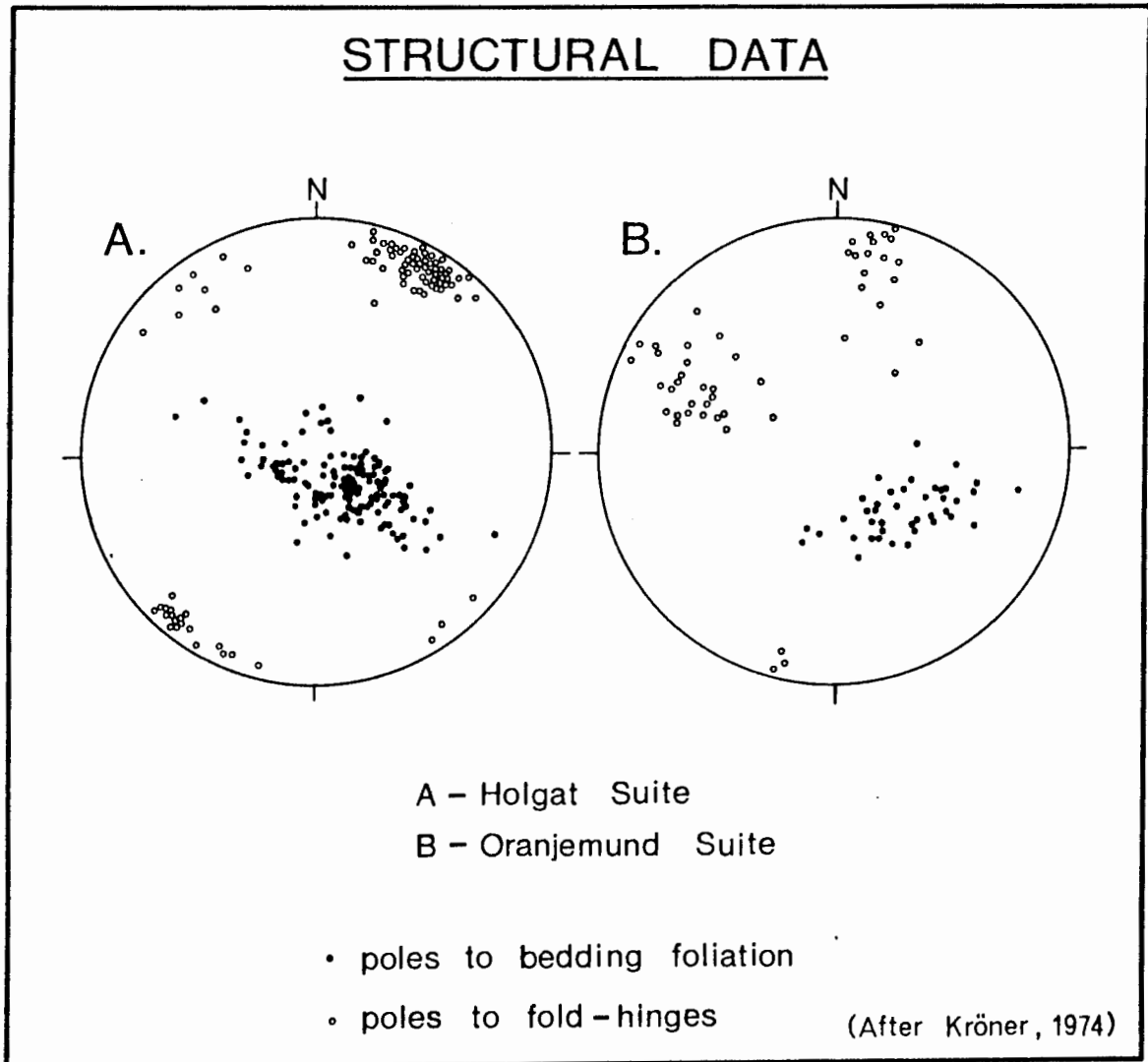


FIGURE 1.11

resulted in widely separated fractures, expressed by severe jointing that trend between 320° and 340° (NW to NNW) (Kröner, 1974)

Bedrock exposed on the inner shelf may be expected to show prevalent north-northeast to north-northwest lineaments on sonographs reflecting the trend of the regional schistosity, the original lithological stratification and the preferred orientation of dolerite dykes seen along the coast (Fig.1.10). Lineaments that trend northwest to north-northwest are likely to have formed as the result of the erosion of fractures and jointing in the bedrock. The east-northeast trending thrust faults at Cape Voltas and (possibly) Alexander Bay could be reflected in a strong cross-cutting lineament, across the general trend. Conversely, these faults may have been eroded into extensive gullies or depressions that are now filled with sediment. Gullies eroded along these planes of weakness have been found to harbour rich diamondiferous deposits (Keyser, 1972) on the raised marine terraces. Positive identification of similarly formed gullies on the inner shelf would therefore be of assistance in the exploration of diamonds in this region as well. In Chapter 4 the surface structure of the exposed bedrock, interpreted from side-scan sonar records, will be discussed.

1.4.2 Cretaceous and Tertiary deposits

Cretaceous deposits: Major sediment basins formed along the western continental margin as a result of tensional rift-faulting during the late Jurassic-early Cretaceous separation of South America from Africa. The Orange Basin has been the main depocentre for sediments supplied mostly by the Orange River, with smaller contributions from the Olifants and Berg Rivers

(Dingle and Scrutton, 1974). The sediments supplied to the basin covered the downfaulted basement blocks, forming a prograding sediment wedge that had evolved to its present outline by the end of the Cretaceous period (Dingle, 1977). Figure 1.12 shows that the middle shelf consists of an approximately 50 km wide outcrop of shallow seaward-dipping (ave. 3° , Dingle, 1973a) Upper Cretaceous deposits (Dingle et al., 1983) lapping onto the Precambrian basement rocks (Fig.2.1).

The oldest sediments onland covering the Precambrian basement rocks are marine deposits of Upper Cretaceous age. These beds are restricted to a table-top size outlier found at Bogenfels in Namibia (Klinger, 1977). The deposit consists of a basal layer of yellowish brown fossiliferous silty sand, overlain by a calcified horizon with marine shells. The top layer is formed by unfossiliferous olive green silt (SACS, 1980; Dingle et al., 1983).

Palaeogene deposits: On the continental shelf a thin belt of lower Tertiary strata unconformably follow on the Cretaceous beds, also dipping westward at about 2.5° (Fig.1.12; Dingle, 1973a).

Small outcrops of Palaeogene age occur along the Namibian coast south of Luderitz. The basal strata, called the Pomona Beds, were originally dated as Cretaceous (Du Toit, 1954) but Dingle et al. (1983) "tentatively" place them in the Palaeocene. The Pomona Beds are mostly fluvial sandstones with a basal pebble conglomerate, capped by dolomitic silcrete and calcrete (Dingle et al., 1983). Diamondiferous, largely unfossiliferous marine conglomerates and clayey fine-grained sandstone lie on a wave-cut terrace at 120 to 140 m above sea level at Buntfeldschuh

GEOLOGY OF THE CONTINENTAL SHELF

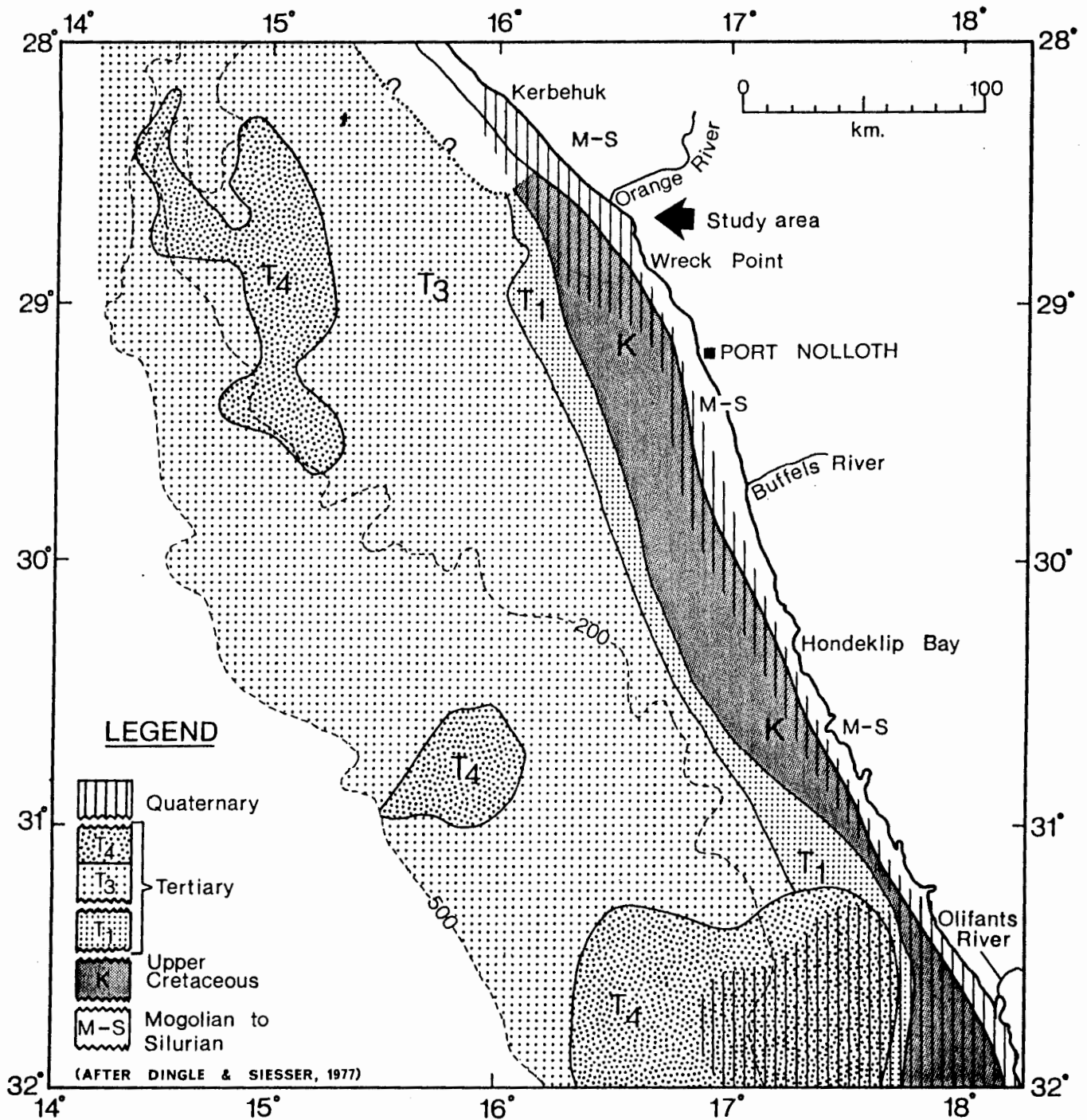


FIGURE 1.12

160 km north of the Orange River. These strata are overlain by aeolian sandstones and capped by a calcrete layer (Siesser and Salmon, 1979). At Bogenfels, 20 km farther north, they report about 4 m of fossiliferous marine pebbly sandstones on a marine terrace at an elevation of about 70 m. This has been overlain by calcareous and marly sandstones and silts that have been dated as middle-upper Eocene (Bohm, 1926 in Siesser and Salmon, 1979). The latter authors ascribe an age of upper Palaeocene - lower Eocene to the marine deposits at Buntfeldschuh. Hendey (1981a) mentions "possible Eocene" deposits at about 140 m elevation from Kamaggas, on the Buffels River (Fig.1.12), where a shark's tooth deposit in beach gravels is found. He correlates it with marine deposits near Vanrhynsdorp, 60 km east of the Olifants River mouth (Fig.1.12) for which Lamont (1947, in Dingle et al., 1983) gives an elevation of 150 to 230 m.

Neogene deposits and raised marine terraces: The largest part of the continental shelf is underlain by subhorizontal deposits of Upper Tertiary age (Fig.1.12). The lower sequence of the Upper Tertiary (T3) constitutes most of the middle shelf, and lies with a strong unconformity on the Lower Tertiary deposits. Upper Upper Tertiary (T4) sediments are found as outliers, forming the extensive Orange Banks off the Orange River, and Childs Bank farther south (Fig.1.12). These beds lie with an unconformity on the older rocks (Dingle 1973c).

Neogene deposits along the Namaqualand coastal zone include the important diamondiferous beach deposits found on the raised wave-cut terraces. These terraces occur at various elevations along the coast and are covered by deposits consisting of marine gravels with rounded pebbles and boulders of basement rocks.

These are set in a matrix of sand which is partly cemented by lime or gypsum; shells are also a common constituent of the gravel deposits (Keyser, 1972). The diamonds found with the littoral deposits are usually associated with the gravels and heavy sediment fraction, trapped in gullies and potholes or at the foot of a cliff cut by wave-action into the bedrock (Hallam, 1964; Keyser, 1972; Maree, 1966).

During the Upper Cretaceous and Tertiary periods sea level rose and fell as a consequence of changes in the rate of sea-floor spreading superimposed on the variations in volume of continental ice-caps and isostatic imbalance of the continental margin (Donovan and Jones, 1979; Vail and Hardenbol, 1979; Nunn 1984). The result of these different effects was that sea level did not change eustatically. Local influences may have caused transgressions or regressions in one area to occur at a different time and rate than in another area. This is well illustrated on the west coast, where "the convergence of the Mio-Pliocene beach terraces along the north Namaqualand-south Namibia coast illustrates the degree of differential crustal movement that can be detected in well-documented regions" (Dingle et al., 1983, p.305).

The oldest and highest raised wave-cut terrace recognised in the Alexander Bay area, the Grobler terrace, lies at between 64 m and 84 m and extends up to 7.5 km inland from the coast (Keyser, 1972). Other terraces found are the Upper Terrace, at 34 m to 47 m, the Middle Terrace which lies between 17 m and 26 m and the Lower Terrace, found between sea level and 9 m (Keyser, 1972). The latter two terraces form important elements in the coastal plain that is found between the beach and the 30 m contour (Map

2). North of the Orange River two sets of marine terraces are recognized. They are lettered A to F, with A,B and C corresponding to the Lower Terrace and D,E and F to the other terraces. The terraces lie at progressively lower elevations northward and eventually merge at Affenrucken, 100 km north of the Orange River (Anonymous, 1982).

The deposits on the higher terraces - the Middle, Upper and Grobler Terraces of Keyser (1972) and the D-, E- and F-beaches of Anonymous (1982) and Corvinus (1983) at Oranjemund contain a thermophilic molluscan fauna, including Striostrea margaritacea, Donax haughtoni, Fissurella robusta, and Chamelea krigei (Carrington and Kensley, 1969), and Thais praecingulata (Keyser, 1972) that indicate a warm water milieu. These terraces have consequently been placed in the Late Miocene (Hendey, 1981b and Corvinus, 1983). The well known "Oyster Line" (Merensky, 1927; Haughton, 1931) is found on the Middle Terrace (the D beach at Oranjemund). At Arris Drift, 30 km upstream from the Orange River mouth, highly fossiliferous estuarine Neogene deposits are found at elevations between 27 m and 63 m above sea level (Corvinus and Hendey, 1978). The inference is that the estuarine deposits and those marine terraces at similar elevations are synchronous.

The Lower Terrace (beaches A, B and C) is of Quaternary age and shows the cold-water faunal assemblages found along the coast today, including Donax serra, Patella granularis and Bullia sp. (Hallam, 1964, p.714) and also Burnupena lagenaria, B. limbosa, Cominella sp., Crepidula rugulosa, Helcion pectunulus and Mytilus crenatus (Keyser, 1972).

In Chapter 8 these raised marine terraces will be placed in the context of the distribution of diamonds along the west coast.

1.4.3. Quaternary deposits.

Initial studies of the Quaternary sediments along the west coast were made in the course of prospecting for diamonds. Hoyt et al. (1965a) found that the sediment deposits on the inner continental shelf between the Olifants River and Luderitz are orientated parallel to the shoreline. This has been verified by subsequent studies (Birch and Rogers, 1973; Birch 1975; Rogers, 1977 etc). A prominent, continuous wedge-like body of acoustically transparent mud lies south of the Orange Delta and is about 25 m thick along the inshore edge where it lies against the steepening seaward slope of the inner shelf bedrock and across the inner shelf - middle shelf boundary in water depths between 60 and 90 m (Birch, in prep). Another sediment body north of the delta lies inshore of a series of bedrock ridges just seaward of the surf zone, averages 6 m in thickness and consists of silty sand and shell, with occasional gravels near the base of the sequence. This sequence Hoyt et al. (1965a) consider to represent Pleistocene shoreline deposits.

The geological environment of diamondiferous deposits on the west coast has been described by Murray et al. (1970). From numerous vibrocores they conclude that the typical stratigraphic sequence on the inner shelf fines upward. At the bedrock a layer of gravel and shell, usually 0,5 m thick is followed by about 1 m of a shell horizon with a few pebbles and then 2 m of silty sand with occasional shells. Hoyt et al. (1969) discuss the evolution of the Orange Delta ("lens"), although they do not present a stratigraphic sequence of the deposits forming the delta. They suggest that this sediment body could have been formed since 18000 y. B.P., but calculate an apparent building time of only

530 years. The implication is that most of the sediment that was introduced onto the inner shelf by the Orange River during the Quaternary has been carried away by wave action and longshore drift. A large part of the sand fraction will have been blown inland from the beaches to form the extensive Namib Sand Sea (Rogers, 1977). Finer material will have been carried offshore and then southward by currents on the shelf, thereby forming the extensive terrigenous mudbelt (Fig. 1.12; Rogers, 1977).

O'Shea (1971) presented a detailed description of the inner shelf deposits between the Olifants River and Walvis Bay. From his seismic records he was able to distinguish an "intermediate sediment" layer overlying the Precambrian bedrock and which in turn is covered by "Recent" unconsolidated sediment. The 'intermediate sediment' has subsequently been interpreted (Dingle, 1973a) as Cretaceous-Tertiary deposits. O'Shea (1971) presents the same stratigraphic sequence as Murray et al. (1970) for the unconsolidated sediments.

Regional investigations of parts of the continental margin adjacent to the Cape West Coast were undertaken by Birch (1975) and Rogers (1977). These studies concentrated on the surficial sediments, although aspects of Quaternary sedimentation were discussed, particularly by Rogers. Birch (in prep.) describes sediments of Quaternary age between Cape Town and Baker Bay on the Namibian coast. His contact between the Quaternary and Tertiary deposits is based on the initial stratigraphy by Dingle (1973b). Off the Olifants River Birch (in prep.) places this boundary at the top of the lowermost horizontally stratified unit, although he does not substantiate his interpretation. Two Honours projects (Petersen, 1983 and Price, 1984) detailed the

lithostratigraphy of the top few metres of Quaternary deposits. Both workers could identify six lithofacies based on compositional and textural characteristics of the sediment downcore. The data were obtained from vibrocores drilled by CDM along coast-perpendicular lines 60 km and 70 km north of the Orange River and extending between 64 m and 190 m below sea-level.

Approximately 38% of the Quaternary sediments on the continental shelf is contained in the Orange Delta, with a volume of $44505 \times 10^6 \text{ m}^3$. Off the Olifants and Berg Rivers a further 27% is located (Birch, in prep.). With the exception of a small Pleistocene palaeodelta off the Orange River (Rogers, 1977), there is very little Quaternary sediment on the middle shelf (Dingle, 1973b; Rogers, 1977; Birch, in prep.).

Quaternary strandline oscillations were primarily due to changes in the polar ice-volumes, with isostatic adjustment of the continental margin playing a progressively smaller role (Walcott, 1972; Tankard, 1976). The level to which sea level rose during transgressions in the Quaternary remains in dispute, ranging from between 50 and 60 m (Tankard, 1976) to 6 m (Hendey, 1983). On the other hand, Siesser and Dingle (1981) suggested a late Pliocene-early Pleistocene regression on the west coast to 210 m below sea level. A pre-Holocene regression to -110 m (Hoyt et al., 1965b; O'Shea, 1971; Rogers, 1977 and others) caused the erosion of much of the marine deposits that occur on the raised marine terraces. The Flandrian transgression was accompanied by the development of the Orange Delta and the extensive, acoustically transparent terrigenous mudbelt seaward of the inner-shelf slope (Fig.1.12).

CHAPTER 2BATHYMETRY2.1 Introduction

The following three chapters form a trilogy in which the bathymetry, the buried bedrock-morphology and the structure of exposed bedrock are discussed. Brief mention of the morphology of the continental shelf was made in Chapter 1. This chapter presents a general discussion of the inner shelf from the Orange River to Port Nolloth (100 km farther south), since the various elements that define the inner shelf in general are particularly well developed in this area. This will give perspective to the more anomalous nature of the inner shelf in the study area. The study area is presented in three parts (Fig.1.2):

- a) A delta-dominated inner shelf between the Orange River and Cape Voltas.
- b) A region between Rietfontein and Wreck point that is typical of most of the inner shelf farther southward.
- c) A transitional area between Cape Voltas and Rietfontein.

In subsequent chapters on subbottom bedrock morphology (Chapter 3), bedrock surface structure (Chapter 4) and seismic stratigraphy (Chapter 5) the study area will be discussed also in three parts.

Dingle (1973a, p.346); Birch et al. (1976, p.2) and Rogers (1977, p.12) define the inner shelf off the west coast as the region beside the coast underlain by pre-Mesozoic basement (Fig.1.12). O'Shea (1971, p.14) mentions it only in passing, referring to it as "the rocky inshore area". Birch (1975, p.13)

uses the term "inner shelf" in a general sense, but refers to a "nearshore rocky platform" when subdividing the continental margin into morphological zones.

In this study the inner shelf (Fig.1.8) is defined as the region between the coast and the shoreward edge of a terrigenous mudbelt that is continuous for most of the West Coast and is termed the Orange River mudbelt (Rogers, 1977). Where the mudbelt is absent, for example over the Orange Delta, the 50 m isobath will be used as the boundary, since bedrock forming the relatively steep seaward slope of the inner shelf, hereafter referred to as the "inner-shelf slope", generally dips beneath unconsolidated sediments at that depth (Fig.2.1). This is also the approximate depth of the shoreward side of the Orange prodelta farther north. The area thus differs little from that generally defined as the inner shelf, but by using the edge of the mudbelt the contact is both at the seafloor surface and easily traced on bathymetric maps. This is then a morphological boundary, similar to boundaries outlining the middle and outer continental shelves.

Initial bathymetric maps of the inner shelf in the study area (O'Shea, 1971) were drawn with isobaths at 12,2 m (40 ft) and 30,5 m (100 ft) intervals. A concise description of the bathymetry of the continental margin between the Buffels River ($29^{\circ}45'S$) in the south and Sylvia Hill ($25^{\circ}S$) on the Namibian coast was given by Rogers (1977) who also presented a bathymetric map with 10 m-intervals. Subsequently, Dingle et al. (1977) published a map of the entire South African and Namibian continental shelf, incorporating Rogers' (1977) data for the west coast. The bathymetry of the study area and of the inner shelf

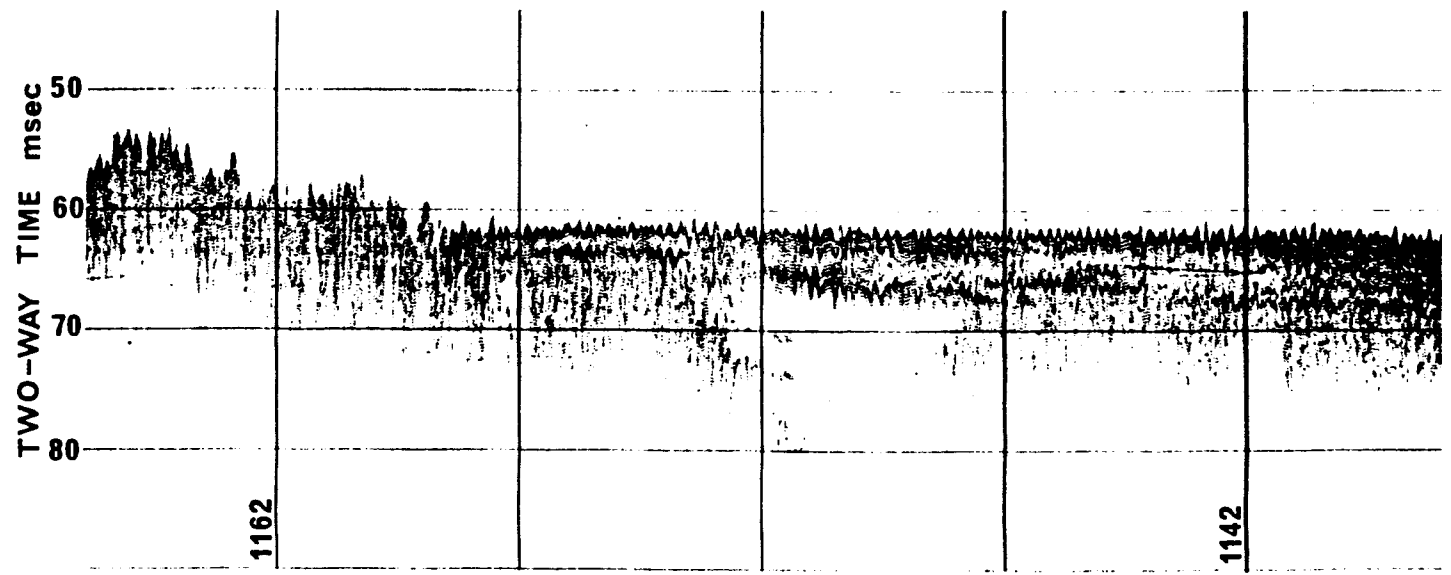
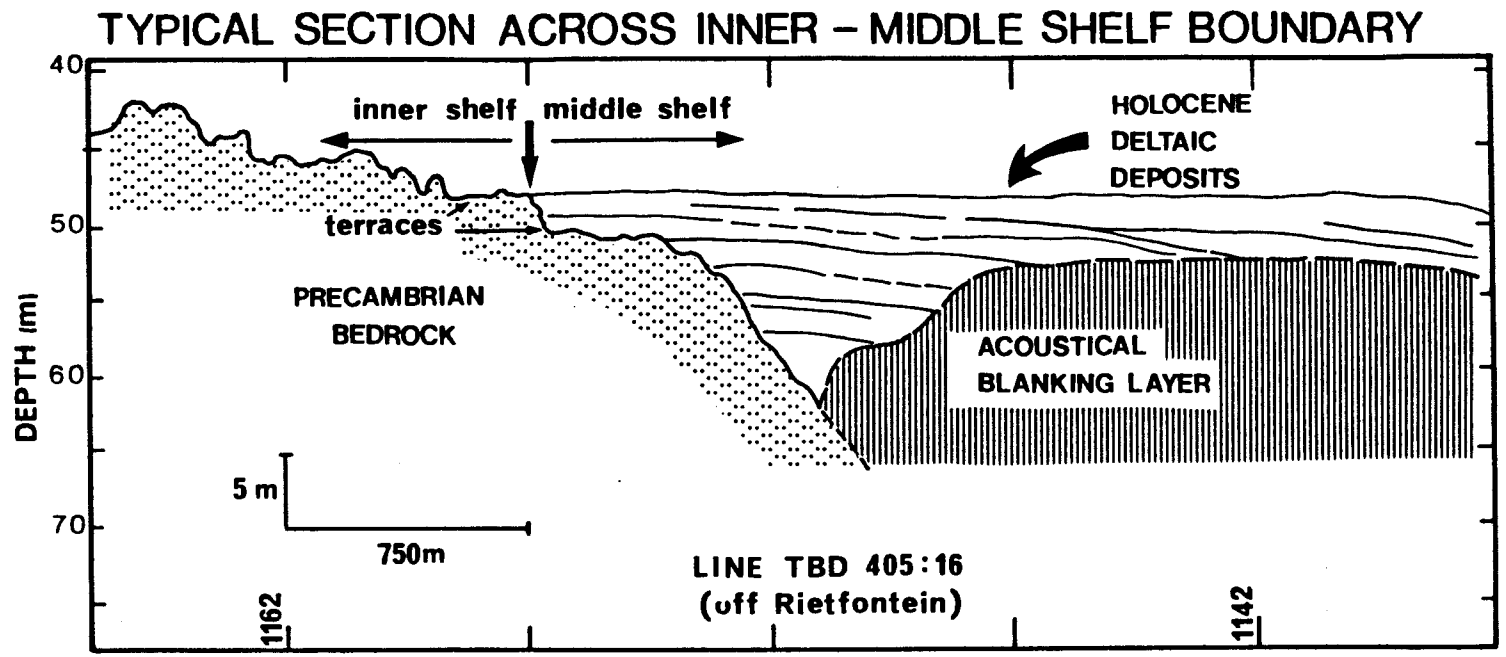


FIGURE 2.1

farther southward to Port Nolloth was contoured at 2 m intervals and discussed by De Decker (1982). The bathymetry maps of the study area, drawn at 1 m-intervals and an original scale of 1:2000, therefore represent the most detailed work on the inner shelf thus far. Coupled with the sonographic interpretation at the same 1:2000 scale, bathymetry becomes a useful tool in identifying areas where diamondiferous deposits are most likely to occur.

2.2 Morphology of the inner shelf between Orange River and Port Nolloth.

The area between the Orange River and Port Nolloth, 100 km farther south, displays the different morphologies of the inner shelf particularly well (Fig.2.2). Rogers (1977) highlighted the changes in the character of the inner shelf and related them to the variation in bedrock lithology.

Southward from Herring Bay the inner shelf is narrow (2-3 km) with no distinct inner shelf break (Fig.2.2). Instead, it slopes smoothly down to -75 m where it dips beneath the overlapping mudbelt (Fig.2.3, section 6). The bedrock forming the inner shelf in this region consists of highly resistant felspathic quartzites, arkoses, conglomerates and minor volcanics of the Stinkfontein Formation (Joubert and Kröner, 1971) (Fig.2.2). These rocks grade into the Holgat Suite (Fig.2.2) at Cliff Point, consisting of schists, greywackes, conglomerates, felspathic quartzites and hornfels (De Villiers and Söhnge, 1959) that are more readily eroded by wave action. Consequently the inner shelf widens to between 5 and 8 km north of Herring Bay (Figs.2.2 and 2.3). From here to Wreck Point, 60 km farther north, the inner

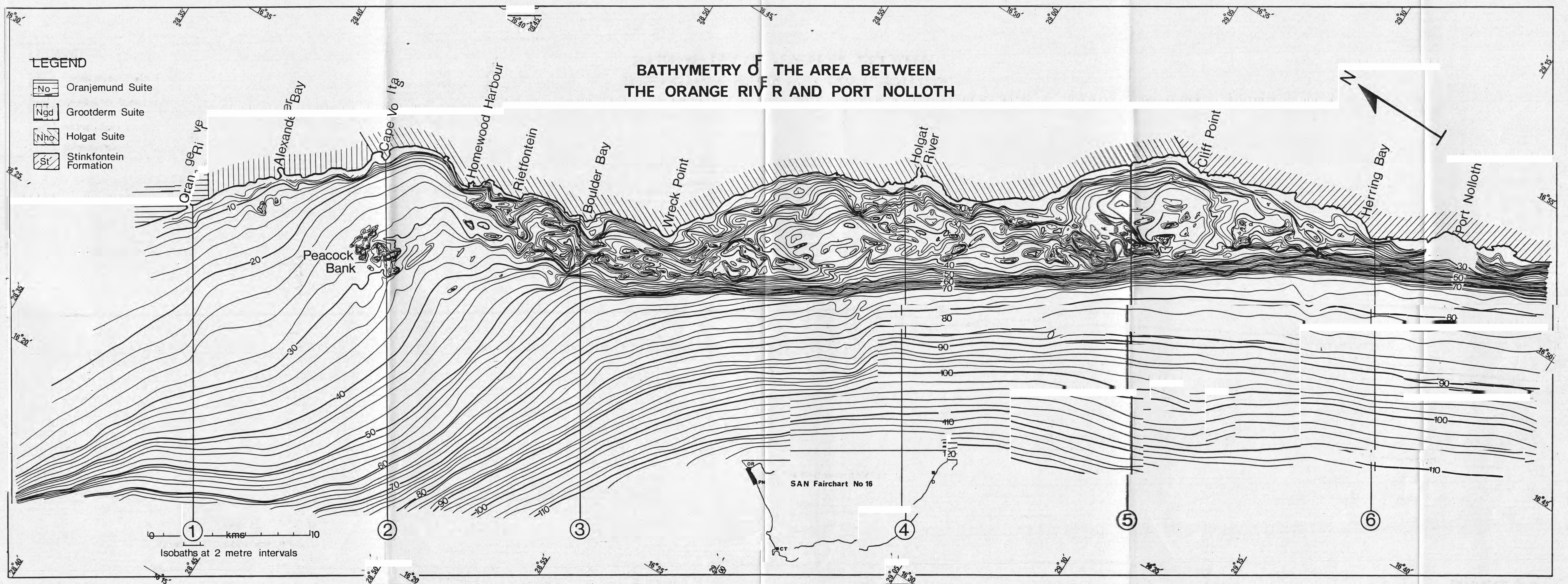


FIGURE 2.2

SECTIONS ACROSS THE INNER SHELF
 BETWEEN ORANGE RIVER AND PORT NOLLOTH
 (cf. Figure 2.2 for positions of section lines.)

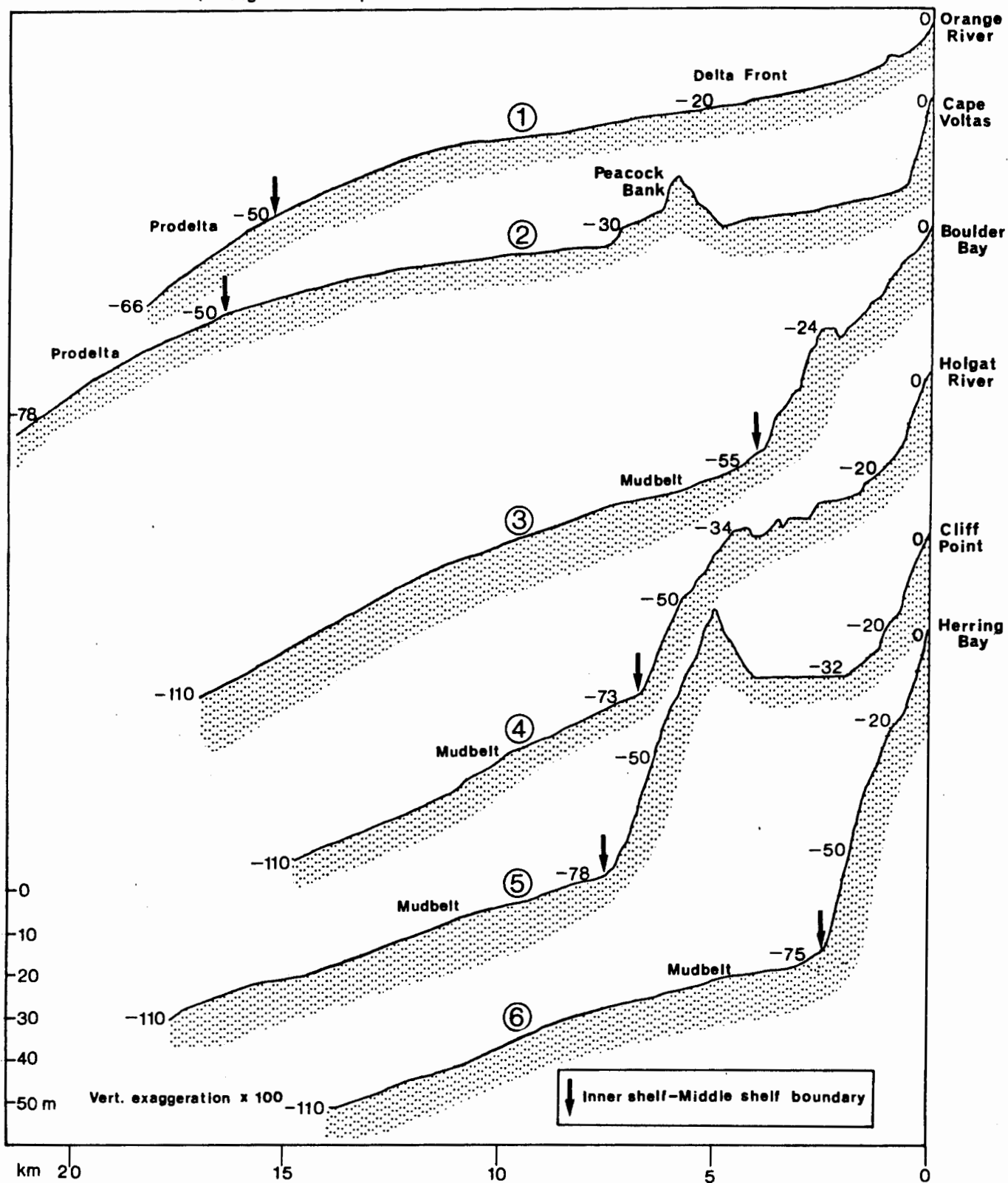


FIGURE 2.3

shelf maintains this width. The bathymetry shows a rugged, undulating inner shelf, bounded on the east by an irregular coastline and on the west by a straight, continuous inner-shelf slope trending between 332°N and 333°N shoreward of the terrigenous mudbelt (Fig.2.2). Northward from Wreck Point the inner shelf becomes increasingly covered by sediment as the seafloor seaward of the inner-shelf slope shoals in the transition from terrigenous mudbelt to prodelta to delta front. Between Homewood Harbour and the Orange River the inner shelf is mostly covered by sediments of the Orange Delta. However, seismic evidence (discussed in Chapter 3) shows that the inner-shelf bedrock north of Homewood Harbour extends over 10 km seaward (cf Maps 3A and B). Here the bedrock is composed of lavas, agglomerates and tuff of the Grootderm Suite and friable schists, phyllites and lavas of the Oranjemund Suite (De Villiers and Sohngé, 1959; Kroner, 1974) (Fig.1.10). Peacock Bank, part of which is interpreted to be granitic (Chapter 4), juts through the deltaic sediments 6 km west of Homewood Harbour.

The shoreface bedrock along the coast slopes down from the shore to about -20 m, usually at an angle of between $1,1^{\circ}$ and $2,0^{\circ}$. Seaward, the seafloor levels out to a gradient of less than $0,5^{\circ}$ to form the major part of the inner shelf between -20 m and -40 m. Several ridges, generally standing 10 to 15 m above the surrounding seafloor, strike due south and cut diagonally across the inner shelf. These ridges separate areas of smoother, gentler topography, identified as sediment-filled embayments (Fig.2.3, section 5). Whereas the 20 m isobath outlines the base of the ridges and extends to the shoreward edge of the embayments, the 40 m isobath is relatively straight, marking the

seaward edge of the inner shelf (Fig 2.2).

Although the Holgat River has not contributed any sediments to the inner shelf in recent memory - it last flowed in 1925 (Keyser, 1972) - its incised course across the coastal plain shows it to have been an active river during the Quaternary. This previous fluvial activity is substantiated by O'Shea (1971, map 3) who shows a wedge of sediment less than 6 m thick extending from the Holgat River mouth, whereas Fig.2.2 shows a deflection of the isobaths between -40 m and -50 m, suggesting the existence of a channel. However, the continuation of the channel towards the river mouth is not clear from the bathymetry alone. It is probable though that with sea-level receding as much as 200 m during the Quaternary (Siesser and Dingle, 1981), the river would have cut a channel across the inner shelf. In comparison, the Orange River has two palaeo-channels buried beneath deltaic sediments extending to -63 m and -85 m respectively (O'Shea, 1971) and are thought by Hoyt et al. (1969) to have been formed during regressions in the Late Pleistocene.

The inner-shelf slope extends, with a slight curvature, for over 230 km northwestward, from the Olifants River to Wreck Point (Fig.1.8) (Dingle et al., 1977, Rogers, 1977). It then swings north and disappears beneath the deltaic sediments of the Orange River at Homewood Harbour (Fig.2.2). The gradient of the inner shelf-slope, between the 40 m and 70 m isobaths, varies from $1,1^{\circ}$ to $1,9^{\circ}$ (Fig.2.3, sections 3 to 6). Between Wreck Point and Homewood Harbour the inner-shelf slope is dissected by several sediment-filled channels that cut across the inner shelf from north-east to southwest.

In contrast to the gradient of the inner-shelf slope, the

average gradient seaward of the slope is $0,25^{\circ}$ over the terrigenous mudbelt (Fig.2.3, sections 3 to 6). The gradient decreases even further on the middle shelf seaward of the -120 m isobath and the mudbelt (Fig.1.8).

Figure 1.8 shows the regional extent of the Orange Delta. It influences the bathymetry of the area for over 100 km, extending 30 km southward to Wreck Point and northward for almost 80 km (Hoyt et al., 1969; Rogers, 1977). On the inner shelf in the study area however, it affects the isobaths only as far south as Homewood Harbour (Fig.2.2). Cross-sections drawn from the Orange River mouth and Cape Voltas (Fig.2.3, sections 1 and 2) show the convex outline of the delta. Hoyt et al. (1969) estimate the width of the delta opposite the river mouth to be 25km, with a maximum thickness of more than 60 m. To the south the muds of the Orange prodelta abut against the inner-shelf slope between Homewood Harbour and Wreck Point, and increase in depth with an average gradient of $0,09^{\circ}$ from -40 m to -60 m in the same direction (Maps 3B and C). However, the deltaic sediments in this area do not cover the inner shelf itself. The toe of the prodelta lies at approximately -70 m slightly south of Wreck Point and continues south in the form of the terrigenous mudbelt. Seaward, the prodelta edge dips at $0,1^{\circ}$ to a maximum depth of about -120 m (Rogers, 1977) forming a broad arc that outlines the Holocene deltaic deposits.

2.3 Seafloor morphology of the study area.

The bathymetric maps presented here at 1:60 000 scale (Maps 3A, B and C), combine data obtained from seismic records with a sonographic interpretation distinguishing exposed bedrock from

sediment-covered areas.

The seismic profiler and side-scan sonar reveal the nature of the bedrock in section and plan respectively (cf. Appendix). The high-resolution, 3,5kHz seismic records allow accurate depth measurements of both the seafloor and the sub-bottom, thereby outlining all features in section. However, interpolation between traverses, particularly over rugged topography, is difficult. Sonographs allow one, inter alia, to delineate bedrock outcrops and sediment-covered areas. Combined, the two interpretations supplement each other, by giving substance to the isobaths and dimensions to the seafloor features.

The bathymetry, drawn at 1 m-isobath intervals, covers the area between the breaker zone and the seaward limit of the coast-parallel survey lines. Fence diagrams are drawn from the tielines that extend seaward across the outer edge of the inner-shelf slope. The sea-surface lines of the fence diagrams represent the ship's track-lines.

Where place names are first introduced, they are underlined and their location shown on Maps 3A,B and C. Whereas most of the names used appear on previously published topographic maps, orthophotomaps, etc., I have created a few new place-names to guide the reader through the diverse topography of the study area.

2.3.1. Orange River to Cape Voltas: (Map 3A)

The principal features in this area are the subdued seafloor north of Alexander Bay, the rugged shoreface bedrock outcrop that is in places interrupted by sediment-filled embayments, and the influence of the Orange Delta on the bathymetry. The isobaths off the Orange River mouth indicate a seafloor gradient of $0,16^\circ$

(1:350) seaward of the -11 m isobath (Fig.2.4A). From the surf zone to the 11 m isobath the gradient increases to 1,05° (1:55). The fence diagram (Map 3A), shows that farther seaward the delta front has an even gentler gradient (1:1000). It reaches a depth, approximately 9 km offshore, of just over -20 m off the Orange River and -25 m off Cape Voltas.

The shoreface outcrop consisting of Grootderm Suite lithologies (Fig.1.10), first appears as the seaward extension of the southern bank of the Orange River floodplain (Map 3A). It forms a broad reef extending up to 1 km offshore and has a very indented contact with the sediment at about -12 m, indicating the presence of many sediment-filled gullies. Several ridges, 10 to 60 m wide and about 150 m long, extend from the reef, rising a few metres above the sediment.

Tripp Shoal consists of two isolated bedrock outcrops, 1 km apart and about 2 km from the coast directly west of Alexander Bay. The bedrock probably belongs to the Grootderm Suite, as the contact onshore lies slightly north of Tripp Shoal. The northern outcrop rises to -12 m, from -15 m on the shoreward side and from -17 m on the seaward side. The other, more pronounced peak rises to 8 m below sea level, standing between 7 m and 9 m above the surrounding sediment. Both outcrops are elongated northeast-southwest, the northern one being the larger of the two (0,50 km² and 0,32 km²). The sediment-bedrock contact along the northern edges is quite linear, whereas several sediment-filled channels extend up to 100 m into the southern and western sides of the outcrops. Another isolated outcrop, approximately 2 km south of Tripp Shoal, rises to -16 m from the surrounding sediment at 20 m below sea level. The fence diagram in Map 3A shows bedrock

SECTIONS ACROSS THE INNER SHELF
BETWEEN ORANGE RIVER AND WRECK POINT
(cf. Maps 3,4 and 6 for positions of sections)

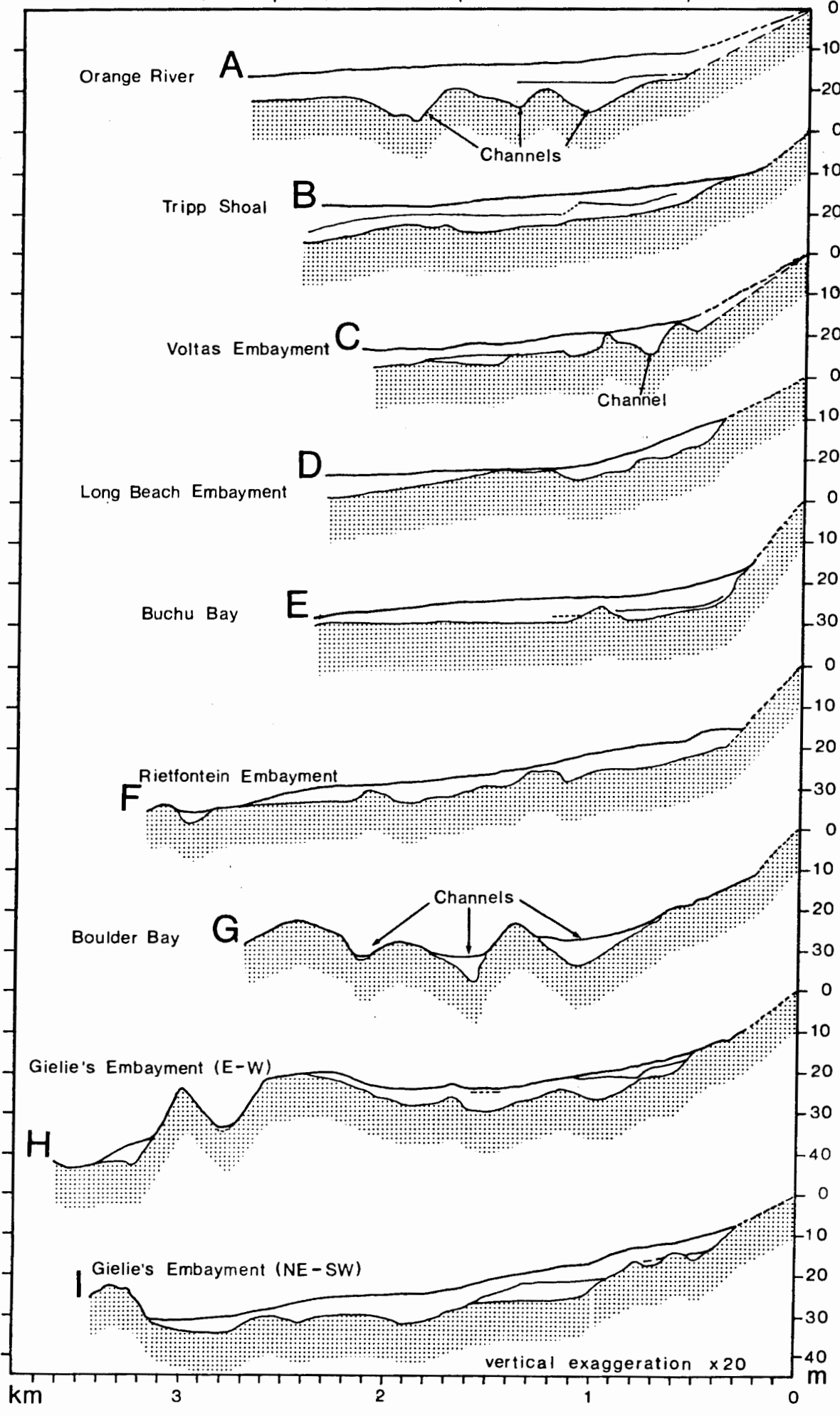


FIGURE 2.4

apparently cropping out at the inshore end of Line 32. This would indicate that the outcrop continues beyond the shore-parallel survey lines for at least another kilometre, giving it a typical northeast-southwest trend.

The shoreface outcrop north of Alexander Bay is rugged, although large areas of the bedrock have a thin sediment veneer. On the seaward side bedrock dips beneath the sediment at -11 m to -13 m, the contact being 400 m from the coast (Map 3A and Fig.2.4B).

Three sediment-filled embayments cross the shoreface outcrop area between Alexander Bay and Cape Voltas, linking the offshore sediments with the beach (Map 3A). Isobaths over the bedrock outcrop area show a decrease in gradient between -8 and -12 m (Fig.2.4B), suggesting some planation at this depth. Bedrock below -10 m has a gradient of about $1,0^{\circ}$, increasing in depth to between 17 m and 20 m below sea level before disappearing beneath the onlapping sediment. Several large sediment-filled channels extend into the shoreface bedrock, thus creating a highly indented seaward boundary between the bedrock outcrop and the sediment.

Alexander Bay itself is a distinctive, elongate coastal re-entrant measuring 200 m wide by 600 m long, with a sediment-filled embayment extending seaward to the edge of the shoreface outcrop. Versuipgat Embayment is similar to Alexander Bay, in that it is parallel-sided and aligned towards the east-northeast; it is about 300 m wide and 1000 m long. Voltas Embayment narrows rapidly from slightly over 1.5 km wide at the seaward side, to a sediment-filled channel that connects the embayment with the beach (Map 3A). North of Voltas Embayment prominent channels, up

to 200 m wide, cut shoreward across the shoreface outcrop, giving rise seaward to a highly irregular bedrock-sediment contact at -17 m to -20 m (Map3A). Isolated outcrops seaward of the shoreface outcrop indicate that the sediment adjacent to the contact covers the rock with a thin veneer.

The sediment-bedrock contact in Voltas Embayment is very irregular. The southern edge in particular has a highly indented outline, accentuated by a prominent ridge extending northwestward, at about 20 m below sea level.

At Cape Voltas, bedrock lies exposed along the shoreface for approximately 2 km and extends offshore for 1 km, at which point it is covered by a thin veneer of sediment (Map 3B). Along the northern edge, however, Voltas Reef continues farther seaward for 1 km, extending beyond the limits of the coast-parallel survey lines. The reef has an average width of 400 m and trends southwestward, although its outline is quite irregular. Voltas Reef rises to -19 m from the sediment contact at about -22 m.

2.3.2. Cape Voltas to Rietfontein (Map 3B)

From Cape Voltas southwards to Homewood Harbour the orientation of the coastline changes to form the wide northwest-facing Buchu Bay (Map 3B). Bedrock lithology changes from the volcanic schists and tuffs of the Grootderm Suite to the more resistant quartzites and greywackes and conglomerates of the Holgat Suite. This northern part of the middle section of the study area is mostly sediment covered, whereas the seafloor from Homewood Harbour southwards to Rietfontein is mainly bedrock outcrop.

Voltas Reef defines the northern boundary of Long Beach

Embayment. The embayment deepens quickly from the coast to -20 m, then slopes at $0,42^{\circ}$ to a depth of -25 m at the edge of the survey area (Map 3B). Agate Reef rises 5 m above its surroundings to -19 m to form the southern boundary of the embayment. The reef reaches seaward for about 2 km, is 400 m wide and has a 300 m wide arm extending north towards Long Beach (Map 3B). The bedrock-sediment contact along the northern and southern edges of Long Beach Embayment are characterised by several subdued ridges that extend into the embayment, measuring between 150 and 300 m in length and 50 to 100 m in width. A particularly prominent 50 m-wide ridge lies at -20 m, trends to the northwest and continues for over 500 m (Map 3B).

Agate Embayment (Map 3B) is divided by Lone Ridge, a subdued ridge between 10 m and 18 m below sea level that runs from the beach southwestward for 600 m. A thinly sediment-covered, rectangular, bedrock outcrop at -20 m to -22 m, lies between Lone Ridge and Agate Reef. The subdued relief and sub-horizontal slope that persists for about 500 m suggest that this could be a wave-cut terrace; it is separated from Agate Reef by a 100 m wide sediment-filled channel.

The seafloor in Agate Embayment grades evenly with a slope of about $0,7^{\circ}$ to -24 m before levelling off farther seaward. Another terraced area is found south of the embayment off Agate Bay. The planated, square-shaped surface of the terrace is outlined by the -18 m isobath and has a surface-area of about 0.2 km^2 (Map 3B). Shoreward of this terrace the gradient steepens markedly to the beach. On both the northern and southern side of the terrace, broad sediment-filled channels extend towards Agate Bay. The terrace therefore forms a broad promontory jutting out

towards the southwest into the surrounding sediment (Map 3B).

The sediment cover in Buchu Bay is reflected in the smooth subparallel isobaths that grade at about $0,8^{\circ}$ from -16 m inshore to -23 m in the middle of the bay (Fig.2.4E). The seafloor slope decreases farther offshore (Map 3B). At Peacock Bay the sediment encroaches in a large tongue towards the mouth of the bay. From Cape Voltas to Agate Bay the seaward edge of the shoreface outcrop lies at a fairly constant depth of -22 m, but in Buchu Bay the bedrock-sediment contact is found at -16 m.

Peacock Bank, 6 km from the coast and directly west of Peacock Bay, consists of a northern part with peaks at -20 m, trending east-west, and a southern portion that runs north-south, rising to -16 m (Fig.2.5). On its northern side the seafloor at the bedrock-sediment contact lies at -27 m, increasing 4 km farther south to -34 m; shoreward the depth remains at about 30 m below sea level. The fence diagram (Map 3B) shows an undulating topography over Peacock Bank, with the channels and depressions generally filled with sediment. A north-south trending channel divides that part of Peacock Bank covered by sonographs into two parts (Fig.1.2 and Map 5B). The eastern half has a rugged topography, contrasting with the subdued topography of the western half and inferring a lithological change.

From Homewood Harbour to Collins Reef, the coastline is fringed by bedrock that quickly gives way to the sediment-filled Collins Embayment. The embayment continues for about 1 km towards Collins Reef, narrowing eastward to 500 m. Collins Reef extends westwards for almost 2 km, increasing in depth from the sea surface to -17 m at its seaward limit; the -10 m isobath outlines an area of almost $0,65 \text{ km}^2$.

BATHYMETRY OF PEACOCK BANK

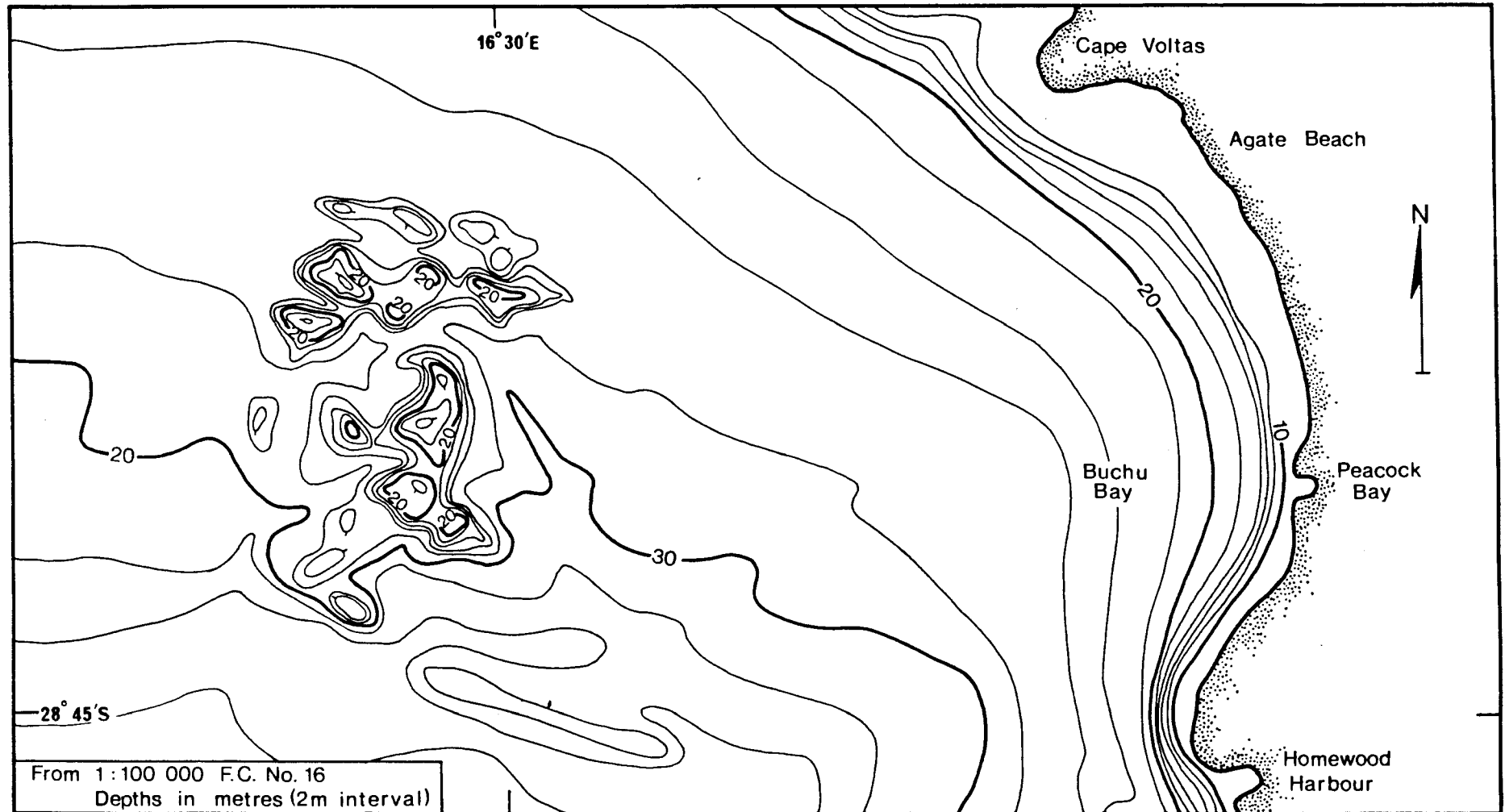


FIGURE 2.5

The inner shelf between Collins Reef and Rietfontein Embayment is formed by a rugged, exposed bedrock area that extends for almost 3 km seaward, lying between -10 and -20 m. The numerous channels that cut across this region contain little sediment and the water depth in them varies from approximately -15 m to -25 m. The seaward boundary of this shallow bedrock outcrop terrain is well defined, runs north-south and increases from -20 m, with a slope of between 1.4° and 2.0° , to -30 m, about 400 m farther west (Map 3B). The seafloor then levels off, continuing seaward for over 5 km to form a broad, dissected terrace between -30 and -40 m to the shoreward edge of the terrigenous mudbelt (Map 3B, Line 19). Kloppers Reef 1,5 km west of Collins Reef rises from this terrace to -22 m. It runs due south, curving slightly east to eventually merge with the seaward edge of the shoreface bedrock outcrop off Rietfontein Embayment. A 50 to 75 m wide sediment-filled channel cuts southward along the shoreward edge of the -30 m terrace (Map 3B).

Sediment-filled channels on either side of Kloppers Reef (cf Fig.1.2) narrow southward to a width of about 50 m, although they range over a distance of several hundred metres.

2.3.3. Rietfontein to Wreck Point (Map 3C)

This section of the study area is representative of most of the inner shelf southward. The seafloor between Rietfontein and Wreck Point is generally underlain by exposed bedrock. The two sediment-filled embayments crossing the inner shelf are almost entirely encircled by exposed bedrock, allowing sediment continuity seaward to the terrigenous mudbelt only through pronounced channels.

Rietfontein Embayment extends 2 km seaward, the seafloor sloping at $0,5^{\circ}$ from -12 m to -29 m (Fig.2.4F). The northern boundary is formed by a ridge rising to -10 m, with several sediment-filled channels cutting through it. The sediment in the embayment abuts, 1,2 km farther southward, against the steeply dipping ($1,3^{\circ}$ to $3,1^{\circ}$) shoreface bedrock outcrop (Fig.2.4F). The bedrock-sediment contact here is not as indented as along the northern edge, and for the most part remains at -20 m (Map 3C).

On its seaward side the embayment ends against a series of parallel ridges that trend southward (Map 3C). These ridges rise to between 20 and 25 m below sea level and are separated by relatively straight and narrow channels that extend for several kilometres out to the edge of the inner shelf (Map 3C and Fig.1.2). The sides of the channels are steeply dipping, usually exceeding $5,0^{\circ}$ (Fig.2.4G and H). The channel floor, where it opens into the embayment, lies at about -29 m. The seaward exit from the embayment is through a broad channel 300 m to 400 m wide. The water depth increases from -30 m at the entrance to the embayment to -38 m at the edge of the surveyed area (Map 3C). Northwestward the ridges die out within the embayment, usually in a series of smaller isolated outcrops (Map 3C).

From Rietfontein Embayment the channels continue along the northern side of Boulder Reef, which itself extends southwestward for over 1,2 km. The -10 m isobath on Boulder Reef outlines an area of about 1 km^2 . Seaward of the reef the seafloor descends rapidly to -28 m, levelling off at this depth to form a terrace 200 m wide in places (Map 3C). The bedrock then increases in depth to -41 m, to form one of the extensive north-south trending channels. A side channel trends shoreward to end abruptly at -

22 m against the steeply dipping shoreface bedrock. The main channel continues northward, narrowing to 50 m in width and shoaling progressively from -32 m to -27 m where it debouches into Rietfontein Embayment (Map 3C).

Gielie's Embayment descends from -12 m to -25 m (Fig. 2.4I). As with Rietfontein Embayment, a series of ridges and channels mark the seaward boundary, 2.5 km from the coast, of this southwestward-trending embayment (Map 3C). The bedrock-sediment contact along the northern edge of the embayment lies at about -20 m (Map 3C). The shoreface bedrock between Gielie's Bay and Wreck Point extends 500 m offshore before being covered by sediment; the contact lies between -13 m and -22 m and trends almost due south.

The ridges marking the seaward edge of the embayment are not as pronounced as those off Rietfontein. A very subdued ridge protrudes for over 2 km into the embayment (Map 3C). A wide terrace at its southern end at -23 to -24 m divides the ridge into two parts. The northern part has little topography and lies between -25 and -27 m. In the south the ridge rises to -22 m. A 300 m wide sediment-filled channel runs along the seaward side of the ridge, the waterdepth ranging from -32 m to -36 m at the inner-shelf slope. The channel has a steep seaward side that rises to form a reef with a crest at -28 m. The embayment opens westward onto the shelf-edge via a 600 m wide sediment-filled channel (Map 3C).

The inner-shelf slope is generally formed by exposed bedrock (Map 3C). Between Rietfontein and Wreck Point the seaward boundary of the inner shelf lies between -30 and -35 m. Farther seaward the inner-shelf slope dips at approximately $4,5^{\circ}$ to

between -40 and -45 m, after which the gradient decreases up to the shoreward edge of the terrigenous mudbelt. The mudbelt has a seaward gradient of $0,15^{\circ}$. The contact between the inner-shelf slope and the mudbelt is very regular and forms the inner shelf-middle shelf boundary (Fig.1.2). The depth of this boundary increases southwards from -50 m off Rietfontein to -65 m west of Wreck Point (Map 3C). Off Wreck Point the shelf-slope gradient ($1,3^{\circ}$) is continuous, with some evidence of a lower gradient at -40 m (Map 3C, Line 26F). The tielines off Rietfontein show that the inner-shelf slope has below average gradients at -35 m (Line 17) and -45 m (Lines 16,17 and 18). Lines 26A to F show lower than average gradients at -40 m, -45 m, -50 m, -55 m, and -60 m.

2.4 Discussion.

Hallam (1964), Keyser (1972) and Gurney et al.(1982) show from work on the raised terraces and in the surf zone that diamondiferous deposits are more likely to occur in the following localities: along the base of a wave-cut cliff, within gullies and potholes eroded into terraces, on the southern side of reefs that trend northeastward and the northern side of south-facing bays and also along palaeo-channels scoured by fluvial action. Exploration of the inner shelf for diamonds can thus be facilitated by recognizing these features in the bathymetry.

Off the Orange River and south to Homewood Harbour the bedrock outcrops are found along the shoreface, seldom extending beyond 1 km seaward. Isolated outcrops are indeed found farther offshore, such as Tripp Shoal at Alexander Bay and Peacock Bank, 6 km west of Peacock Bay, but they are limited in extent.

Generally, the bedrock topography in the northern part is not very rugged (i.e. micro-topographic differences are less than 5 m) and is characterised by an average dip of $1,4^{\circ}$ from the shoreline to where it disappears beneath the sediment at approximately -20 m. Maps 3B and C and the cross-sections (Figs. 2.3 and 2.4) show that the largest part of the inner shelf lies between the 20 m and 30 m isobaths. This is a recurring depth for sea-level transgressions in the Late Quaternary (Barwis and Tankard, 1983). Flemming (1976a) reasons that at -20 m wave abrasion would be effective to -35 m and cites evidence from Rocky Bank at the mouth of False Bay south of Cape Town. The inner shelf could therefore be the erosional expression of a sea-level stand at -20 m.

Abrupt and distinct changes in the general gradient of the bedrock in a particular area (nick-points in seafloor sections) may be indicative of wave erosion during periods of lower sea-level stands in the Cainozoic (Dietz, 1964; Flemming, 1965 and Flemming, 1976a). Nick-points in the bedrock are commonly found at -10 m, the gradient being less than the average down to -13 m. Both Collins Reef and Boulder Bay have large areas that lie at about -10 m (Map 3B and C), whereas the ridges of Tripp Shoal rise to -12 m and -8 m respectively. The bedrock gradient from the shore to the 10 m isobath is invariably steeper than between that depth and -13 m. Another evident nick-point is found at about -16 m. Terraces lying between -16 m and -19 m are well developed west of Cape Voltas and Agate Bay, whereas the crests of Voltas and Agate Reefs rise to between 18 and 19 m below sea level, standing up to 5 metres above the surrounding seafloor. Regionally, within the study area this depth interval also has a

lower than average gradient. Similar gradient changes are found at greater depths, but they are generally covered by sediment and will be discussed in the next chapter.

Murray et al. (1970) and O'Shea (1971) give no evidence of wave-cut erosion features at depths shallower than -20 m. They do, however, refer to a prominent cliff with its base cut at -18 to -20 m, which Murray et al. (1970) were able to trace for 550 km between Kerbehuk (just north of the Orange River) and Conception Bay (south of Walvis Bay), along the Namibian coast. The cliff varies in height between 1,5 m and 5 m and a distinct wave-cut nick-point is usually found at its base. O'Shea (1971) found evidence for this cliff slightly north of the Orange River, although he found the cliff to be extremely dissected by gullies. In the study area bedrock exposures below -20 m are not commonly found, but evidence for a steepening of the bedrock gradient at approximately -20 m is particularly well displayed on the exposed shoreface area between Collins Reef and Rietfontein (Map 3B). The depth of the sediment-bedrock contact, which often lies at -20 m, may be another indication of a possible sudden increase in bedrock slope. The subbottom bedrock morphology will be discussed in the following chapter, when further evidence for possible wave-cut features in the bedrock will be produced.

Erosional features at depths shallower than -20 m could have formed since the time sea-level reached its present level about 6500 y B.P. (Flemming, 1977). The possibility of a previous sea-level stand at this datum cannot however be discarded. Milliman and Emery (1968) and Curray (1965) suggest a sea-level at approximately the present-day position between 35 000 to 30 000 y B.P., and Barwis and Tankard (1983) quote evidence for a

stillstand at this level 120 000 to 130 000 y B.P.

2.5 Conclusions

On a regional scale, the bathymetry between the Orange River and Port Nolloth (Figs.2.2 and 2.3) shows four geomorphic areas between the shoreline and the 120 m isobath (De Decker, 1982):

1. The submerged Orange Delta.
2. A rugged inner shelf, well developed south of Homewood Harbour and extending to -40 m.
3. The inner-shelf slope, lying between the 40 m and 70 m isobaths.
- 4) The smooth, gently sloping zone from -50 m to -120 m, underlain mainly by the terrigenous muds from the Orange River and the Orange prodelta.

Within the study area these four zones are represented to a greater or lesser degree. Deltaic sedimentation influences the bathymetry as far south as Wreck Point (Fig.2.2). Inshore, however, the effect on the bathymetry extends southwards only to Homewood Harbour (Maps 3A, B and C). Southward from Homewood Harbour the inner shelf is well developed, forming a rugged, relatively sediment-free area between the coast and -20 m, with another terraced area between -30 m and -35 m and extending more than 2 km offshore. The study area can therefore be divided into a relatively sediment-covered northern half and a southern half that is mostly underlain by exposed bedrock (cf. Fig.1.2).

The inner-shelf slope north of Wreck Point is not as pronounced as the slope found farther southward (Fig.2.2 and 2.3; Woodborne, 1985). At Wreck Point the bedrock dips down evenly and steeply ($1,3^{\circ}$) for about 1.5 km from -30 m to where it

disappears beneath the sediment at about- 62 m. Off Homewood Harbour the inner shelf has broadened to over 6 km with no distinct, exposed inner-shelf slope (cf Lines 15 and 19, Map3B). The bedrock at this point dips beneath the offshore sediments at -40 m. Northward the width of the inner shelf therefore increases, the gradient of the inner-shelf slope decreases and the depth at which the Orange River mudbelt laps onto the bedrock decreases.

CHAPTER 3SUBBOTTOM BEDROCK-MORPHOLOGY3.1 Introduction

In the sections below, those portions of the inner shelf underlain by Precambrian bedrock and covered by unconsolidated sediment are described. It is therefore essentially a discussion on the morphology of the sediment-filled embayments that cross the shoreface bedrock, the channels that extend from the embayments and cross the inner shelf, and that part of the inner-shelf slope covered by the Orange Delta and its terrigenous mudbelt. Areas of the seafloor that exhibit exposed bedrock have been discussed in the previous chapter on bathymetry and are therefore excluded here. The discussion builds on the previous one and incorporates data from exposed bedrock areas as well.

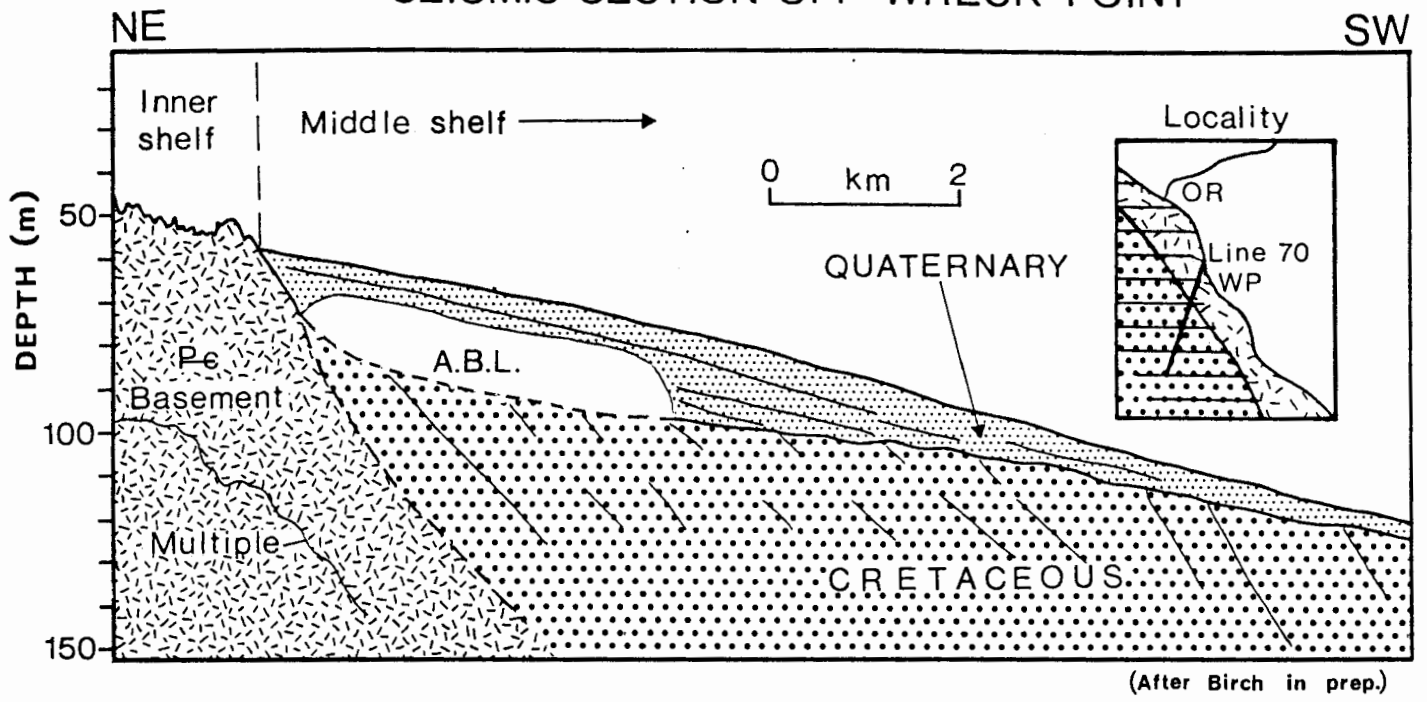
Without the second dimension from sonographs to assist in the interpretation of seismic profiles, the interpretation of subbottom bedrock areas will be less refined and reveal fewer subtleties in bedrock character. Nevertheless, the same morphological features considered in the previous chapter to be essential in locating diamondiferous deposits, need to be recognized in the bedrock isobaths beneath sediment-covered areas.

To facilitate meaningful conclusions to be drawn from the descriptions of the bedrock morphology, analogies for features interpreted from the seismic records are found onshore. The raised marine terraces, exposed through mining activities (cf Plate 4.4A and B; Hallam, 1964, Plates I and IV; Keyser, 1972, Plates II and VIII), allow a visualisation of the processes that

must have operated to form them. This permits a greater degree of confidence in the interpretation of the relatively low-resolution seismic records from the inner shelf.

The 3.5kHz pinger sub-bottom profiler used for the study has too high a frequency to penetrate lithified material and pebble horizons. "Acoustic basement" is therefore the deepest reflector recorded at a position, unless an internal horizon is so indurated or comprises pebbles, cobbles and boulders that further penetration is prevented. The sediment cover on the inner shelf reaches a maximum thickness of only 10 m (cf. Chapter 5) so that "acoustic basement" usually represents the bedrock reflector. On the inner shelf the bedrock reflector can be traced seaward to where it dips beneath the terrigenous mudbelt, which is to a large extent impervious to seismic pulses because of an Acoustical Blanking Layer (ABL) (Fig.3.1). O'Shea (1971, p21) remarks that "... the ABL represents a sediment with a high gas content and which would therefore tend to strongly reflect acoustic pulses and thereby screen details of the underlying sediments." (In fact, the gas would attenuate and scatter the seismic pulses, resulting in loss of signal (Whelan et al., 1977)). The bedrock reflector cannot therefore be traced below the ABL. O'Shea (1971, p.21) suggests that the gas, identified from drilling activities to be sulphurous, "...probably generated by decaying organic matter which could be expected to be plentiful in the biologically productive waters." The extent of the ABL off the study area and southward to beyond the Buffels River (Fig.1.12) is shown by Rogers (1977 , figs.VII-7 and 8). Details of the seismic system used, the method of recording and the resolution achieved are given in the Appendix.

SEISMIC SECTION OFF WRECK POINT



3.2 Orange River to Cape Voltas. (Map 4A)

Except for a shallow depression parallel to the shore, bedrock off the Orange River is very subdued, grading gently at $0,18^{\circ}$ down from -18 m inshore to -25 m, 2.5 km offshore (Map 4A). Bedrock lithology here comprises the phyllites, schists and quartzites of the Oranjemund Suite (De Villiers and Söhnge, 1959).

At the southern edge of the Orange River floodplain the nature of the subbottom bedrock changes abruptly. Two prominent channels are cut into the bedrock to a depth of between -25 m and -28 m (Fig.2.4A). The northern channel, cut into the Oranjemund Suite, runs due south for approximately 1.9 km, before making a right turn to the west, continuing for another 700 m (Map 4A). The channel is approximately 300 m wide at the -20 m isobath, which defines the top of the western side, but the channel-floor at -26 m is less than 100 m wide. Although shown to die out on both the seaward and landward edges, the channel probably continues, at least seaward. The other channel, bisecting Tripp Shoal at right angles to the coast, is about 75 m wide, lies at -24 to -26 m, and appears to open onto the -25 m terrace that extends farther offshore (Map 4A). The channel shallows rapidly shoreward of the shoal and is split by a pronounced pinnacle, rising 8 m above the surroundings (Map 4A). The southern branch seems to extend to the coast slightly north of Alexander Bay. The other branch extends to the north and dies out at -13 m against the shoreface bedrock. Tripp Shoal has a ridge extending from it northwards towards the coast, rising to 15 m below sea level and joining the shoal with the shoreface bedrock. These channels were cut into the Grootderm Suite.

In contrast to the rugged topography of the exposed bedrock between the shore and 20 m isobath (described in the previous chapter), the bedrock from Alexander Bay to Cape Voltas deeper than -21 m has a subdued, subhorizontal surface, lying at an average depth of -24 m (Fig.2.4A to D). Channels have however been cut into this subdued surface, reaching up to 28 m below sea level on the seaward edge of the shore-parallel survey area (Map 4A). Prominent channels between 50 m and 100 m wide are found in the embayments at Alexander Bay and Versuipgat, cut about 5 m deep into the bedrock to at least -20 m. In Voltas Embayment (Map 4A) a shallow channel extends westward along the southern edge of the embayment, reaching -28 m on the seaward side. The meandering aspect of the channels cutting the shoreface bedrock would indicate that these may have developed as river-courses during sea-level regressions in the Quaternary, when sea-level receded as much as 200 m (Siesser and Dingle, 1981).

Lines 31, 32, 33 and 34 (Map 4A and 4B and Fig.5.2), extending to the seaward edge of the inner shelf, have subhorizontal bedrock surfaces at -25 m, -30 m and a very broad undulating region at -40 m. Bedrock grades from $1,14^{\circ}$ to $1,9^{\circ}$ between these terraces, whereas the terraces slope seaward at about $0,15^{\circ}$. The -40 m terrace is the broadest and reaches a width of 1.5 km along Line 31 (Fig.5.2). Line 33, running perpendicular to the coastline, shows that the -30 m terrace is 600 m wide in this region; it is not seen on Line 31, and only partly on Line 32. The shoreward edge of the -30 m terrace lies 3.0 km offshore, whereas that of the -40 m terrace lies 4.5 km from the coast. The possibility that these terraces are wave-cut features will be investigated in the discussion section of this chapter.

3.3 Cape Voltas to Rietfontein. (Map 4B)

The morphological pattern established south of Alexander Bay continues through this area to Homewood Harbour, although the lithology changes at Cape Voltas from volcanic schists of the Grootderm Suite to quartzitic schists of the Holgat Suite (Map 4B). In general the shoreface bedrock is rugged, whereas seaward it is characterised by more subdued and subhorizontal topography (Fig. 2.4D and E).

The sediment embayments off Long Beach, Agate Beach and Homewood Harbour display similar, stepped bedrock floors. Long Beach Embayment (Fig. 2.4D) has a sloping floor with nick points (where the slope of the bedrock flattens appreciably seawards) between -17 m and -27 m. The changes in the bedrock slope occur at -18 m, -20 m and -24 m. The sides of the embayment, and the bedrock along the shoreface dip down quickly to -17 m from a depth of -10 m. South of Voltas Reef the bedrock has a level surface with no channels cut into it. The area defines a broad terrace at -24 m, measuring 800 x 400 m. Seaward of the terrace, the bedrock surface deepens steadily to -30 m before levelling off, remaining at about that depth until it rises to form Peacock Bank, 3 km to the southwest (Map 4B, Lines 1 and 20C).

In a similar fashion the bedrock underlying Agate Embayment has nick points in its general seaward slope at -16 m, -21 m and -24 m. Lone Ridge shows a shallower gradient between -14 m and -16 m, with a nick point at -16 m. The extensive terrace off Agate Bay lies at -18 m and its seaward edge descends rapidly to -24 m, with a slope of up to 1:10 (5.7°) in places. This edge is to a certain extent maintained on both the northern and southern sides of the terrace where shallow channels run towards Agate

Bay. The terrace between Agate Reef and Lone Ridge lies at -19 m, with a steeper gradient to -25 m.

The slope of the shoreface outcrop varies between Agate Bay and Peacock Bay, where rugged bedrock continues for over 800 m offshore before levelling off at -24 m. Nick points are found at several depths, but the more pronounced are at -11 m, -15 m and -19 m. From Peacock Bay to Homewood Harbour the unusually steep seaward slope of the bedrock fringing Buchu Bay (Fig.2.4E) is constant at 1:4 (14°) down to a prominent nick point at -24 m. Ill-defined ridges farther seaward in Buchu Bay head almost due south, rise to -27 m and are separated by wide channels that cut down to between -29 m and -31 m.

The floor of Collins Embayment lies between 26 and 30 m below sea level with the deepest part forming an almost circular depression in the southwestern corner of the embayment (Map 4B). The surrounding bedrock rises to -22 m in the west and -16 m in the south, where it forms the western extension of Collins Reef. West of Homewood Harbour the bedrock levels out at -27 m, then increases gradually to -31 m and remains at this depth for over 1 km seaward.

The exposed bedrock between Collins Reef and Rietfontein (Map 4B) is cut by numerous channels and gullies. Ridges in this area generally rise to -10 m; others rise only to -15 m. At between -13 m and -17 m the bedrock makes a step with the gradient being gentler. The same change in slope occurs at -24 m. The interval between these two depths (17 to 24 m below sea level) is characterised by significantly steeper slopes. From a depth of -24 m the bedrock increases in depth more gently to -30 m, where it levels off completely to form a broad terrace. This terrace extends for about 300 m offshore before bedrock dips to -

38 m. Westward, bedrock again rises to form Kloppers Reef (Map 4B). The depression thus forms a north-south channel on the shoreward side of the reef. This channel broadens as it shallows northward to -34 m, continuing beyond the survey limits. At its southern end the channel floor rises steadily to the -30 m terrace. This depth is maintained for 750 m southward before a second channel is formed that trends due south. The channel floor reaches -40 m, and continues for over 1 km at that depth. At its narrowest, the channel floor is between 75 m and 100 m wide. The channel banks, with steep gradients of 5.7° , rise to -29 m on the west and east. Along the eastern side, though, the bedrock continues to rise, with a gentler slope, to 10 m below sea level, whereas Kloppers Reef forms the western channel bank. Bedrock seaward of Kloppers Reef increases in depth to -40 m, then remains at that depth for some distance to form a broad terrace (Map 4B, Line 19).

The fence diagram (Map 4B), shows that north-east and south-east of Peacock Bank the bedrock remains level at -30 m. Several channels cut into this terrace between Peacock Bank and Homewood Harbour. Peacock Bank itself rises about 10 m above the surrounding bedrock. Several sediment-filled gullies and channels cut across Peacock Bank. From the seismic record these seem to be between 2 m and 3 m deep. Bedrock seaward of Peacock Bank (Lines 1,2 and 34, Map 4B) remains at about -40 m for almost 3 km before dipping down to -50 m at the end of the lines.

The bedrock seaward of Kloppers Reef and south of Peacock Bank, reflects the change in the morphology from north to south which was already evident in the bathymetry. The fence diagram (Maps 4A and B) shows that the bedrock is much more rugged south of Peacock Bank. This can be correlated with a change in bedrock

lithology (cf section 1.4.1) from quartzitic schists and conglomerates in the south to sheared lavas and phyllites in the north (Map 4B). Lines 15, 19 and 20 indicate that the most extensive areas of the bedrock lie at approximately -40 m to -45 m and that this depth interval continues seaward for over 2 km (Line 15). From -45 m the bedrock gradually descends to -50 m ($0,57^\circ$) then increases sharply in gradient below -50 m (7°) until it disappears beneath the ABL. Several channels, some sediment filled, cut across this part of the inner shelf, probably extending to the shelf edge and water depths of over 50 m.

3.4 Rietfontein to Wreck Point. (Map 4C)

Rietfontein Embayment (Fig.2.4F) is underlain by bedrock that dips steeply at about $2,3^\circ$ from the shore to -25 m before levelling out, so that most of the floor of the embayment lies between 25 and 30 m below sea level. Between -20 and -25 m the gradient increases again to approximately $2,9^\circ$. A poorly defined, shallow, north-south trending channel skirts the eastern edge of the embayment floor. At the -29 m isobath this channel turns westward to break through a reef formed on the seaward side of the embayment. The reef rises 10 m above the channel floor. The channel continues to meander westward, remaining at -34 m for about 1 km, then drops to -40 m at the seaward edge of the survey area.

Three channels (Fig.2.4G) extend southward off Boulder Bay from the southern edge of Rietfontein Embayment, separated by reefs that rise to between 19 and 25 m below sea level (Map 4C). The channels cut into the bedrock to depths of between -34 m and -42 m; channel widths are about 100 m at their floor level. Two of the channels continue for over 4 km to the edge of the inner

shelf. The channel lying closer inshore runs along the northwestern edge of Boulder Reef. A broad tributary of this channel extends northeastwards towards the coast, but ends abruptly against the sharply rising shoreface bedrock. The channel floor, at -33 m, remains level to where it joins the north-south channel about 1 km southwestward. Smaller channels enter Rietfontein Embayment along its northern edge. These channels generally meander northeastward across the exposed bedrock between Rietfontein and Collins Reef.

The form of Giellie's Embayment (Map 4C, Fig.2.4H and I) is determined by Boulder Reef, that defines the northwestern boundary, and an ill-defined channel running along the north-south axis of the embayment. The channel branches at -29 m, with one tributary extending westward to the shelf-edge, whereas the other branch continues southward, narrowing in the same direction. The larger part of the embayment floor lies below -25 m, increasing to -35 m on its seaward edge. The bedrock gradient from the shore to -25 m shows a relative increase between the 20 m and 25 m isobaths.

Southward, Giellie's Embayment narrows to a series of channels, separated by reefs that rise to between -25 m and -22 m. The channels are between 75 m and 200 m wide at the 30 m isobath and the depth to the bedrock within the channels is between -38 m and -40 m. Seaward of the channels bedrock rises steeply (gradients of 1:20 are found) to an average depth of -30 m at the inner-shelf slope. Giellie's Embayment decreases rapidly in size southward until only the channels remain as connections between the deeper regions offshore and the embayment itself.

The fence diagram (Maps 4B and C) shows that from north to south, the width of the inner shelf decreases and the gradient of

the inner-shelf slope increases. This is a consequence of the increasingly indurated nature of the bedrock as the phyllites and volcanic schists of the Grootderm Suite are replaced south of Cape Voltas by the quartzites, conglomerates and phyllites of the Holgat Suite. West of Kloppers Reef (Map 4B, Lines 19 and 15) the depth of the bedrock increases gently from -35 m to -45 m, although the topography is generally rugged. At -45 m, almost 3 km seaward of the 35 m isobath, the bedrock gradient increases appreciably, and -60 m is reached only 600 m farther seaward. The bedrock dips beneath the ABL at -50 m. Off Rietfontein the inner shelf beyond the -30 m terrace (Map 4C, Lines 16, 17 and 18) slopes down to -45 m within 2 km, remaining at about that depth for a further 2 km before increasing in gradient and disappearing at -60 m beneath the ABL. Bedrock on the inner-shelf slope off Boulder Reef remains between -40 m and -45 m for almost 2,5 km (Map 4C, Lines 26A to C) before increasing in depth and disappearing once more beneath the ABL. Here the contact between the ABL and the bedrock lies at -75 m and bedrock can be followed to 80 m below sea level. West of Giellie's Embayment the inner shelf remains between -25 m and -35 m for another kilometre offshore (Map 4C, Lines 26D to F). The bedrock then increases in gradient, to form the inner-shelf slope dipping down to -80 m within 2,5 km, with a constant gradient down to 60 m below sea level. At this depth, and between -70 and -80 m, the bedrock has two nick points where the gradient is much less than the general 1.7° found at shallower depths.

3.5 Discussion

Bedrock underlying the sediment-filled embayments shows

changes in gradient at several depths. These depths correspond well with similar nick-points found on the exposed bedrock and discussed in the previous chapter. Evidence of nick-points in the study area have been found at -11 m, -16 m, -19 m to -21 m, -25 m, -28 m to -30 m, -35 m, -40 m, -50 m and -60 m. To express these changes in bedrock slope graphically, eight transects, each 1 km wide, have been selected (Fig.3.2), and the surface-area between 2 m-interval isobaths (from Maps 4A,B and C) summed between the -10 m isobath and the deepest isobath at the locality, which varies from -26 m to -34 m. Whereas this method of calculating areas is rather crude in that it uses second-order data (i.e. isobaths that have been drawn from spot heights), histograms of the data reflect the depths at which bedrock-gradient changes occur. The average distribution of gradient for the eight areas studied is shown in Figure 3.3. The histogram (Fig.3.3) shows maxima (shallower gradients) at the 14 m to 16 m and 26 m to 28 m isobath intervals and minima (steeper gradients) at the 10 m to 12 m and 20 m to 22 m isobath intervals.

Seaward of the shoreface the subbottom bedrock north of Homewood Harbour lies mainly at -22 to -25 m, -30 to -35 m and -40 to -45 m; steeper slopes separate these depth intervals in places (Maps 4A and B, Fig.2.4A to E). Whilst these depth intervals are also prominent south of Homewood Harbour (Maps 4B and C, and Fig.2.4F to I), particularly in the embayments and channels, the bedrock here shows a more continuous increase in depth, reaching a maximum depth in the study area of -80 m off Wreck Point. Bedrock in the south also has shallower gradients at -50 m and -60 m. O'Shea (1971) commented on the low bedrock gradient at -20 m off the Orange River and found that bedrock along the West Coast has "flatter" areas at several depths. On

HISTOGRAMS OF BEDROCK SURFACE AREA AT 2m. INTERVALS

(c.f. maps 4 A, B and C for localities)

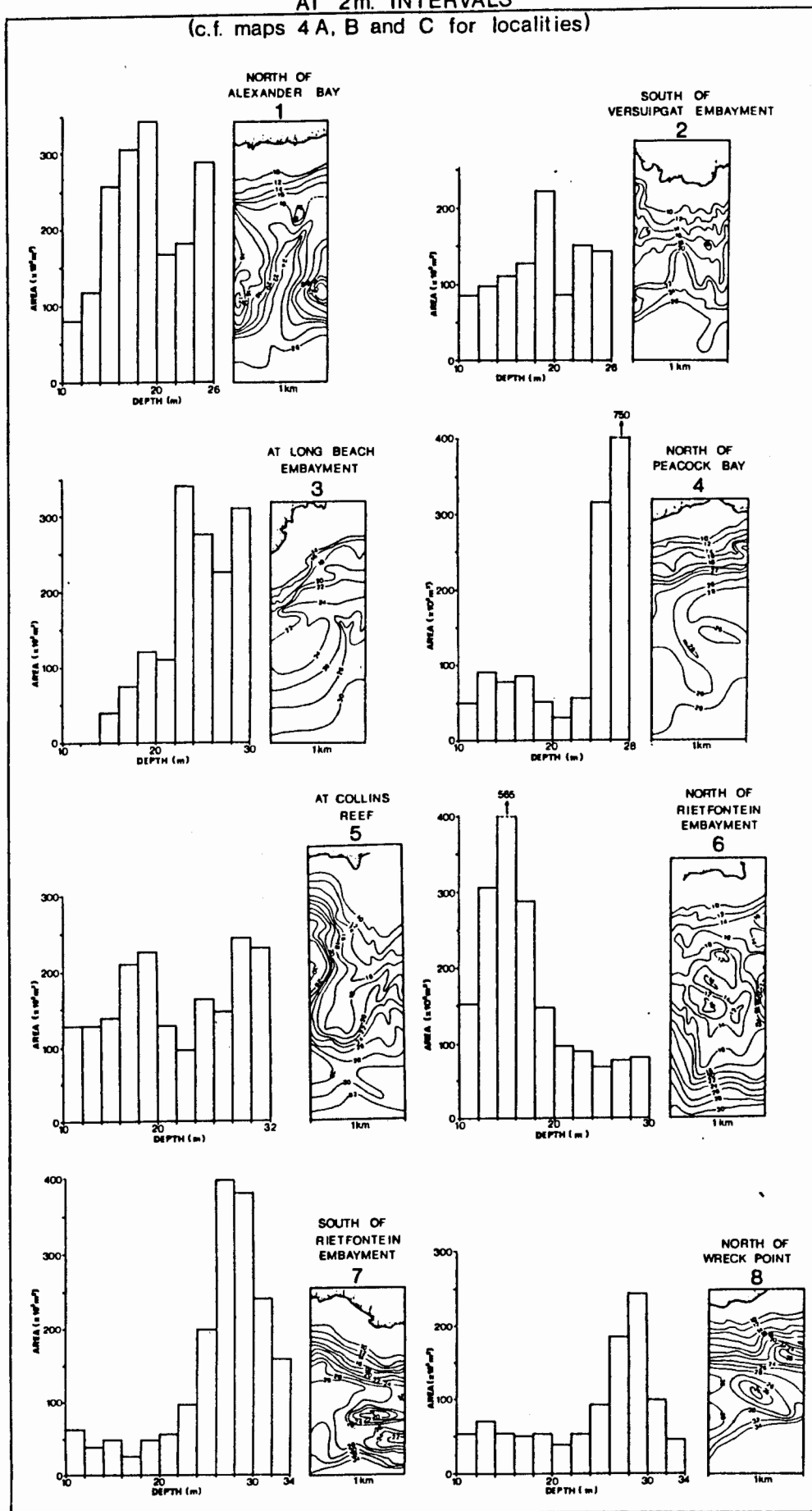


FIGURE 3.2

AVERAGE FOR EIGHT TRANSECTIONS

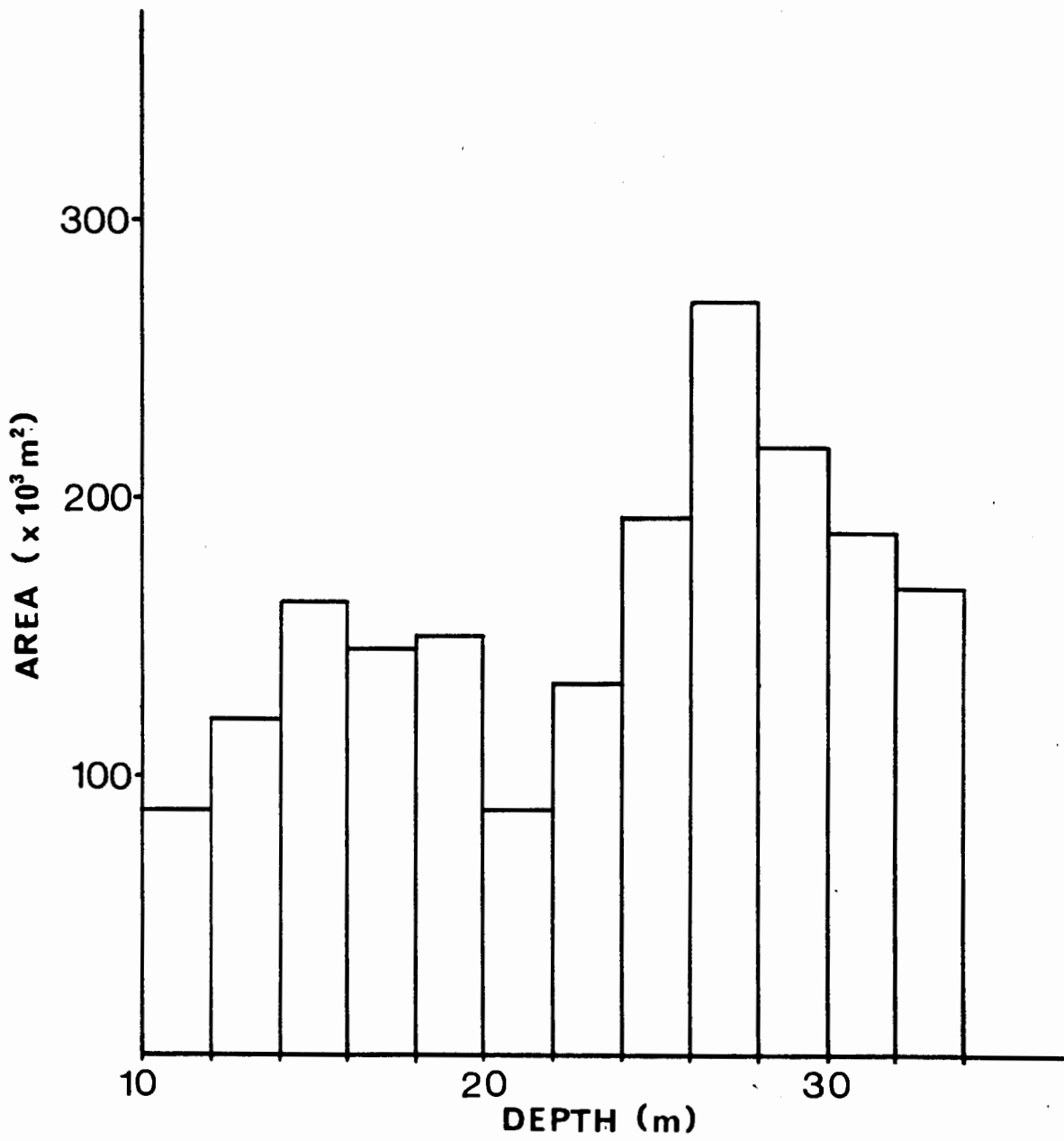


FIGURE 3.3

the east coast Maud (1968, p.185) reported "submarine platforms" interpreted from "detailed bathymetric charts". Table 3.1 lists the depths quoted by O'Shea (1971) and Maud (1968) and compares them with the depths found in the study area.

Table 3.1

Bedrock-terrace depths on the South African continental shelf (m)

Depth interval (m)	20	30	40	50	60	70	80	90
Study Area	14-16 18-20	22-25	30-35	40-45	50	60		
O'Shea (1971)	18-24	26-28	32-34	40-42	52-54 56-59		82-84	
Maud (1968)	11 18		36	47			70	80 95

The reasonable correlation of the depths indicates that these terraces probably developed eustatically during Quaternary sea-level oscillations.

The two channels cut 5 m to 10 m into the bedrock between -20 m and -28 m just south of the Orange River and between the outcrops of Tripp Shoal do not appear to extend across the broad terrace at -30 m. This is also the situation with the channels in the embayments at Cape Voltas, Long Beach and Agate Beach, all of which cut down to below -25 m (Maps 4A and B). The Orange River itself has however cut two channels across the inner shelf just north of the present mouth (Fig.3.4) (Hoyt et al., 1969; O'Shea, 1971). The main channel was detected to a depth of at least -80 m before it was masked by the ABL. (Off Wreck Point the ABL also masked bedrock seaward of the -80 m bedrock isobath). The other channel can be traced down to -60 m, having

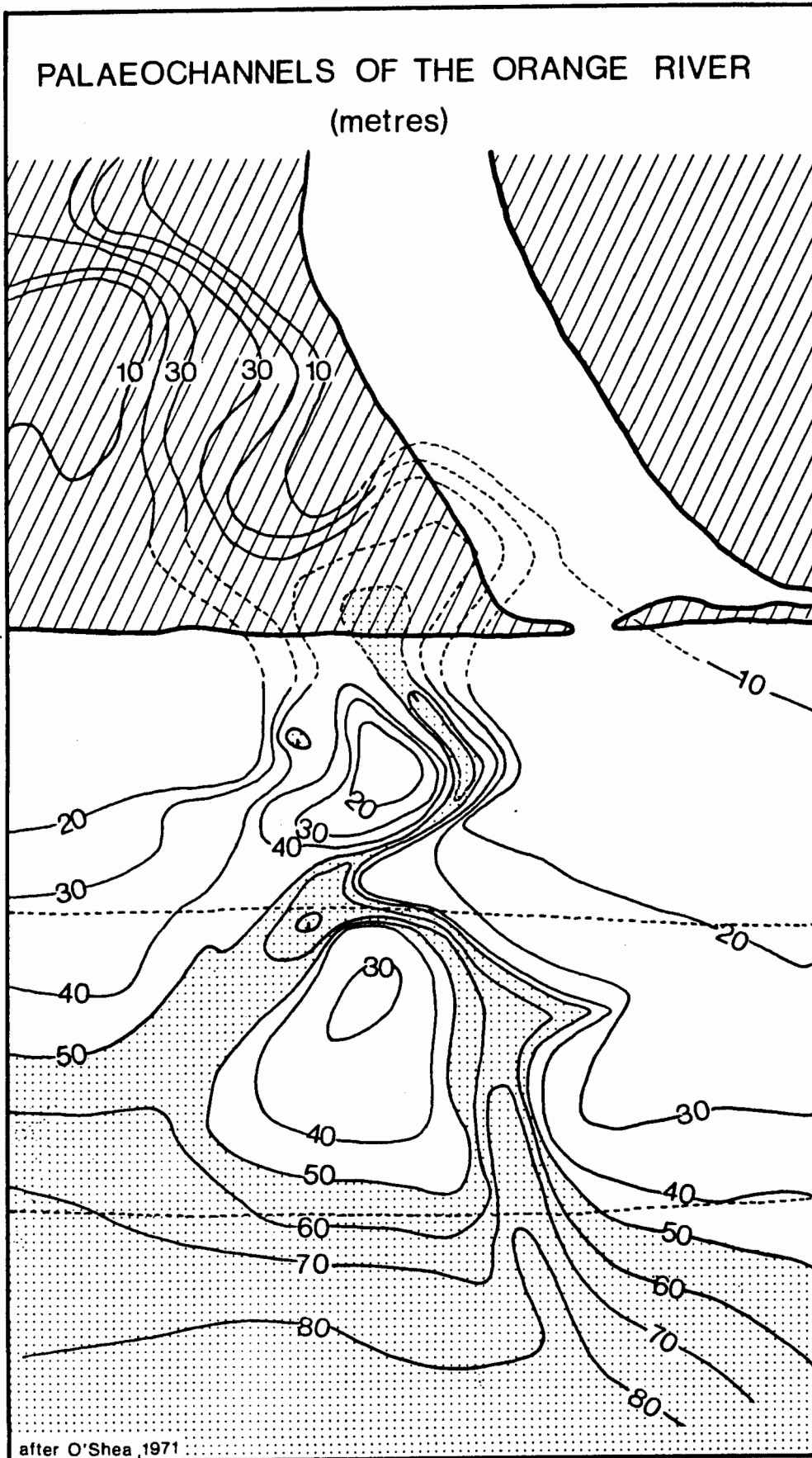


FIGURE 3.4

eight transects (Fig.3.3) is strong evidence for a wave-cut cliff at that depth. This is substantiated by the observations made by O'Shea (1971) and Murray et al. (1970, p.128) who report: "Probably the most clear-cut evidence of a former stand in sea level is provided by a cliff which ranges in height from 1,5 to 5 m. This feature has been mapped for about 20 km of its length in the Kerbehuk-Affenrucken area. It has a base at about -20 m where a distinct wave-cut nick is usually found." Marked steepening of bedrock gradients between -20 m and -24 m are found throughout the study area as is shown by the histograms for the eight transects (Fig.3.2). Foster (1974, in Petersen, 1983) reports carbon-isotope dates of 7340y. and 7080y. B.P. from deposits seaward of this cliff. The last sea-level stillstand at that depth therefore occurred during the rapid Holocene transgression, although here again one cannot rule out previous stillstands at these depths.

Map 2 shows that the channels crossing the inner shelf bedrock can be correlated with fluvial channels onland. Prominent channels trend inland from where they enter the sea at Alexander Bay, Agate Bay and Peacock Bay, extending more than 100 m above sea-level. Keyser (1972) believes that these channels would have transported diamondiferous sediment eroded from all the raised marine terraces. He suggests that the channel entering the sea at Agate Bay from the north was a tributary of the Orange River. Submerged channels continue seaward from the coast and reach down to at least -30 m (Maps 2, 4A and 4B). Farther south, in the embayments at Rietfontein and Giellie's Bay, several large channels extend to the edge of the inner shelf and water depths of over 40 m. Keyser (1972) suggested that the

level transgressions and the subaerial agencies of wind and water during periods of regressions.

A sea-level stand at -20 m is proposed from the seismic evidence that shows a marked increase in bedrock gradient between -20 m and -24 m, and this conclusion is supported by Murray et al. (1970) and O'Shea (1971) who report a wave-cut cliff with its base at -18 m to -20 m.

In the study area, terraces appear to increase in width and extent alongshore with depth. The -40 m terrace is the most prominent, with large parts of the inner shelf north of Rietfontein lying at about this depth (cf fence diagrams on Maps 4A and B). Also extensively developed is the -30 m terrace, best displayed between Kloppers and Collins Reefs (Map 4B) but also found throughout the study area. The -25 m terrace is not very striking in the southern part, but is fairly continuous north of Homewood Harbour, whereas the -20 m terrace is often not developed at all in the south; it is best displayed off the Orange River. The -16 m and -10 m terraces are manifest as the crests of some reefs and along the shoreface-bedrock outcrop and are areally not very extensive. However in terms of diamond recoveries the latter two terraces are most important as they are generally free of sediment and within reach of presently used mining techniques using divers. The decrease in size and extent of terraces with shallower water depth can be related to the number of times a terrace was re-occupied during relatively slow sea-level transgressions. (In comparison regressions were very rapid and continuous (Vail et al., 1977), therefore not allowing sufficient time for terrace development). Figure 8.1 shows that sea-level rose to between -40 m and -20 m on several occasions

since the Eemian transgression about 130 000y. B.P. which reached present-day sea levels (Barwis and Tankard, 1983).

Simultaneously with the terrace development, the abrading force of the waves would have formed gullies, potholes and other microtopographical erosional features. This aspect of the bedrock morphology will be described in the following chapter.

CHAPTER 4SURFACE STRUCTURE OF THE EXPOSED INNER SHELF BEDROCK4.1 Introduction.

The study of bedrock surface structures and microtopography with side-scan sonar is crucial to the exploration of diamonds on the inner shelf. Hallam (1964) and Keyser (1972) pointed out that onshore along the West Coast, diamondiferous deposits are concentrated in certain localities, primarily determined by the nature of the bedrock surface. Gurney et al. (1982) concluded from work in the surf zone north of the Olifants River that gully orientation is an important factor in the location of diamondiferous deposits. It is necessary, therefore, to identify from the sonographs features such as gullies, channels, cliffs and ridges, and to quantify the microtopography in terms of seafloor "ruggedness". Microtopography refers to variations in bedrock elevation of the order of metres and over distances of tens of metres.

Whereas the description of the seafloor is mostly qualitative, the following terms are now rigorously defined to quantify the microtopographic nature of the seafloor:

subdued - topographic differences are less than 2 m.

rugged - topographic differences vary from 2 m to 5 m.

very rugged - topographic differences are more than 5 m.

sediment-covered bedrock - more than 75% of the bedrock

has a sediment cover that can be

recognized on the sonographs.

exposed, bare bedrock - less than 25% of the bedrock has

a recognizable sediment veneer over it.

Through the interpretation of sonographs one hopes to gain a detailed understanding of the seafloor. Verification of the interpretation by means of bottom sampling, photography, video-taping or, optimally, diver observations, is an important aspect of this process, which is commonly termed "ground-truthing". A restriction to the diver approach is the basic scale to be used in sonographic interpretations. Severe limitations imposed on a diver by his work environment demand that results are obtained through a minimum effort on the part of the diver. The descriptive scale used here falls within the working range of an exploration diver, enabling him to convey an accurate picture of the nature of the seafloor traversed. The diver's task may be greatly facilitated by using an intercom system from the supply vessel. Such a method has been suggested by the author (De Decker, 1983c) who devised a simple questionnaire that has proved to be rigorous enough to enable non-geologist divers to gather valuable data during exploration of the seafloor.

The bedrock descriptions presented here are based on the "texture", or pattern, recognized on the side-scan records. Bedding planes, fractures, intrusive dykes, cliffs, ridges, gullies and other structural elements appear as distinct lineaments on the sonograph records. Their identification per se is based largely on inferences drawn from onland bedrock features exposed in mined-out areas (Keyser, 1972, Plate II) and by comparison with aerial photographs of the rocky stretches of the coastline.

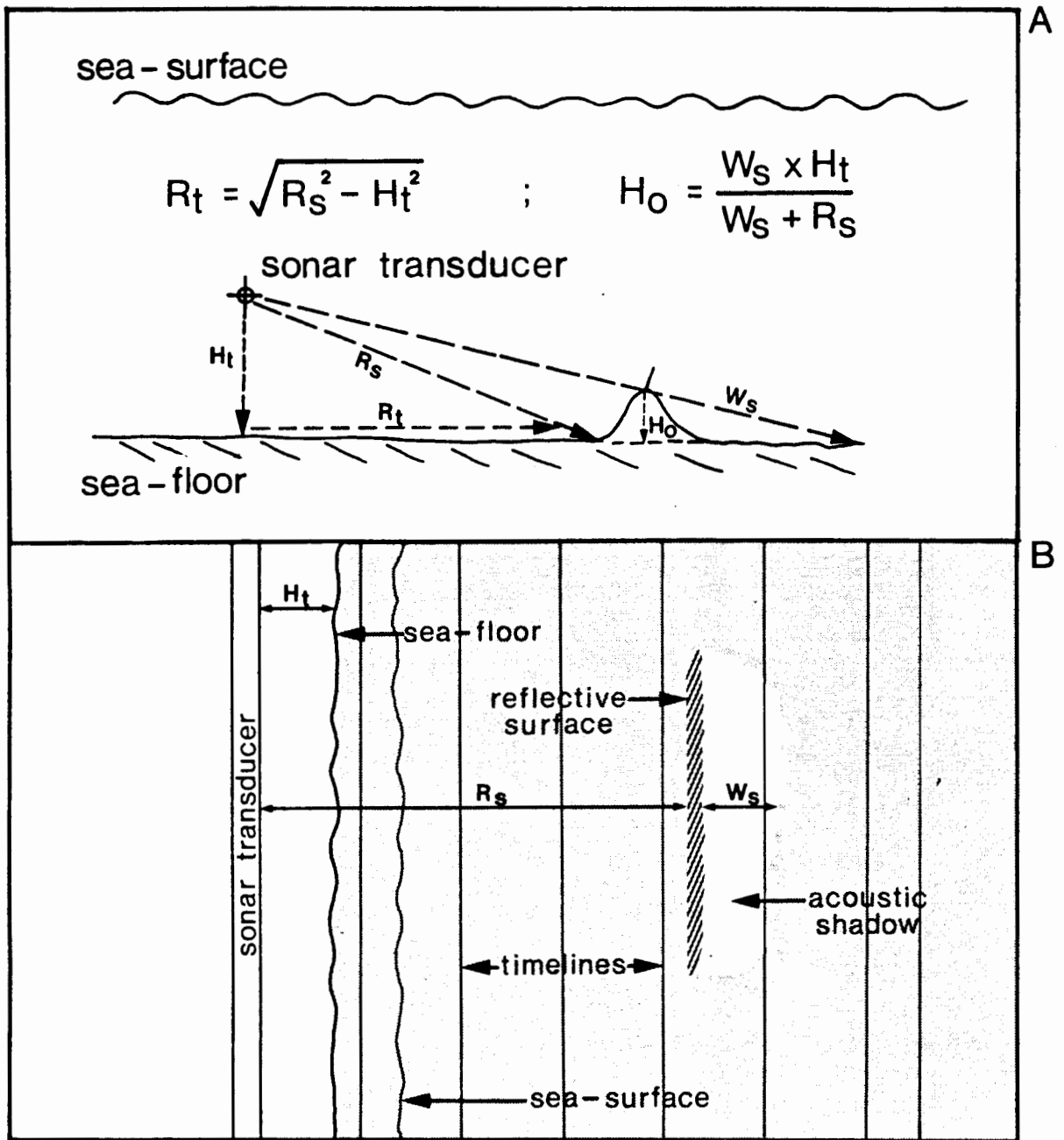
The seafloor is often described in terms such as "highly, moderately and weakly reflective", "granular", "even-toned", "blotchy", etc (eg. Knebel et al., 1982). These descriptions

group features with similar acoustic reflectivities together, even though the features themselves may be quite different.

The distinction between "bedrock" and "sediment cover" lies in the nature of the sonograph image: signal returns from bedrock surfaces parallel to the ship's track, i.e. facing the sonar transducer, are strong and usually contrast sharply with the areas of no signal return, termed "acoustic shadow zones" (Fig.4.1).

The surface detail of bedrock outcrops varies as a function of the amount of sediment cover over it and of the microtopography of the bedrock itself. The resultant effect of microtopography and sediment cover determines whether the bedrock is classified as "rugged" or "subdued". Thus, although the bedrock microtopography may be extremely "rugged", due to a sediment veneer the seafloor expression may warrant a "subdued" classification. Plate 4.1 shows examples of these patterns seaward of Boulder Reef (Map 5C, 3). Areas defined as "rugged" include the crests of reefs such as Voltas, Collins and Agate Reefs and inshore areas where the shoreface bedrock is exposed, as at Rietfontein, Wreck Point and between Versuipgat and Cape Voltas. "Subdued" bedrock generally occurs in deeper areas and is particularly prevalent offshore between Collins Reef and Rietfontein, northwest of Boulder Reef and on the terraces between -18 m and -20 m at Agate Reef and off Peacock Bay.

The resolution of the side-scan sonar depends on the paper feed rate, ship's speed and scanning range (cf. Appendix). In the terminology used here, "gullies" are identifiable from their form within the bedrock, i.e. their linearity and group-relationship are typical. It is however not possible



KEY

R_t = true range

H_o = height of object

R_s = slant range

W_s = width of acoustic shadow

H_t = transducer height above seafloor

FIGURE 4.1

to distinguish on the sonograph whether a gully contains sediment or not, as the gully-floor generally falls within the acoustic shadow zone cast by the sides, i.e. the sides are only 2 or 3 m apart. Murray et al. (1970) have analysed the variety and types of gullies encountered and the reader is referred to the discussion section below for details. Channels are larger features (5-200 m wide) that are found in isolation with the channel-floor cut down to 10 m into the bedrock. They are generally filled with sediment and have an average depth to width ratio of 0.5 to 0.05.

It is possible to gauge the texture of the sediment from the strength of the return signal - an aspect that will be discussed in Chapter 7. Suffice to say here that muddy and sandy unconsolidated sediments usually produce an even, homogeneous reflection, the coarser grain sizes giving a stronger return signal. Megaripples are easily recognized on the records and are best displayed when the sonar scans perpendicular to their crestlines. On Maps 5A, B and C areas interpreted from sonographs to be covered by coarse-grained sediment (mainly gravelly-sand) and megaripples are outlined. Although scale-limitations precluded representing the lineaments on the bedrock outcrops in terms of the interpretations given to them, the orientation, shape and length of all lineaments are accurately traced from the sonographs.

A review of the literature reveals that side-scan sonar has mainly been used as a tool to locate and identify specific seafloor features and not for systematic regional seafloor mapping. Examples of side-scan sonar applications to marine geology are Sanders et al. (1969), Mudie et al. (1970), Langhorne

SECTIONS ACROSS THE INNER SHELF BETWEEN ORANGE RIVER AND PORT NOLLOTH (cf. Figure 2.2 for positions of section lines.)

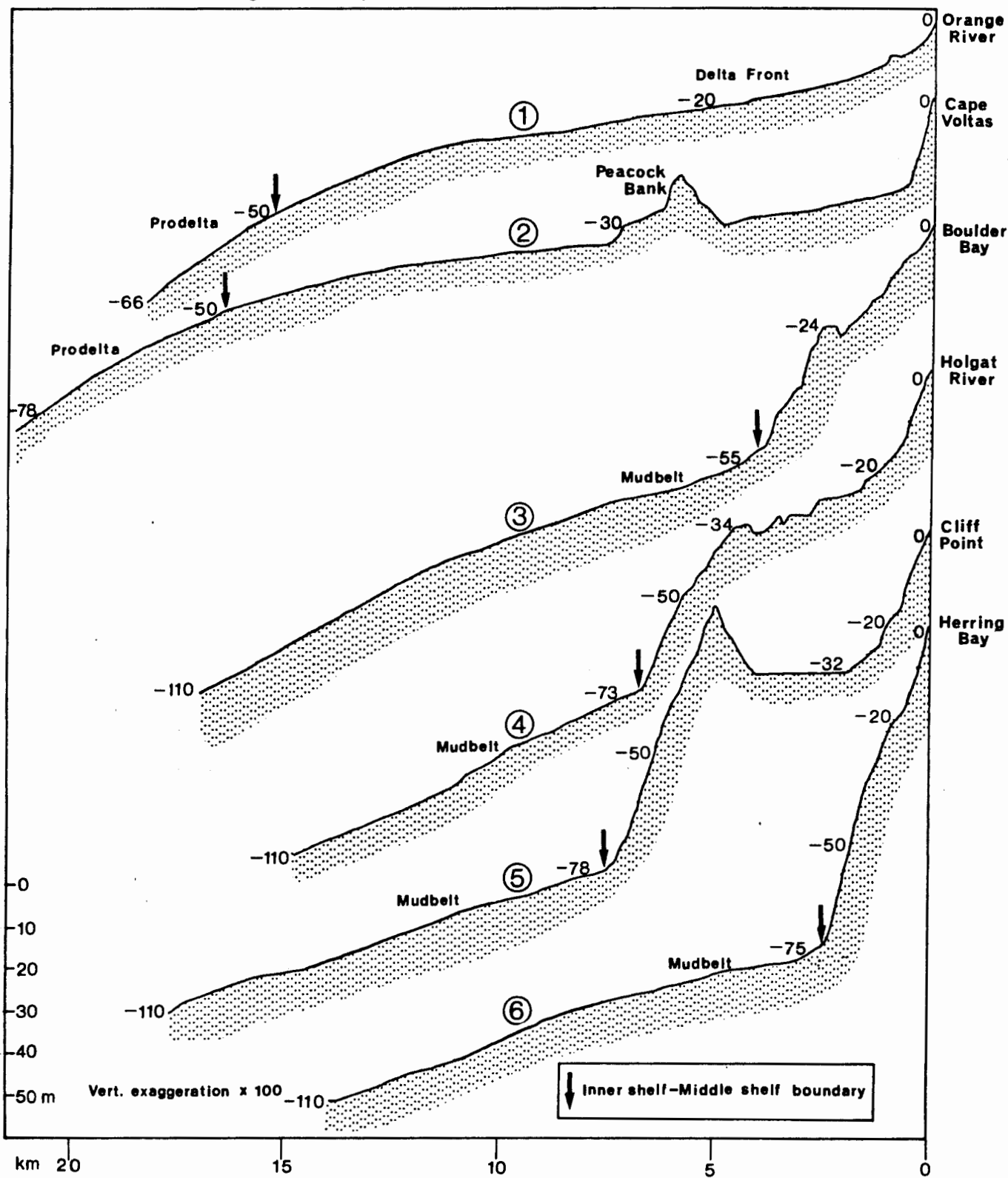


FIGURE 2.3

shelf maintains this width. The bathymetry shows a rugged, undulating inner shelf, bounded on the east by an irregular coastline and on the west by a straight, continuous inner-shelf slope trending between 332°N and 333°N shoreward of the terrigenous mudbelt (Fig.2.2). Northward from Wreck Point the inner shelf becomes increasingly covered by sediment as the seafloor seaward of the inner-shelf slope shoals in the transition from terrigenous mudbelt to prodelta to delta front. Between Homewood Harbour and the Orange River the inner shelf is mostly covered by sediments of the Orange Delta. However, seismic evidence (discussed in Chapter 3) shows that the inner-shelf bedrock north of Homewood Harbour extends over 10 km seaward (cf Maps 3A and B). Here the bedrock is composed of lavas, agglomerates and tuff of the Grootderm Suite and friable schists, phyllites and lavas of the Oranjemund Suite (De Villiers and Sohngé, 1959; Kroner, 1974) (Fig.1.10). Peacock Bank, part of which is interpreted to be granitic (Chapter 4), juts through the deltaic sediments 6 km west of Homewood Harbour.

The shoreface bedrock along the coast slopes down from the shore to about -20 m, usually at an angle of between $1,1^{\circ}$ and $2,0^{\circ}$. Seaward, the seafloor levels out to a gradient of less than $0,5^{\circ}$ to form the major part of the inner shelf between -20 m and -40 m. Several ridges, generally standing 10 to 15 m above the surrounding seafloor, strike due south and cut diagonally across the inner shelf. These ridges separate areas of smoother, gentler topography, identified as sediment-filled embayments (Fig.2.3, section 5). Whereas the 20 m isobath outlines the base of the ridges and extends to the shoreward edge of the embayments, the 40 m isobath is relatively straight, marking the

seaward edge of the inner shelf (Fig 2.2).

Although the Holgat River has not contributed any sediments to the inner shelf in recent memory - it last flowed in 1925 (Keyser, 1972) - its incised course across the coastal plain shows it to have been an active river during the Quaternary. This previous fluvial activity is substantiated by O'Shea (1971, map 3) who shows a wedge of sediment less than 6 m thick extending from the Holgat River mouth, whereas Fig.2.2 shows a deflection of the isobaths between -40 m and -50 m, suggesting the existence of a channel. However, the continuation of the channel towards the river mouth is not clear from the bathymetry alone. It is probable though that with sea-level receding as much as 200 m during the Quaternary (Siesser and Dingle, 1981), the river would have cut a channel across the inner shelf. In comparison, the Orange River has two palaeo-channels buried beneath deltaic sediments extending to -63 m and -85 m respectively (O'Shea, 1971) and are thought by Hoyt et al. (1969) to have been formed during regressions in the Late Pleistocene.

The inner-shelf slope extends, with a slight curvature, for over 230 km northwestward, from the Olifants River to Wreck Point (Fig.1.8) (Dingle et al., 1977, Rogers, 1977). It then swings north and disappears beneath the deltaic sediments of the Orange River at Homewood Harbour (Fig.2.2). The gradient of the inner shelf-slope, between the 40 m and 70 m isobaths, varies from $1,1^{\circ}$ to $1,9^{\circ}$ (Fig.2.3, sections 3 to 6). Between Wreck Point and Homewood Harbour the inner-shelf slope is dissected by several sediment-filled channels that cut across the inner shelf from north-east to southwest.

In contrast to the gradient of the inner-shelf slope, the

average gradient seaward of the slope is $0,25^{\circ}$ over the terrigenous mudbelt (Fig.2.3, sections 3 to 6). The gradient decreases even further on the middle shelf seaward of the -120 m isobath and the mudbelt (Fig.1.8).

Figure 1.8 shows the regional extent of the Orange Delta. It influences the bathymetry of the area for over 100 km, extending 30 km southward to Wreck Point and northward for almost 80 km (Hoyt et al., 1969; Rogers, 1977). On the inner shelf in the study area however, it affects the isobaths only as far south as Homewood Harbour (Fig.2.2). Cross-sections drawn from the Orange River mouth and Cape Voltas (Fig.2.3, sections 1 and 2) show the convex outline of the delta. Hoyt et al. (1969) estimate the width of the delta opposite the river mouth to be 25km, with a maximum thickness of more than 60 m. To the south the muds of the Orange prodelta abut against the inner-shelf slope between Homewood Harbour and Wreck Point, and increase in depth with an average gradient of $0,09^{\circ}$ from -40 m to -60 m in the same direction (Maps 3B and C). However, the deltaic sediments in this area do not cover the inner shelf itself. The toe of the prodelta lies at approximately -70 m slightly south of Wreck Point and continues south in the form of the terrigenous mudbelt. Seaward, the prodelta edge dips at $0,1^{\circ}$ to a maximum depth of about -120 m (Rogers, 1977) forming a broad arc that outlines the Holocene deltaic deposits.

2.3 Seafloor morphology of the study area.

The bathymetric maps presented here at 1:60 000 scale (Maps 3A, B and C), combine data obtained from seismic records with a sonographic interpretation distinguishing exposed bedrock from

sediment-covered areas.

The seismic profiler and side-scan sonar reveal the nature of the bedrock in section and plan respectively (cf. Appendix). The high-resolution, 3,5kHz seismic records allow accurate depth measurements of both the seafloor and the sub-bottom, thereby outlining all features in section. However, interpolation between traverses, particularly over rugged topography, is difficult. Sonographs allow one, inter alia, to delineate bedrock outcrops and sediment-covered areas. Combined, the two interpretations supplement each other, by giving substance to the isobaths and dimensions to the seafloor features.

The bathymetry, drawn at 1 m-isobath intervals, covers the area between the breaker zone and the seaward limit of the coast-parallel survey lines. Fence diagrams are drawn from the tielines that extend seaward across the outer edge of the inner-shelf slope. The sea-surface lines of the fence diagrams represent the ship's track-lines.

Where place names are first introduced, they are underlined and their location shown on Maps 3A,B and C. Whereas most of the names used appear on previously published topographic maps, orthophotomaps, etc., I have created a few new place-names to guide the reader through the diverse topography of the study area.

2.3.1. Orange River to Cape Voltas: (Map 3A)

The principal features in this area are the subdued seafloor north of Alexander Bay, the rugged shoreface bedrock outcrop that is in places interrupted by sediment-filled embayments, and the influence of the Orange Delta on the bathymetry. The isobaths off the Orange River mouth indicate a seafloor gradient of $0,16^\circ$

(1:350) seaward of the -11 m isobath (Fig.2.4A). From the surf zone to the 11 m isobath the gradient increases to $1,05^{\circ}$ (1:55). The fence diagram (Map 3A), shows that farther seaward the delta front has an even gentler gradient (1:1000). It reaches a depth, approximately 9 km offshore, of just over -20 m off the Orange River and -25 m off Cape Voltas.

The shoreface outcrop consisting of Grootderm Suite lithologies (Fig.1.10), first appears as the seaward extension of the southern bank of the Orange River floodplain (Map 3A). It forms a broad reef extending up to 1 km offshore and has a very indented contact with the sediment at about -12 m, indicating the presence of many sediment-filled gullies. Several ridges, 10 to 60 m wide and about 150 m long, extend from the reef, rising a few metres above the sediment.

Tripp Shoal consists of two isolated bedrock outcrops, 1 km apart and about 2 km from the coast directly west of Alexander Bay. The bedrock probably belongs to the Grootderm Suite, as the contact onshore lies slightly north of Tripp Shoal. The northern outcrop rises to -12 m, from -15 m on the shoreward side and from -17 m on the seaward side. The other, more pronounced peak rises to 8 m below sea level, standing between 7 m and 9 m above the surrounding sediment. Both outcrops are elongated northeast-southwest, the northern one being the larger of the two (0,50 km² and 0,32 km²). The sediment-bedrock contact along the northern edges is quite linear, whereas several sediment-filled channels extend up to 100 m into the southern and western sides of the outcrops. Another isolated outcrop, approximately 2 km south of Tripp Shoal, rises to -16 m from the surrounding sediment at 20 m below sea level. The fence diagram in Map 3A shows bedrock

SECTIONS ACROSS THE INNER SHELF
BETWEEN ORANGE RIVER AND WRECK POINT
(cf. Maps 3,4 and 6 for positions of sections)

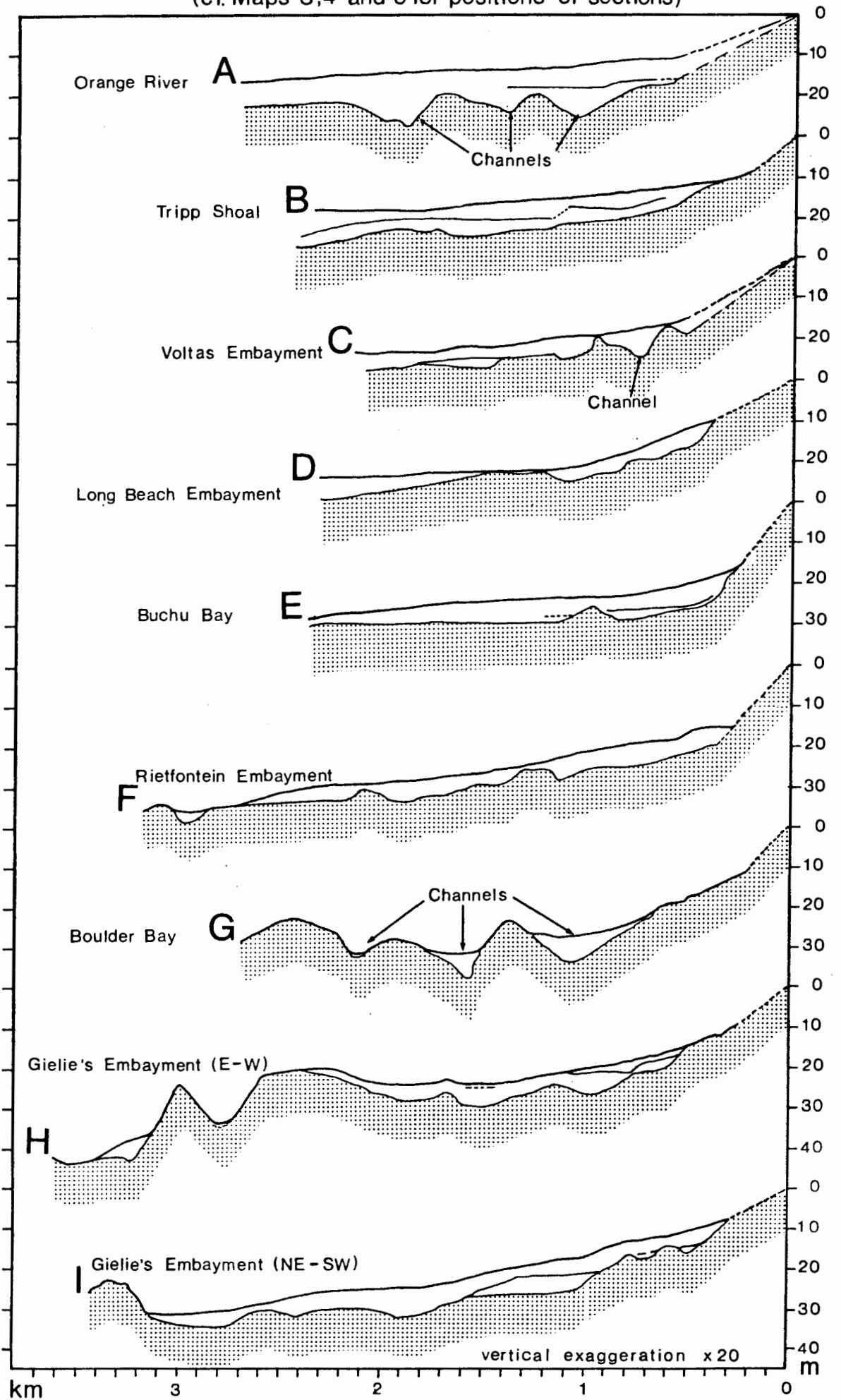


FIGURE 2.4

apparently cropping out at the inshore end of Line 32. This would indicate that the outcrop continues beyond the shore-parallel survey lines for at least another kilometre, giving it a typical northeast-southwest trend.

The shoreface outcrop north of Alexander Bay is rugged, although large areas of the bedrock have a thin sediment veneer. On the seaward side bedrock dips beneath the sediment at -11 m to -13 m, the contact being 400 m from the coast (Map 3A and Fig.2.4B).

Three sediment-filled embayments cross the shoreface outcrop area between Alexander Bay and Cape Voltas, linking the offshore sediments with the beach (Map 3A). Isobaths over the bedrock outcrop area show a decrease in gradient between -8 and -12 m (Fig.2.4B), suggesting some planation at this depth. Bedrock below -10 m has a gradient of about $1,0^{\circ}$, increasing in depth to between 17 m and 20 m below sea level before disappearing beneath the onlapping sediment. Several large sediment-filled channels extend into the shoreface bedrock, thus creating a highly indented seaward boundary between the bedrock outcrop and the sediment.

Alexander Bay itself is a distinctive, elongate coastal re-entrant measuring 200 m wide by 600 m long, with a sediment-filled embayment extending seaward to the edge of the shoreface outcrop. Versuipgat Embayment is similar to Alexander Bay, in that it is parallel-sided and aligned towards the east-northeast; it is about 300 m wide and 1000 m long. Voltas Embayment narrows rapidly from slightly over 1.5 km wide at the seaward side, to a sediment-filled channel that connects the embayment with the beach (Map 3A). North of Voltas Embayment prominent channels, up

to 200 m wide, cut shoreward across the shoreface outcrop, giving rise seaward to a highly irregular bedrock-sediment contact at -17 m to -20 m (Map3A). Isolated outcrops seaward of the shoreface outcrop indicate that the sediment adjacent to the contact covers the rock with a thin veneer.

The sediment-bedrock contact in Voltas Embayment is very irregular. The southern edge in particular has a highly indented outline, accentuated by a prominent ridge extending northwestward, at about 20 m below sea level.

At Cape Voltas, bedrock lies exposed along the shoreface for approximately 2 km and extends offshore for 1 km, at which point it is covered by a thin veneer of sediment (Map 3B). Along the northern edge, however, Voltas Reef continues farther seaward for 1 km, extending beyond the limits of the coast-parallel survey lines. The reef has an average width of 400 m and trends southwestward, although its outline is quite irregular. Voltas Reef rises to -19 m from the sediment contact at about -22 m.

2.3.2. Cape Voltas to Rietfontein (Map 3B)

From Cape Voltas southwards to Homewood Harbour the orientation of the coastline changes to form the wide northwest-facing Buchu Bay (Map 3B). Bedrock lithology changes from the volcanic schists and tuffs of the Grootderm Suite to the more resistant quartzites and greywackes and conglomerates of the Holgat Suite. This northern part of the middle section of the study area is mostly sediment covered, whereas the seafloor from Homewood Harbour southwards to Rietfontein is mainly bedrock outcrop.

Voltas Reef defines the northern boundary of Long Beach

Embayment. The embayment deepens quickly from the coast to -20 m, then slopes at $0,42^{\circ}$ to a depth of -25 m at the edge of the survey area (Map 3B). Agate Reef rises 5 m above its surroundings to -19 m to form the southern boundary of the embayment. The reef reaches seaward for about 2 km, is 400 m wide and has a 300 m wide arm extending north towards Long Beach (Map 3B). The bedrock-sediment contact along the northern and southern edges of Long Beach Embayment are characterised by several subdued ridges that extend into the embayment, measuring between 150 and 300 m in length and 50 to 100 m in width. A particularly prominent 50 m-wide ridge lies at -20 m, trends to the northwest and continues for over 500 m (Map 3B).

Agate Embayment (Map 3B) is divided by Lone Ridge, a subdued ridge between 10 m and 18 m below sea level that runs from the beach southwestward for 600 m. A thinly sediment-covered, rectangular, bedrock outcrop at -20 m to -22 m, lies between Lone Ridge and Agate Reef. The subdued relief and sub-horizontal slope that persists for about 500 m suggest that this could be a wave-cut terrace; it is separated from Agate Reef by a 100 m wide sediment-filled channel.

The seafloor in Agate Embayment grades evenly with a slope of about $0,7^{\circ}$ to -24 m before levelling off farther seaward. Another terraced area is found south of the embayment off Agate Bay. The planated, square-shaped surface of the terrace is outlined by the -18 m isobath and has a surface-area of about 0.2 km^2 (Map 3B). Shoreward of this terrace the gradient steepens markedly to the beach. On both the northern and southern side of the terrace, broad sediment-filled channels extend towards Agate Bay. The terrace therefore forms a broad promontory jutting out

towards the southwest into the surrounding sediment (Map 3B).

The sediment cover in Buchu Bay is reflected in the smooth subparallel isobaths that grade at about $0,8^\circ$ from -16 m inshore to -23 m in the middle of the bay (Fig.2.4E). The seafloor slope decreases farther offshore (Map 3B). At Peacock Bay the sediment encroaches in a large tongue towards the mouth of the bay. From Cape Voltas to Agate Bay the seaward edge of the shoreface outcrop lies at a fairly constant depth of -22 m, but in Buchu Bay the bedrock-sediment contact is found at -16 m.

Peacock Bank, 6 km from the coast and directly west of Peacock Bay, consists of a northern part with peaks at -20 m, trending east-west, and a southern portion that runs north-south, rising to -16 m (Fig.2.5). On its northern side the seafloor at the bedrock-sediment contact lies at -27 m, increasing 4 km farther south to -34 m; shoreward the depth remains at about 30 m below sea level. The fence diagram (Map 3B) shows an undulating topography over Peacock Bank, with the channels and depressions generally filled with sediment. A north-south trending channel divides that part of Peacock Bank covered by sonographs into two parts (Fig.1.2 and Map 5B). The eastern half has a rugged topography, contrasting with the subdued topography of the western half and inferring a lithological change.

From Homewood Harbour to Collins Reef, the coastline is fringed by bedrock that quickly gives way to the sediment-filled Collins Embayment. The embayment continues for about 1 km towards Collins Reef, narrowing eastward to 500 m. Collins Reef extends westwards for almost 2 km, increasing in depth from the sea surface to -17 m at its seaward limit; the -10 m isobath outlines an area of almost $0,65 \text{ km}^2$.

BATHYMETRY OF PEACOCK BANK

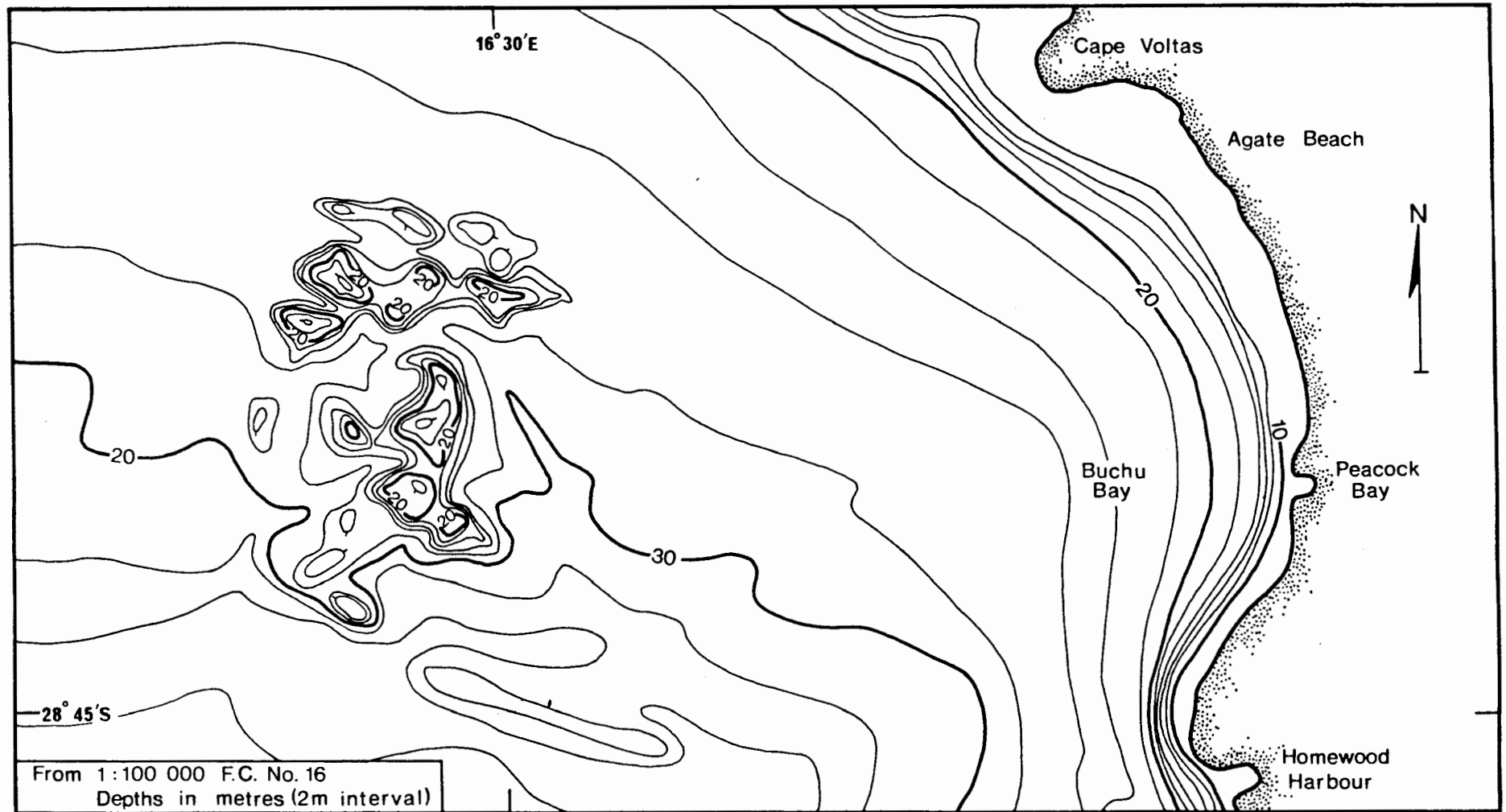


FIGURE 2.5

The inner shelf between Collins Reef and Rietfontein Embayment is formed by a rugged, exposed bedrock area that extends for almost 3 km seaward, lying between -10 and -20 m. The numerous channels that cut across this region contain little sediment and the water depth in them varies from approximately -15 m to -25 m. The seaward boundary of this shallow bedrock outcrop terrain is well defined, runs north-south and increases from -20 m, with a slope of between 1.4° and 2.0° , to -30 m, about 400 m farther west (Map 3B). The seafloor then levels off, continuing seaward for over 5 km to form a broad, dissected terrace between -30 and -40 m to the shoreward edge of the terrigenous mudbelt (Map 3B, Line 19). Kloppers Reef 1,5 km west of Collins Reef rises from this terrace to -22 m. It runs due south, curving slightly east to eventually merge with the seaward edge of the shoreface bedrock outcrop off Rietfontein Embayment. A 50 to 75 m wide sediment-filled channel cuts southward along the shoreward edge of the -30 m terrace (Map 3B).

Sediment-filled channels on either side of Kloppers Reef (cf Fig.1.2) narrow southward to a width of about 50 m, although they range over a distance of several hundred metres.

2.3.3. Rietfontein to Wreck Point (Map 3C)

This section of the study area is representative of most of the inner shelf southward. The seafloor between Rietfontein and Wreck Point is generally underlain by exposed bedrock. The two sediment-filled embayments crossing the inner shelf are almost entirely encircled by exposed bedrock, allowing sediment continuity seaward to the terrigenous mudbelt only through pronounced channels.

Rietfontein Embayment extends 2 km seaward, the seafloor sloping at $0,5^{\circ}$ from -12 m to -29 m (Fig.2.4F). The northern boundary is formed by a ridge rising to -10 m, with several sediment-filled channels cutting through it. The sediment in the embayment abuts, 1,2 km farther southward, against the steeply dipping ($1,3^{\circ}$ to $3,1^{\circ}$) shoreface bedrock outcrop (Fig.2.4F). The bedrock-sediment contact here is not as indented as along the northern edge, and for the most part remains at -20 m (Map 3C).

On its seaward side the embayment ends against a series of parallel ridges that trend southward (Map 3C). These ridges rise to between 20 and 25 m below sea level and are separated by relatively straight and narrow channels that extend for several kilometres out to the edge of the inner shelf (Map 3C and Fig.1.2). The sides of the channels are steeply dipping, usually exceeding $5,0^{\circ}$ (Fig.2.4G and H). The channel floor, where it opens into the embayment, lies at about -29 m. The seaward exit from the embayment is through a broad channel 300 m to 400 m wide. The water depth increases from -30 m at the entrance to the embayment to -38 m at the edge of the surveyed area (Map 3C). Northwestward the ridges die out within the embayment, usually in a series of smaller isolated outcrops (Map 3C).

From Rietfontein Embayment the channels continue along the northern side of Boulder Reef, which itself extends southwestward for over 1,2 km. The -10 m isobath on Boulder Reef outlines an area of about 1 km^2 . Seaward of the reef the seafloor descends rapidly to -28 m, levelling off at this depth to form a terrace 200 m wide in places (Map 3C). The bedrock then increases in depth to -41 m, to form one of the extensive north-south trending channels. A side channel trends shoreward to end abruptly at -

22 m against the steeply dipping shoreface bedrock. The main channel continues northward, narrowing to 50 m in width and shoaling progressively from -32 m to -27 m where it debouches into Rietfontein Embayment (Map 3C).

Gielie's Embayment descends from -12 m to -25 m (Fig. 2.4I). As with Rietfontein Embayment, a series of ridges and channels mark the seaward boundary, 2.5 km from the coast, of this southwestward-trending embayment (Map 3C). The bedrock-sediment contact along the northern edge of the embayment lies at about -20 m (Map 3C). The shoreface bedrock between Gielie's Bay and Wreck Point extends 500 m offshore before being covered by sediment; the contact lies between -13 m and -22 m and trends almost due south.

The ridges marking the seaward edge of the embayment are not as pronounced as those off Rietfontein. A very subdued ridge protrudes for over 2 km into the embayment (Map 3C). A wide terrace at its southern end at -23 to -24 m divides the ridge into two parts. The northern part has little topography and lies between -25 and -27 m. In the south the ridge rises to -22 m. A 300 m wide sediment-filled channel runs along the seaward side of the ridge, the waterdepth ranging from -32 m to -36 m at the inner-shelf slope. The channel has a steep seaward side that rises to form a reef with a crest at -28 m. The embayment opens westward onto the shelf-edge via a 600 m wide sediment-filled channel (Map 3C).

The inner-shelf slope is generally formed by exposed bedrock (Map 3C). Between Rietfontein and Wreck Point the seaward boundary of the inner shelf lies between -30 and -35 m. Farther seaward the inner-shelf slope dips at approximately $4,5^{\circ}$ to

between -40 and -45 m, after which the gradient decreases up to the shoreward edge of the terrigenous mudbelt. The mudbelt has a seaward gradient of $0,15^{\circ}$. The contact between the inner-shelf slope and the mudbelt is very regular and forms the inner shelf-middle shelf boundary (Fig.1.2). The depth of this boundary increases southwards from -50 m off Rietfontein to -65 m west of Wreck Point (Map 3C). Off Wreck Point the shelf-slope gradient ($1,3^{\circ}$) is continuous, with some evidence of a lower gradient at -40 m (Map 3C, Line 26F). The tielines off Rietfontein show that the inner-shelf slope has below average gradients at -35 m (Line 17) and -45 m (Lines 16,17 and 18). Lines 26A to F show lower than average gradients at -40 m, -45 m, -50 m, -55 m, and -60 m.

2.4 Discussion.

Hallam (1964), Keyser (1972) and Gurney et al.(1982) show from work on the raised terraces and in the surf zone that diamondiferous deposits are more likely to occur in the following localities: along the base of a wave-cut cliff, within gullies and potholes eroded into terraces, on the southern side of reefs that trend northeastward and the northern side of south-facing bays and also along palaeo-channels scoured by fluvial action. Exploration of the inner shelf for diamonds can thus be facilitated by recognizing these features in the bathymetry.

Off the Orange River and south to Homewood Harbour the bedrock outcrops are found along the shoreface, seldom extending beyond 1 km seaward. Isolated outcrops are indeed found farther offshore, such as Tripp Shoal at Alexander Bay and Peacock Bank, 6 km west of Peacock Bay, but they are limited in extent.

Generally, the bedrock topography in the northern part is not very rugged (i.e. micro-topographic differences are less than 5 m) and is characterised by an average dip of $1,4^{\circ}$ from the shoreline to where it disappears beneath the sediment at approximately -20 m. Maps 3B and C and the cross-sections (Figs.2.3 and 2.4) show that the largest part of the inner shelf lies between the 20 m and 30 m isobaths. This is a recurring depth for sea-level transgressions in the Late Quaternary (Barwis and Tankard, 1983). Flemming (1976a) reasons that at -20 m wave abrasion would be effective to -35 m and cites evidence from Rocky Bank at the mouth of False Bay south of Cape Town. The inner shelf could therefore be the erosional expression of a sea-level stand at -20 m.

Abrupt and distinct changes in the general gradient of the bedrock in a particular area (nick-points in seafloor sections) may be indicative of wave erosion during periods of lower sea-level stands in the Cainozoic (Dietz, 1964; Flemming, 1965 and Flemming, 1976a). Nick-points in the bedrock are commonly found at -10 m, the gradient being less than the average down to -13 m. Both Collins Reef and Boulder Bay have large areas that lie at about -10 m (Map 3B and C), whereas the ridges of Tripp Shoal rise to -12 m and -8 m respectively. The bedrock gradient from the shore to the 10 m isobath is invariably steeper than between that depth and -13 m. Another evident nick-point is found at about -16 m. Terraces lying between -16 m and -19 m are well developed west of Cape Voltas and Agate Bay, whereas the crests of Voltas and Agate Reefs rise to between 18 and 19 m below sea level, standing up to 5 metres above the surrounding seafloor. Regionally, within the study area this depth interval also has a

lower than average gradient. Similar gradient changes are found at greater depths, but they are generally covered by sediment and will be discussed in the next chapter.

Murray et al. (1970) and O'Shea (1971) give no evidence of wave-cut erosion features at depths shallower than -20 m. They do, however, refer to a prominent cliff with its base cut at -18 to -20 m, which Murray et al. (1970) were able to trace for 550 km between Kerbehuk (just north of the Orange River) and Conception Bay (south of Walvis Bay), along the Namibian coast. The cliff varies in height between 1,5 m and 5 m and a distinct wave-cut nick-point is usually found at its base. O'Shea (1971) found evidence for this cliff slightly north of the Orange River, although he found the cliff to be extremely dissected by gullies. In the study area bedrock exposures below -20 m are not commonly found, but evidence for a steepening of the bedrock gradient at approximately -20 m is particularly well displayed on the exposed shoreface area between Collins Reef and Rietfontein (Map 3B). The depth of the sediment-bedrock contact, which often lies at -20 m, may be another indication of a possible sudden increase in bedrock slope. The subbottom bedrock morphology will be discussed in the following chapter, when further evidence for possible wave-cut features in the bedrock will be produced.

Erosional features at depths shallower than -20 m could have formed since the time sea-level reached its present level about 6500 y B.P. (Flemming, 1977). The possibility of a previous sea-level stand at this datum cannot however be discarded. Milliman and Emery (1968) and Curray (1965) suggest a sea-level at approximately the present-day position between 35 000 to 30 000 y B.P., and Barwis and Tankard (1983) quote evidence for a

stillstand at this level 120 000 to 130 000 y B.P.

2.5 Conclusions

On a regional scale, the bathymetry between the Orange River and Port Nolloth (Figs.2.2 and 2.3) shows four geomorphic areas between the shoreline and the 120 m isobath (De Decker, 1982):

1. The submerged Orange Delta.
2. A rugged inner shelf, well developed south of Homewood Harbour and extending to -40 m.
3. The inner-shelf slope, lying between the 40 m and 70 m isobaths.
- 4) The smooth, gently sloping zone from -50 m to -120 m, underlain mainly by the terrigenous muds from the Orange River and the Orange prodelta.

Within the study area these four zones are represented to a greater or lesser degree. Deltaic sedimentation influences the bathymetry as far south as Wreck Point (Fig.2.2). Inshore, however, the effect on the bathymetry extends southwards only to Homewood Harbour (Maps 3A, B and C). Southward from Homewood Harbour the inner shelf is well developed, forming a rugged, relatively sediment-free area between the coast and -20 m, with another terraced area between -30 m and -35 m and extending more than 2 km offshore. The study area can therefore be divided into a relatively sediment-covered northern half and a southern half that is mostly underlain by exposed bedrock (cf. Fig.1.2).

The inner-shelf slope north of Wreck Point is not as pronounced as the slope found farther southward (Fig.2.2 and 2.3; Woodborne, 1985). At Wreck Point the bedrock dips down evenly and steeply ($1,3^{\circ}$) for about 1.5 km from -30 m to where it

disappears beneath the sediment at about- 62 m. Off Homewood Harbour the inner shelf has broadened to over 6 km with no distinct, exposed inner-shelf slope (cf Lines 15 and 19, Map3B). The bedrock at this point dips beneath the offshore sediments at -40 m. Northward the width of the inner shelf therefore increases, the gradient of the inner-shelf slope decreases and the depth at which the Orange River mudbelt laps onto the bedrock decreases.

CHAPTER 3SUBBOTTOM BEDROCK-MORPHOLOGY3.1 Introduction

In the sections below, those portions of the inner shelf underlain by Precambrian bedrock and covered by unconsolidated sediment are described. It is therefore essentially a discussion on the morphology of the sediment-filled embayments that cross the shoreface bedrock, the channels that extend from the embayments and cross the inner shelf, and that part of the inner-shelf slope covered by the Orange Delta and its terrigenous mudbelt. Areas of the seafloor that exhibit exposed bedrock have been discussed in the previous chapter on bathymetry and are therefore excluded here. The discussion builds on the previous one and incorporates data from exposed bedrock areas as well.

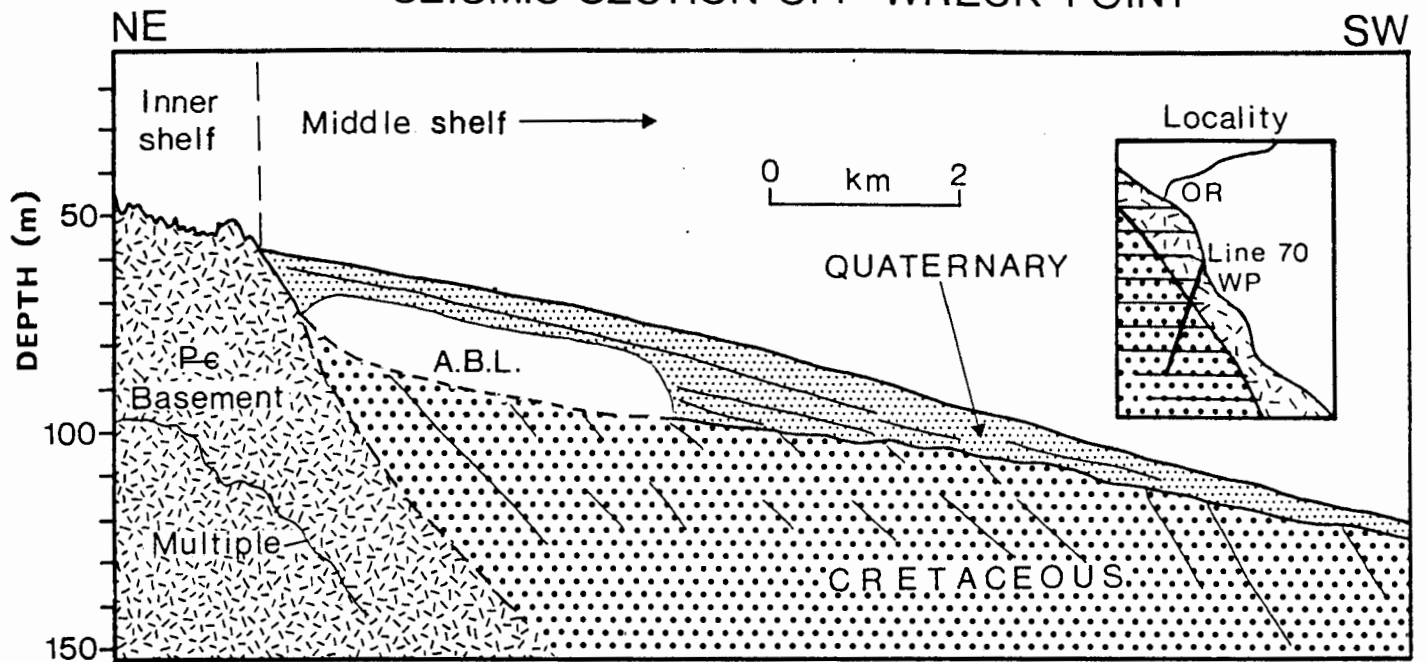
Without the second dimension from sonographs to assist in the interpretation of seismic profiles, the interpretation of subbottom bedrock areas will be less refined and reveal fewer subtleties in bedrock character. Nevertheless, the same morphological features considered in the previous chapter to be essential in locating diamondiferous deposits, need to be recognized in the bedrock isobaths beneath sediment-covered areas.

To facilitate meaningful conclusions to be drawn from the descriptions of the bedrock morphology, analogies for features interpreted from the seismic records are found onshore. The raised marine terraces, exposed through mining activities (cf Plate 4.4A and B; Hallam, 1964, Plates I and IV; Keyser, 1972, Plates II and VIII), allow a visualisation of the processes that

must have operated to form them. This permits a greater degree of confidence in the interpretation of the relatively low-resolution seismic records from the inner shelf.

The 3.5kHz pinger sub-bottom profiler used for the study has too high a frequency to penetrate lithified material and pebble horizons. "Acoustic basement" is therefore the deepest reflector recorded at a position, unless an internal horizon is so indurated or comprises pebbles, cobbles and boulders that further penetration is prevented. The sediment cover on the inner shelf reaches a maximum thickness of only 10 m (cf. Chapter 5) so that "acoustic basement" usually represents the bedrock reflector. On the inner shelf the bedrock reflector can be traced seaward to where it dips beneath the terrigenous mudbelt, which is to a large extent impervious to seismic pulses because of an Acoustical Blanking Layer (ABL) (Fig.3.1). O'Shea (1971, p21) remarks that "... the ABL represents a sediment with a high gas content and which would therefore tend to strongly reflect acoustic pulses and thereby screen details of the underlying sediments." (In fact, the gas would attenuate and scatter the seismic pulses, resulting in loss of signal (Whelan et al., 1977)). The bedrock reflector cannot therefore be traced below the ABL. O'Shea (1971, p.21) suggests that the gas, identified from drilling activities to be sulphurous, "...probably generated by decaying organic matter which could be expected to be plentiful in the biologically productive waters." The extent of the ABL off the study area and southward to beyond the Buffels River (Fig.1.12) is shown by Rogers (1977 , figs.VII-7 and 8). Details of the seismic system used, the method of recording and the resolution achieved are given in the Appendix.

SEISMIC SECTION OFF WRECK POINT



(After Birch in prep.)



3.2 Orange River to Cape Voltas. (Map 4A)

Except for a shallow depression parallel to the shore, bedrock off the Orange River is very subdued, grading gently at $0,18^{\circ}$ down from -18 m inshore to -25 m, 2.5 km offshore (Map 4A). Bedrock lithology here comprises the phyllites, schists and quartzites of the Oranjemund Suite (De Villiers and Söhnge, 1959).

At the southern edge of the Orange River floodplain the nature of the subbottom bedrock changes abruptly. Two prominent channels are cut into the bedrock to a depth of between -25 m and -28 m (Fig.2.4A). The northern channel, cut into the Oranjemund Suite, runs due south for approximately 1.9 km, before making a right turn to the west, continuing for another 700 m (Map 4A). The channel is approximately 300 m wide at the -20 m isobath, which defines the top of the western side, but the channel-floor at -26 m is less than 100 m wide. Although shown to die out on both the seaward and landward edges, the channel probably continues, at least seaward. The other channel, bisecting Tripp Shoal at right angles to the coast, is about 75 m wide, lies at -24 to -26 m, and appears to open onto the -25 m terrace that extends farther offshore (Map 4A). The channel shallows rapidly shoreward of the shoal and is split by a pronounced pinnacle, rising 8 m above the surroundings (Map 4A). The southern branch seems to extend to the coast slightly north of Alexander Bay. The other branch extends to the north and dies out at -13 m against the shoreface bedrock. Tripp Shoal has a ridge extending from it northwards towards the coast, rising to 15 m below sea level and joining the shoal with the shoreface bedrock. These channels were cut into the Grootderm Suite.

In contrast to the rugged topography of the exposed bedrock between the shore and 20 m isobath (described in the previous chapter), the bedrock from Alexander Bay to Cape Voltas deeper than -21 m has a subdued, subhorizontal surface, lying at an average depth of -24 m (Fig.2.4A to D). Channels have however been cut into this subdued surface, reaching up to 28 m below sea level on the seaward edge of the shore-parallel survey area (Map 4A). Prominent channels between 50 m and 100 m wide are found in the embayments at Alexander Bay and Versuipgat, cut about 5 m deep into the bedrock to at least -20 m. In Voltas Embayment (Map 4A) a shallow channel extends westward along the southern edge of the embayment, reaching -28 m on the seaward side. The meandering aspect of the channels cutting the shoreface bedrock would indicate that these may have developed as river-courses during sea-level regressions in the Quaternary, when sea-level receded as much as 200 m (Siesser and Dingle, 1981).

Lines 31, 32, 33 and 34 (Map 4A and 4B and Fig.5.2), extending to the seaward edge of the inner shelf, have sub-horizontal bedrock surfaces at -25 m, -30 m and a very broad undulating region at -40 m. Bedrock grades from $1,14^{\circ}$ to $1,9^{\circ}$ between these terraces, whereas the terraces slope seaward at about $0,15^{\circ}$. The -40 m terrace is the broadest and reaches a width of 1.5 km along Line 31 (Fig.5.2). Line 33, running perpendicular to the coastline, shows that the -30 m terrace is 600 m wide in this region; it is not seen on Line 31, and only partly on Line 32. The shoreward edge of the -30 m terrace lies 3.0 km offshore, whereas that of the -40 m terrace lies 4.5 km from the coast. The possibility that these terraces are wave-cut features will be investigated in the discussion section of this chapter.

3.3 Cape Voltas to Rietfontein. (Map 4B)

The morphological pattern established south of Alexander Bay continues through this area to Homewood Harbour, although the lithology changes at Cape Voltas from volcanic schists of the Grootderm Suite to quartzitic schists of the Holgat Suite (Map 4B). In general the shoreface bedrock is rugged, whereas seaward it is characterised by more subdued and subhorizontal topography (Fig. 2.4D and E).

The sediment embayments off Long Beach, Agate Beach and Homewood Harbour display similar, stepped bedrock floors. Long Beach Embayment (Fig. 2.4D) has a sloping floor with nick points (where the slope of the bedrock flattens appreciably seawards) between -17 m and -27 m. The changes in the bedrock slope occur at -18 m, -20 m and -24 m. The sides of the embayment, and the bedrock along the shoreface dip down quickly to -17 m from a depth of -10 m. South of Voltas Reef the bedrock has a level surface with no channels cut into it. The area defines a broad terrace at -24 m, measuring 800 x 400 m. Seaward of the terrace, the bedrock surface deepens steadily to -30 m before levelling off, remaining at about that depth until it rises to form Peacock Bank, 3 km to the southwest (Map 4B, Lines 1 and 20C).

In a similar fashion the bedrock underlying Agate Embayment has nick points in its general seaward slope at -16 m, -21 m and -24 m. Lone Ridge shows a shallower gradient between -14 m and -16 m, with a nick point at -16 m. The extensive terrace off Agate Bay lies at -18 m and its seaward edge descends rapidly to -24 m, with a slope of up to 1:10 (5.7°) in places. This edge is to a certain extent maintained on both the northern and southern sides of the terrace where shallow channels run towards Agate

Bay. The terrace between Agate Reef and Lone Ridge lies at -19 m, with a steeper gradient to -25 m.

The slope of the shoreface outcrop varies between Agate Bay and Peacock Bay, where rugged bedrock continues for over 800 m offshore before levelling off at -24 m. Nick points are found at several depths, but the more pronounced are at -11 m, -15 m and -19 m. From Peacock Bay to Homewood Harbour the unusually steep seaward slope of the bedrock fringing Buchu Bay (Fig.2.4E) is constant at 1:4 (14°) down to a prominent nick point at -24 m. Ill-defined ridges farther seaward in Buchu Bay head almost due south, rise to -27 m and are separated by wide channels that cut down to between -29 m and -31 m.

The floor of Collins Embayment lies between 26 and 30 m below sea level with the deepest part forming an almost circular depression in the southwestern corner of the embayment (Map 4B). The surrounding bedrock rises to -22 m in the west and -16 m in the south, where it forms the western extension of Collins Reef. West of Homewood Harbour the bedrock levels out at -27 m, then increases gradually to -31 m and remains at this depth for over 1 km seaward.

The exposed bedrock between Collins Reef and Rietfontein (Map 4B) is cut by numerous channels and gullies. Ridges in this area generally rise to -10 m; others rise only to -15 m. At between -13 m and -17 m the bedrock makes a step with the gradient being gentler. The same change in slope occurs at -24 m. The interval between these two depths (17 to 24 m below sea level) is characterised by significantly steeper slopes. From a depth of -24 m the bedrock increases in depth more gently to -30 m, where it levels off completely to form a broad terrace. This terrace extends for about 300 m offshore before bedrock dips to -

38 m. Westward, bedrock again rises to form Kloppers Reef (Map 4B). The depression thus forms a north-south channel on the shoreward side of the reef. This channel broadens as it shallows northward to -34 m, continuing beyond the survey limits. At its southern end the channel floor rises steadily to the -30 m terrace. This depth is maintained for 750 m southward before a second channel is formed that trends due south. The channel floor reaches -40 m, and continues for over 1 km at that depth. At its narrowest, the channel floor is between 75 m and 100 m wide. The channel banks, with steep gradients of 5.7° , rise to -29 m on the west and east. Along the eastern side, though, the bedrock continues to rise, with a gentler slope, to 10 m below sea level, whereas Kloppers Reef forms the western channel bank. Bedrock seaward of Kloppers Reef increases in depth to -40 m, then remains at that depth for some distance to form a broad terrace (Map 4B, Line 19).

The fence diagram (Map 4B), shows that north-east and south-east of Peacock Bank the bedrock remains level at -30 m. Several channels cut into this terrace between Peacock Bank and Homewood Harbour. Peacock Bank itself rises about 10 m above the surrounding bedrock. Several sediment-filled gullies and channels cut across Peacock Bank. From the seismic record these seem to be between 2 m and 3 m deep. Bedrock seaward of Peacock Bank (Lines 1,2 and 34, Map 4B) remains at about -40 m for almost 3 km before dipping down to -50 m at the end of the lines.

The bedrock seaward of Kloppers Reef and south of Peacock Bank, reflects the change in the morphology from north to south which was already evident in the bathymetry. The fence diagram (Maps 4A and B) shows that the bedrock is much more rugged south of Peacock Bank. This can be correlated with a change in bedrock

lithology (cf section 1.4.1) from quartzitic schists and conglomerates in the south to sheared lavas and phyllites in the north (Map 4B). Lines 15, 19 and 20 indicate that the most extensive areas of the bedrock lie at approximately -40 m to -45 m and that this depth interval continues seaward for over 2 km (Line 15). From -45 m the bedrock gradually descends to -50 m ($0,57^\circ$) then increases sharply in gradient below -50 m (7°) until it disappears beneath the ABL. Several channels, some sediment filled, cut across this part of the inner shelf, probably extending to the shelf edge and water depths of over 50 m.

3.4 Rietfontein to Wreck Point. (Map 4C)

Rietfontein Embayment (Fig.2.4F) is underlain by bedrock that dips steeply at about $2,3^\circ$ from the shore to -25 m before levelling out, so that most of the floor of the embayment lies between 25 and 30 m below sea level. Between -20 and -25 m the gradient increases again to approximately $2,9^\circ$. A poorly defined, shallow, north-south trending channel skirts the eastern edge of the embayment floor. At the -29 m isobath this channel turns westward to break through a reef formed on the seaward side of the embayment. The reef rises 10 m above the channel floor. The channel continues to meander westward, remaining at -34 m for about 1 km, then drops to -40 m at the seaward edge of the survey area.

Three channels (Fig.2.4G) extend southward off Boulder Bay from the southern edge of Rietfontein Embayment, separated by reefs that rise to between 19 and 25 m below sea level (Map 4C). The channels cut into the bedrock to depths of between -34 m and -42 m; channel widths are about 100 m at their floor level. Two of the channels continue for over 4 km to the edge of the inner

shelf. The channel lying closer inshore runs along the northwestern edge of Boulder Reef. A broad tributary of this channel extends northeastwards towards the coast, but ends abruptly against the sharply rising shoreface bedrock. The channel floor, at -33 m, remains level to where it joins the north-south channel about 1 km southwestward. Smaller channels enter Rietfontein Embayment along its northern edge. These channels generally meander northeastward across the exposed bedrock between Rietfontein and Collins Reef.

The form of Giellie's Embayment (Map 4C, Fig.2.4H and I) is determined by Boulder Reef, that defines the northwestern boundary, and an ill-defined channel running along the north-south axis of the embayment. The channel branches at -29 m, with one tributary extending westward to the shelf-edge, whereas the other branch continues southward, narrowing in the same direction. The larger part of the embayment floor lies below -25 m, increasing to -35 m on its seaward edge. The bedrock gradient from the shore to -25 m shows a relative increase between the 20 m and 25 m isobaths.

Southward, Giellie's Embayment narrows to a series of channels, separated by reefs that rise to between -25 m and -22 m. The channels are between 75 m and 200 m wide at the 30 m isobath and the depth to the bedrock within the channels is between -38 m and -40 m. Seaward of the channels bedrock rises steeply (gradients of 1:20 are found) to an average depth of -30 m at the inner-shelf slope. Giellie's Embayment decreases rapidly in size southward until only the channels remain as connections between the deeper regions offshore and the embayment itself.

The fence diagram (Maps 4B and C) shows that from north to south, the width of the inner shelf decreases and the gradient of

the inner-shelf slope increases. This is a consequence of the increasingly indurated nature of the bedrock as the phyllites and volcanic schists of the Grootderm Suite are replaced south of Cape Voltas by the quartzites, conglomerates and phyllites of the Holgat Suite. West of Kloppers Reef (Map 4B, Lines 19 and 15) the depth of the bedrock increases gently from -35 m to -45 m, although the topography is generally rugged. At -45 m, almost 3 km seaward of the 35 m isobath, the bedrock gradient increases appreciably, and -60 m is reached only 600 m farther seaward. The bedrock dips beneath the ABL at -50 m. Off Rietfontein the inner shelf beyond the -30 m terrace (Map 4C, Lines 16, 17 and 18) slopes down to -45 m within 2 km, remaining at about that depth for a further 2 km before increasing in gradient and disappearing at -60 m beneath the ABL. Bedrock on the inner-shelf slope off Boulder Reef remains between -40 m and -45 m for almost 2,5 km (Map 4C, Lines 26A to C) before increasing in depth and disappearing once more beneath the ABL. Here the contact between the ABL and the bedrock lies at -75 m and bedrock can be followed to 80 m below sea level. West of Gielie's Embayment the inner shelf remains between -25 m and -35 m for another kilometre offshore (Map 4C, Lines 26D to F). The bedrock then increases in gradient, to form the inner-shelf slope dipping down to -80 m within 2,5 km, with a constant gradient down to 60 m below sea level. At this depth, and between -70 and -80 m, the bedrock has two nick points where the gradient is much less than the general 1.7° found at shallower depths.

3.5 Discussion

Bedrock underlying the sediment-filled embayments shows

(1973), McKinney et al. (1974), Flemming (1978), Morang and McMaster (1980), Knebel et al. (1982) and Twichell (1983).

Along the South African coast, mapping the seafloor by means of sonographs has been carried out in Algoa Bay (Bremner, 1981; Du Plessis and Glass, 1981), Saldanha Bay (De la Cruz, 1978), Table Bay (Woodborne, 1982), along the West Coast in Diamond Concession Area 3 (Macrae, 1983 and Terhorst, 1983) and in Area 4 (Woodborne, 1986). The west coast has been a focal point for this type of survey, specifically in the search for diamondiferous deposits (Murray 1969). None of the data have yet been published, however, or made available as open file Geological Survey reports. O'Shea (1971) makes brief mention of the use of mosaics constructed from sonographs and states that the prominent wave-cut cliff at -20 m has been mapped in this way and its position later verified by divers.

4.2 Orange River to Cape Voltas (Map 5A)

The shoreface north of Alexander Bay consisting of volcanic schists of the Grootderm Suite exhibits prominent lineaments that are continuous for up to 150 m and trend in two directions, namely east-west and coast-parallel i.e. northwest-southeast. Superimposed on these strong lineaments are a set of short, less distinct, linear reflectors also orientated northwest-southeast. The prominent east-west lineaments are interpreted as being slope gullies (cf section 4.5), whereas the more numerous coast-parallel northwest-southeast lineaments reflect structural trends in the bedrock (jointing, fracturing) or possibly low ridges and cliffs. Faint lineaments represent megaripples in bedrock depressions, the sediment occurring as a thin veneer over large

parts of the outcrop. Acoustic shadow zones associated with the prominent lineaments indicate a rugged bedrock topography with pockets of sediment found between ridges or in gullies.

Tripp Shoal is covered for the most part by a veneer of sediment, only the shallowest parts exhibiting prominent lineaments (Map 5A, 1). Here, the sonographs show intersecting lineaments and the seismic records indicate rugged topography with a relief of up to 5 m. The majority of these lineaments extend northeast - southwest representing lithological trends and foliation direction, or northwest - southeast, representing structural trends in the bedrock such as fractures and joints (Fig. 1.10).

Bedrock between Alexander Bay and Cape Voltas has numerous prominent lineaments, trending north-south or north-northwest south-southeast. Plate 4.2 (Map 5A, 2) shows a prominent lineament with two parallel reflectors about 20 m apart. The lineament continues northward across the sedimentary embayment; southward, it extends for over 800 m. These features are continuous for up to 1 km in length and often trend subparallel to each other; occasionally they may be curved, coalesce, or even appear to cross each other (Map 5A). Well-defined, broad, shadow zones are associated with the lineaments. The orientation and length suggest that these lineaments represent dolerite dykes, known from onland exposures to have similar characteristics (Fig. 1.10) (De Villiers and Söhnge, 1959; Kröner, 1974). Shorter, fainter lineaments generally trend northwest-southeast to east-west and rarely continue for more than 100 m. These are interpreted as east-west orientated slope gullies (Murray et al., 1970), or northwest-southeast oriented bedding planes and

structural trends in the bedrock.

The continuity of these lineaments southward is interrupted by a very subdued 200 m wide area, flanked by sediment-filled depressions, that extends across the shoreface bedrock (Map 5A, 3). The lineaments re-emerge about 300 m farther south along the northern edge of Voltas Embayment. Their disappearance across the subdued zone can be attributed to a thick sediment veneer that almost completely masks the lineaments on the sonographs, yet is not resolved on seismic records (i.e. the sediment is less than 1 m thick). This emphasizes the value of side-scan-sonar areal surveys to complement the lower-resolution seismic-line surveys.

The shoreface bedrock at Cape Voltas is similar to that described farther north: continuous lineaments extend southwards for several hundred metres; another set of shorter lineaments has a northwest to northeast orientation. At Voltas Reef the crest is rugged with little sediment cover. Bedrock surface features therefore remain the same for the region between Alexander Bay and Cape Voltas, indicating little variation in lithology or structure within the area. No evidence of the northwest-trending thrust fault (Fig.1.10) was found on the sonographs.

4.3. Cape Voltas to Rietfontein (Map 5B)

A prominent lineament extends for about 4 km southward from the seaward edge of the shoreface outcrop at Cape Voltas (Map 5B, 1) to the terrace off Agate Bay (Map 5B). Off Cape Voltas it is exposed for about 600 m, trending southeastward. It crops out again on the southern side of Long Beach Embayment, forming a narrow, 600 m long ridge that juts out through the sediment (Map

5B, 2). Continuing southeastward, another lineament cuts across Agate Reef and the adjacent outcrop on its southern side to disappear beneath the sediments in Agate Embayment. The -20 m bedrock terrace south of Agate Embayment (Map 5B) is also crossed by a prominent lineament, aligned along the same NW-SE direction. The coast-parallel orientation, prominent appearance on the sonographs and consistent depth between -19 m and -21 m of these lineaments suggests that they could be segments of the prominent cliff at -20 m to -24 m described in Chapters 2 and 3.

Several other, long NNW/SSE-trending lineaments (possibly dykes) cut across Agate Reef and Lone Ridge (Map 5B). Besides these features, the bedrock shows few prominent lineaments, indicating a subdued topography covered by a veneer of sediment. The lineaments seen on the sonographs are generally faint and not very extensive.

The terraces south of Agate Reef and off Agate Bay (described in Chapter 2) generally show little topographic detail and very few distinct lineaments. The shoreface between Agate Embayment and Peacock Bay remains subdued with few distinct lineaments; several sediment-filled depressions extend offshore at right angles to the coast. These are about 100 m long and vary in width between 10 m and 30 m. Towards Peacock Bay the bedrock becomes more rugged and long lineaments (>200 m) trend in several directions. The two dominant directions are towards the northwest and northeast. Many short lineaments and associated shadow-zones indicate that the bedrock is not as extensively covered by sediment as is found, for example, on the terrace nearby. The two predominant directions for the lineaments may be a function of the two surveys that cross each other at high

angles in this area (Map 1). Onshore, the bedrock lithology changes from phyllites and schists of the upper stage of the Holgat Suite between Cape Voltas and Peacock Bay (De Villiers and Söhnge, 1959) to the schistose quartzites that form the Buchu Berg Twins and the prominent northeast trending ridge farther inland (Map 2) and conglomerates of the Holgat Suite farther south (Fig. 1.10). The change in bedrock sonograph "texture" mirrors this change in onshore lithology.

The 100 m-wide strip of bedrock that fringes Buchu Bay dips steeply down to the sediment cover which lies at about -16 m. It shows few lineaments and the sediment contact is very indented (Map 5B).

The subdued eastern section of Peacock Bank has lineaments similar to those found along the shoreface outcrop. The lithology is probably the same, i.e. schists and phyllites with a predominant northeast-southwest structural pattern. In contrast bedrock in the western part is characterized by numerous rounded features that cast broad acoustic shadows, indicating a rugged topography (Maps 5B, 3 and Plate 4.3). Few lineaments are present and where there are no rounded features, the bedrock surface has a distinct "granular" texture. The rounded features are aligned in a northwest-southeast and northeast-southwest direction, forming prominent ridges 150 m to 300 m wide. The ridges can be followed for over 200 m and rise between 3 and 5 m above the surrounding bedrock. This "granular", rounded sonographic pattern is very similar to sonographs described by Flemming (1976b, Fig.17) which were recovered from an area of granitic outcrop near Cape Town. Peacock Bank lies directly west of the Swartbank granite pluton (cf. Fig.1.10) and approximately

12 km from the closest granitic outcrop onland. Bedrock forming the western part of Peacock Bank is therefore tentatively interpreted as a submarine outcrop of the Swartbank Pluton. This pluton forms part of the Cape Granite Suite (SACS, 1980, p489) and is estimated to be 525 ± 60 my. old (from a date obtained on the genetically related Kuboos Pluton (Allsopp et al. 1979) farther inland). Peacock Bank is also aligned with the northeast-trending thrust fault exposed at Cape Voltas (Fig.1.10).

The inner shelf from Homewood Harbour to Rietfontein Embayment consists of bedrock covered by a thin veneer of sediment. The outcrop between Collins Embayment and Collins Reef (Map 5B) has a very subdued topography with few lineaments, the bedrock being covered by a thick veneer of sediment. This zone stretches from Collins Beach westward for almost 1 km and in places is over 500 m wide.

Collins Reef is very rugged only locally along the crest where it is devoid of sediment (Map 5B). Lineaments criss-cross this sediment-free area, but only a few are continuous for more than 50 m. The general trend is north-south or NNE-SSW. The extensive lineaments at Collins Reef trend northwest-southeast, parallel to the orientation of the jointing in the bedrock onshore. These continue for over 200 m and have eroded to form gullies seen as lineaments on the sonographs.

The bedrock south of Collins Reef (Map 5B) has few prominent lineaments. Where present, the lineaments are faint, closely spaced, generally parallel-aligned and with no prominent acoustic shadow-zones, thus generally reflecting a subdued microtopography. These lineaments usually trend NNE-SSW. Locally, at the crests of ridges, the bedrock microtopography is

rugged and numerous lineaments cross in several directions, but they are not very extensive.

The shoreface off Rietfontein has prominent, NNE-SSW to north-south trending lineaments that continue for almost 200 m. These contrast with the lineaments at Collins Reef which have a northwesterly orientation. More sub-parallel, short lineaments, that frequently have a shadow zone associated with them, indicate that the microtopography is rugged. Several sediment-filled depressions are associated with the prominent lineaments (Map 5B, 4).

The bedrock across the -30 m terrace (Map 5B, 5), is subdued with few lineaments or other reflectors. However, Kloppers Reef shows several extensive lineaments running northwest-southeast, interpreted as fracture or joint gullies, with another set of shorter, less prominent but more numerous lineaments trending north-south reflecting the bedding plane schistosity (De Villiers and Söhnge, 1959). Several sediment-filled channels extend southward across the inner-shelf slope with smaller channels trending southwest or northwest. Lineaments trend both NNE-SSW and NNW-SSE. The more prominent lineaments generally continue for over 400 m (Map 5B, Lines 15, 16 and 19).

4.4 Rietfontein to Wreck Point. (Map 5C)

At Rietfontein the shoreface bedrock north and south of the embayment is generally sediment-free and numerous short (<100 m), parallel lineaments, trending north-south are present. These usually have an acoustic shadow zone associated, indicating a rugged micro-topography. These lineaments are cut by more continuous lineaments that have a curving outline and trend

north-south to northwest-southeast and are interpreted to be intrusive dykes. The seafloor along the northern edge of the embayment varies from rugged, with many distinct but short lineaments on the ridge crests, to very subdued, with very few lineaments. Farther seaward, south of Rietfontein Embayment there are fewer short, parallel reflectors and the continuous lineaments are absent; the subdued microtopography indicates a thick sediment veneer (Map 5C, 1). Nearer Boulder Reef the sonographs show only a few prominent lineaments. Here the short, finer, sub-parallel set of lineaments, extensively developed elsewhere, is found only on the crests of the ridges (Map 5C). The bedrock outcrop seaward of Rietfontein Embayment has several continuous and prominent lineaments. These trend northwest-southeast and cut across the crests of the ridges. The sediment-filled channels that extend south-southwestward across the inner shelf to the shelf edge are not well defined on the sonographs. The bedrock adjacent to the channels is topographically subdued, particularly offshore and a sediment veneer covers extensive area of the bedrock.

The northwestern edge of Gielie's Embayment (Map 5C) has many short, indistinct lineaments trending north-northeast; no prominent ones are present. Channels cut into the shoreface bedrock are generally sediment-filled. Along the shoreface and directly west of Boulder Reef, isolated patches of sediment are found on the bedrock (Map 5C, 2). Farther offshore the general trend of the short lineaments remains north-northeast, but a few cross-cutting lineaments are present and these trend north-northwest.

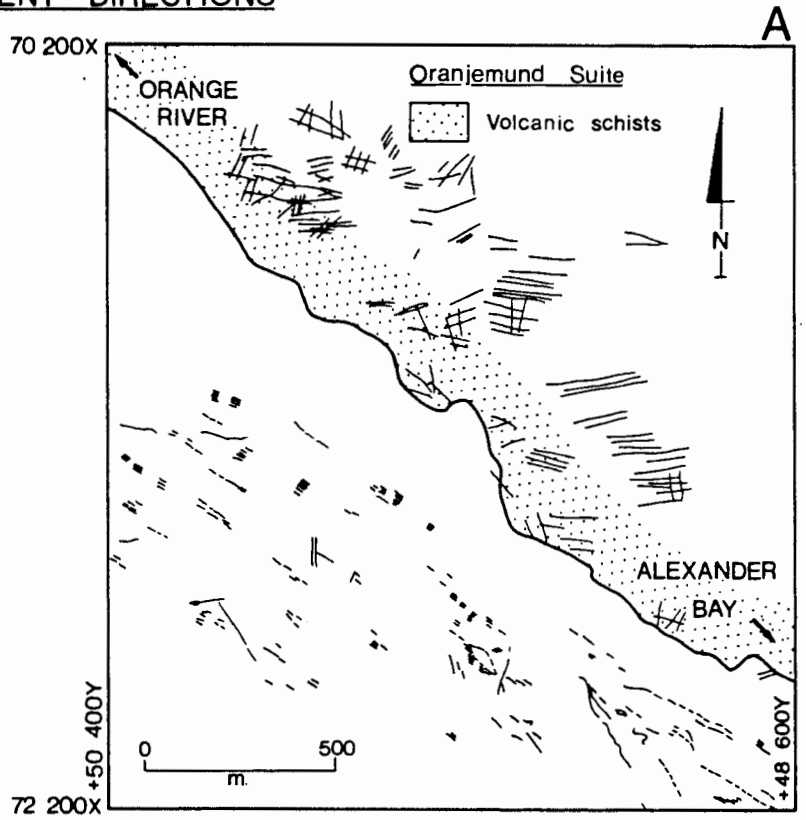
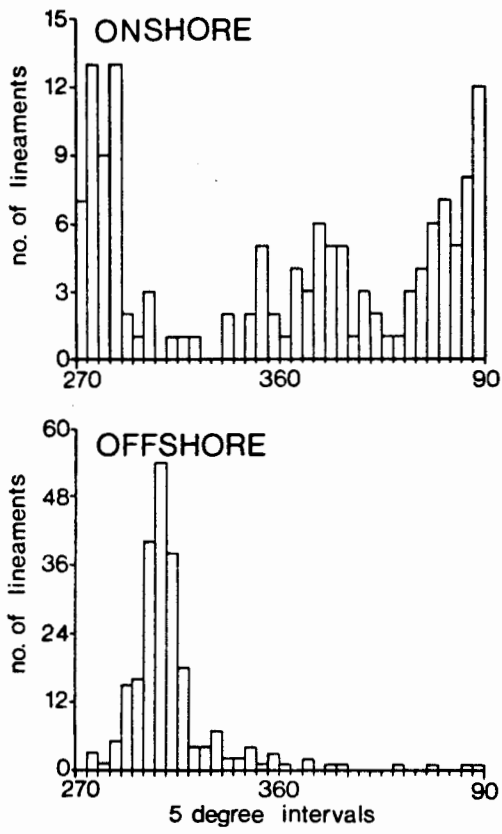
A major cross-cutting feature (Map 5C, 3 and Plate 4.1),

were investigated. Within the study area bedrock consists of indurated, resistant quartzites and conglomerates, greywackes easily-erodible phyllites, volcanics, tuffs and schists (cf Chapter 1). The more resistant lithologies, forming positive relief, give rise to some of the lineaments seen on the sonographs. Lineaments due to schistosity, foliation, jointing and faulting are visible on the sonographs only where erosion has etched them out to form gullies. Dolerite dykes frequently give rise to linear features on the sonographs as well. Secondary products of erosion and deposition may also result in linear reflectors on the sonographs: gullies, channels and wave-cut cliffs are examples. Intense deformation of the bedrock underlying the inner shelf (cf Chapter 1) gave rise to pronounced foliation and schistosity, roughly parallel to the bedding, that trends northeastwards with a shallow dip towards the northwest (Fig. 1.10). Jointing and fracturing of the bedrock is prevalent at between 320° and 340° (i.e. NW-NNW). Large parts of the bedrock onland have been denuded of sediment in the course of diamond mining, thus exposing the bedrock structures. Erosion gullies, along foliation and schistosity directions, ridges, dykes and bedding planes form lineaments that are readily traced from aerial photographs. Using 1:10 000 orthophotomaps, these onland lineaments have been transferred onto selected portions of the sonograph maps (Figs.4.2A-C). The trends of these onshore lineaments have been plotted at 5° intervals and compared with a similar analysis of the offshore lineaments. Histograms of the two data-sets show that both areas have preferred lineament directions, and by inference from the onland lineaments therefore, the inner-shelf lineaments can be interpreted. Wright

(1964) studying gully patterns on the raised beach terraces north of the Orange River, however found that there was little correlation between structural trends in the bedrock and the orientation of gullies.

Three areas were selected for analysis of onland-offshore structural trends. The northernmost area lies between the Orange River and Alexander Bay (Fig. 4.2A). Here sediment covers most of the bedrock seaward of the -20 m isobath (Map 5A). Lineaments trend mostly parallel to the coast, whereas the onshore lineaments generally trend east-west. The onshore-offshore correlation of lineaments is therefore not very good. An oblique view of the Lower Terrace north of Alexander Bay (Plate 4.4) shows the predominance of northeast-southwest gullies over the much fainter NNW-SSE trend in foliation and jointing. If the microtopography is similar for the shoreface bedrock adjacent to the area shown in the photograph, the lack of correlation of lineaments can be ascribed either to, a) the gullies being filled with sediment from the Orange River, or, b) the unfavourable orientation of gullies parallel to the northeast-southwest scanning direction of the side-scan sonar. It is probably a combination of both. Slope gullies are the most commonly found gullies on the raised -beach terraces, but they are not nearly as abundant offshore. Wright (1964) found that the offshore gullies trend normal to the coast and have a regular spacing in any one area regardless of bedrock lithology or structure. The spacing may vary between 4.5 m and 10 m, but is seldom wider than 10 m. Their width to depth ratio ranges from 0.3 to 1.0, with the depth usually varying between 1 m and 6 m. The usual outline for this type of gully is U-shaped (Murray et al., 1970).

COMPARISON OF LINEAMENT DIRECTIONS



COMPARISON OF LINEAMENT DIRECTIONS

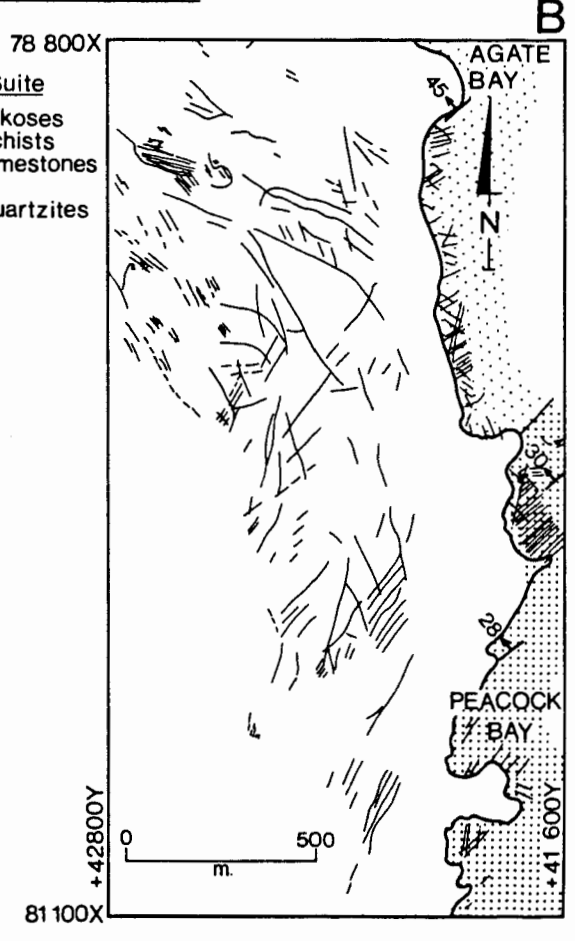
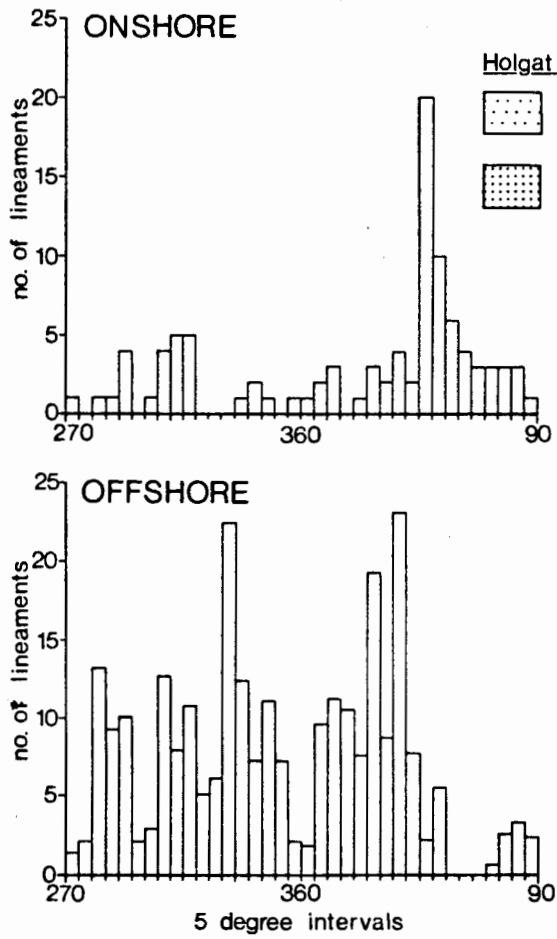


FIGURE 4.2

This type of gully is also very common on the terraces onshore at Alexander Bay (Plate 4.4), but it has not been identified on the sonographs of the adjacent area (Fig.4.2A). In other areas lineaments trending offshore are too few to suggest slope gullies. This conclusion supports Murray et al. (1970) who claim that slope gullies are not very common below sea level, bearing in mind that their coast-perpendicular orientation would make it difficult to detect them during a coast-parallel side-scan sonar survey scanning along their length. The best results would be from scanning lines perpendicular to the coast.

The centrally located area lies just north of Peacock Bay (Fig.4.2B). The onland area has lineaments on the orthophotomaps that arise from bedding planes, foliation, jointing and a few dolerite dykes. From Figure 4.3 it is deduced that the inner shelf lineaments trending northeast result from foliation and bedding planes. The dolerite dykes are shown as slightly meandering lines trending north-south, whereas jointing and fracturing occur as two sets of lineaments orientated northwest-southeast and northeast-southwest. Dyke gullies, according to Murray et al. (1970), form as a result of the differential erosion of intrusive dykes and the contiguous country rock. The centre of the dyke would erode more easily, the chill-zones at the lithological boundaries forming the gully walls. A possible example from an area just south of Versuipgat Embayment (Map 5A, 2) has been described in section 4.2 and is shown on Plate 4.2. According to Murray et al. (1970) this type of gully is not commonly found, although it does appear to be common north of Peacock Bay. Fracture zone gullies may extend for several kilometres along fracture zones or faults. They are somewhat U-

shaped in outline and their depth and width are about equal. According to Murray et al. (1970) these are best developed in areas of finely foliated schists. This agrees with what is found in the study area. North of Peacock Bay the Holgat Suite is represented by phyllite and quartzitic schists which are followed at Cape Voltas by the Grootderm Suite consisting mainly of highly foliated volcanic schists. The bedrock displays numerous extensive lineaments extending north-south, parallel to the faulting exposed onshore (Fig.1.10). The thrust fault that separates the Grootderm from the Holgat Suite, entering the sea at Cape Voltas, does not show on the sonographs.

The most striking correlations found were between Giellie's Bay and Wreck Point where the bedding planes and the foliation both trend due north, whereas the jointing strikes east-west (Fig.4.2C). The lineaments on the inner shelf adjacent to this part of the coastline show the two orientation directions prominently displayed (Map 5C). According to the interpretation of Murray et al. (1970), joint gullies are generally found in harder bedrock and are often associated with wave-cut cliffs. The width to depth ratio of this type of gully is 0,3 to 0,25, with the depth ranging from 3 m to 5 m. The gully is usually pear shaped and the gully floor frequently has a little trough along the joint plane (Murray et al., 1970). The much more numerous north-south lineaments represent strike gullies, arising from erosion along foliation planes, parallel to the bedding. These gullies also occur in areas where the schistosity in the bedrock varies with the lithology, such as between Collins Reef and Rietfontein. Strike gullies assume a V-shaped outline; the width usually approximates to the depth (Murray et al., 1970).

COMPARISON OF LINEAMENT DIRECTIONS

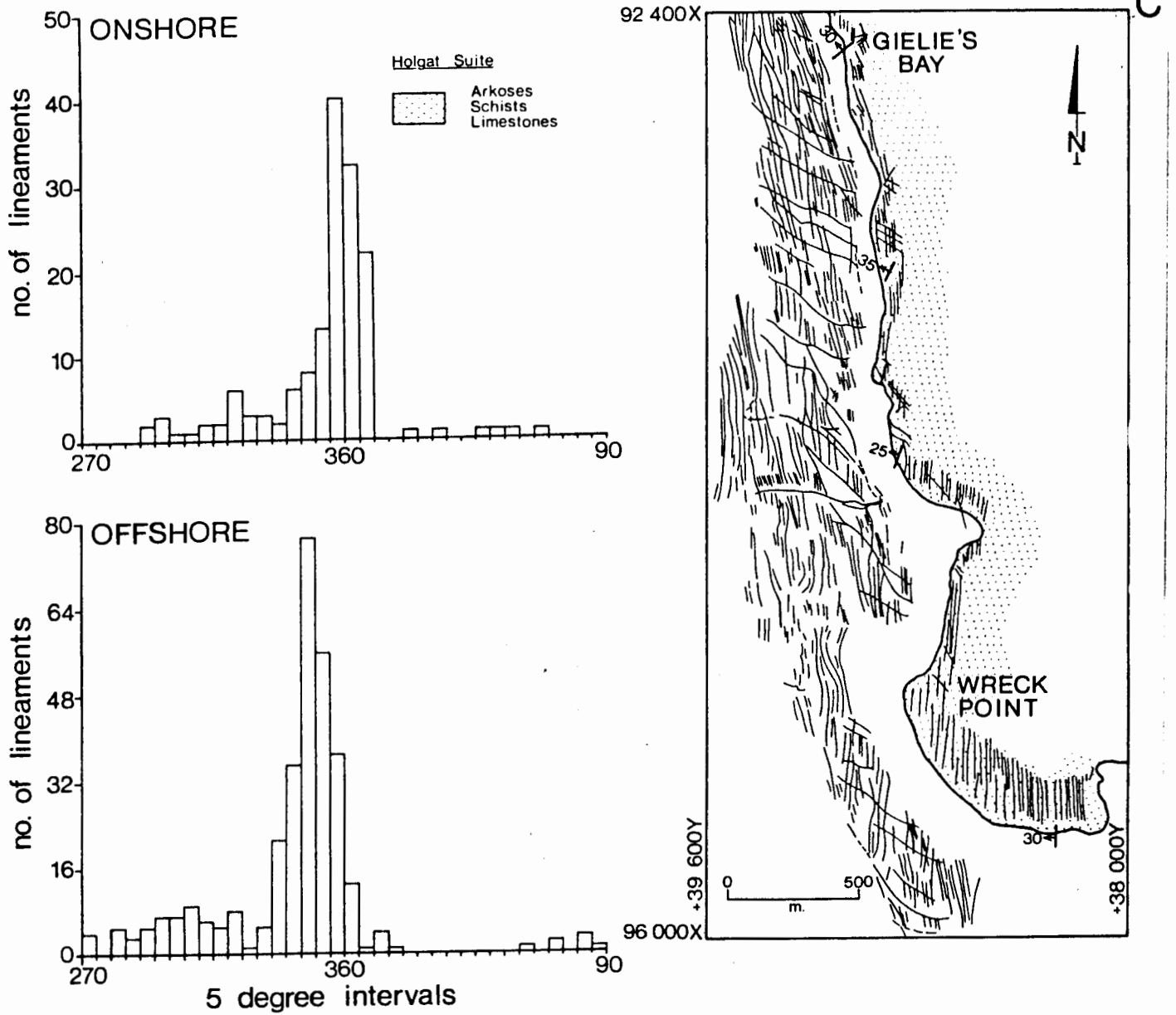


FIGURE 4.2

Murray et al. (1970) and O'Shea (1971) mention that north of the Orange River a wave-cut cliff up to 5 m high at approximately -20 m can be traced on sonographs for a distance of 20 km. They mention that it is closely associated with gullies that have cut across the cliff face. Murray et al. (1970, p.128) describe the feature as follows: "The cliff, which generally runs northwest and parallel to the present coastline, is composed of sections alternately controlled by the strike of the foliation and the direction of jointing." The irregular trend of the cliff-face, dissected by numerous gullies, makes it difficult to identify from numerous other lineaments. The cliff-face lineament will be best displayed in topographically subdued areas where bedrock lithology gives rise to a regular pattern of lineaments. The bedrock north of Peacock Bay, consisting of homogeneous quartzitic schists and phyllites of the Holgat Suite, and farther north, of volcanic schists from the Grootderm Suite, gives rise to a regular lineament pattern in which the lineament arising from a cliff-face may be recognized. Plate 4.5 shows a meandering, coast-parallel reflector off Cape Voltas, interpreted to be the cliff-face at -20 to -24 m.

4.6 Conclusions

The inner-shelf bedrock has been shaped by wave-action and, to a much lesser extent, fluvial processes, mostly during the Quaternary. The resultant morphology shows the presence of marine terraces, wave-cut cliffs and associated gullies on these terraces and sediment-filled channels of possible fluvial origin. From the sonographs it is possible to identify and delineate these features and then to comment on their diamondiferous

potential.

The position and orientation of gullies and other bedrock microtopographic features are very important factors in the entrapment of diamonds on the inner shelf. Gullies trending northeast, that is, parallel to the propagation direction of the incoming ocean swell, are more likely to contain diamondiferous deposits (Gurney et al., 1982). Northeast-trending strike gullies, fracture gullies and possibly dyke gullies therefore appear to be the most promising in terms of diamond recovery.

The significance of wave-cut cliffs is apparent, considering the location of relict beach deposits which are very likely to be diamond-bearing since diamondiferous deposits are generally concentrated in the high-energy surf zone. Analysis of sonographic records only will not disclose the most promising diamondiferous area. A comprehensive program of "ground-truthing" sonographic interpretations using video-cameras, photography and diver-investigations, is required. This must be followed by an analysis of the economic returns based on the systematic exploration of those areas considered, from sonographs, to be potentially diamondiferous. The results could indicate whether sonographs could be used to predict, a priori, diamondiferous deposits.

PLATE 4.1

Sonograph displaying various seafloor features.

Locality: Boulder Reef. (Map 5C).
Line 14C: 50 - 55. (Map 1).

Explanation: a - gravelly, coarse sand.
b - fine-grained sand.
c - gullies in bedrock outcrop.
d - channel.
e - bedrock lineaments.
f - cross-cutting feature (possibly fractures) in bedrock.
g - open folding in bedrock.
h - fish shoal.

PLATE 4.2

Sonograph image of lineaments in bedrock, interpreted as a dolerite dyke.

Locality: Versuipgat Embayment. (Map 5A).
Line 205: 1422 - 1424. (Map 1).

Explanation: a - cross-cutting dolerite dyke, showing two parallel reflective sides.
b - megaripples; wavelength $+1,5$ m; amplitude $+0,5$ m.
c - megaripples covering subdued bedrock.
d - rugged bedrock, (2 to 5 m relief).
e - fine-grained sand.

PLATE 4.3

Sonograph image of part of Peacock Bank, showing different bedrock reflectors.

Locality: Peacock Bank. (Map 5B).
Line 10: 937-947. (Map 1).

Explanation: a - Rounded, "granular" reflectors, typical of very rugged granitic bedrock.
b - sediment-filled channel.
c - subdued bedrock (<2 m relief) with prominent lineaments, typical of phyllites and schists.

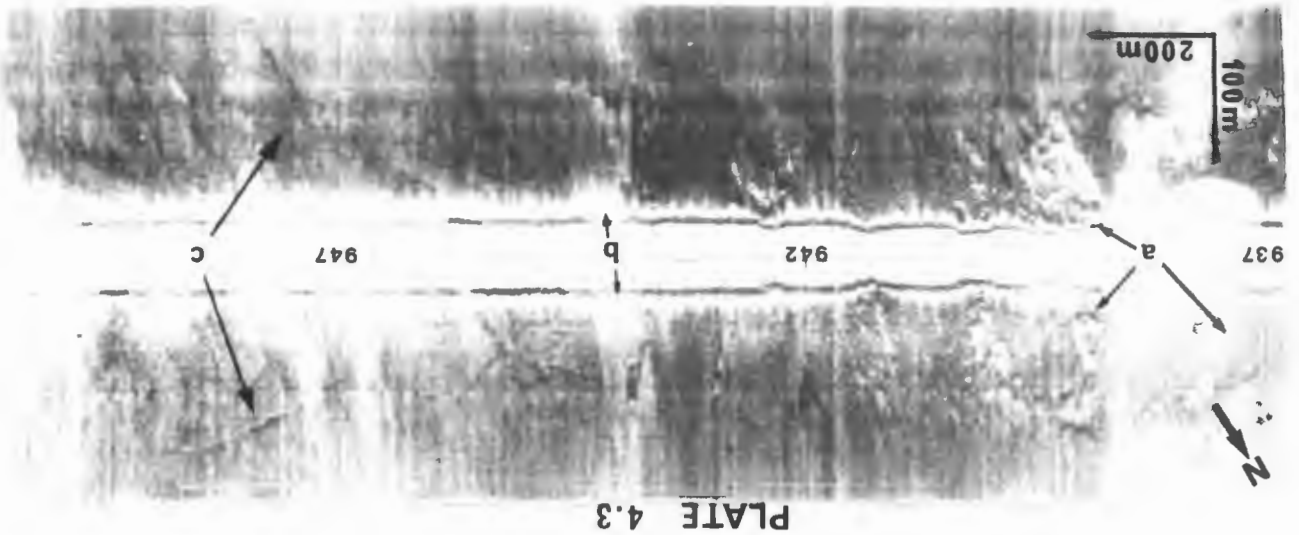


PLATE 4.3

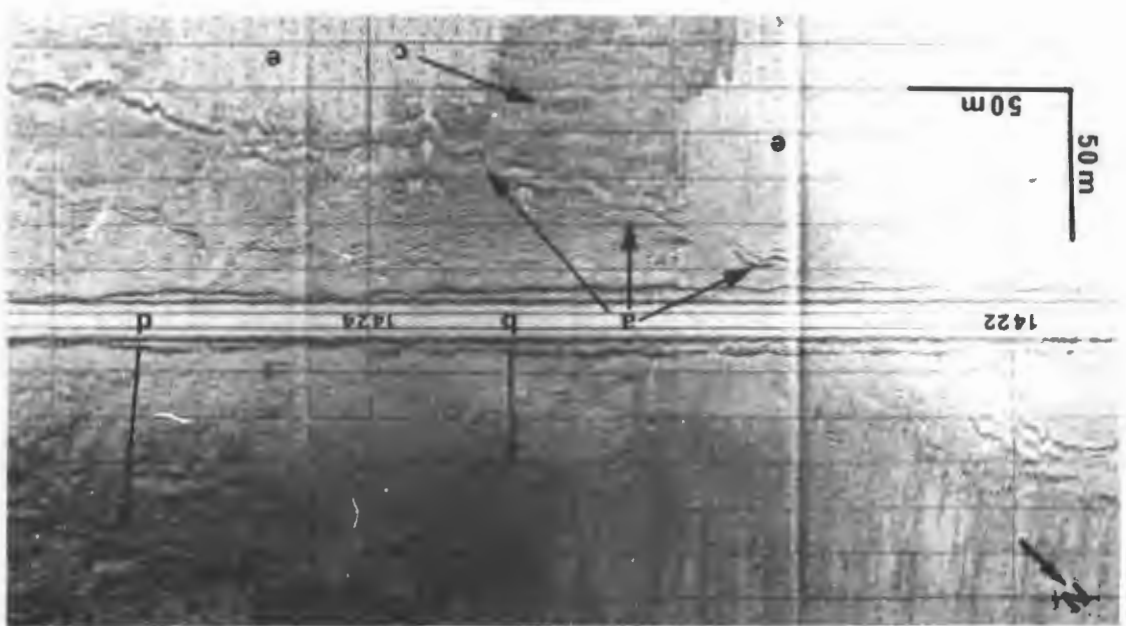


PLATE 4.2

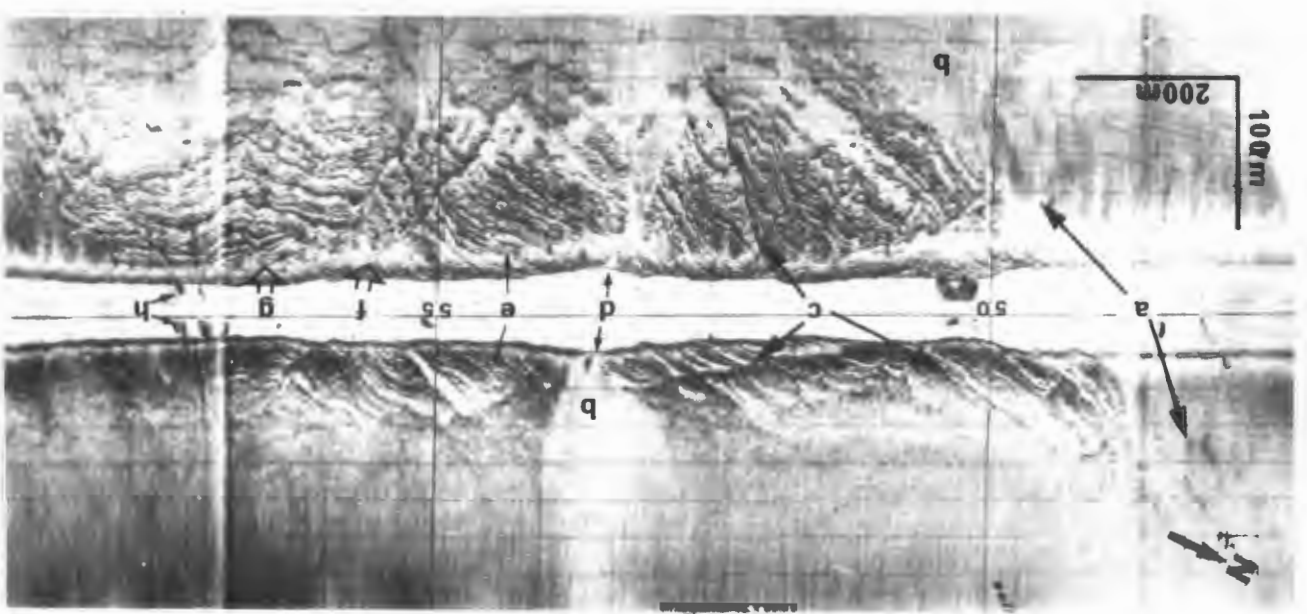


PLATE 4.1

PLATE 4.4

Oblique view of Lower Terrace gullies.

Locality: Alexander Bay, facing west-northwest.

Explanation: a - SW-NE trending slope-gullies on the Lower Terrace. Gully-spacing approximately 5 to 10 m; gully width 2 to 5 m.

PLATE 4.5

Sonograph showing a bedrock lineament, interpreted as a wave-cut cliff.

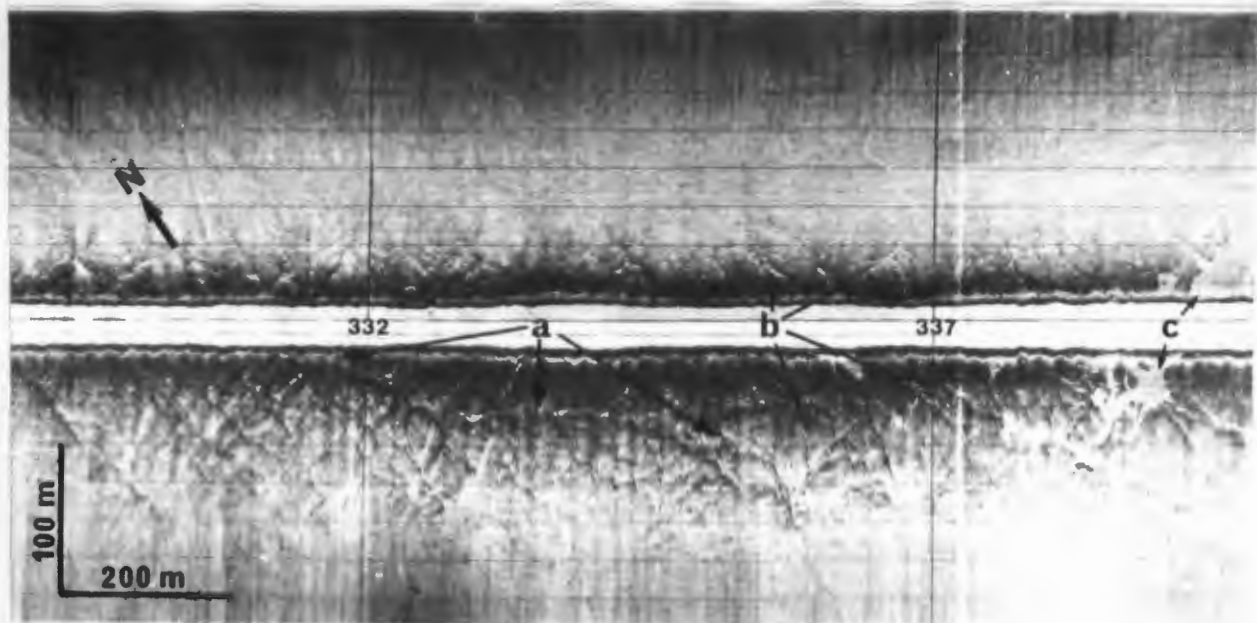
Locality: Seaward side of Voltas Reef. (Map 5A).
Line 4: 332 - 337. (Map 1).

Explanation: a - lineament representing wave-cut cliff with base at +24 m.
b - fracture and jointing gullies.
c - sediment-filled channel.

PLATE 4.4



PLATE 4.5



CHAPTER 5SEISMIC STRATIGRAPHY5.1 Introduction

Having focussed with increasing detail on bedrock morphology in the preceding three chapters, we now turn our attention to the sediments on the inner shelf. In Chapter 5 we shall study the dimensions and seismic stratigraphy of the thicker sediment bodies, whereas in Chapter 6 we shall discuss the sedimentology of grab samples from the upper surface of these sediment bodies. Wave data will be evaluated in Chapter 7 to explain the formation of sedimentary bedforms. The thesis is concluded in Chapter 8 with a discussion of the evolution of diamondiferous sediments in the study area.

Data from all the cruises (cf Appendix) were originally plotted onto 1:10 000 scale basemaps. No tidal corrections were made because the west coast is a microtidal region (<2 m tidal range) with a spring-tide range of only 1,8 m (Heydorn and Tinley, 1980). This is within the resolution of the seismic records recovered, considering the relatively high-energy wave conditions along the west coast.

The 3.5kHz EDO WESTERN pinger used in the study area is ideally suited for silty sand and muddy deposits, giving a theoretical resolution down to 20 cm and a theoretical maximum penetration of up to 50 m (D'Olier, 1979). In the study area the maximum penetration of 30 m was obtained in the sediments of the Orange Delta. Elsewhere, the sediment cover on the inner shelf was thin enough to allow penetration to bedrock. Within the

corrections were made for the change in the velocity of the acoustic pulse from water into unconsolidated sediment. The conventional value of 1500 m/s was assumed for all calculations, although the velocity in unconsolidated sediments may vary between 1519 m/s in silty clay to 1836 m/s in coarse sand (Hamilton, 1979; D'Olier, 1979). The thicknesses involved are such that the correction would have been within the limits of resolution of the records. However, the thicknesses should be regarded as minima since a minimum sound velocity has been assumed.

Subbottom seismic reflectors arise from the partial reflections of the acoustic pulse. The strength of the return signal is dependant on several factors. Most important is the compaction, grain size and porosity of the sediment. In addition, the frequency of the sound source will determine the reflectivity of the horizon in question. The resolution of the records is determined by the frequency of the sound source; the normal frequency range for subbottom profiling is between 0,2 and 14 kHz (D'Olier, 1979). Higher frequencies will permit better resolution, but the energy will be more rapidly attenuated and therefore penetration will be more limited. Penetration is improved by using lower frequencies allowing more energy to be transmitted, but the result is a loss in resolution.

A consequence of selecting the high-resolution 3,5kHz seismic system used for the survey is that penetration of the subbottom suffers. Sargent (1969) observes that seismic profilers with frequencies below 3,5 kHz achieve similar "acoustic penetration" in most sediments, whereas using frequencies above 3,5 kHz e.g. a standard 12kHz echo-sounder,

only muds are acoustically transparent. This study shows that at times the signal did not reach bedrock, but was completely reflected by an internal horizon of cemented sediment or "false bedrock" as described by O'Shea (1971). Penetration was however also limited in the compact delta-front sands and the sediments found in the embayments.

Lines extending across the inner-shelf slope show the seismic stratigraphy of the Orange prodelta in detail; in places four internal horizons were penetrated before bedrock was reached. The seismic coverage across the prodelta deposits (mainly terrigenous muds and therefore acoustically transparent) (Rogers, 1977) is however restricted by the ABL near the surface of the sediment (O'Shea, 1971), masking all reflectors beneath it. The shoreward boundary of this layer is sharp and rises steeply from the bedrock. This acoustic impedance zone does not allow penetration of any seismic signal, irrespective of the signal's energy or frequency (at least for the range generally used).

5.2 Sediment isopachs to acoustic basement

5.2.1. Orange River to Cape Voltas (Map 6A)

Map 6A shows that the sediment isopachs on the inner shelf between the Orange River and Cape Voltas generally mirror the bedrock contours (cf Map 4A). The prominent channel extending seaward just south of the Orange River is clearly displayed, with sediment up to 14 m thick within the channel. Likewise, the channels north of Tripp Shoal and between the outcrops forming the shoal (Fig.5.1) are reflected in the increase in sediment thickness (Map 6A). This is also found for the sediment isopachs within the sediment-filled embayments at Alexander Bay,

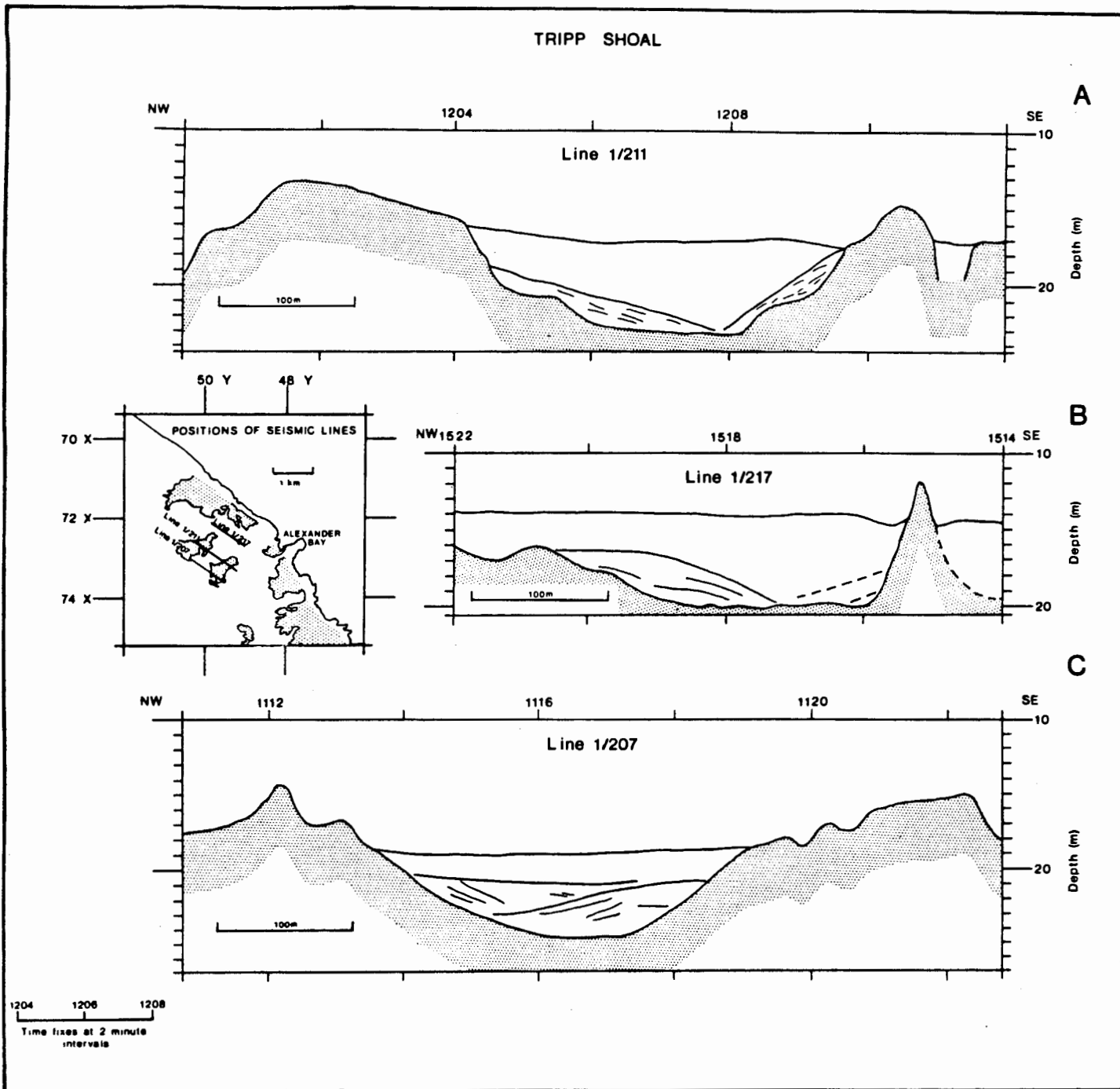


FIGURE 5.1

Versuipgat and Voltas.

The average sediment thickness seaward of the shoreface bedrock outcrop is 4 m, increasing locally to 8 m in bedrock depressions (Map 6A). On the shoreface outcrop itself, several large (at least 500 m²) sediment deposits are identified from the sonograph records, but are not resolved on the seismic records, indicating a sediment thickness of less than about one metre. These sediment patches correspond with the "sediment-covered bedrock" areas described in Chapter 4.

The tielines extending offshore (Map 6A and Fig.5.2) indicate that the sediment steadily increases in thickness seaward, but decreases in thickness southward away from the Orange River Delta. Over the -40 m terrace the average isopach value is 20 m (Fig.5.2A); in comparison, the sediment thickness over the same terrace farther south (Fig.5.2C) is only 12 m.

5.2.2. Cape Voltas to Rietfontein (Map 6B)

The isopachs in Long Beach Embayment increase for 500 m seaward to 7 m, after which the sediment thickness reduces to about 4 m. The isopachs thereby outline a 200 m wide sediment body with the axis of maximum thickness lying coast-parallel. The area west of Long Beach Embayment and south of Voltas Reef is covered by 2 to 3 m of sediment, increasing to a maximum of 7 m along the southern edge of Voltas Reef.

Farther south, the sediments on either side of Lone Ridge have isopach values of 6 m, decreasing to 3 m on the seaward edge of Agate Embayment and 4 m farther offshore. Sediment thicknesses of only 2 m are found over the buried bedrock ridges seaward of the shoreface outcrop south of Agate Reef (Map 6B). The maximum isopach values in Buchu Bay lie towards the shoreward

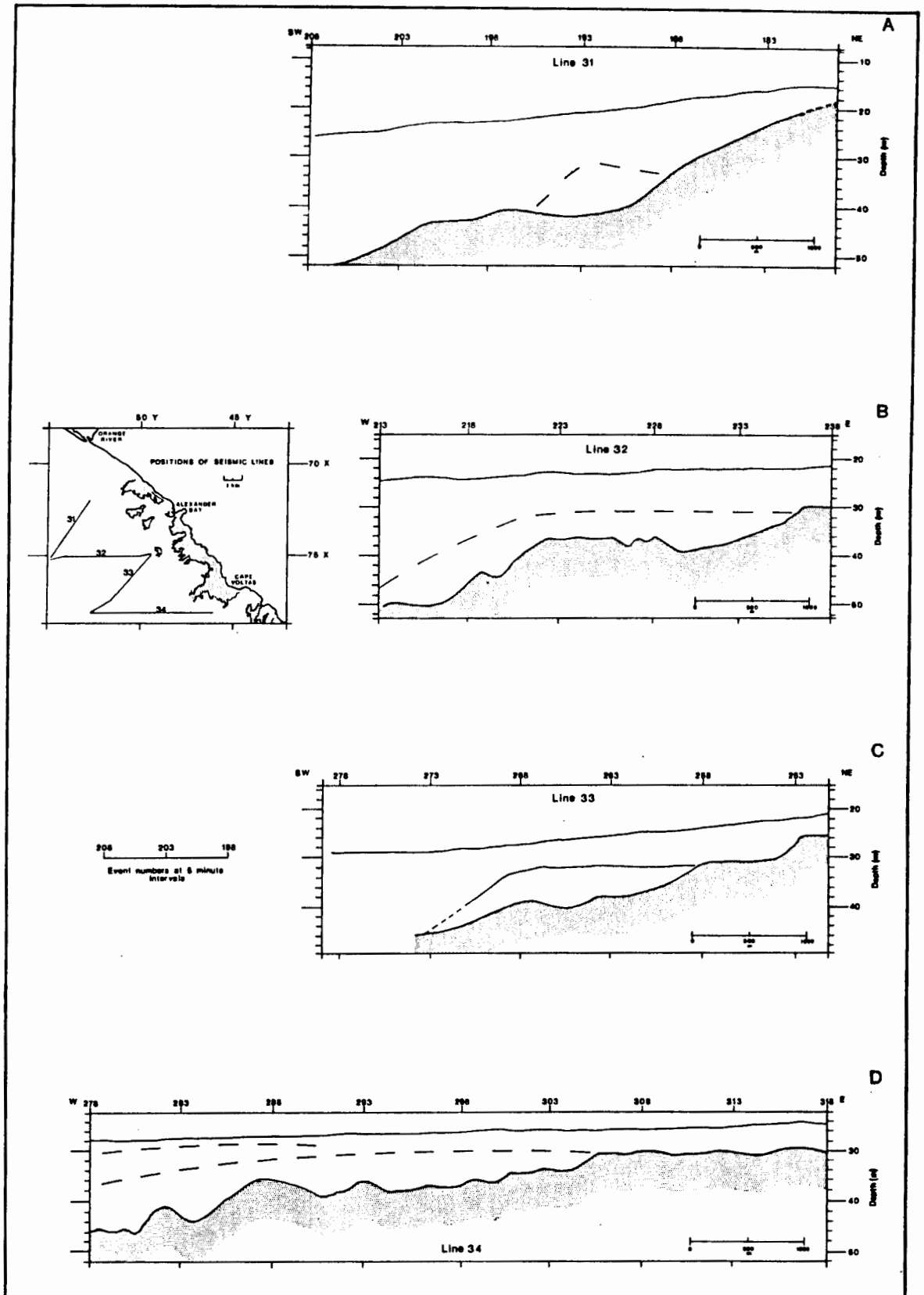


FIGURE 5.2

edge of the sediment body in the bay, attaining a thickness of 6 m. Farther seaward the isopachs show a decrease in sediment thickness to about 4 m and even less over the bedrock ridges. The channels cutting towards Agate Bay and Peacock Bay into the shoreface bedrock contain up to 4 m of sediment in them (Map 6B). Figure 5.3 shows that the sediment thickness decreases seaward from Homewood Harbour, bedrock eventually cropping out along Line D3 towards Kloppers Reef (Map 6B).

Lines 1 and 10 (Map 4B) that run from Homewood Harbour across Peacock Bank, indicate a maximum thickness of 5 m of sediment on the shoreward side of the bank; the average isopach value is between 2 and 3 m. The sediment cover also decreases in thickness southward from Peacock Bank. Only the channels on either side of the north-south trending Kloppers Reef have any appreciable amount of sediment, the isopachs showing a cover of up to 5 m.

Sediment reaches a thickness of between 7 and 8 m on the seaward side of Collins Embayment. Farther inshore poor-quality seismic records mask any indications of bedrock. From Collins Reef to Rietfontein Embayment the inner shelf has no seismically identifiable sediment cover, except for the channels that cut towards the inner-shelf slope. These channels contain less than 3 m of sediment (Map 6B).

5.2.3. Rietfontein to Wreck Point (Map 6C)

Sediment in the southern section of the study area is restricted to large embayments off Rietfontein and Gielie's Bay, the channels that extend seaward to the inner-shelf slope and the Orange prodelta muds abutting against this slope.

Within the embayments the isopachs generally reflect the

seaward slope. Within the sediment between the shoreface bedrock outcrop and Tripp Shoal, a reflector is draped in a lobate fashion southeastward between -16 m and -19 m (Map 7A and Fig.5.1B). Sediment in the channel dividing the shoal has two separate reflectors over the north-western and south-eastern channel banks, dipping between -17 m and -23 m towards the centre of the channel (Fig.5.1A). Both reflectors extend for over 500 m along the length of the channel, but overlap only on the seaward side of the shoal (Fig.5.1C). Faint, reflective horizons generally parallel the outline of these sediment bodies, indicating progradational deposition of the bodies.

Seaward of Tripp Shoal a subhorizontal reflector dips coast-perpendicularly from -22 m to -26 m, extending laterally for over 2 km southwestward to a bedrock outcrop off Versuipgat Embayment (Map 7A). The embayments at Alexander Bay, Versuipgat and Voltas have gently seaward-dipping reflectors, lying between -16 m and -19 m for the first two embayments and from -21 m to -25 m in the latter. The reflectors lie 2 to 5 m below the seafloor in the embayments and increase by about a metre in depth at the centre relative to the edges of the embayments.

Figure 5.2A to D shows the internal reflectors along the tielines run in this section of the study area. The reflectors all abut bedrock at approximately -30 m, continue with a subhorizontal aspect for between 1 km and 3 km seaward, before increasing in gradient to pinch out against the bedrock at about -40 m to -50 m below sea level. The horizon is generally not more than 10 m above the bedrock, whereas the overburden can be as much as 24 m.

5.3.2. Cape Voltas to Rietfontein (Map 7B)

Long Beach Embayment has a subbottom horizon on its shoreward side that extends the width of the embayment and is continuous seaward between -15 m and -19 m below sea level. A similar reflector is found on both sides of Lone Ridge in Agate Embayment. Here the horizon extends from -13 m to pinch out against the bedrock at -18 m. The other embayments and the sediments in Buchu Bay do not have internal reflectors at depths shallower than -20 m.

Between -24 m and -28 m at the seaward edges of all the embayments and particularly in Boulder Bay, there is a prominent seaward-dipping horizon. Although the reflectors are not continuous from one embayment to another (Map 7B), the constant depth-interval suggests that they formed concurrently. The sediment bodies encompassed by the reflectors do not show any internal feature.

Tielines D3 and D5, that run seaward from Peacock Bay and Homewood Harbour respectively (Fig.5.3), reveal several reflectors dipping offshore. On the shoreward side of the lines steeper-dipping reflectors correspond in depth to the subbottom horizon contoured in Buchu Bay (Map 7B), but the subhorizontal reflector present farther seaward is not seen on the coast-parallel survey lines run during cruise TBD 405. Tieline D4, extending offshore from Long Beach Embayment (Fig.5.3A), has several gently seaward-dipping, subparallel horizons at approximately -27 m to -32 m, partially overlapping each other. Each reflector is continuous for over 400 m before it pinches out against the bedrock. These reflectors correspond in depth and attitude to the subhorizontal reflectors on Lines D3 and D5 and

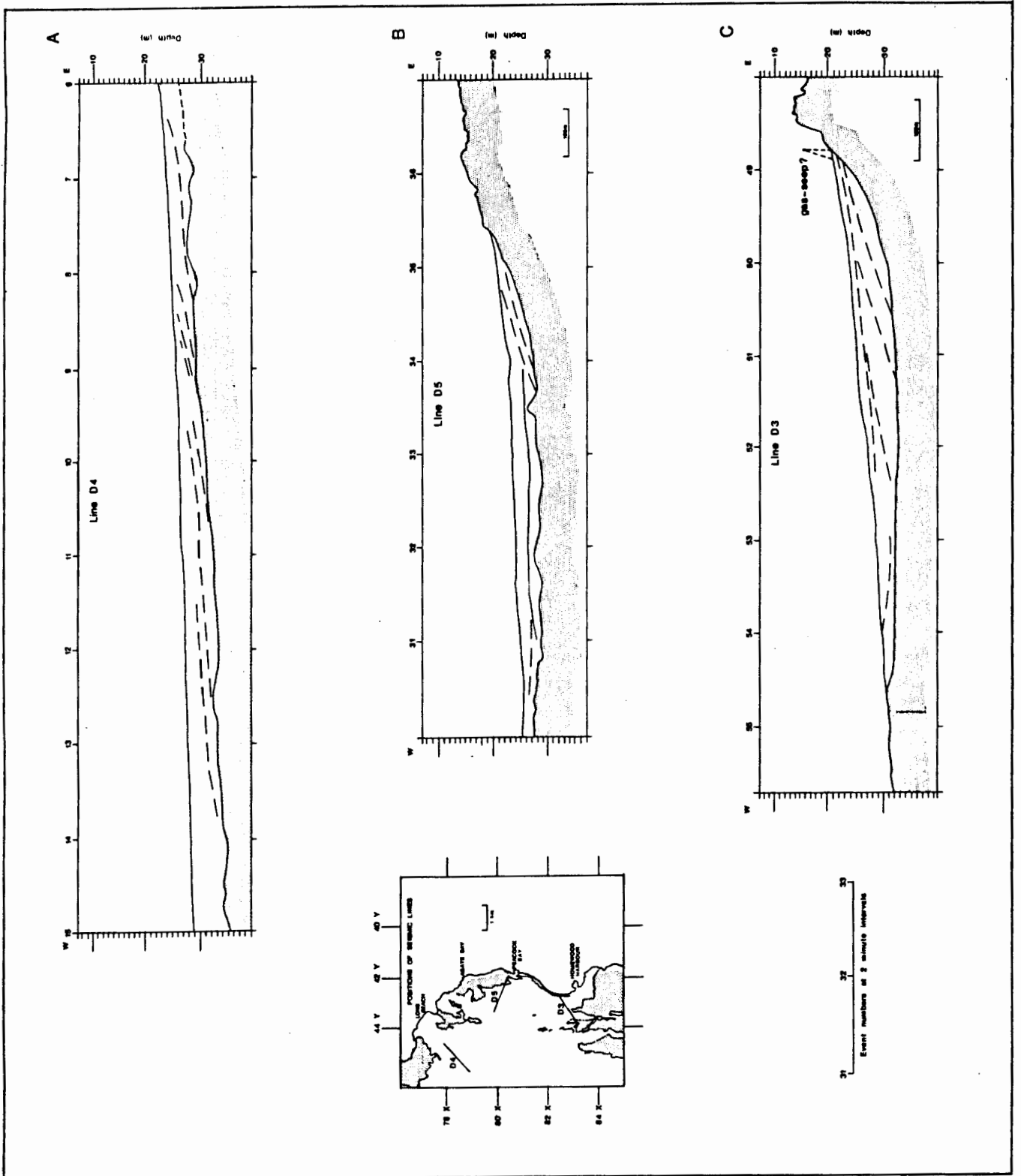


FIGURE 5.3

are probably of the same origin. Towards Peacock Bank another subhorizontal reflector is present at -32 m (Map 7B, Line 1), continuing at that depth to the edge of the bank. Seaward of Peacock Bank, along the same line, are two horizons. The upper one is continuous and extends from -30 m to -35 m, whereas the other horizon remains between -33 m and -36 m, but appears to be discontinuous on the record.

South of Peacock Bank the tielines (Map 7B, Lines 15, 19 and 20) show three continuous, subparallel reflectors between the inner-shelf slope and the ABL in the sediments of the Orange prodelta. The horizons have a seaward dip of $0,1^{\circ}$ to $0,3^{\circ}$ and all end on their shoreward side against bedrock. The abutment point increases in depth southward: the upper horizon lies at -38 m on Line 20, -43 m on Line 19 and -50 m on Line 15; the middle and lower horizons abut in the same direction at depths of -41 m, -44 m and -53 m (middle), and -44 m, -48 m and -57 m (lower) respectively.

The ABL is found at the seaward ends of the tielines south of Peacock Bank (Maps 7B and C). Its shoreward boundary is typically steep, rising from bedrock to just below the seafloor. It extends beyond the seaward limits of the tielines and appears to continue for several kilometres offshore (cf Fig.3.1, and O'Shea, 1971; Rogers, 1977 and Birch, in prep.).

5.3.3. Rietfontein to Wreck Point (Map 7C)

Subbottom reflectors are restricted to the two embayments and to the Orange prodelta deposits seaward of the inner shelf-slope.

In Rietfontein Embayment the subbottom horizon, which first appears 300 m from the shore, dips from -23 m to end within the

sediment body 500 m farther offshore, at -28 m. The reflector remains about 2 to 3 m above the bedrock and dips seaward at less than $0,6^{\circ}$ (1:100), increasing somewhat in gradient on the seaward end. Laterally this reflector extends across to abut against the rising bedrock forming the northern and southern boundaries.

No horizon is found at the western end of the embayment, seaward of the ridge dividing the embayment, although up to 8 m thickness of sediment is found here (Map 7C). Internal reflectors are also absent from the channels that continue southward from the embayment, although the sediment deposit reaches a thickness of 8 m in them.

Where the subbottom horizon in Giellie's Embayment lies shallower than -20 m it appears only locally, straddling the palaeo-channel cutting through the embayment (Map 7C). From -22 m to -29 m the horizon is more extensively developed. It continues across the width of the embayment in the north and extends southward for about 2 km, remaining on the shoreward side of the ridge jutting into the embayment from the south. As in the embayment at Rietfontein, there are no reflectors present seaward of the ridge dividing Giellie's Embayment; in both areas the seafloor lies at -25 m to -30 m.

Although described as one horizon, the subbottom reflectors present may in fact be two separate horizons. Figure 5.4 shows that other reflectors, limited to bedrock depressions, are also present. It is not possible to contour the lower reflectors as they are too limited in areal extent and occur only on the lines depicted in Figure 5.4. Line 715 shows the lower reflector at -24 m extending subhorizontally across the palaeo-channel; the other two lines show this horizon present only along the edges of

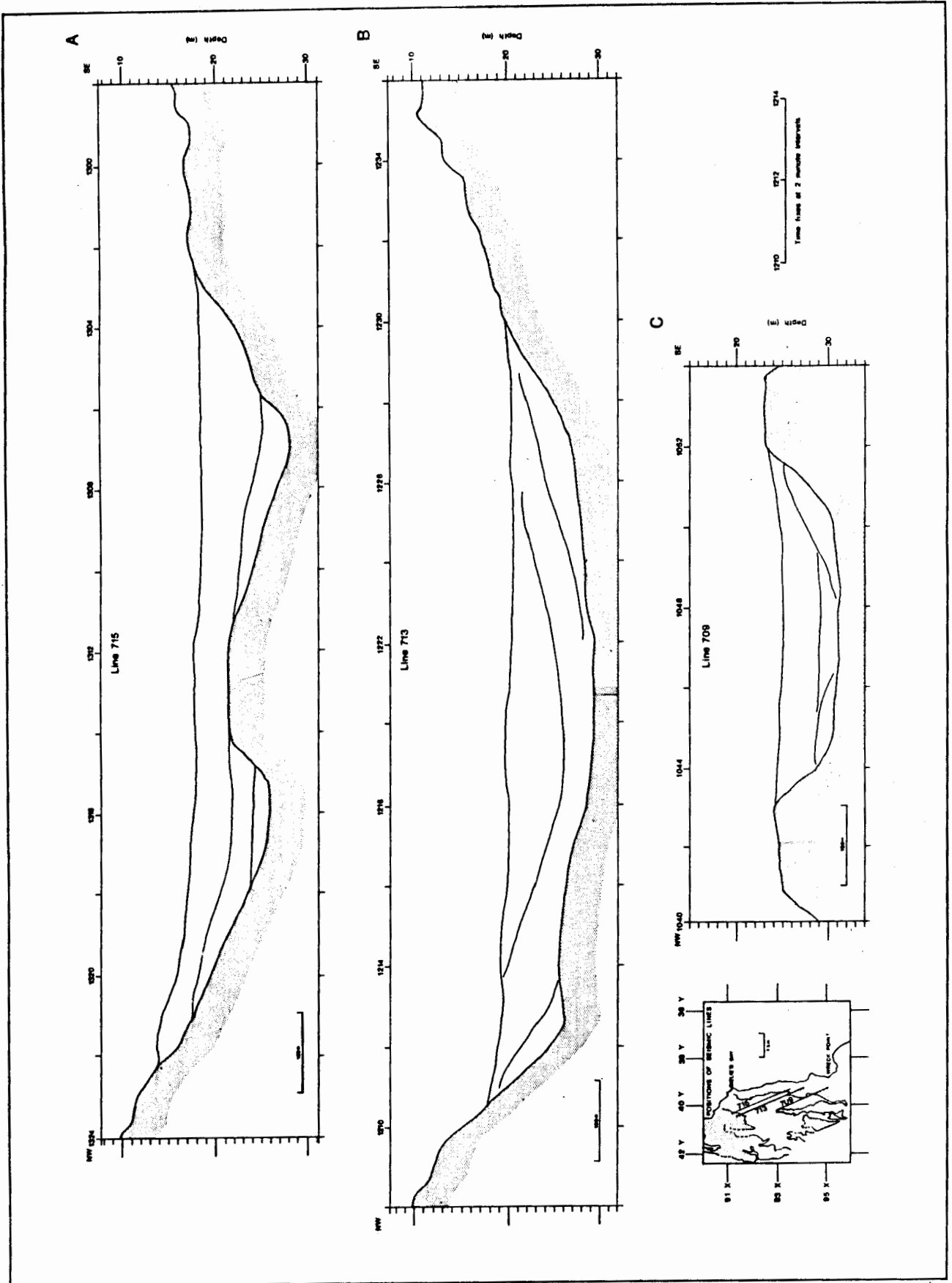


FIGURE 5.4

the bedrock depressions.

Reflectors within the Orange prodelta sediments, recorded on the tielines, are similar in attitude to those farther northward and described above. Off Rietfontein (Map 7C), Lines 16, 17 and 18 have four subparallel horizons that are very gently inclined seaward. All the reflectors except the topmost one are attenuated by the ABL. The depths at which the horizons abut against the bedrock is -50 m for the upper, then at -52 m for the second, -55 m for the third and -58 m for the lowermost one. The depth does not increase southward, contrary to what was found along Lines 15, 19 and 20 (Map 7B). Lines 26A to E have only one subbottom horizon, about 3 m below the seafloor. The ubiquitous ABL rises steeply for about 5 to 10 m from the bedrock, then levels off seaward to continue offshore parallel to the reflector, but 5 to 10 m beneath it. The contact between the ABL and bedrock increases in depth southward: -60 m off Rietfontein and -83 m off Wreck Point (Map 7C). The subbottom horizon abuts against bedrock at -60 m in the north and increases to -65 m off Wreck Point. It maintains a seaward gradient on Lines 26A to E of 1:400 ($0,14^{\circ}$) or even less. The horizon seems to be cropping out at -63 m along Line 26E, but the seismic record is not clear enough to show it convincingly.

5.4 Discussion

On the inner shelf the isopach values show that within the confines of the shoreface outcrop, the Precambrian bedrock is covered on average by 6 m of sediment, mostly confined to embayments. North of Homewood Harbour, the sediment is present

as a seaward-thickening layer on the bedrock, maintaining a thickness of approximately 10 m over the -30 to -40 m terrace, but increasing rapidly to form the main body of the Orange Delta as bedrock dips away to form the inner-shelf slope (Fig.5.2A to D). The relatively thin deposit covering the terraces could be attributed to the high-energy wave regime on the inner shelf preventing deposition of the very fine to fine terrigenous sand brought down by the Orange River (Rogers 1977) onto the delta front. In discussing the Orange prodelta muds, Rogers (1977) comes to the conclusion that the -40 m boundary between the delta-front sands and the prodelta muds is related to the wave regime. Preliminary studies of sediment transport on the inner shelf (Chapter 7) show that average wave conditions are sufficient to transport coarse sand as deep as -30 m below sea level, thus supporting Rogers' conclusions for the Orange Delta itself.

Estimating the sediment flux on the inner shelf in the study area is a subjective exercise with the data available. Sediment input is chiefly from the Orange River, with a minor contribution from the south through longshore drift. The contribution from the river itself is extremely variable. Rogers (1977) considers the average mass of sediment transported to the sea annually to be 60×10^6 t, but ranging up to 205×10^6 t per year. Rooseboom and Harmse (1979) showed that there has been a 50% decline in the sediment load, from 90.3×10^6 t in the 1930's to 41.5×10^6 t in the 1960's. However, as Rogers (1977, p.79) explains in detail, modern sediment yields are unnaturally high due to accelerated soil erosion and are "more indicative of sediment discharge during Late-Pleistocene interglacials than of modern conditions."

Extrapolating back in time, Hoyt et al. (1969) suggested that the sediment of the Orange Delta could have been deposited within 530 years, although the mouth has been in its present position for 5000 years. They conclude from this that most of the sediment deposited on the inner shelf by the Orange River is transported northward via longshore drift and wave-induced bottom currents with little remaining on the delta itself.

The lack of a general sediment cover on the inner shelf south of Homewood Harbour (cf Maps 6B and C) is also attributable to the high-energy wave regime and the paucity of sediment input from the south. Sediment bodies are restricted to embayments formed along possible palaeo-channels of the Holgat and other, now non-existent, rivers. The channels are reflected in the increase in isopach values. The conclusion drawn from the absence of delta-front aggradation north of Homewood Harbour and the restricted distribution of sediments southward, is that under prevalent conditions sediment accumulation does not take place on the inner shelf. Only along the shoreface is there, in places, a suggestion of the development of a sediment wedge. This is best displayed in the coast-parallel increase in isopachs in Long Beach Embayment (Map 6A) and Gielie's Embayment (Map 6C).

The calculation of sediment masses from volumes determined using isopach values, depends on the average bulk density value given to the sediment. Flemming and Hay (1983) report a value of 1.5 g/cm^3 as the average bulk density for marine sands, whereas Birch (in prep.) uses a value of 2.0 g/cm^3 as the basis for his calculations. It is essential that the average bulk density of the diamondiferous deposits be determined to an acceptable degree of accuracy, as the resultant calculation of sediment masses

could vary widely depending on the figure chosen.

Within the confines of the shoreface bedrock outcrop, i.e. in the sedimentary embayments, internal reflectors generally lie between -15 m and -19 m, pinching out at both top and bottom against bedrock. These reflectors have a slightly lobate outline, the gradient being steepest at the toe (eg. Fig.5.1B). The apparent dip of the reflector is generally towards the centre of the sediment embayment (where the bedrock is often cut by a channel), that is, either southeastward or northwestward; otherwise the dip is seaward, usually at about 2° . Evidence of this reflector is found at Tripp Shoal (Fig. 5.1) and the embayments at Alexander Bay, Versuipgat, Voltas, Agate Beach and Gielie's Bay. It lies between 3 m and 5 m below the seafloor, but also occurs as shallow as 1 m and extends down to 7 m.

The seismic records do not show internal structures within the sediment encompassed by the lobate reflector, except at Tripp Shoal, where faint layering is found to parallel the prominent reflector, suggesting that here this facies developed by progradation (Fig.5.1). The location of this reflector, its outline and the relation with the bedrock suggests that this facies is best described as a beach deposit, although this will only be verified by vibrocoreing. Equivalent deposits have been described by Hallam (1964, Plates II and III), Keyser (1972, Folder 1) and Corvinus (1983, Fig.1a) from onland marine sediments. Cross-sections through these deposits show seaward-dipping marine gravel beds overlain by beach and aeolian sand. The gravel beds are interpreted as storm-beach deposits that dip seaward at up to 4° . The outline of these beds resembles that seen on the seismic records. Murray et al. (1970) and O'Shea

(1971) give descriptions of vibrocores retrieved from the inner shelf north of the Orange River. They found that there is a 1,5 m thick gravelly-shell horizon with occasional pebbles, usually only 1 m beneath the seafloor. The gravel is described by Murray et al. (1970, p.135) as "... well rounded, spherical, well sorted ... termed 'terrace' gravel because of its similarity to the material mined on the local raised beaches." Assuming that the horizon described by Murray et al. (1970) north of the Orange River is the same as the internal reflector described from the seismic records in the study area (a preliminary study of vibrocores from selected areas (De Decker, 1985a) suggests that this could well be the case) the horizon must be regarded as an important potentially diamondiferous deposit. Exploration onland has shown that diamonds are concentrated in gravel horizons that are found at the base of palaeo-beach deposits (Keyser, 1972).

Apart from one instance, this reflector is not found below - 20 m, and therefore does not straddle over the wave-cut cliff found between -20 m and -24 m (Chapter 3). The presence of a wave-cut cliff, and an associated terrace at -30 m, indicates that the sea stood at that depth interval for an extended period. A sea-level curve (Fig.8.1) of the Late Pleistocene by Barwis and Tankard (1983) shows that the sea stood at -20 m for extensive periods within the last 125 000y. During these stillstands deposits below -20 m would have been reworked, leaving little trace of the original beach facies, forming a transgressive gravel-lag deposit instead as sea-level rose further. During the most recent period (the Flandrian transgression) when sea level rose from -120 m to the present strandline, the transgression may have been sufficiently rapid to prevent the complete reworking of

the beach deposits, leaving the lobate reflectors as remnants of a beach facies.

The second type of internal reflector is found seaward of the -20 m bedrock isobath. Typically sub-horizontal in section, it is more continuous than the inshore lobate reflector and commonly extends across the width of the sediment embayments. It has a gentle seaward dip of about $0,7^{\circ}$ and does not abut against bedrock on its seaward side. This reflector extends beyond the confines of the sediment embayments and generally dips from -21 m to -28 m. The tielines extending from Agate Beach and Buchu Bay (Fig.5.3B and C) show that there are several en echelon reflectors in this area, dipping seaward at approximately 2° to 3° . In the absence of vibrocore samples to characterize these horizons, it is nevertheless postulated that the deposit represents a prograding deltaic sequence, interspersed with storm-lag horizons consisting mainly of shell-hash and gravel. Murray et al. (1970, fig.8) show a general stratigraphic sequence of sediments on wave-cut terraces on the inner shelf north of the Oange River. Their sequence shows a succession consisting of a thin ($\pm 0,5$ m) layer of basal gravel that is overlain by a shell bed of about 1 m thickness. The shell bed is capped by 1 to 2 m of silty sand to complete the sequence.

The third type of reflector is found in the seismically transparent sediment lying over and seaward of the inner-shelf slope, south of Peacock Bank (Maps 7B and C). Up to four reflective horizons dip at less than $0,5^{\circ}$ seaward and southward. Their continuation offshore is masked by the ubiquitous ABL. Establishing their lateral extent and regional correlations is therefore not possible. The absence of these subbottom horizons

south of Boulder Bay (Map 7C) infers that these horizons are related to the Orange Delta, and probably represent prograding foreset beds in the prodeltaic deposits, commonly consisting of silts and clays (Coleman and Prior, 1980). The Orange prodelta muds continue southward to form the terrigenous mudbelt that extends south of the Olifants River (Rogers, 1977).

5.5 Conclusions

There are three major sedimentary facies covering the inner shelf and draped over the inner-shelf slope onto the middle shelf. Most extensive in the study area are the deposits of the Orange Delta (Figs. 1.8 and 2.2). These sediments extend 30 km south of the Orange River mouth, up to 80 km northward and at their widest they cover the shelf seawards for over 25 km (Hoyt et al., 1969). A second facies is the elongated belt of fine terrigenous sediments, mostly mud lying along the inner-shelf slope, forming the Orange prodelta in the study area. The mudbelt extends for several hundred kilometres southward (Hoyt et al. 1965a; O'Shea, 1971; Rogers, 1977, and Fig. 6.1A). The third sedimentary unit is found in the embayments, particularly south of Homewood Harbour. Grab samples show that these sediments are characteristically rich in carbonates (>25%), contain very little mud and a minor proportion of terrigenous detritus, particularly of the heavy mineral suite (Chapter 6). The seismic stratigraphies of these three sedimentary facies differ markedly in certain aspects, while they do share common elements as well. The seismic records across the inner shelf show that there are several internal reflectors, or horizons, within the unconsolidated sediment overlying the Precambrian basement. It

is possible to distinguish three types of reflectors, each characterised by its form and location. These reflectors may be related to the various sedimentary facies present on the inner shelf and seaward of the inner-shelf slope.

Without any data on sedimentology, stratigraphy and diamond content, the economic significance of the internal reflectors has to be inferred from the onland deposits. The inshore lobate reflectors are potentially the most important diamondiferous deposits. The depositional environment associated with storm-beach gravels is conducive to the concentration of the hydrodynamic coarse fraction in the sediment. It is therefore expected that diamonds would be found associated with these reflectors in the gravel fraction. The horizontal reflectors interpreted as gravel-lag deposits would likewise be of economic importance as they are formed, presumably, from reworked beach deposits. Fractionation of the sediment bedload during reworking of these beach deposits may have enriched the lag deposits in the heavier constituents, including diamonds. Systematic drilling of these internal horizons using a vibrocore capable of drilling 10 m is essential to determine their origin and age and to establish their economic viability. The following chapter, which deals with the surficial sediments on the inner shelf, may be regarded as only the first step toward establishing an accurate stratigraphic sequence for the diamondiferous deposits on the inner shelf.

CHAPTER 6SURFICIAL SEDIMENTS6.1 Introduction

The ninety-nine sediment samples retrieved from the inner shelf were principally recovered to verify, or "ground-truth", the sonographic interpretations of the sediment-covered areas of the inner shelf. To that end the samples were positioned in areas where the seafloor had a specific feature, such as sedimentary bedforms, coarse lag deposits or a thin sediment cover over the bedrock outcrop. Very few samples were retrieved from positions not dictated by side-scan sonar. This meant that sample-recovery lacked a rigorous grid-pattern necessary for a more thorough analysis. All of the samples were from water depths less than 40 m and 85% were from depths shallower than 25 m (cf Appendix, Table B1). The result is a lack of sampling continuity across sediment that is homogeneous in sonar character. The samples were first described by De Decker (1985).

Rogers (1977) considers four possible sources for the sediments found on the entire Orange shelf: 1) Reworked, residual sediments of Late Tertiary age; 2) Relict sediments of the Pleistocene regressions; 3) Recent terrigenous sediments, and 4) Recent biogenic sediments. Shelf sediments are found in facies parallel to the present coastline (Fig.6.1A). Recent terrigenous sediment is present on the inner shelf along the whole coast. A belt of terrigenous mud up to 40 km wide (Birch et al., 1976) is found along the seaward edge of the inner shelf (Fig.6.1B). It forms the continuation of the Orange prodelta

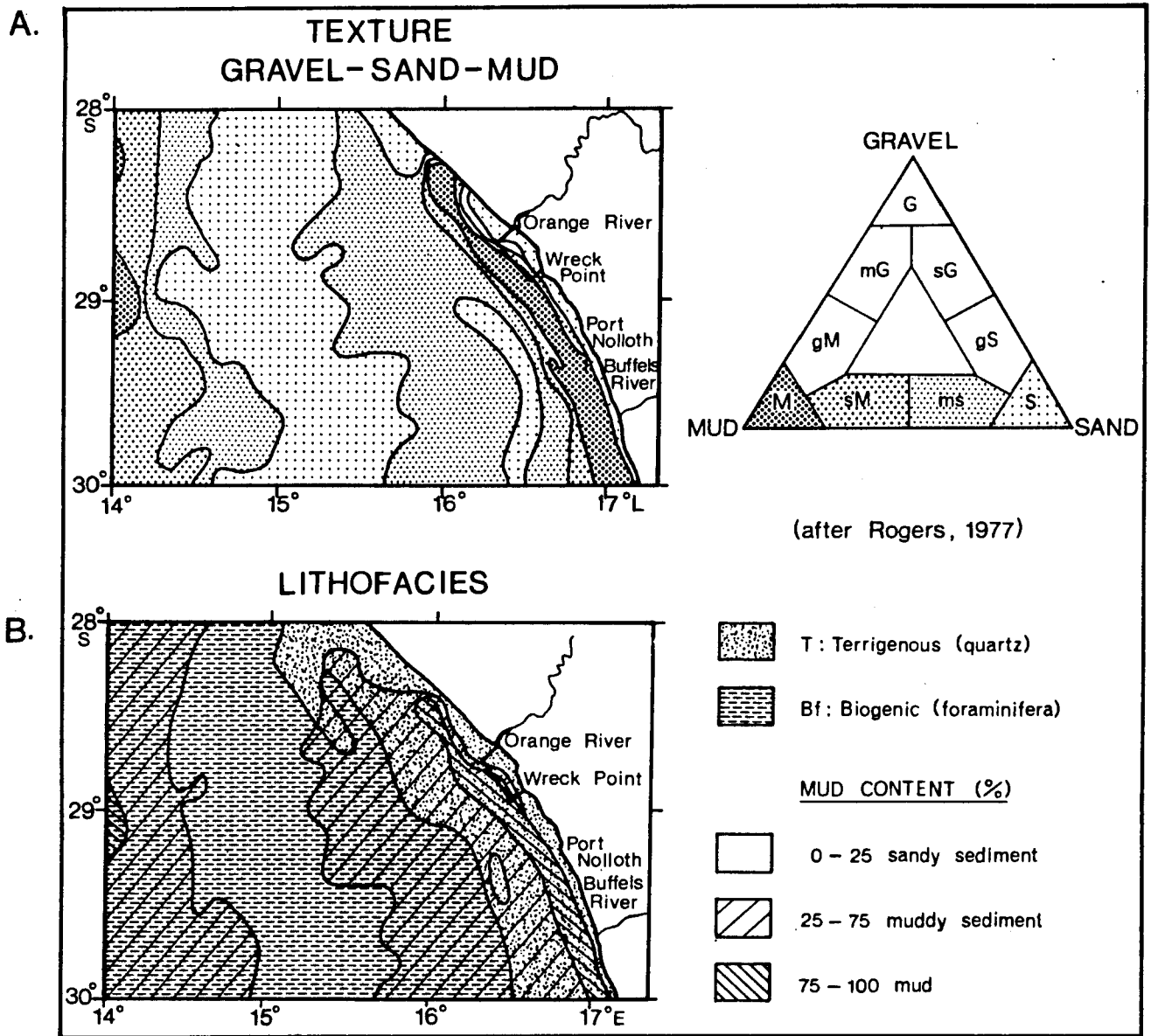


FIGURE 6.1

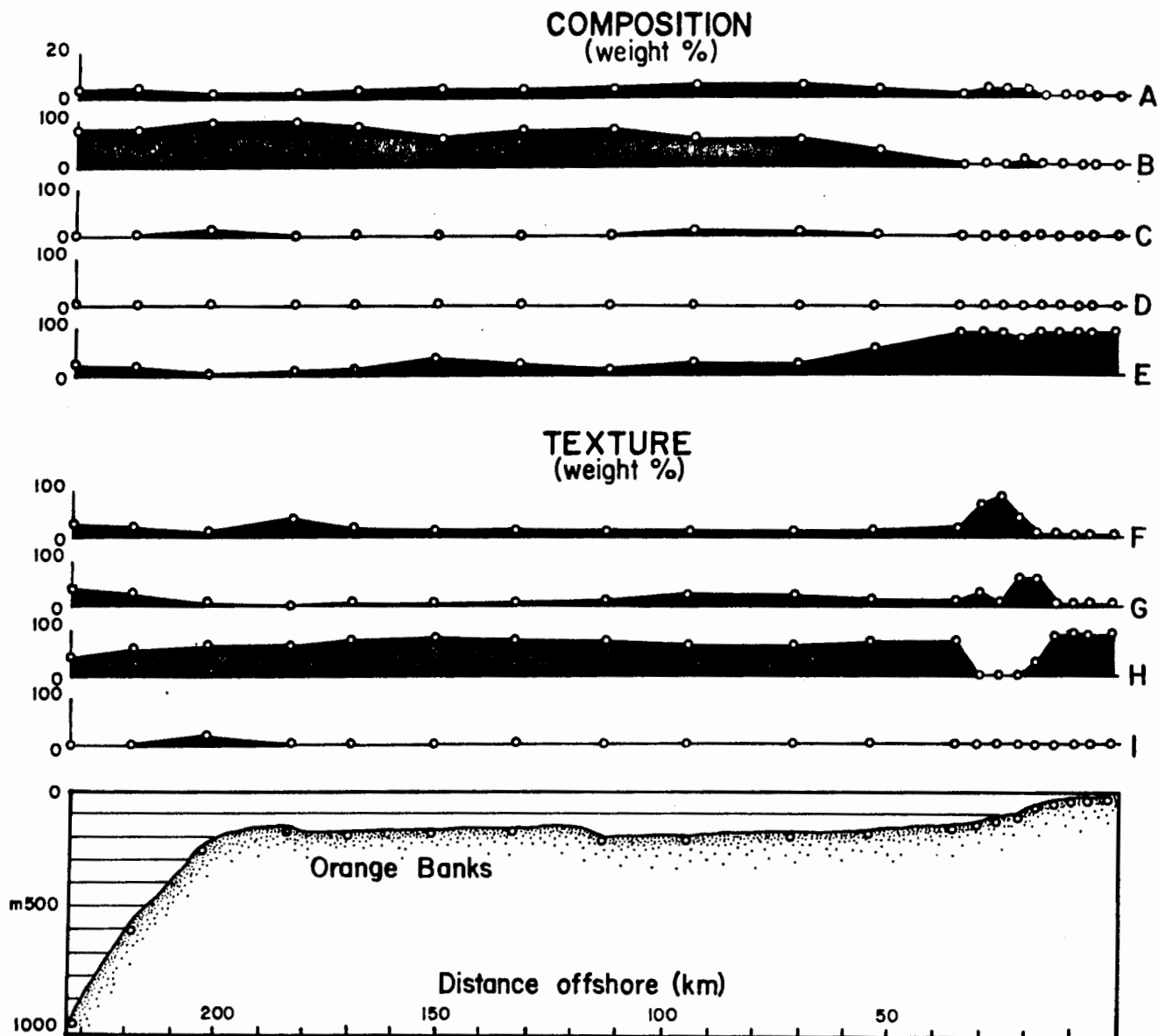
stretching southward for over 500 km between the Orange and Olifants Rivers, the former being the chief source for most of the terrigenous material.

Seaward of this mudbelt the continental shelf is mantled by a coarse, relict terrigenous sand, diluted with Holocene mud. Off the Orange River the middle and outer shelves are draped by foraminiferal biogenic sediment (Rogers, 1977).

Calcium-carbonate percentages on the Orange Delta and the terrigenous mudbelt are minimal (<5%), increasing to 25% inshore and seaward of the mudbelt south of Homewood Harbour (Fig.6.2). The organic carbon content in the sediment is less than 0,5% beside the coast, probably because of the oxidising effect of wave action on the sediments (Rogers 1977) and the very high terrigenous input from the Orange River. Further dilution of the organic carbon is found in the terrigenous mudbelt. The most important, potentially economic authigenic minerals, phosphorite and glauconite, occur in all types of sediments on the middle and outer continental shelf, except in the inner shelf terrigenous muds and sands (Rogers, 1977). The prevalence of terrigenous sand on the inner shelf is very evident from Figure 6.2.

6.1.1 Sediments in the study area

The inner shelf between Wreck Point and the Orange River is described in some detail by O'Shea (1971) from numerous grab samples and vibrocores. He finds that south of Wreck Point "ponds" of sediment consist of a thin layer of shelly, angular gravel overlain by sand, whereas north of Wreck Point rounded gravel is an added constituent. A hard green clay is found to underlie the sediment body where the latter thickens inshore. The sediment-filled embayment off Rietfontein (Fig.6.3) has large



- A. Organic matter
- B. Calcium carbonate
- C. Carbonate apatite
- D. Glauconite
- E. Terrigenous
- F. Clay
- G. Silt
- H. Sand
- I. Gravel

(after Rogers 1977)

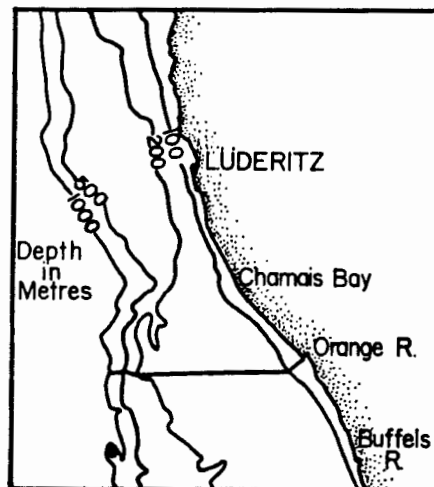


FIGURE 6.2

amounts of subangular gravel and clay. O'Shea (1971) notes further that the sediment in Buchu Bay (Fig.6.3) has a large proportion of shell and a hard greenish and musty smelling clay in the southern part. Nearer the surf zone the sediments have coarser, angular gravel that pinches out towards Cape Voltas and Peacock Bank. The sediments grade into silty sand with abundant shells and some "basal" clay at Cape Voltas. North of Cape Voltas the sediments show the influence of the Orange River, being brown, finer-grained and with few shells. Well-rounded gravel is found interbedded with brown mud; green clay is found well inshore. O'Shea (1971) however, does not show the relationship between the gravel and the clay.

6.2 Composition

Sub-samples of the sand-size fractions of the 99 sediment samples were described using a binocular microscope and percentage-frequency comparison charts (Ingram, 1965). The four main constituent groups outlined are: 1) "Quartz and feldspar" essentially the lighter density fraction of terrigenous detritus; 2) "Rock fragments" including heavy minerals, constituting the heavier fraction of terrigenous detritus; 3) "Biogenic fragments" fragments of molluscs, benthic-foraminiferal tests, ostracods, etc; and 4) "Micas" chiefly biotite and muscovite. Table B2 (Appendix) lists the percentage-range of components identified for each sample. In the sections below each of the above component groups will be described in turn, followed by a general discussion at the end of the chapter.

6.2.1 Quartz and Feldspar

The preponderance of terrigenous material in the marine

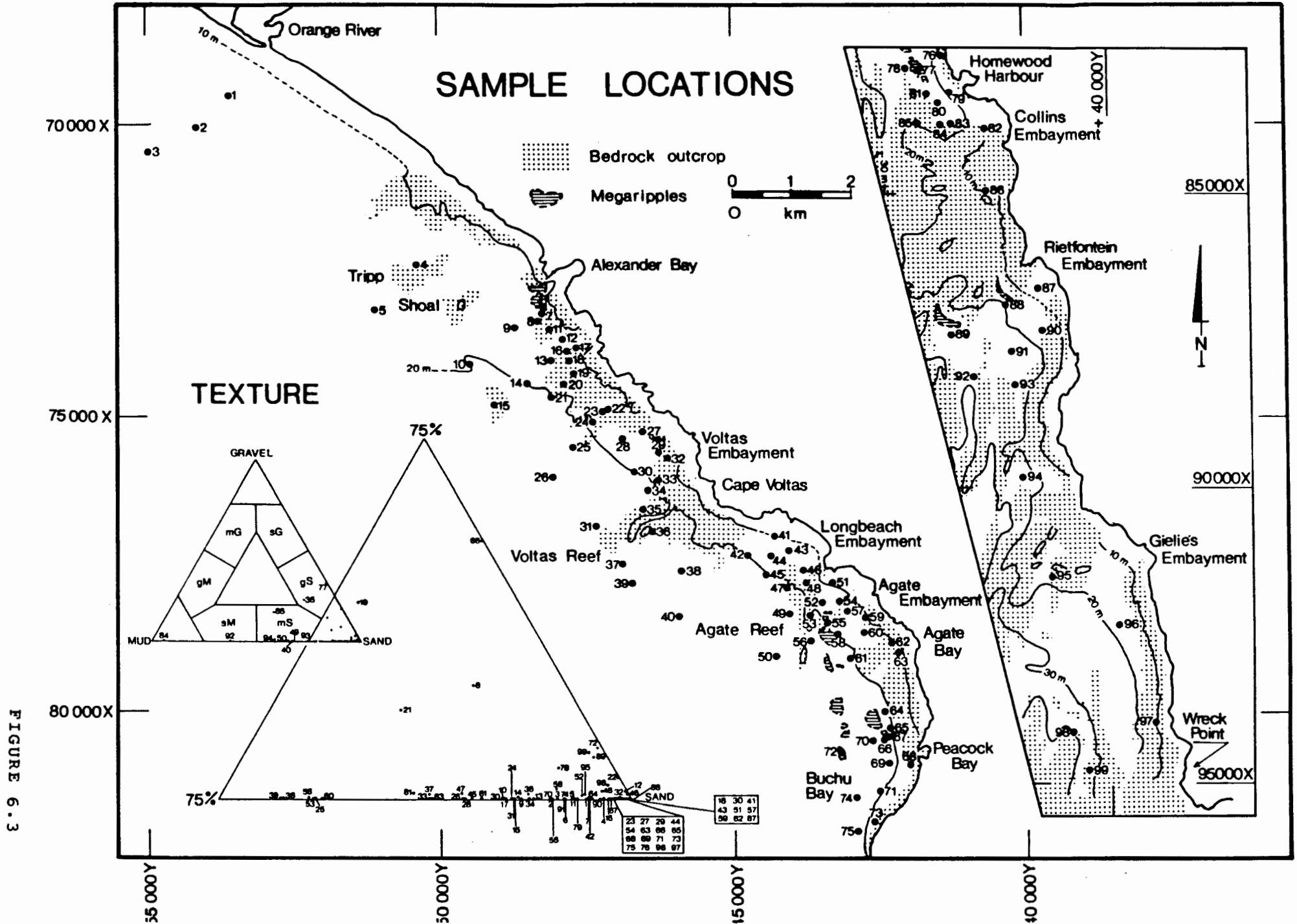


FIGURE 6.3

sediments of the study area is seen in Figure 6.4. The Orange Delta exerts its influence on the inner shelf as far south as Wreck Point (Fig.2.2), but the effects are particularly strong north of Peacock Bay. Away from bedrock exposures, the sediments north of Peacock Bay show between 75 and 90% by volume quartz and feldspar. Close to the Orange River mouth (Samples 1 to 5, Fig.6.3), the quartz grains generally have a reddish-brown staining of iron hydroxide on their surfaces (cf O'Shea, 1971; Rogers, 1977), probably indicating their relatively recent introduction to the reducing marine environment. Quartz grains from sediment samples south of Alexander Bay have little or no staining, it probably being abraded during northward transport on the inner shelf.

Where the percentage quartz and feldspar is less than 75% in the area between Alexander Bay and Peacock Bay, the samples invariably lie on bedrock outcrop or were retrieved from areas covered by megaripples. The predominance of the quartz-and-feldspar fraction in the sediment decreases from Homewood Harbour to Wreck Point. Here the trend is reversed and sediment recovered from areas underlain by exposed bedrock with only a thin veneer of sediment show a higher percentage of this component-fraction than the sediment embayments. This reversal in trend indicates that the predominance of the Orange Delta as the principal source of the quartz-and-feldspar fraction is limited to north of Homewood Harbour, where the sediment is very strongly biased towards the terrigenous fraction.

6.2.2 Rock Fragments

Off the Orange River, the percentage of this component is about 25% but decreases southward away from the influence of the

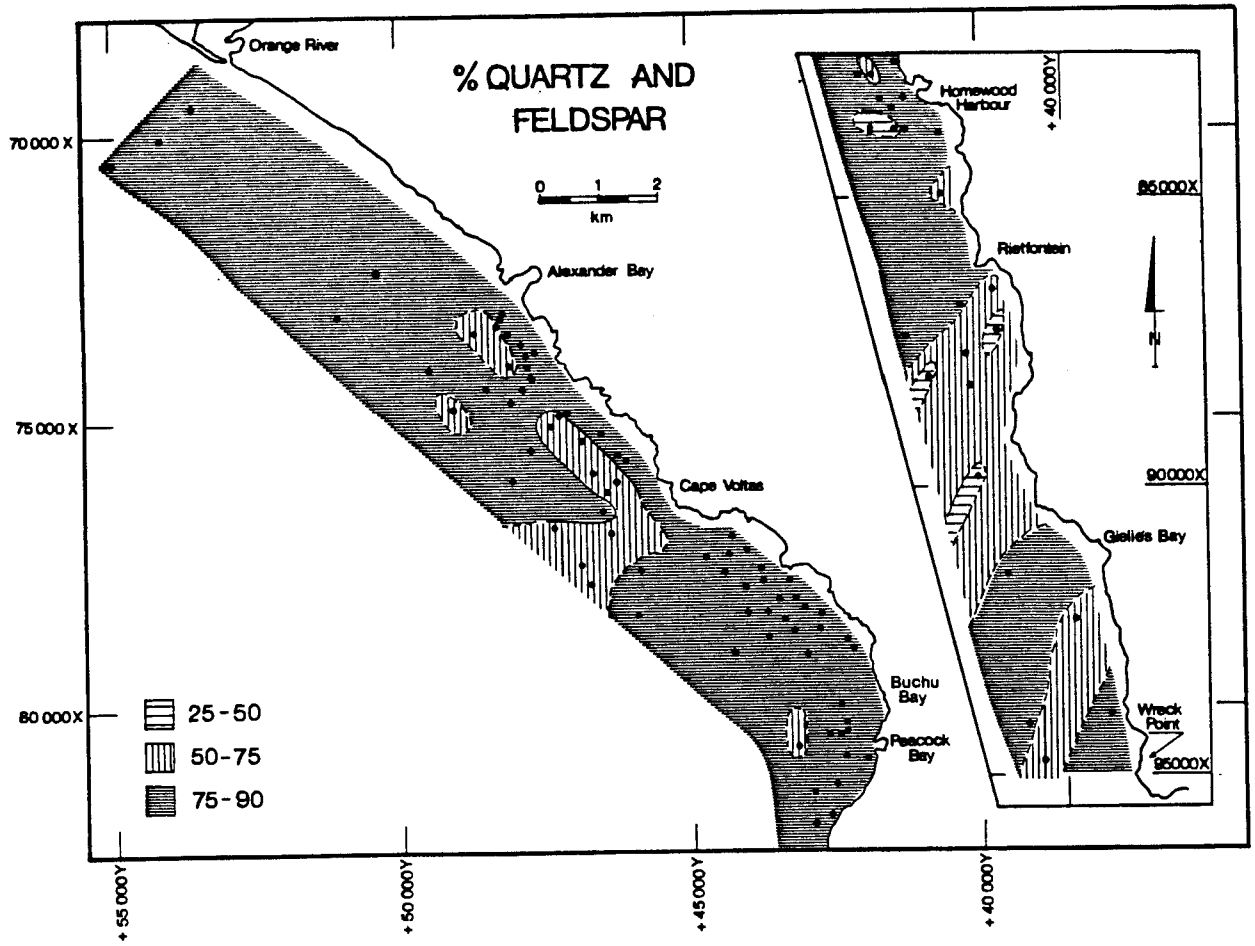


FIGURE 6.4

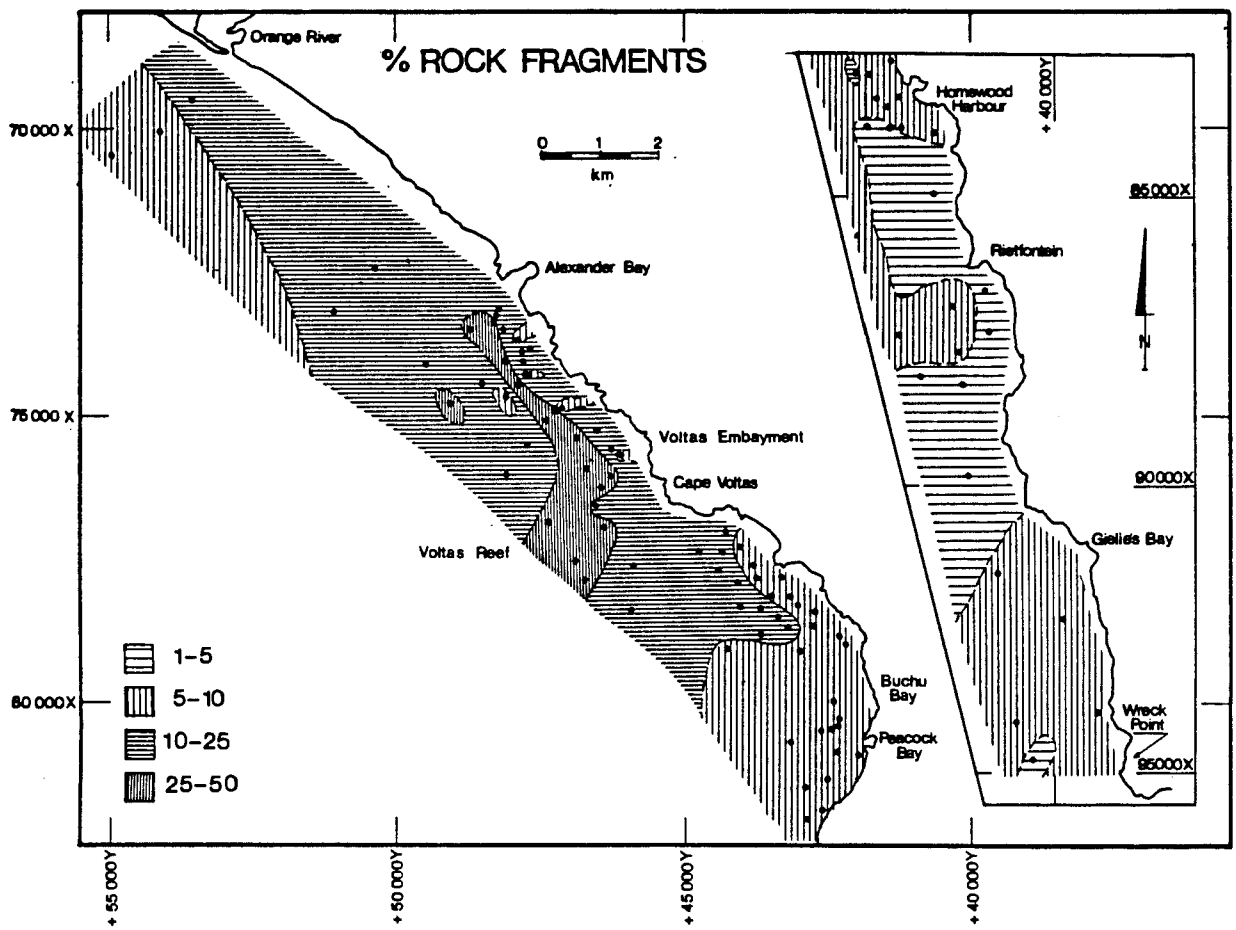


FIGURE 6.5

river mouth (Fig.6.5). The percentage heavy minerals within the "rock fragment" component has not been estimated, but from Figure 1.9 it is clear that the percentage also drops off rapidly southwards.

Between Alexander Bay and Cape Voltas there is an increase in the percentage rock fragments along a narrow zone in a water depth of about 20 m. This zone swings offshore just north of Voltas Reef, so that most of Voltas Embayment has between 25% and 50% rock fragments. Across Voltas Reef the percentage decreases to between 10 and 25%, decreasing even farther in the sediments of Buchu Bay. South of Homewood Harbour the percentage "rock fragments" in the sediment samples decreases for samples taken from the sediment veneer on rock outcrops, and increases in the sediments found in the sediment embayments. Thus one finds that Rietfontein and Giellie's Embayments have up to 10% of this component, whereas the sediments on the rock outcrops between these embayments show only about 5% or less. In the south heavy minerals form the larger part of the rock fragment group which has a very-fine-sand mode (cf Appendix, Table B2). The rock fragments per se and heavy minerals are mainly introduced by the Orange River. O'Shea (1971) found that in 5 samples from the study area, heavy minerals occur in "trace" amounts. Epidote predominates and is present in all the samples along with garnet, ilmenite and tourmaline. Zircon and kyanite are found in four of the samples, while rutile is only found in a sample off Wreck Point.

6.2.3 Biogenic Fragments

This component-group of the sediment is constituted mostly of shell fragments and benthic foraminifera. The total "biogenic

fragments" percentage distribution is thus represented by the CaCO₃ percentage (Fig.6.6 and Table B3). The distribution of benthic foraminifera is shown in Figure 6.7.

6.2.3.1 Calcium Carbonate

The trend in the CaCO₃ values within the confines of the study area shows a decrease offshore towards the mudbelt and an increase southward (Fig.6.6). This pattern is very well established north of Peacock Bay. The percentages between the Orange River and Peacock Bay vary from 10% in the north to 32% at Peacock Bay. This percentage difference is the same for inshore-offshore trends in this area. O'Shea (1971) estimates the average percentage carbonate south of the Orange River to be 16.5%, increasing southward.

South of Homewood Harbour the percentage carbonate remains between 30 and 35%. Only 3 samples (87, 92 and 99) have more than 50% and 2 samples (88 and 89) less than 25% (Table B3).

While the percentage carbonate in the sediment remains about the same from Peacock Bay southward, the biogenic fragments contributing to it change from dominantly mollusc remains in the north to benthic foraminiferal tests in the sediment farther south.

6.2.3.2. Benthic Foraminifera

Martin (1981) showed that five foraminiferal zones can be distinguished on the continental margin. In zones 1 and 2, covering the inner shelf and middle shelf from sea level to -34 m and between -34 m and -162 m respectively, the dominant species present are Ammonia beccarii (zones 1 and 2), Elphidium spp (zone 1) and Cassidulina carinata (zone 2), with the main supplementary species being Pararotalia nipponica (zone 1), Elphidium advenum,

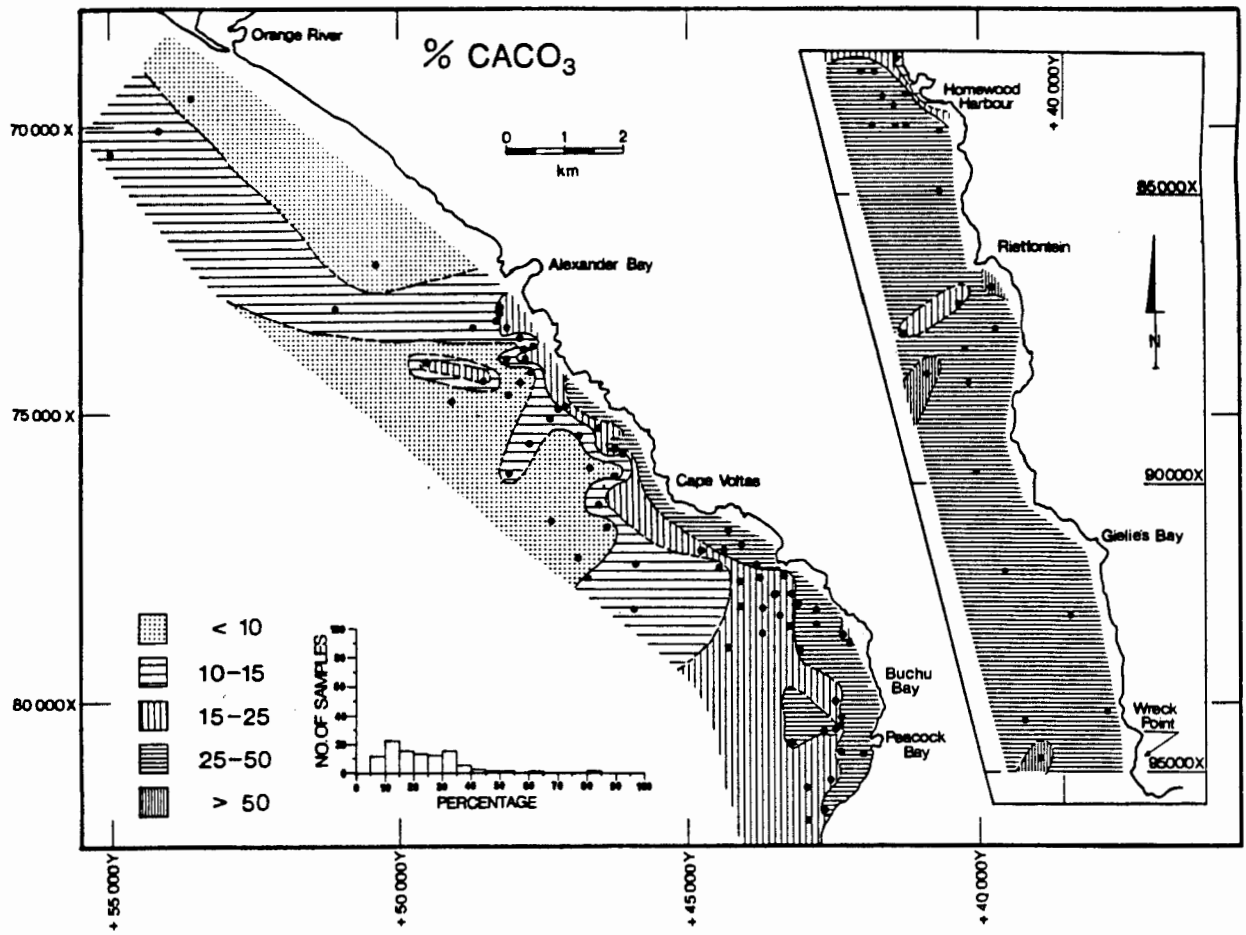


FIGURE 6.6

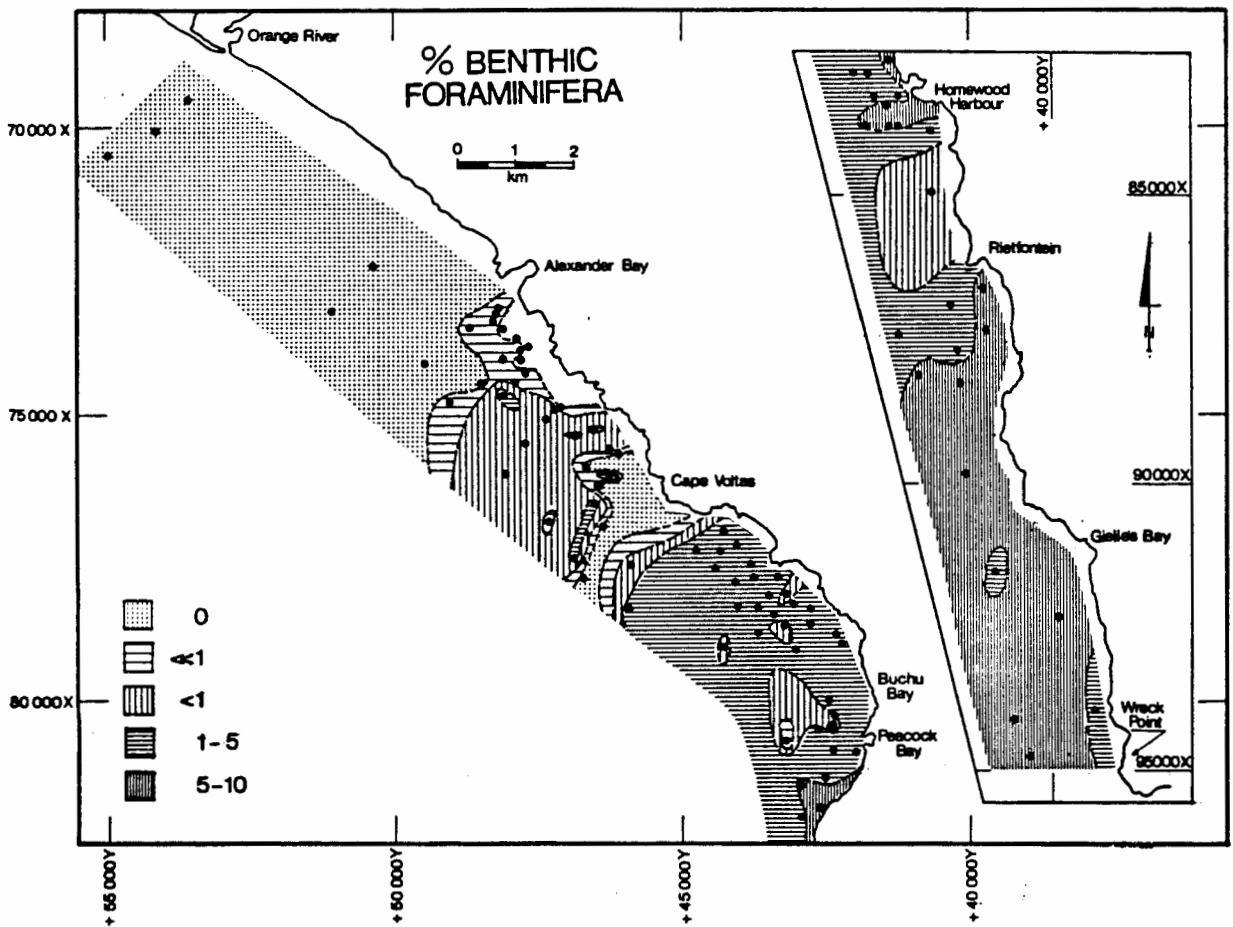


FIGURE 6.7

Ammobaculites americanus and Florilus boueanum (zone 2) (Martin, 1981).

The percentage benthic foraminifera as a group has been determined separately from the other components that constitute the biogenic fragments. From Martin's (1981) work, it seems that Ammonia beccarii, Elphidium spp. and Pararotalia nipponica are the most common benthic foraminifera found in the sediment. These species have been identified while routinely determining the percentage components in the sediment with a binocular microscope.

North of Alexander Bay there are no benthic foraminifera in the deltaic sediments (Fig.6.7). Between Alexander Bay and Cape Voltas the abundance is still less than 1%, except locally where the percentage may rise to 5%. There are very few (<<1%) or no benthic foraminifera in the sediment that overlies the shoreface bedrock outcrop. Martin (1981) notes that Elphidium spp. is commonly found in river samples and was the dominant species in her sample from the sand bar at the Orange River mouth. Ammonia beccarii and Pararotalia nipponica are "well-known nearshore dwellers capable of withstanding extremes of temperature and salinity." (Martin, 1981, p.11). The absence of foraminifera close to the Orange River mouth must therefore be related to the high sedimentation rate which would dilute the Foraminifera.

The area between Cape Voltas and Buchu Bay has up to 5% benthic foraminifera in the sediment. Lower percentages are associated mostly with areas covered by megaripples, or close inshore. The higher-energy regime associated with these environments would prevent any accumulation of this light fraction. In Buchu Bay the foraminiferal abundance increases to

10% along the base of the steeply dipping bedrock fringing the coast (Map 3B). The water depth is 15 to 20 m close inshore and the calmer, sheltered conditions probably account for the relatively high percentages.

Across the bedrock-outcrop area south of Homewood Harbour to Rietfontein, the percentage Foraminifera decreases to less than 1%. The value increases rapidly within Rietfontein Embayment, reaching up to 10% in the samples along the southern edge of the embayment. Southwards the percentage remains at that level, except inshore at Wreck Point, where Sample 97 has between 1 and 5% benthic foraminifera. This sample was retrieved from an area of exposed bedrock, inferring a high-energy environment which would prevent the deposition of fine grained sediment.

6.2.3.3 Organic Carbon

The percentage distribution of organic carbon is presented in Table B3 (Appendix). Rogers (1977) shows that the percentage organic carbon in the sediments on the inner shelf, particularly off the Orange River, is less than 0,5%, whereas the middle shelf has up to 4% organic carbon. The sediments at the shoreward edge of the middle shelf are diluted by terrigenous muds and the concentration remains below 1%. Fifteen samples between the Orange River and Wreck Point were analysed for organic carbon. The percentages vary from 0.37% (Sample 37) to 1.38% (Sample 50) with a weak correlation between mud and organic carbon percentages (Appendix, Table B3). These values confirm the general finding of Rogers (1977) that the terrigenous detritus from the Orange River severely dilutes the organic carbon concentration (Fig.6.2A).

6.2.4. Micas

The two minerals identified were brownish flakes of biotite and transparent platy flakes of muscovite. The percentage decreases steadily southwards from the Orange River and beyond Homewood Harbour the value is usually less than 1%, reflecting the diminishing influence of the Orange Delta (Fig.6.8). Mica is thus shown to be a particularly useful marker for deltaic sedimentation.

6.3 Texture

The distribution of the various size-fractions is presented, followed by a discussion of the distribution of the mean grain size, sorting and skewness of the sand-size fraction. Table B3 (Appendix) gives the percentage distribution of the size intervals, along with mud and gravel percentages. The statistical parameters of mean, sorting, skewness and the first percentile are presented in Table B4. The chapter is concluded with a discussion of the distribution of the textural parameters. The textural distribution of the sediments is presented in a triangular diagram, based on Shepard's (1964) classification. Notice that there are very few samples that do not fall within the "sand" category, so that a textural distribution map would not be particularly revealing of any trend on the inner shelf.

6.3.1 Grain size fractions

The description of the size fractions is divided into three sections: 1) Mud and very fine sand, 2) Fine sand and 3) Medium sand, coarse sand, very coarse sand and gravel.

6.3.1.1. Mud and very fine sand

Within the study area the mud and very fine sand fractions

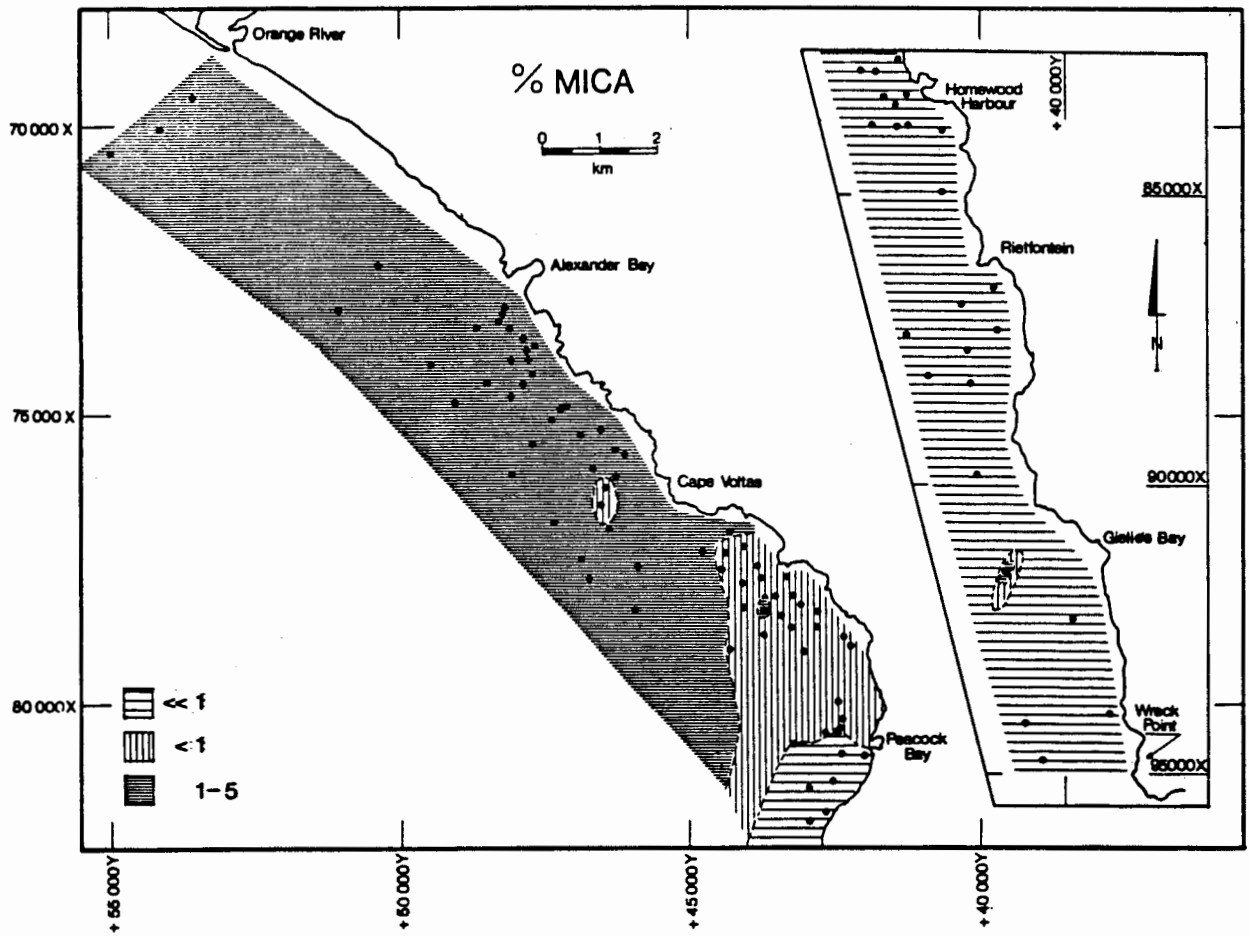


FIGURE 6.8

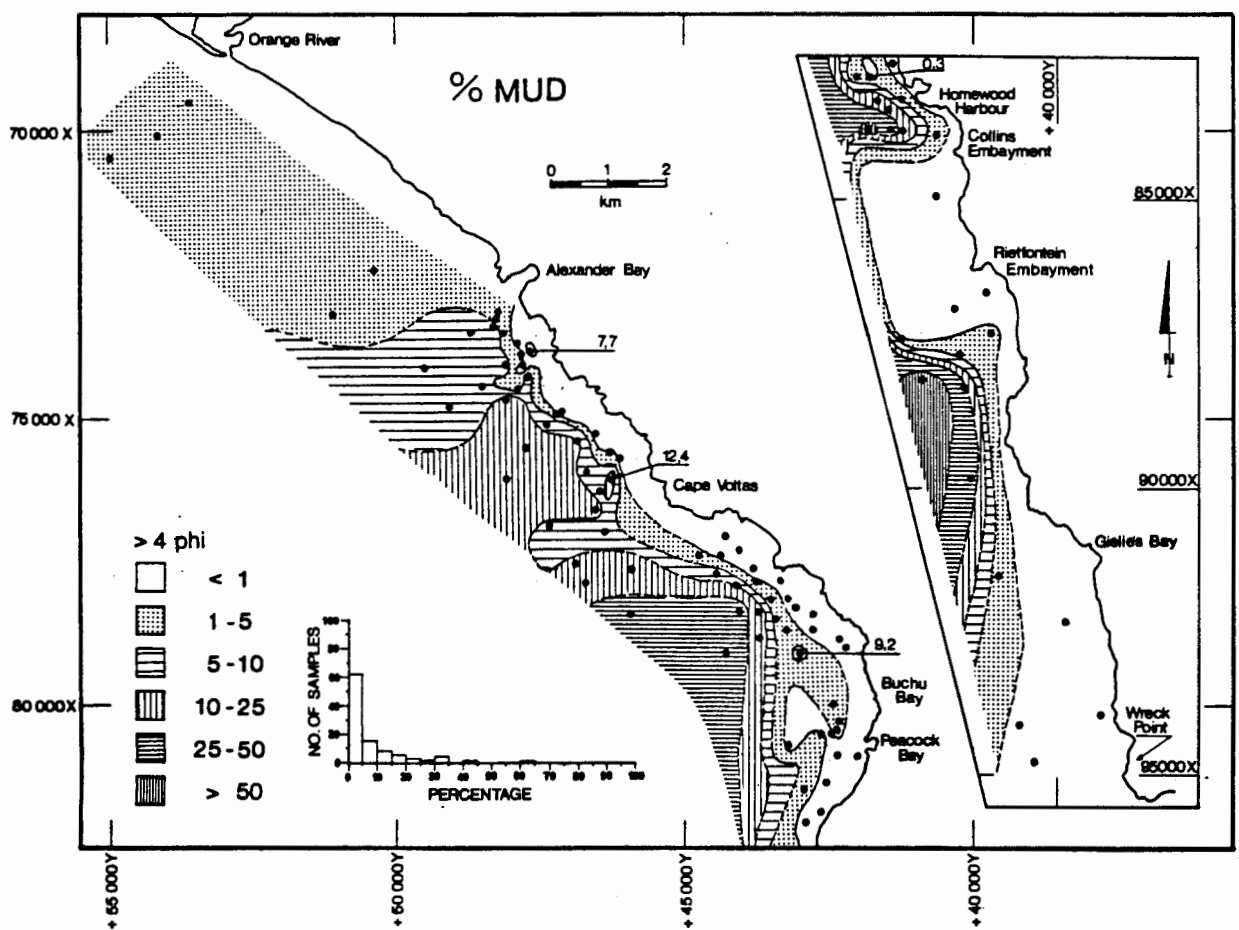


FIGURE 6.9

have similar trends, although the relative abundances differ widely. Figure 6.9 shows that near the Orange River mouth there is very little mud (<5%), up to 3 km from the coast, in a water depth of 30 m. However, Table 6.1 shows the sudden increase in mud content for a set of samples along a line seaward of the Orange River mouth, analysed by Rogers (1977).

Table 6.1

Increase in Weight Percentage Mud off the Orange River mouth
(from Rogers, 1977)

Sample No.	Distance offshore (km)	Depth (m)	Mud %
2695	1.6	12	4.7
2961	5.9	23	9.8
3280	8.8	24	7.2
3281	11.7	34	14.4
3282	15.3	50	68.3
3283	18.7	80	99.0
3284	22.7	96	99.3

The trend also clearly defines the boundary at -50 m between the inner shelf and middle shelf on the Orange Delta (cf Chapter 2). The seaward increase in percentage very fine sand occurs over a much shorter distance, ranging from 17.7% at sample 1 to 32% at sample 3 (Fig.6.10). This offshore increase in the fine fraction of the sediment, reflecting the usual trend (Komar, 1976b), can be attributed to the wave regime preventing fines from settling

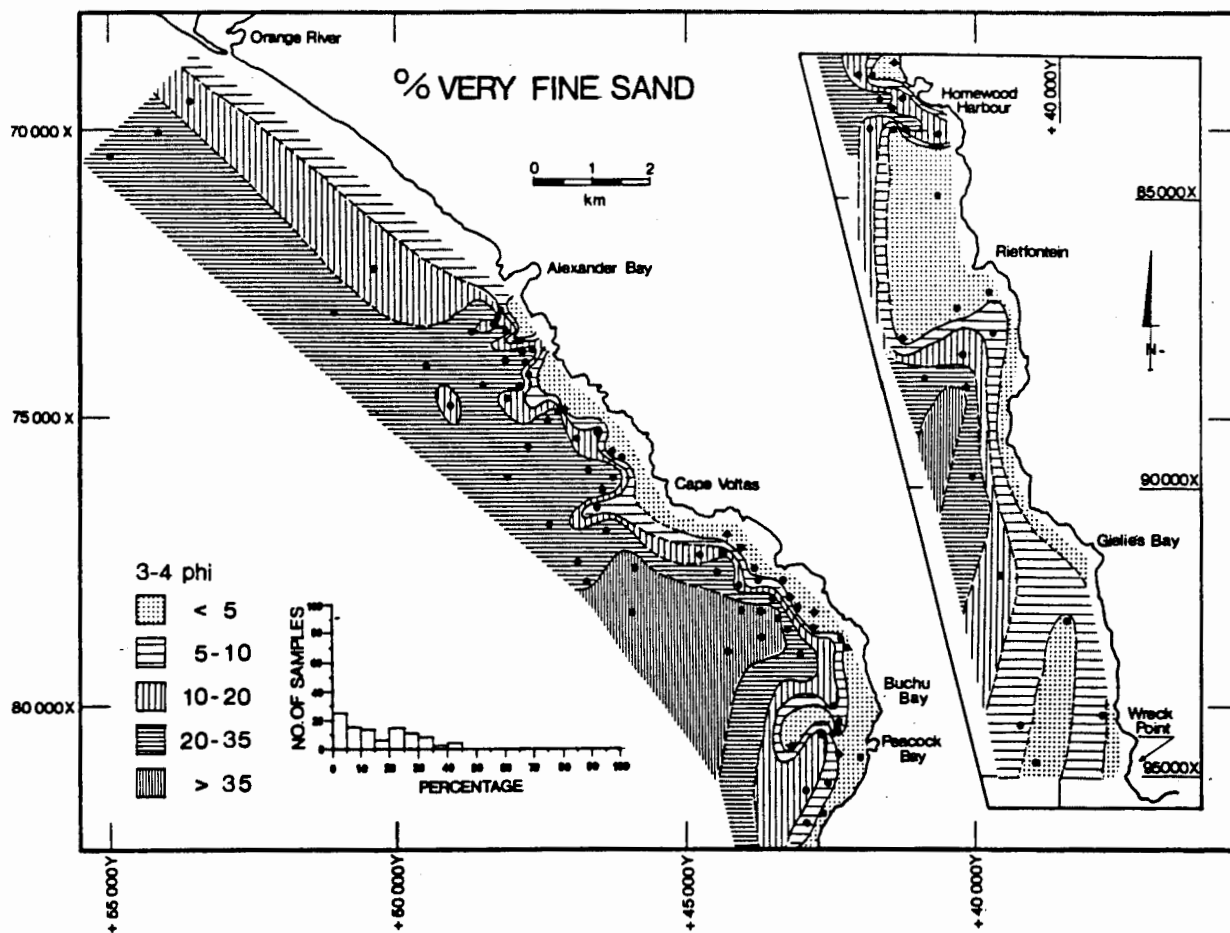


FIGURE 6.10

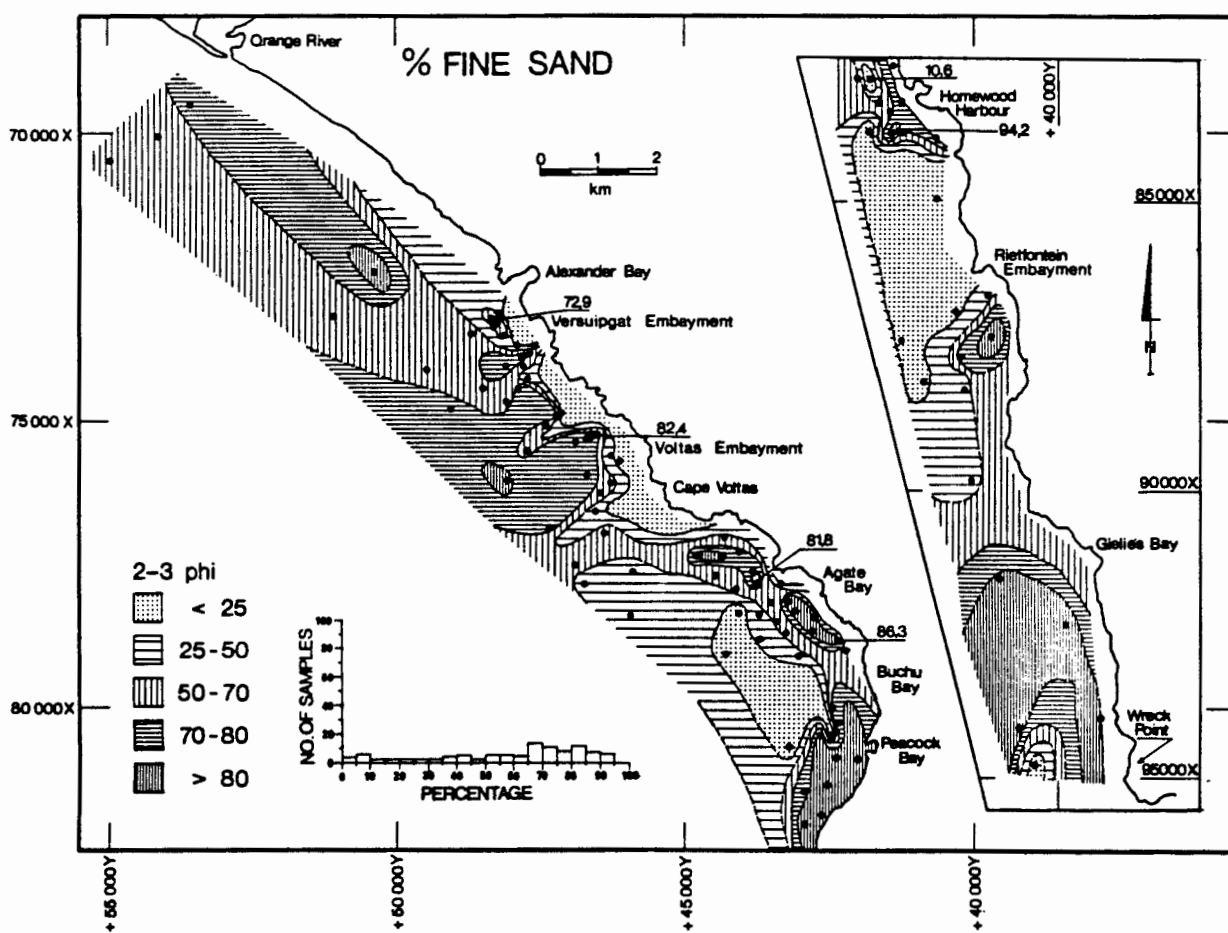


FIGURE 6.11

out at shallower depths. Wave base (Chapter 7) for median wave conditions (waveheight 1,75 m and wavelength 11 sec) is at -42 m, below which depth the mud will normally settle out of suspension. Rogers (1977, Fig.VII-2b) earlier showed that the position of the shoreward edge of the Orange prodelta deposits to be mainly wave-controlled. Off the study area, the shoreward boundary of the mudbelt lies between -40 m and -65 m.

The mud and very-fine-sand size-fractions become more prevalent southward, with the highest percentages off Cape Voltas being 34,6% for mud and 40% for very fine sand (Figs.6.9 and 6.10). Between Cape Voltas and Homewood Harbour both size fractions increase rapidly from <5% at the coast to over 35% within a kilometre of the shore. The overall texture (Fig.6.3) grades from sand inshore to muddy sand offshore. Locally, however, abundances vary, with samples taken on bedrock outcrops with sediment veneer having less of both fractions than samples from within sediment-filled embayments. This is well illustrated by the low-percentage tongue off Cape Voltas (Figs.6.9 and 6.10) that corresponds with the position of Voltas Reef (Fig.6.3). The bedrock outcrop between Homewood Harbour and Rietfontein also has very little of either size fraction. Figures 6.9 and 6.10 also show low concentrations of mud and very fine sand for samples in Buchu Bay. These samples were collected from areas covered by megaripples (Chapter 7), indicative of coarse sand and gravel deposits.

The anomalously high percentage of mud in sample 84 in Collins Embayment (Figs.6.3 and 6.9) is possibly due to slimes effluent being pumped into the area from onland diamond workings. The yellow colour of the sample is unlike other muddy samples,

which are olive green.

The steep isopleth gradient across Rietfontein Embayment (Fig.6.9), and reflected in the sandy-mud texture of sample 92 (Fig.6.3), implies a shoreward incursion of the terrigenous mudbelt along the channels cut into the bedrock and extending to the inner-shelf slope (Chapter 2). Wave-induced, or upwelling currents (the latter reinforced by local bathymetry) could be the transport mechanism for the sediment.

The sediments in Giellie's Embayment (Fig.6.9 and 6.10) contain less than 1% mud while the very fine sand fraction averages only 5%.

6.3.1.2. Fine sand

This is the most abundant size fraction, accounting for more than 50% of the sand-size fraction and corresponding to the mean size of the sand-size fraction in more than 80% of the samples (Fig.6.15). (By comparison medium sand rarely exceeds 50%)(Fig.6.12). The percentage distribution is likewise evenly spread; the modal percentage lies in the 65-70% interval (Fig.6.11).

In the embayments between Alexander Bay and Agate Bay percentages increase from about 50% inshore, to peak at over 80% in a zone about 1 km offshore and then decrease again farther seaward (Fig.6.11). This distribution is also found north of Alexander Bay, but the sample density is too low to show it conclusively. A zone of very high fine-sand content is also present in Rietfontein Embayment. The samples along the northern edge have between 5 and 10% fine sand. This increases to 87% at S90 (Fig.6.3). The samples taken in or close to the sediment-filled channels extending southwestward from the embayment have a

fine-sand content of 31,9% (Sample 94) and 40,6% (Sample 93) respectively.

At the Orange River the percentage fine sand decreases away from the coast, but increases from 62% at the mouth to 78% off Alexander Bay (Fig.6.11). Samples from sediment on bedrock outcrops have less fine sand than samples from the sediment-filled embayments. This is clearly shown north of Cape Voltas and in the area between Homewood Harbour and Rietfontein (Fig.6.11) and reflects a similar trend found for the mud and very fine sand fractions (Figs.6.9 and 6.10).

As with the finer size fractions, this fraction is relatively depleted in areas covered by megaripples (Fig.6.3), which accounts for its lack in the samples for Buchu Bay and west of Homewood Harbour. The percentage varies from 0,9% (Sample 72) and 22% (Sample 66) to 24,3% (Sample 49), while Sample 77 has only 10,6%. This contrasts with the sediment inshore that has an average percentage fine sand of over 85%.

6.3.1.3. Medium sand, coarse sand and very coarse sand, and gravel

At the Orange River mouth the percentage medium sand decreases offshore rapidly from 5,8% inshore to less than 1% on the seaward side of the study area (Fig.6.12). Southward the trend is similar, that is, quite high percentages inshore (46,7% at Sample 6, off Alexander Bay and 56% at Sample 87 near Rietfontein) dropping rapidly to zero percentage offshore. The much higher medium-sand abundances inshore south of Alexander Bay indicates the decreasing influence of "deltaic deposits" (i.e. fine-sand fraction), on the sediments away from the Orange River mouth. Sediment from bedrock outcrops has a higher percentage

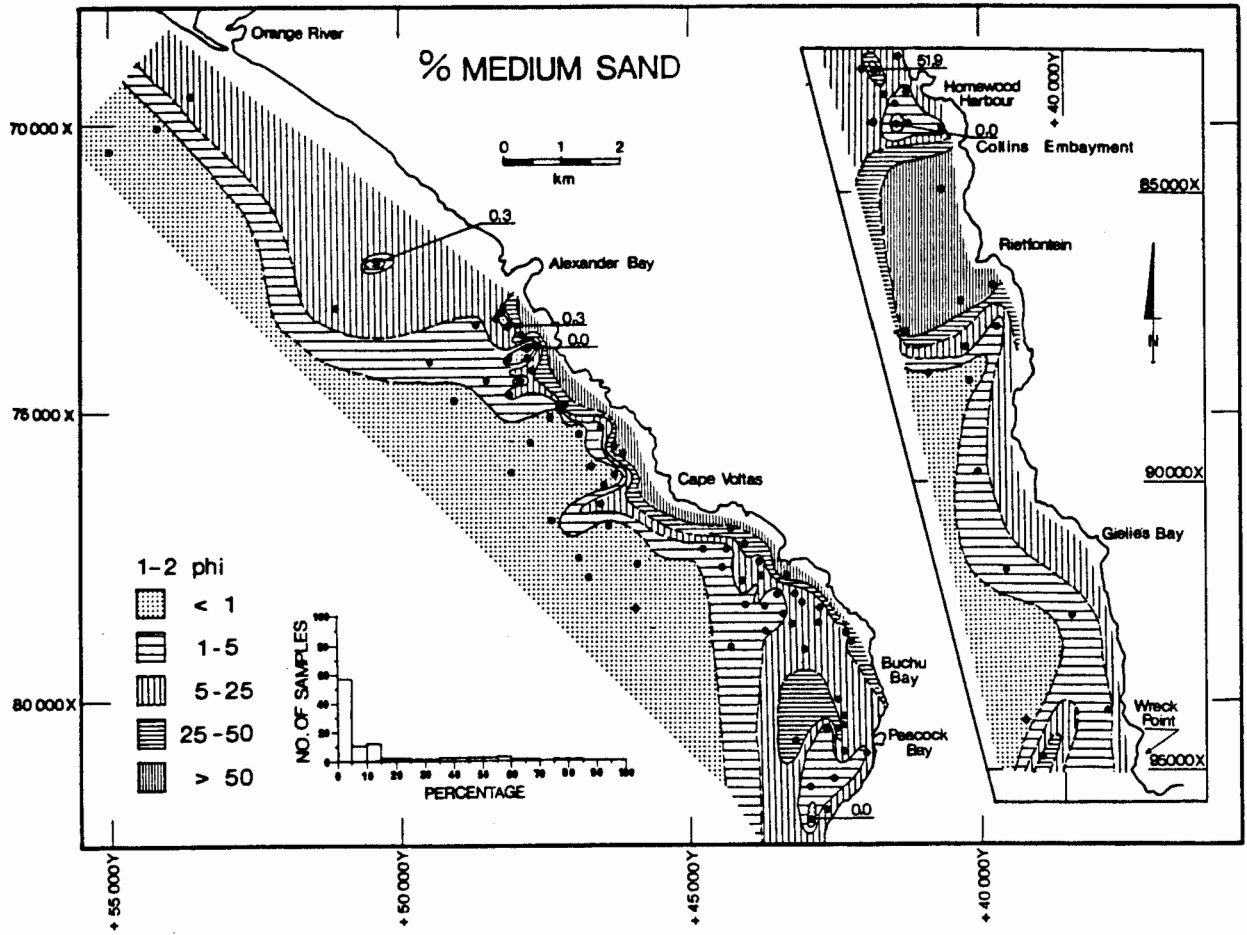


FIGURE 6.12

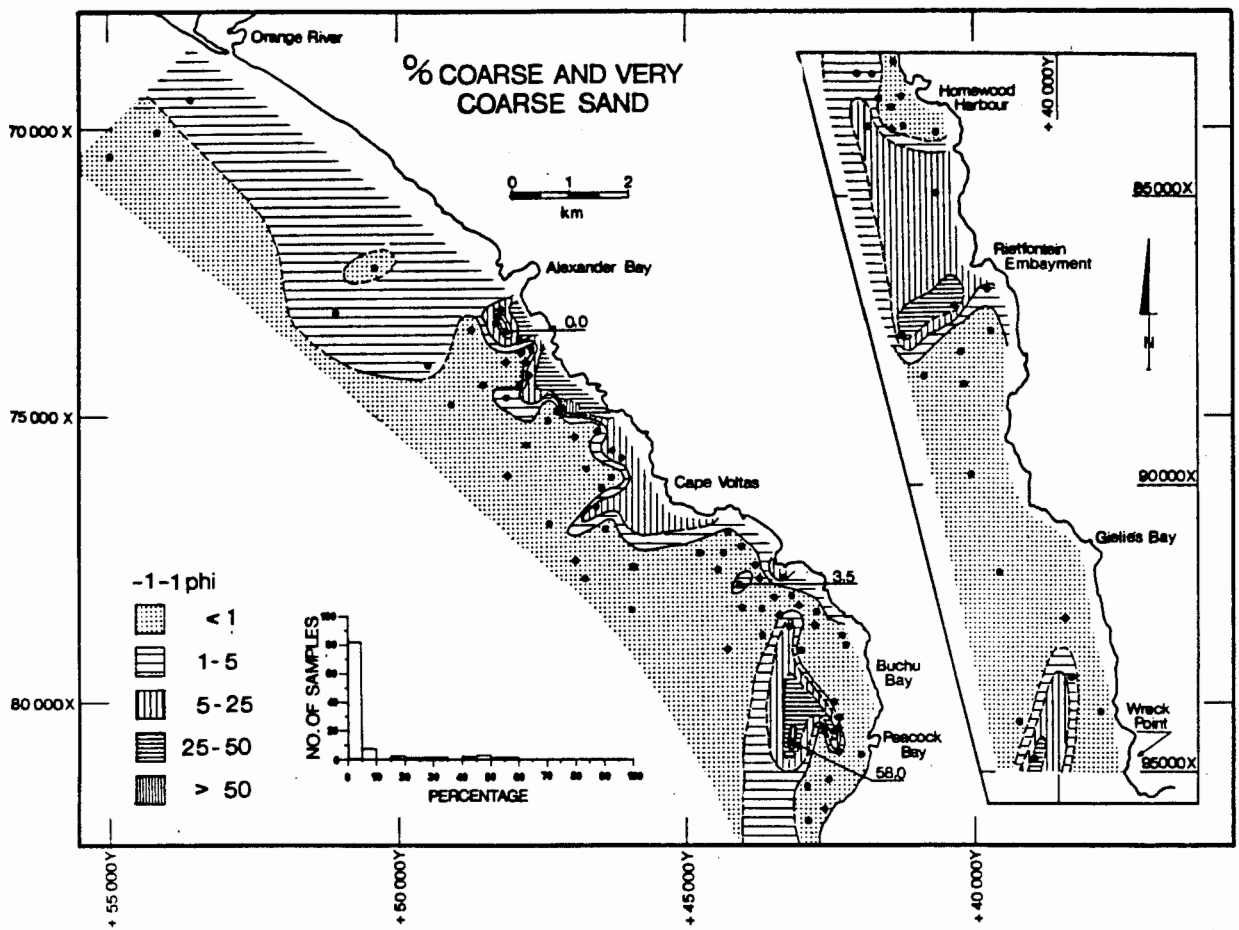


FIGURE 6.13

medium sand than the sediment in the embayments. This is well illustrated in the contrast between Collins Embayment and the rocky area towards Rietfontein (Fig.6.12).

In Buchu Bay the medium sand percentage (Fig.6.12) rapidly decreases away from the coast to an average of less than 3%, except in areas covered by megaripples, where the value rises to over 30%. The distribution of coarse and very coarse sand (Fig.6.13) is almost exclusively limited to sediment on bedrock outcrops and to areas covered by megaripples. Elsewhere, sediments in the embayments and offshore have generally less than 1% or no coarse and very coarse sand fractions at all.

The shoreface from Alexander Bay to Cape Voltas has sediment that in places has up to 52,6% (Sample 22, Fig.6.3) coarse and very coarse sand-fraction, but sediment in the embayments shows no contribution from this size fraction.

The area covered by megaripples in Buchu Bay (Fig.6.13) contains up to 58% coarse and very coarse sand, but inshore this fraction is absent. South of Homewood Harbour the abundance of this size fraction increases, particularly along the northern edge of Rietfontein Embayment, where up to 33,6% (Sample 88) is found. South of Rietfontein only Sample 99 (Fig.6.3), with 46,4%, contains more than 1% of this fraction.

Only two samples have any amount of very coarse sand fraction, namely Sample 8 (0,92%) off Alexander Bay and Sample 66 (3,5%) off Peacock Bay, whereas more than 80% of the samples have less than 5% of both size fractions combined (Fig.6.13). The absence of these size fractions within the sediment-covered areas indicates that the Orange River introduces mainly the finer sediment fractions into the sea, some of which is then

transported southwards into the study area.

The weight percent of gravel (>2 mm) in the sediment is highly variable (Fig.6.14). Samples containing more than 1% of this size fraction are all associated either with bedrock outcrops or sedimentary bedforms. The bulk of the gravel fraction is made up of broken shell fragments and in only a few samples are rock fragments or quartz grains present.

The highest concentrations are found in Buchu Bay and west of Homewood Harbour (Fig.6.14). Sonographs of this area show that it is widely covered by megaripples with up to 1,5 m wavelengths (Fig.6.3). These bedforms will only form in sediment of suitably coarse grain size (Reineck and Singh, 1980).

South of Homewood Harbour the sample distribution is too limited to be able to note trends in the gravel fraction.

6.3.2. Mean

The mean size of the sand-fractions (Fig.6.15) of almost 75% of the samples is between 2.0 and 3.0 phi (fine sand) and 15% fall in the 1.0 to 2.0 phi range (medium sand) (Appendix, Table B4).

The offshore sediment north of Cape Voltas is remarkably uniform in mean size, which generally lies between 2.7 and 2.9 phi (i.e. fine- fine sand). This value fines to >3.0 phi (very fine sand) between Cape Voltas and Peacock Bay. Inshore, from Alexander Bay southward to Peacock Bay medium sand predominates.

A textural traverse across the Orange River Delta by Rogers (1977, Fig.VII-9) shows a gradation from slightly silty, very fine sand on the delta front with a mode at 3 phi, to clayey silts and then silty clays on the prodelta farther offshore. His sampling line ran parallel to the line through samples 1,2 and 3

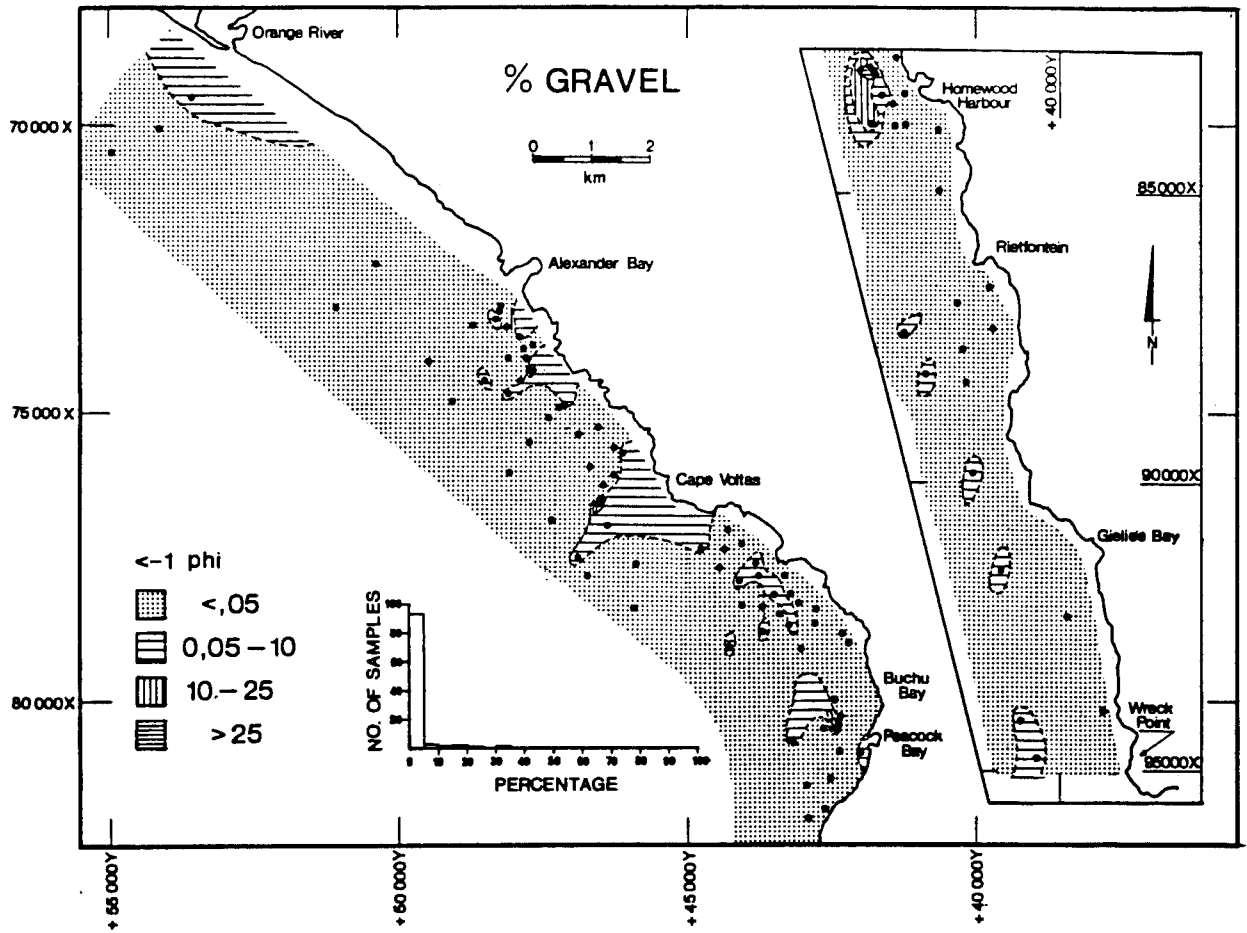


FIGURE 6.14

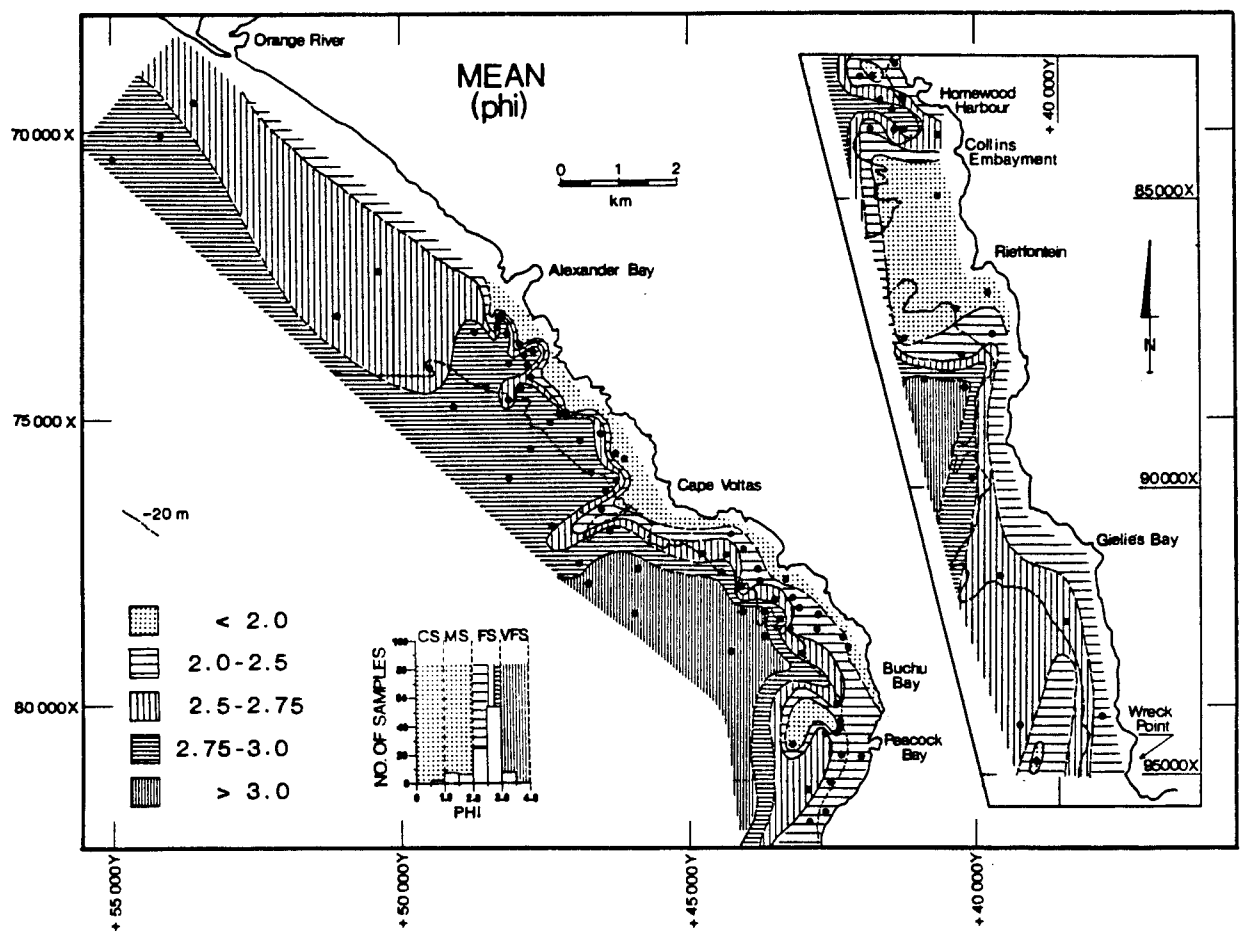


FIGURE 6.15

(Fig.6.3) and started at a position between samples 1 and 2. The slightly finer sand fraction (mean size >3 phi) recovered by Rogers suggests a period of increased terrigenous deposition on the Orange Delta, probably as a result of flooding, or less energetic wave activity preceding the sampling, and that the sediments had not yet attained a hydrodynamic equilibrium with the average wave regime incident on the area. Drake et al. (1972) concluded from a study on the Santa Barbara-Oxmond shelf off California, that over 70% of flood sediments are initially deposited at depths less than 30 m, giving rise to a pronounced disequilibrium. The flood deposits were rapidly eroded by wave-induced bottom currents that transferred the sediment to deeper water on the middle shelf.

The sediment in Buchu Bay is characterised by a large inlier of coarse sand, whereas the sediment closer inshore is generally finer grained, with a mean value of between 2.3 and 2.5 phi. The seaward-fining gradient in Buchu Bay is much steeper than elsewhere. Samples inshore at Agate and Long Beach fall in the "medium-sand" size fraction, whereas the samples on the seaward side have a "muddy-sand" texture with mean grainsize values of >3 phi (very fine sand).

Sediment in Collins Embayment is mainly fine sand, decreasing in mean diameter offshore. An inlier of medium sand lies at the seaward end of the embayment. The sediment covering the exposed bedrock between Collins Embayment and Rietfontein is medium sand (Fig.6.15). Farther south the average grain size remains finer than 2.5 phi, the exception being sample 99, off Wreck Point, that has a value of 1.1 phi (coarse sand).

6.3.3 Standard Sorting

North of Alexander Bay the sand-fraction is well sorted to very well sorted, showing an apparent improvement offshore (Fig.6.16). South of Alexander Bay the influence of the bedrock outcrop is distinct. The sand in the embayments shows sorting values of 0.2 to 0.4 (very well sorted) whereas over bedrock areas the sorting value may reach 1.0, which is only moderately to moderately well sorted sediment.

Most of the samples (89%) have sorting values less than 0.5 (Fig.6.16), indicating that the sand-size fraction is mostly well sorted to very well sorted. The mainly terrigenous sediment north of Peacock Bay is better sorted than the more biogenic sediment farther south.

The trend of better-sorted sediment seaward is maintained to Cape Voltas where the influence of Voltas Reef (Fig.6.3) on the sorting of the sediment is clearly shown (Fig.6.16). Between Cape Voltas and Peacock Bay the trend is from very well sorted inshore through a zone of moderately sorted sediment to well-sorted sediments offshore. South of Homewood Harbour the inshore sediments are very well sorted, becoming moderately well to moderately sorted offshore.

6.3.4 Skewness

The sediment between the Orange River and Alexander Bay is generally strongly coarse-skewed with a seaward trend to near symmetrical and then fine-skewed (Fig.6.17). Sediments from bedrock-outcrop areas south of Alexander Bay to Voltas Embayment are strongly fine-skewed (>0.3), but are coarse-skewed alongside bedrock outcrops. Samples in the embayment are again strongly fine-skewed. Off Cape Voltas the samples become progressively

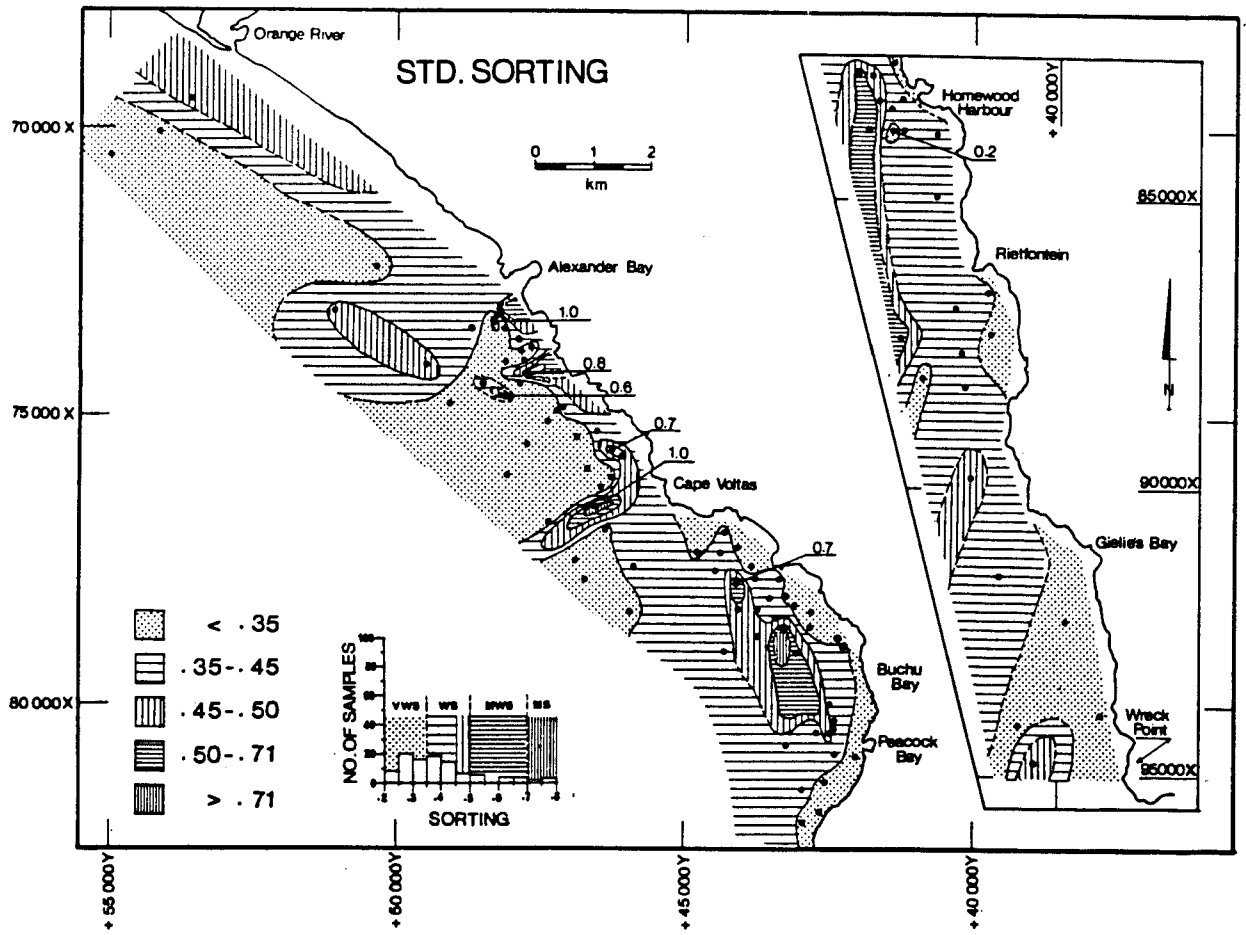


FIGURE 6.16

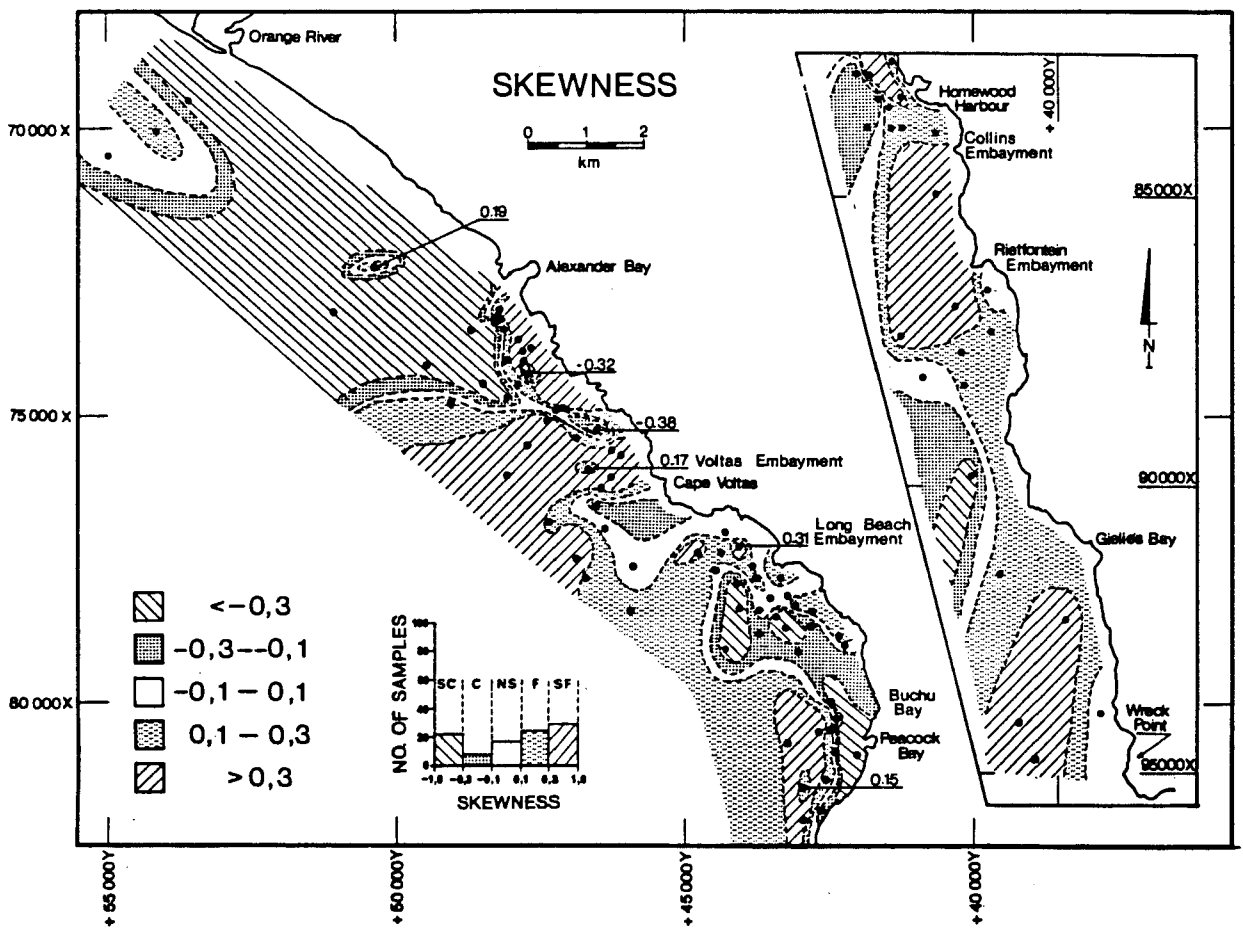


FIGURE 6.17

coarse-skewed, but revert to a fine-skewed distribution in the sediment of Long Beach Embayment south of Cape Voltas.

Between Cape Voltas and Peacock Bay the sediment shows rapid changes from coarse- to fine-skewed. Inshore the sediments are fine-skewed, grading to coarse-skewed and then very coarse-skewed offshore (Fig.6.17). In Buchu Bay the sand-fractions vary from strongly coarse-skewed in turbulent water inshore where a coarse lag fraction could be expected to strongly fine-skewed offshore in sediment with a high mud content. The strongly fine-skewed sediment extends into Collins Embayment, although most of the sediment within the embayment is fine-skewed; seaward the sediment becomes coarse-skewed.

The samples along the northern edge of Rietfontein Embayment, and from the bedrock outcrop towards Collins Embayment are strongly fine-skewed. Within the embayment the sediment is fine-skewed, becoming near-symmetrical inshore and offshore. Gielie's Embayment has strongly fine-skewed sediment, except Sample 97 inshore, which has a near-symmetrical distribution.

6.4. Discussion

Sediments introduced into the sea by the Orange River are dispersed by wave action and longshore drift on the inner shelf (cf Chapter 7). A plot of sorting vs mean grain size for Orange River samples (Rogers, 1977, fig. VII-6) shows that this fluvial sediment is very mixed (poorly sorted to very well sorted, with the average being moderately sorted). Well sorted to very well sorted sediment off the Orange River (Fig.6.16) and the substantial difference in percentages between the size fractions (compare Fig.6.11 (fine sand) with Fig.6.12 (medium sand) and

Fig.6.9 (mud)) suggest the strong influence of the incident waves on the sediment distribution on the inner shelf. Similarly, in the more biogenic sediment between Gielie's Bay and Wreck Point, fine sand is almost exclusively present at the expense of other size fractions (Fig.6.15), and the sediment is very well sorted (Fig.6.16). These terrigenous and biogenic end-members of the sediment "spectrum" indicate that the modern surficial sediment is in dynamic equilibrium with the prevailing wave regime.

Normally swell is from the south-southwest, but during winter storms the swell direction may change to a more westerly direction (Rossouw, 1984), resulting in a southerly transport of sediment (Gurney et al., 1982). The annual median wave height at the Orange River is about 1,75 m and the wave period is 11 secs (Rossouw, 1984 and Chapter 7). The effectiveness of the wave regime in sorting sediments on the Orange Delta has already been mentioned by Rogers (1977, Fig.VII-6). He also reported that beach samples were on average moderately well to well sorted, although the mean size ranges between very coarse sand and fine sand. In the study area the bulk of the sediments have high percentages of the fine and very fine sand-size fractions, and the average sand-sorting is 0,35 (very well sorted).

Further evidence of the strong influence of the wave regime on sediment distribution is seen in the strong separation in size-fractions, particularly inshore, close to the surf zone. In this zone size-fractionation takes place. This is well displayed off Agate Bay, where the fine sand size-fraction increases offshore to a maximum of over 80% just beyond the surf zone. Seaward the percentage decreases again (Fig.6.11). The percentages for the medium and very fine sand fractions

(Figs.6.12 and 6.10) are inversely related along a line extending offshore from the beach, with medium sand percentages decreasing steadily seaward.

A further distinction can be made on the basis of the skewness values: the samples north of Alexander Bay are near symmetrical to strongly coarse skewed, whereas the sediment south of Giellie's Bay is strongly fine skewed to near symmetrical (Fig.6.17). The Orange River introduces moderately sorted sand to the sea (Rogers, 1977) which will continually be fractionated by the incident swell activity, with the finer fractions deposited seaward of the coarser fractions. These coarse fractions, on the other hand, are only transported at times when the energy is sufficiently high, and the net transport direction would be onshore, affected by the stronger onshore component of the wave orbital motion (Komar, 1976b). The sediment distribution therefore develops a coarse tail. In Giellie's Embayment the situation is one of a continual supply of fine biogenic fragments with the introduction of benthic foraminiferal tests to the sediment population beneath surface waters enriched in plankton due to upwelling which occurs throughout the year along this part of the coast (Shannon, 1985). Up to 10% of the biogenic fragments in these samples consists of benthic foraminiferal tests which would give rise to a bias towards the fine-grained end of the sediment population.

This "normal" situation is affected in several ways, reflected in the sediment distribution pattern. The mean grain size (Fig.6.15) decreases offshore in response to the decreasing wave activity at the seafloor, but the smooth gradation, such as off the Orange River or in Buchu Bay, is in places farther south

interrupted by the presence of bedrock, or storm-lag deposits on bedrock-highs. This trend is suggested by the various bivariate plots of skewness vs. mean (Fig.6.18), mean vs. CaCO_3 (Fig.6.19), skewness vs. sorting (Fig.6.20) and sorting vs. mean (6.21). The diagrams differentiate between samples taken from areas that are shown to be exposed bedrock on the sonographs, samples retrieved from sediments that formed into megaripples and other bedforms and sediment samples from areas with no distinguishing features on the sonographs. The effect that bedrock outcrop has on the sediment is evident in the area from Alexander Bay to Rietfontein. Voltas Reef extends about 2 km seaward from Cape Voltas (Fig.6.3) and the samples retrieved from the reef (or close to it) show distinct textural differences from samples elsewhere. Likewise one finds that the exposed bedrock area between Homewood Harbour and Rietfontein is distinguished by sediment that is both compositionally and texturally distinct from the sediment in the embayments (cf. Figs.6.5 and 6.19). The narrow zone of higher percentage rock fragments (which includes heavy minerals) between Alexander Bay and Cape Voltas lies at the seaward edge of the shoreface bedrock outcrop, in approximately 20 m water depth. Hydraulic fractionation of the available sediment due to the higher wave energy in shallower water would preferentially transport the lighter sediment fractions, leaving the sediment enriched in the heavier fraction at the seaward edge of the outcrop.

Megaripples are present in several areas between Alexander Bay and Wreck Point and occur in water depths of less than 15 m to 30 m (cf Chapter 7). The wavelengths of the megaripples (measured on sonographs from the area) range from 0,5 m to 1,5 m.

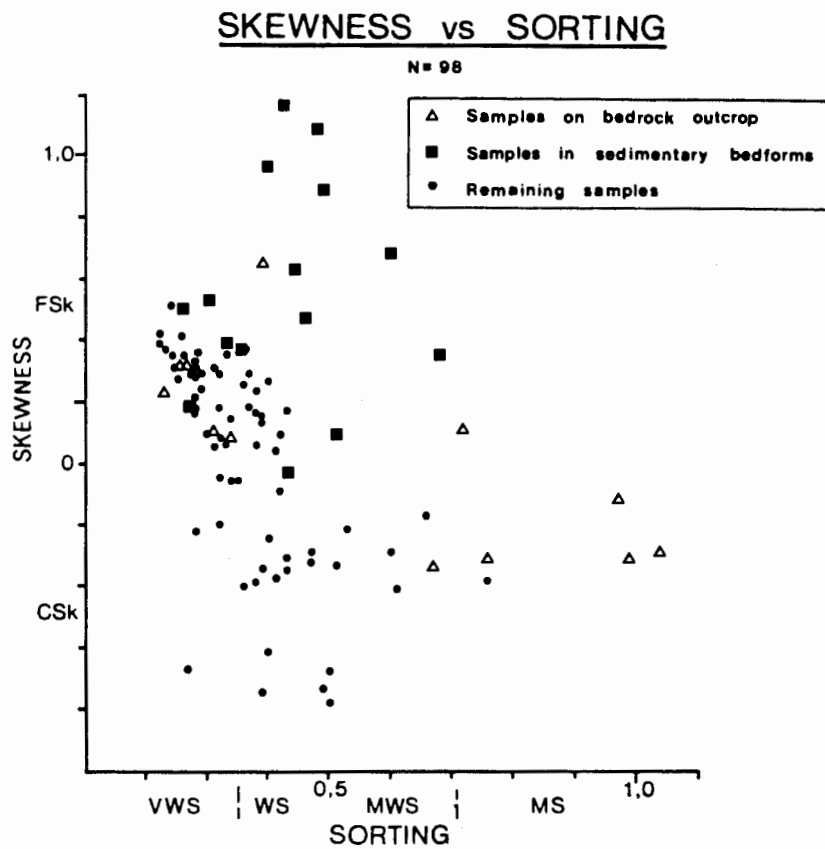


FIGURE 6.20

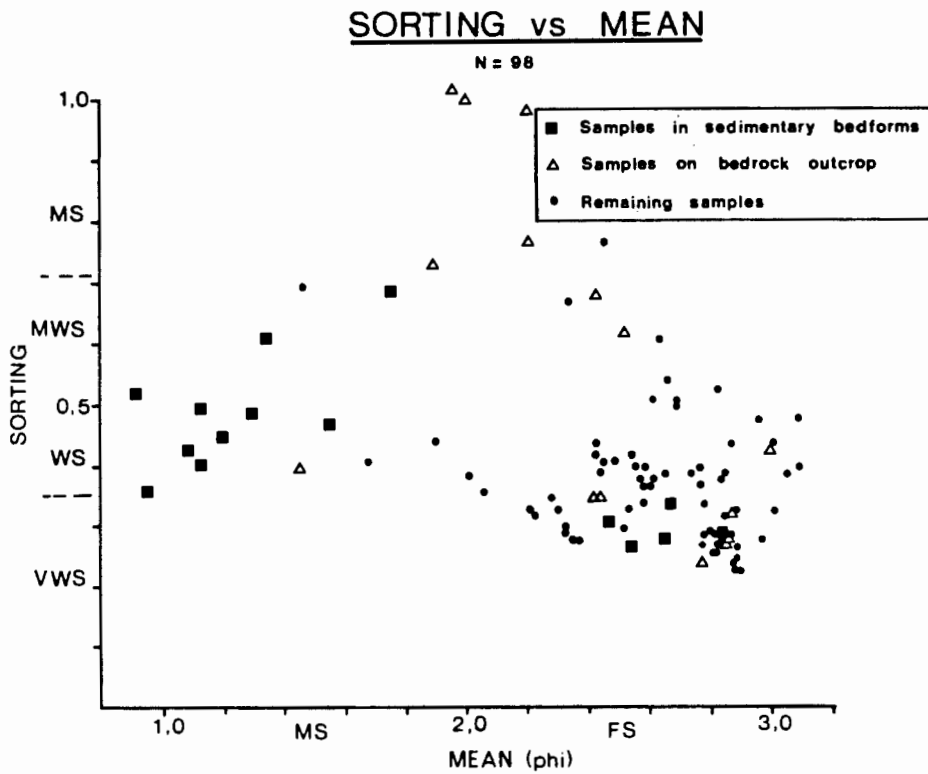


FIGURE 6.21

redeposited on the mudbelt.

6.5 Conclusions

Sampling was primarily aimed at establishing sedimentary control to verify the interpretations of the sonographs. Sample positions are consequently concentrated in areas of sonographic interest. Despite this biased sampling, the analyses, if interpreted in conjunction with the sonograph features on the seafloor, nevertheless reveal interesting sediment-distribution trends.

Compositional and textural distributions indicate that the sediments on the inner shelf are derived from more than one source. South of the Orange River terrigenous mica-bearing fine sand on the Orange delta front grades southwards to slightly muddy fine sand between Alexander Bay and Cape Voltas and muddy very fine sand in Buchu Bay (Fig.6.3). South of Homewood Harbour terrigenous sediment is mixed with biogenic carbonate sediment introduced from the south mainly through northward-directed longshore drift (Harris, 1978). The area between Cape Voltas and Homewood Harbour has elements of both these "end-members", but also a lag fraction consisting of a coarse shelly-gravel deposit found in Buchu Bay. The three sedimentary zones are best defined by the percentage distribution of compositional components (Figs.6.4 to 6.8).

Texturally and compositionally the sediments on the inner shelf may therefore be separated into three populations, with the gravelly, shelly, coarse sand population being storm-lag deposits. The terrigenous fraction, mainly concentrated in the north (on the Orange Delta) and the biogenic fraction which is

found concentrated in the southern embayments appear to be in dynamic equilibrium with the hydrodynamic regime. Megaripples that form in areas like Buchu Bay indicate active sediment movement, presumably by storm-wave-induced currents. The high-energy waves incident on this coastline and the resultant sediment transport are described in the next chapter.

CHAPTER 7WAVE REGIME AND SEDIMENT TRANSPORT7.1 Introduction

The positions of the sediment samples that were collected in the study area were selected to verify the interpretation of specific sonograph images. Included in these images were recognizable sedimentary bedforms, chiefly but not exclusively, megaripples. In the previous chapter the composition and texture of the sediments are described and the distinction made between sediment from areas covered by sedimentary bedforms and sediment retrieved from other areas.

This chapter describes the sedimentary bedforms as interpreted from the sonograph records. Their distribution, morphology and their possible origins are discussed. For proper inferences on sediment dynamics to be made from the study of bedforms, having taken the texture and composition of the sediment into account, a knowledge of the wave and current regime extant in the study area is required. "Waverider" data from Alexander Bay, made available by the Fisheries Development Corporation, have been analysed for this purpose and the results are presented here.

It should be mentioned at the outset that the sediment samples, sonograph records and wave data were not obtained synchronously (the ideal situation), so that detailed correlations are not possible.

7.2 Hydrodynamics

In Chapter 1 the regional water circulation pattern on the continental shelf is described. The conclusion is that water-mass movements on the continental shelf have relatively little influence on the inner shelf. When upwelling occurs inshore, it is areally restricted and its maximum effect is seen some distance from the coast, in the vicinity of the inner-shelf slope. The water circulation pattern on the inner shelf itself is thus mainly the result of the incident swell regime, the resultant wave-induced currents and of wind-driven currents.

Waves are caused by wind blowing over the sea surface. The strength, duration and fetch of the wind will determine the wave dimensions. It is clear that at any time there will be a variety of waves of various dimensions propagating away from the origin. Sets of waves will range from being exactly out of phase with others to being in phase, thereby either cancelling or superimposing and thus creating a new wave set. It follows that there is no unique equation that will describe the whole spectrum of waves incident on a coast. Approximations are made which, out of necessity, are gross simplifications of the true nature of the wave condition. The simplest, or first order, equation assumes a sinusoidal curve for the waves, and the theory used in its derivation is known as linear (or Airy) wave theory. Other, higher-order equations have been developed which require a more sophisticated mathematical treatment. Swart (1983, p.10) describes the development of wave theories in his review on the physical aspects of beaches and concludes that the vocoidal wave theory developed by him "...is simple to apply and is in good correspondence with theory (boundary conditions) and data for all

relative water depths".

To compare the linear wave theory with the vocoidal theory for the conditions pertaining in the study area, a correlation curve for U_d , the horizontal orbital velocity at the seafloor (Komar, 1976a), against U_{bc} , the horizontal orbital velocity at the seafloor measured under the wave crest (Swart, 1981), was drawn (Fig.7.1). A coefficient of 0.99 indicates that there is a very good correlation between the two values for the depth calculated (15 m). This correlation decreases in shallower water, since linear wave theory does not take into account the strong shoreward asymmetry of the near-bottom wave orbital motion of shoaling waves (Komar, 1976b). Despite these shortcomings, the linear wave theory equation remains a widely used approach to determine sediment movement on the seafloor (cf. recent papers by Pickerill, 1983, and Sunamura and Kraus, 1985). Consequently this equation is used in this study to calculate the wave conditions for which sediment transport at -15 m, -20 m and -30 m are possible.

The horizontal orbital velocity (U_d) in linear wave theory has the expression:

$$U_d = \frac{\pi H}{T \sinh(2\pi d/L)} \dots\dots\dots(1)$$

Where H denotes wave height, T is the wave period, d is the water depth and L is the wave length. Equation 1 is applicable in intermediate water depths, ranging from 0.25L (deep water) to 0.05L (shallow water) (Komar, 1976a). Table 7.1, below, shows that most of the study area falls within the "intermediate-water" range.

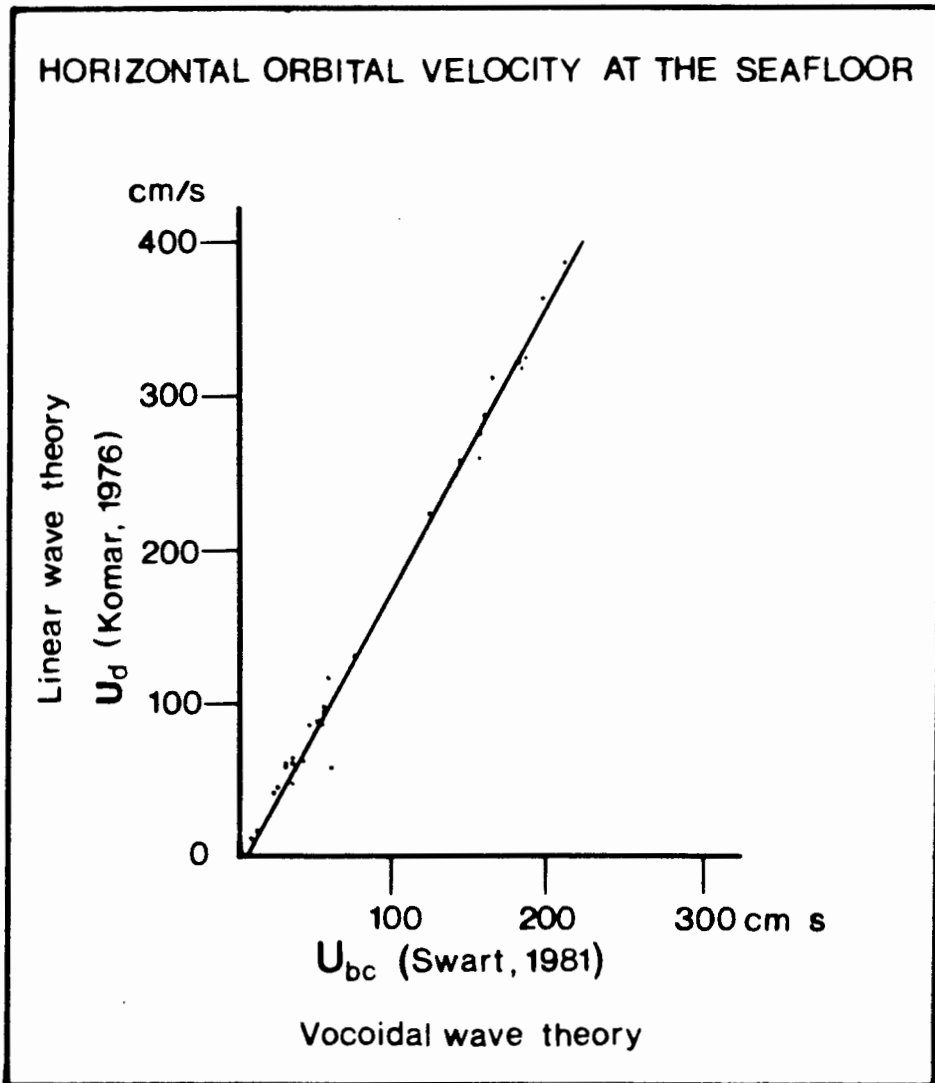


FIGURE 7.1

The wavelength (L) is determined from the equation

$$L = \frac{g}{2\pi} T^2 \tanh \frac{2\pi d}{L} \dots\dots\dots(2)$$

which reduces to $L = \frac{g}{2\pi} T^2 \dots\dots\dots(3)$

for deep to intermediate water and

$$L = T\sqrt{gd} \dots\dots\dots(4)$$

for shallow water.

The threshold of sediment movement can be calculated from the equation (Komar, 1976a)

$$\frac{\rho U_d^2}{(\rho_s - \rho)gd} = 0.21 \left(\frac{d_o}{D} \right)^{1/2} \text{ for } D < 0.5 \text{ mm} \dots\dots\dots(5)$$

and $= 0.46 \pi \left(\frac{d_o}{D} \right)^{1/4} \text{ for } D > 0.5 \text{ mm} \dots\dots\dots(6)$

where $d_o = \frac{U_d T}{\pi} \dots\dots\dots(7)$

D is the grain diameter, ρ is the density of the water, ρ_s is the density of the sediment and d_o is the orbital diameter of the wave motion.

The parameters most commonly used in wave dynamics are (Rossouw, 1984):

T_p - the period of the highest wave amplitude, or the wave period at maximum energy.

T_z - the mean wave period, determined by dividing the duration of each record (normally 20 minutes) by the number of times the record crosses the zero line in an upward direction.

H_s - the significant wave height, calculated as the average one-third of the highest waves in the record.

In this study the maximum-energy wave period T_p and the significant wave height H_s are used.

Table 7.1 shows the range of water depths in the study area that determine the shallow-, intermediate- and deep-water regions for wave-period exceedance values of 50% and 5% (cf. Fig.7.4). The percentage exceedance value indicates the percentage of waves that will exceed that value. For instance in Figure 7.4, 10% of incoming waves will exceed a wave period of 13 secs in summer, whereas 90% will have periods longer than 8 secs.

Table 7.1

Range of depths for deep, intermediate and shallow water (m)

Exceedance	T_p (sec)	Deep Water (m)	Intermediate Water (m)	Shallow Water (m)
50%	11.0	>47.2	47.2 - 9.4	<9.4
5%	14.8	>85.4	85.4 - 17.1	<17.1

Table 7.1 demonstrates that most of the inner shelf lies within the "intermediate water" range. This means that the linear wave equation may be applied to the wave data, it being valid for most of the wave conditions, in all water depths below 17 m.

7.2.1 Waves and currents off the West Coast

Heydorn and Tinley (1980) note that the difference between the highest and lowest tidal range recorded along the west coast is 60 cm and that the tidal range at Port Nolloth is 1,6 m, placing this part of the coast in the microtidal (<2 m) range. The effect of tidal currents on the sediment dynamics of the inner shelf will therefore be negligible. The review by Harris (1978) of coastal currents reveals that data are scarce for the West Coast. Based on wind data (Fig.1.5) he concludes that the predominant coastal currents are most likely northward directed.

The Sea Fisheries Research Institute have two Aanderaa RCM4 current meters on an array deployed at -142 m on the middle shelf (one 102 m above the seafloor, and the other 22 m above the seafloor) about 48 km southwest of Port Nolloth (Fig.1.8). Preliminary interpretation of data taken during the 4-month period, December 1983 to March 1984, indicates a south-southeasterly (138°) bottom current at these depths with average current velocities of 12 cm/sec, ranging up to 25 cm/sec (Nelson pers. comm., 1984).

In a comprehensive review of all the wave data that are available for southern African waters, Rossouw (1984) notes that along the West Coast data have been gathered for several years but until recently the results were not very reliable. In addition, clinometer data from Buchu Bay between 1969 and 1972 were of poor quality according to Rossouw (1984). Initial "Waverider" data gathered by Consolidated Diamond Mines from a position just north of the Orange River mouth for the 12-month period March 1976 to February 1977 have been discarded by him as being of doubtful value.

In their discussion of the wave climate along the coast, Rossouw et al. (1982) conclude that voluntary observer ship (VOS) data is of lower quality than Waverider data. The comparable 0,01% exceedance data at Oranjemund is 7,5 m and 11,1 m for "Waverider" and VOS respectively, whereas at Walvis Bay the values are 3,8 m and 10,4 m. (At 0,01% exceedance one in every 10 000 waves exceeds the value given.) The distribution of wave heights along the West Coast shows a gradual decrease from south to north, ranging from a median annual value of 2,5 m near Cape Town to 1,75 m at Oranjemund and 1,4 m at Walvis Bay (Rossouw,

Town to 1,75 m at Oranjemund and 1,4 m at Walvis Bay (Rossouw, 1984). For hydrodynamic studies on the inner shelf it is therefore necessary to obtain locally derived wave data since the discrepancy between inshore and offshore data is significant and the difference along the coast is large.

The CSIR deployed a "Waverider" buoy in 15 m water-depth 25 km north of the Orange River mouth for an interrupted 3-month period between February 1978 and April 1980 and the data have been summarised by Rossouw (1981). The Fisheries Development Corporation (FDC) collected wave data for the 18-month period, March 1981 to September 1982, for the State Alluvial Diggings using a "Waverider" buoy situated at a position off Alexander Bay in 15 m of water (Fig.7.2). Partially reduced data have been made available for this study (Vonk, pers.comm., 1984).

Van Ieperen (1976) believes the strong southeasterly winds, which occur after the passage of a coastal low (cf Chapter 1) to be principally responsible for the local wind regime. Wind-driven currents have a maximum velocity near the water surface and decrease rapidly with depth. Swart (1983) estimates that for very strong winds blowing northward alongshore (as is found along the West Coast), wind-induced currents could attain velocities of between 25 cm/s and 50 cm/s in the surf zone. He concludes that the effect on sediment movement cannot be neglected. This is borne out by Allen (1970, p171) who finds that "oscillatory currents of the order of 10 cm/s are seen to be all that are needed to set in motion the finest sand."

Rossouw et al. (1982) find along the West Coast that the wave directions on the shelf is predominantly from the south and

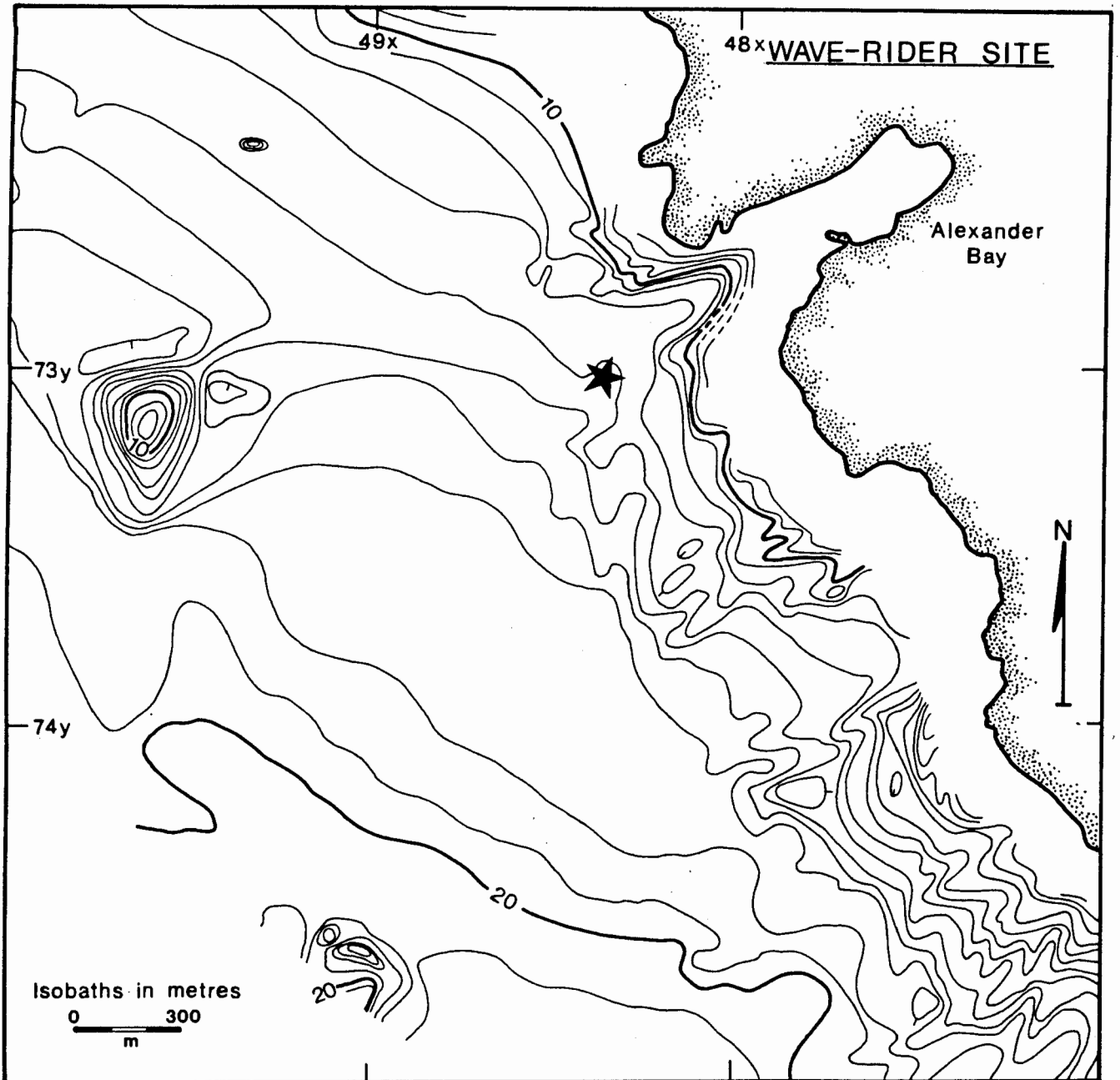


FIGURE 7.2

southeast (Table 7.2 and Fig.7.3A and B), formed by the persistent southeasterly winds that are found along the coast (Fig.1.5). These locally wind-driven waves therefore propagate either parallel to or away from the coast and consequently do not reach the shore. According to Rossouw et al. (1982) this explains the discrepancies in wave height between the data from the VOS (offshore) and the "Waverider" (inshore). It is therefore vital that wave data used to study coastal currents along the west coast are derived from recording stations on the inner shelf itself or, optimally, that the wave propagation direction is known at the time of recording.

Table 7.2

Percentage occurrence of wave directions (VOS data)
(from Rossouw, 1984)

Direction	Summer	Autumn	Winter	Spring
NNE-E	0.5	-	0.6	-
ESE-S	72.6	71.8	57.2	72.8
SSW-W	25.3	26.7	40.3	25.2
WNW-N	1.0	0.5	1.4	1.6

Waves from the southwestern quadrant are much more prevalent during winter (40,3%) than in summer (5,3%)(Table 7.2). This results in an intensification during winter of the pronounced northward littoral drift found along the coast (cf Fig.1.9). Swart (1983) estimates the annual northward littoral drift to be $1,4 \times 10^6 \text{ m}^3$ per year for a section slightly north of the Orange River. Further evidence of the strong northward drift is the pronounced asymmetry of the Orange Delta, extending over 80 km northward (Hoyt et al., 1969) whereas deltaic deposits are no longer in evidence off Wreck Point, 30 km south of the river

WAVE DIRECTIONS FROM VOS
AND WEATHERSHIP DATA
(after Rossouw 1984)

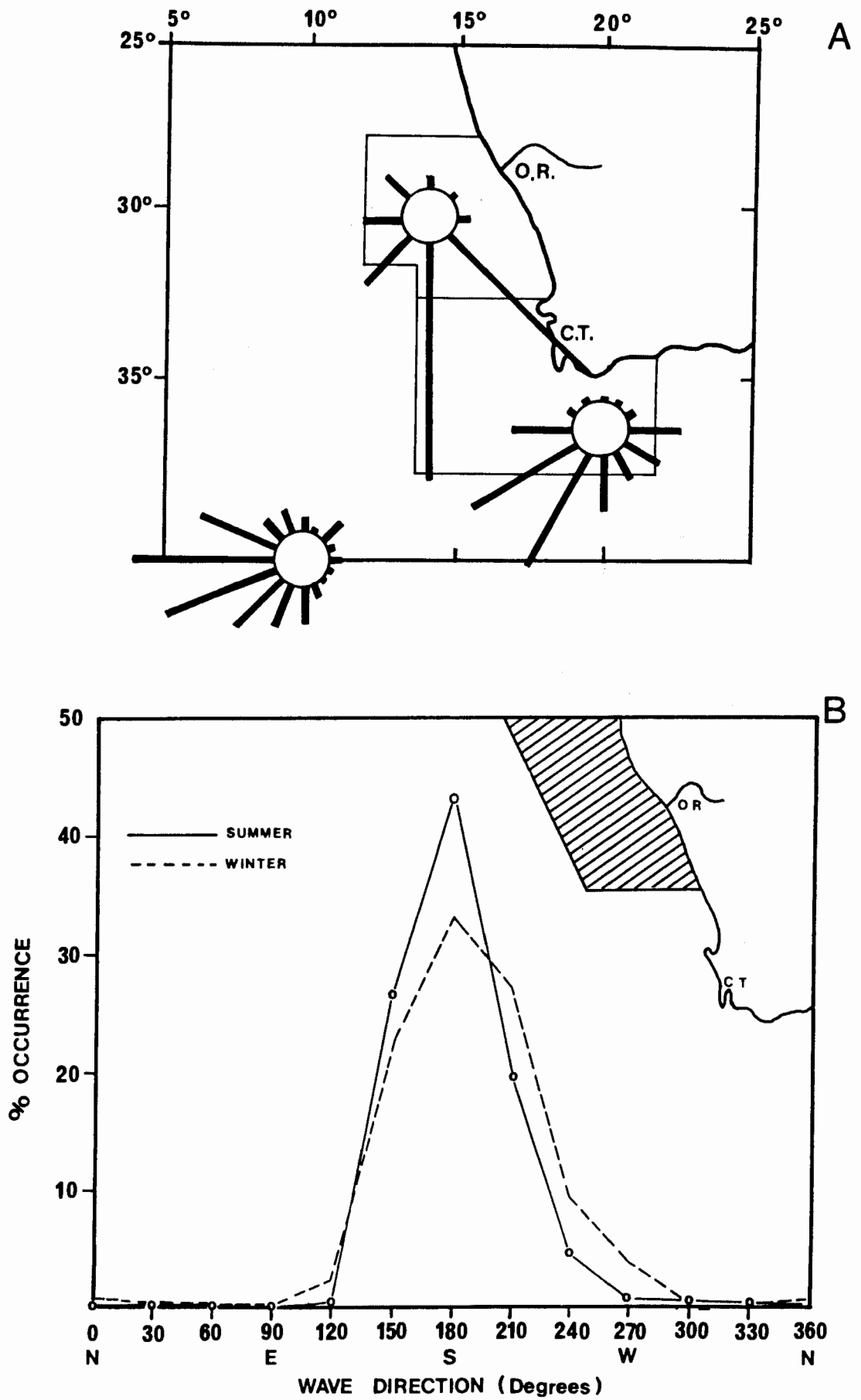


FIGURE 7.3

mouth. Minimal sediment input onto the inner shelf south of the Orange River, plus the strong northward littoral drift, has brought about an inner shelf that is underlain largely by exposed bedrock, with sediment restricted to embayments and the littoral zone (cf Chapter 2 and Woodborne, 1986). Wave directions from the northwestern quadrant are quantitatively insignificant, but are highest in Spring (1,6%) and Winter (1,4%). During periods when waves arrive from this direction, the northward littoral drift may be absent or even reversed. Waves arriving from the southwestern quadrant generally originate from distant storm centres in the Southern Ocean associated with the eastward passage of cyclones (cf Chapter 1). Local storms are the result of strong south-southeasterly winds and easterly bergwinds. The resultant wave direction would be northwestward, or offshore. Waves incident upon the shore that have been generated by distant storms typically have long periods and low amplitudes, whereas local storms generate steeper short-period waves. Swart (1983) suggests that waves from local storms will have a steepness (amplitude : wavelength ratio) between 0,025 and 0,1 and that the ratio for distant storm waves lies between 0,025 and 0,002.

7.2.2 Waves in the study area

The dominant wave periods and wave heights in the study area are shown in Table 7.3.

Table 7.3

Median wave period (sec) and wave height (m), winter (W) summer (S)

	T_p		T_z		H_s	
	W	S	W	S	W	S
Alexander Bay	12.5	10.5	7.5	5.5	1.9	1.5
Oranjemund	-	-	10.0	7.0	1.7	1.5

The median values for the maximum-energy wave period (T_p) from the Waverider records recovered by the FDC at Alexander Bay, range from 10.5 sec in summer to 12.5 sec in winter (Fig.7.4). The equivalent values of T_z are between 5.5 sec and 7.5 sec (Fig. 7.5A). The mean wave period (T_z) at Oranjemund, according to Rossouw (1981), is in the range 7 sec to 10 sec (Fig.7.5B), the longest being in winter. This compares with the range calculated by Van Ieperen (1976) of between 8 sec and 12 sec for values obtained from 'deepwater' (>50 m) wave recording stations at Saldanha Bay, Luderitz and Walvis Bay along the West Coast. Rossouw's (1981) data are from a Waverider deployed about 16 km north of the Orange River mouth in 15 m of water (cf Fig.1.8). The smaller T_z values for waves recorded at Alexander Bay could reflect a lower percentage of distant storm waves during the period when the data were gathered.

Wave heights calculated for Alexander Bay show that 90% of the values fall in the range 0,5 m to 3,5 m (Fig.7.6A). The median for all seasons except winter lies at approximately 1,5 m, whereas for winter it is 1,9 m. The wave heights in Rossouw's (1981) data range between 1,5 m for summer and 1,75 m for the other seasons (Fig.7.6B). There is therefore relatively little variation in the wave height throughout the year with the maximum occurring in winter and the minimum in summer. Rossouw (1981) mentions that wave heights exceeding 5,0 m occur throughout the year which is approximately what was found at Alexander Bay where waveheights between 4,75 and 5,00 m were exceeded in all seasons (Table B5).

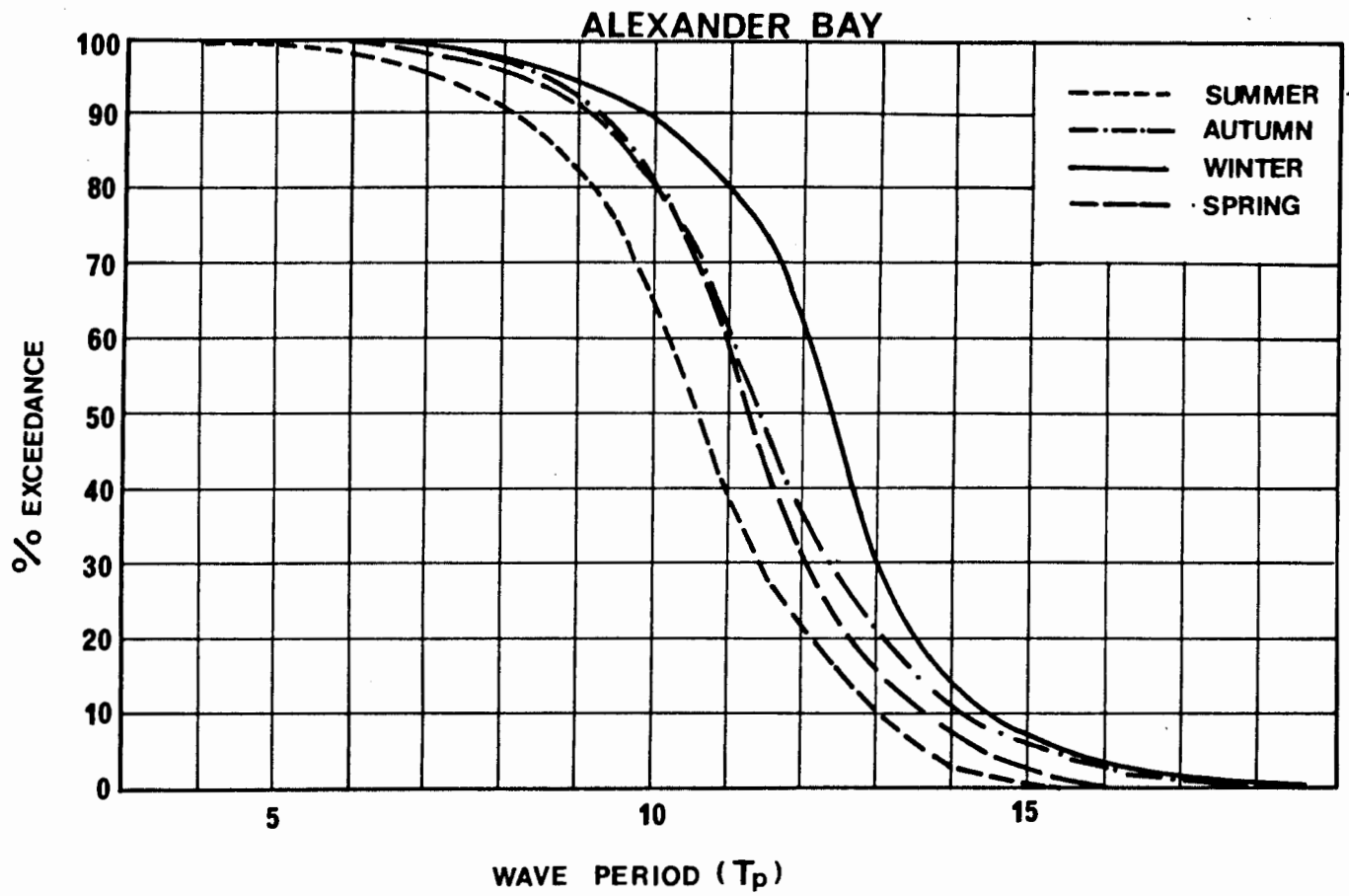


FIGURE 7.4

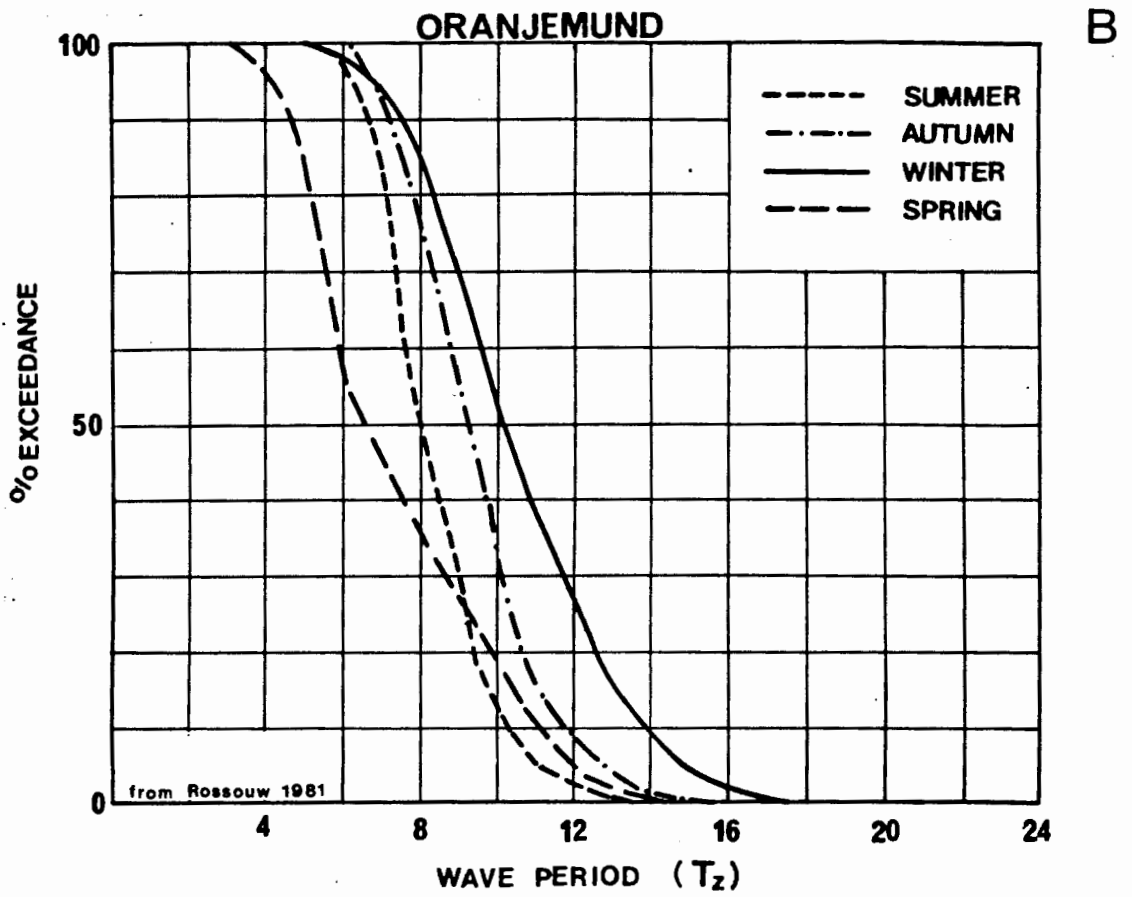
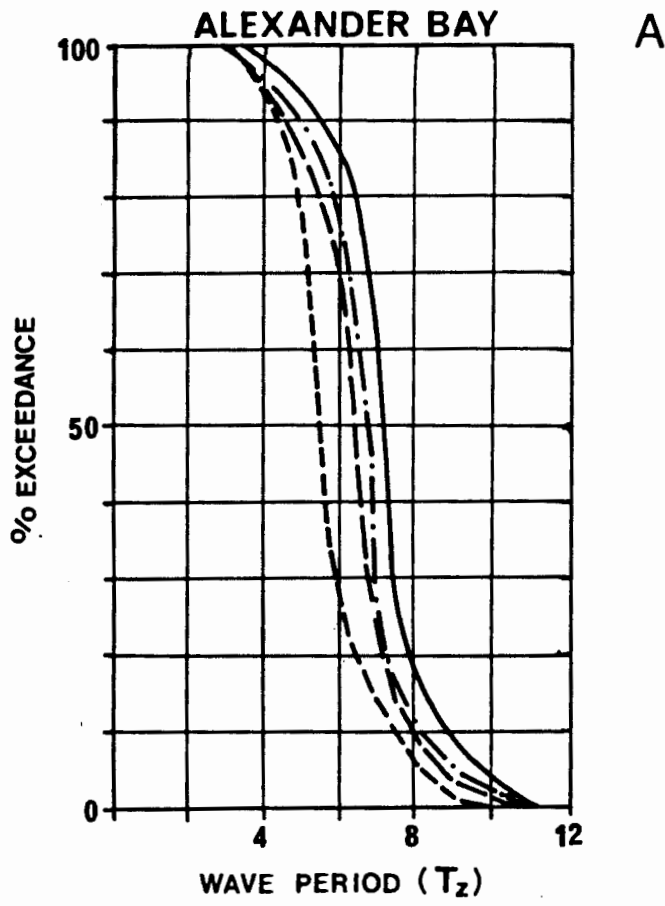


FIGURE 7.5

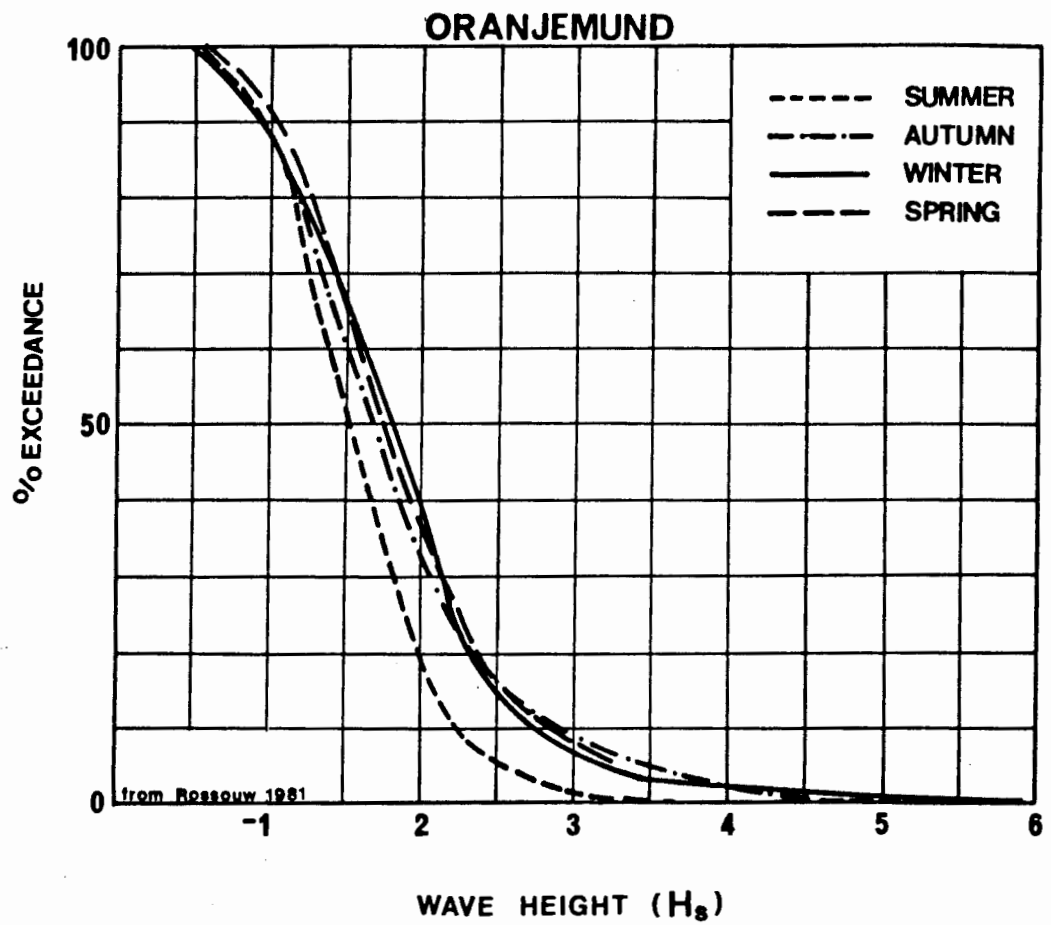
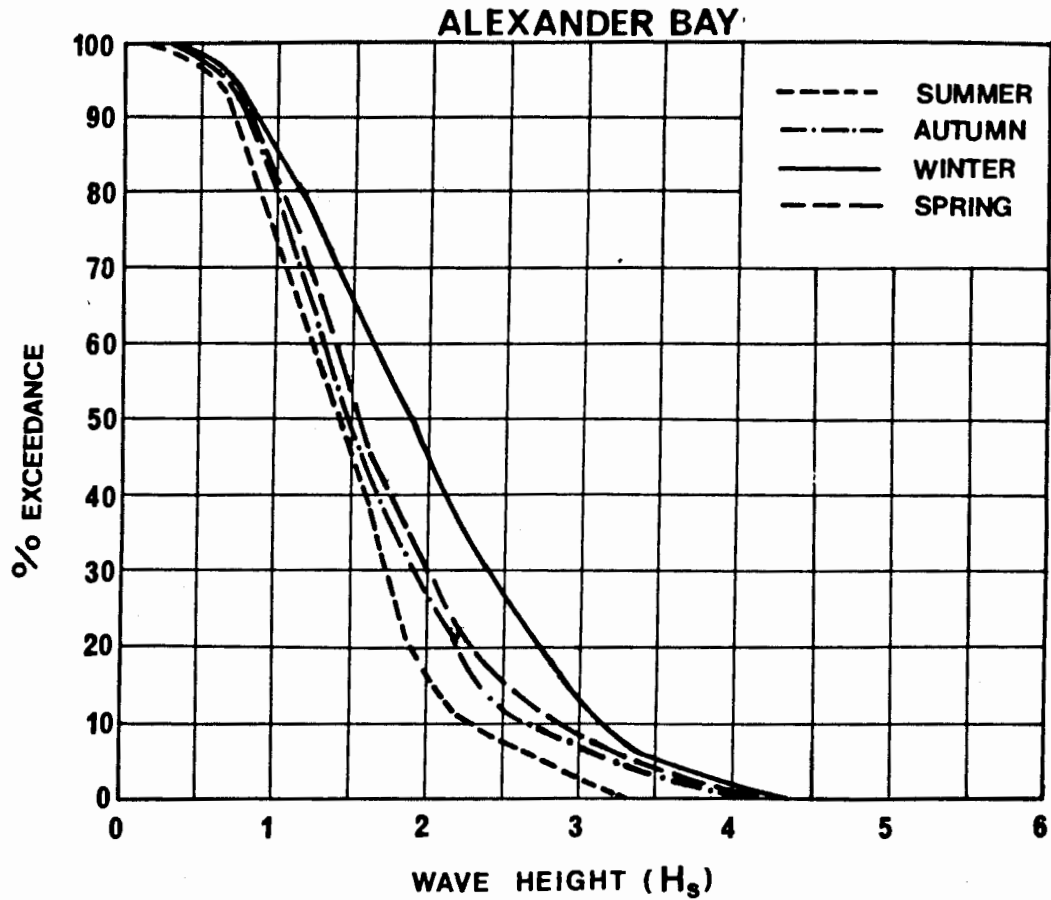


FIGURE 7.6

7.3 Sedimentary bedforms

The sonograph records in the study area reveal the presence of various bedforms, ranging from individual, isolated features to extensive, continuous fields of bedforms covering large areas of the sea floor. The shape, dimensions and orientation of the sedimentary bedforms can be related to the hydrodynamic regime, sediment texture and water depth at the time of formation. A study of the distribution and morphology of the bedforms could therefore give a better insight into the sediment dynamics on the inner shelf. From this the sediment mass movement under specified wave conditions and for given sediment grain-size range can be determined.

The meaningful interpretation of sonographs requires the removal of both the compressional distortion due to ship's speed and the slant-range distortion resulting from the height of the transducer above the seafloor (Flemming, 1976b and 1982, see also Appendix). Having made the necessary corrections for the major distortions, it is possible to determine the true dimensions and orientation of features such as bedforms on the seafloor. Using the acoustic shadow zone of an object protruding above the seafloor, its height (or amplitude, H_o) can be calculated from the equation (Flemming; 1976b, D'Olier, 1979):

$$H_o = \frac{W_s \times H_t}{W_s + R_s} \quad (8)$$

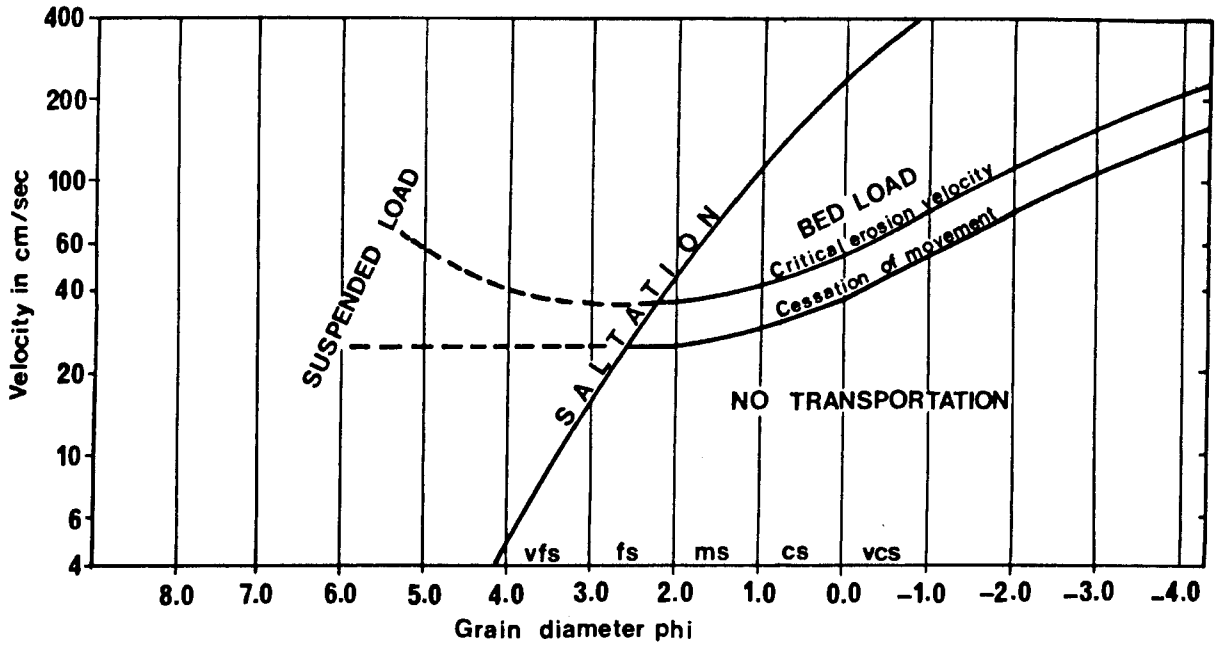
where W_s = width of shadow zone
 H_t = transducer height above seafloor
 R_s = slant range

Figure 4.1 shows the various dimensions that need to be considered. A limitation of this method is the orientation of scan direction relative to the crestline of the bedforms. For an accurate estimate of the amplitude of the bedform these directions should be at right angles to each other, thus effecting the maximum shadow-zone width.

The resolution of the recording system (Flemming, 1976b) determines whether or not an image will be seen on the record (cf Appendix). The resolution parallel to the line of travel (transverse resolution) at 100 m scan range is between 1,75 m and 2,09 m, depending on the recording system used, whereas at 25 m scan range the resolution is 43 cm to 52 cm. The range resolution, at right angles to the ship's course, is also related to the scan range, but also paper width. For a scan range of 100 m the resolution may vary from 49 cm to 80 cm.

Sedimentary bedforms develop in response to an increase (above a critical level) of the flow velocity of the fluid above the sediment. Several forces need to interplay to overcome the retaining (gravity) forces acting on a grain. The moment when entrainment occurs, is mainly influenced by the flow velocity and the sediment grain diameter although factors such as grain shape and composition of the sediment will also affect it (Reineck and Singh, 1980). Depending on the flow velocity and the grain size, Figure 7.7 shows that the sediment will be transported either in suspension or as bedload with an overlap zone of saltating transport at the boundary. The bedload field is of particular importance in the discussion on the development of large-scale sedimentary bedforms. Figure 7.8 shows that under general conditions flow velocity and grain size are critical parameters in determining the type of bedform that will be formed.

The extrapolation of flume experiments to field observations (Fig.7.9) has given rise to a range of descriptive terms for what are perceived to be genetically similar bedforms (cf Middleton



(from Reineck and Singh 1980)

FIGURE 7.7

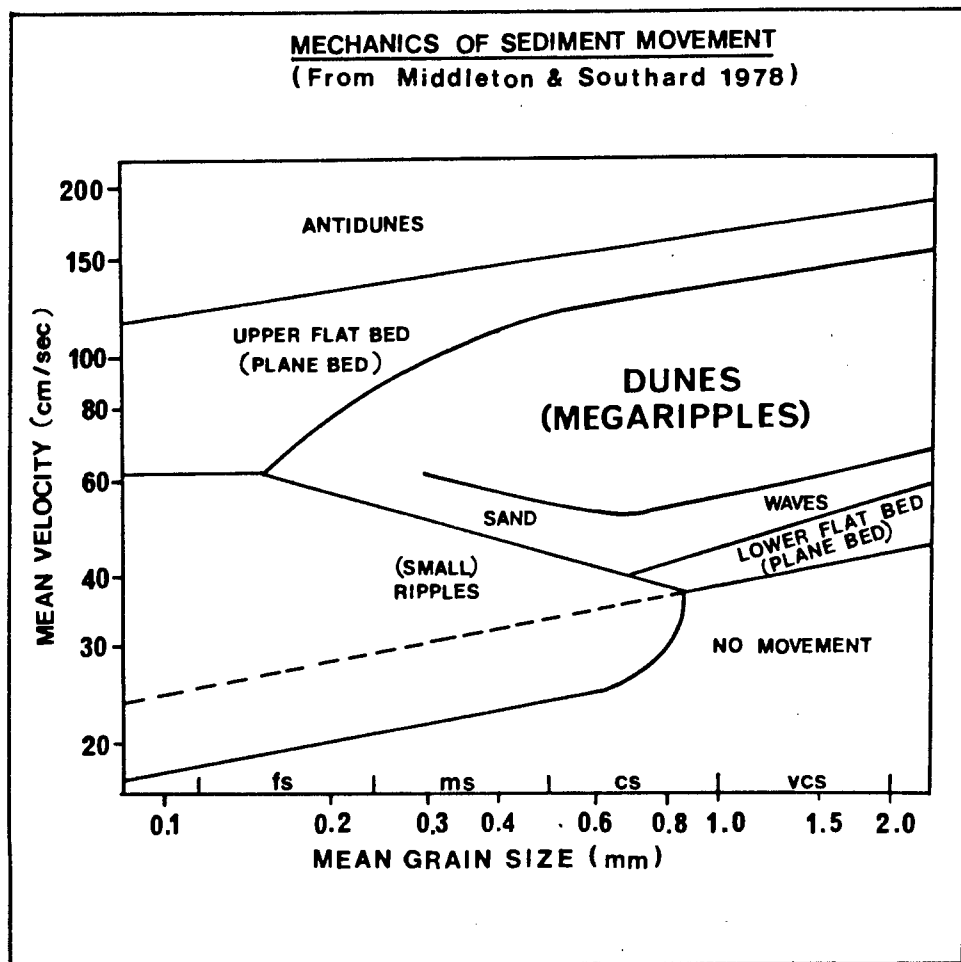


FIGURE 7.8

and Southard (1978) and Reineck and Singh (1980) for discussions on flume experiments). Table 7.4 is a compilation of the parameters used by Amos and King (1984) to define the bedforms they have observed on the southeastern Canadian continental shelf, and from Reineck and Singh (1980) which the latter gleaned from various sources.

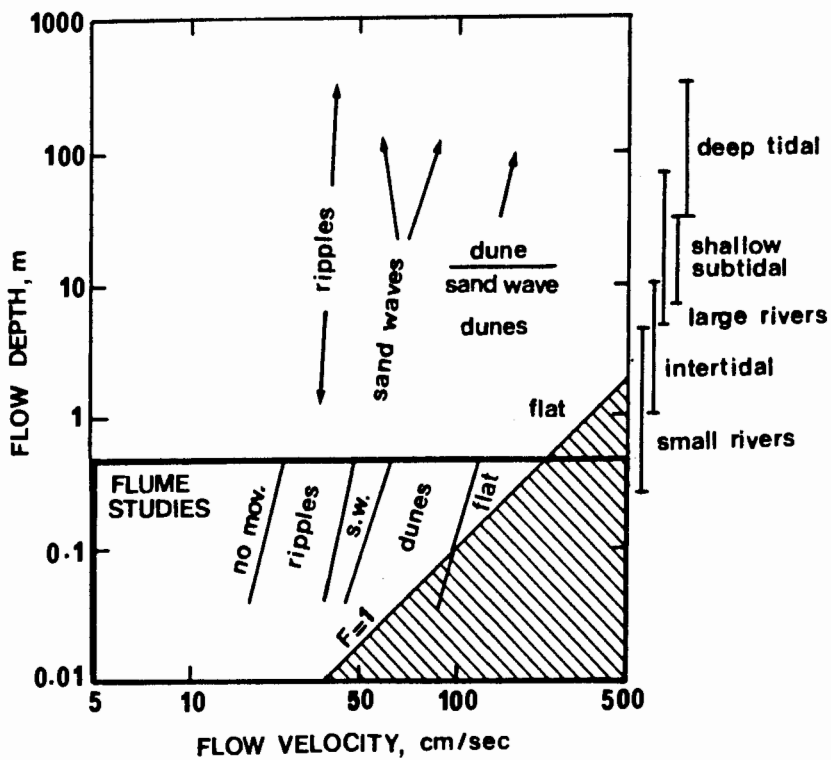
Table 7.4
Nomenclature and dimensions of bedforms.

Bedforms	H(m)	L(m)	U_m (cm/s)	Remarks
a) Small ripples	$\ll 1$	$< 0,6$	20	
b) Sandwave 1.	$H \ll L$	5 - 100	30 - 80	
2.	0.5 - 12	12 - 1000	40 - 100	
c) Megaripples				
1. Two-Dimensional	0.1 - 2	0.2 - 50	40 - 60	Straight-crested megaripples; sand-waves
2. Three-Dimensional	0.1 - 1	0.2 - 50	60 - 150	Sinuus-crested megaripples; dunes
d) Sand ridge	1 - 30	6×10^4	50 - 250	700-8000m wide
e) Sand ribbons	< 0.5	15×10^3	100 - 300	<u>+</u> 200m wide

H - Amplitude of the bedform in metres
L - Wavelength of the bedform in metres
 U_m - Bottom flow velocity

Flemming (1978) in a review states that there is some confusion of bedform nomenclature in the literature which led him to suggest that no genetic connotation should be placed on the names given to bedforms. The extreme range in the dimensions and the multiplicity of terms for the same feature (Table 7.4) emphasizes Flemming's (1978) contention. Amos and King (1984, p.198) consider that bedforms falling within one of their fields (separated by dashed lines in Figure 7.10) are generically indistinguishable and differ only "in terms of degree and not of kind".

FIELD/FLUME COMPARISON
(medium sand)



(from Middleton and Southard 1978)

FIGURE 7.9

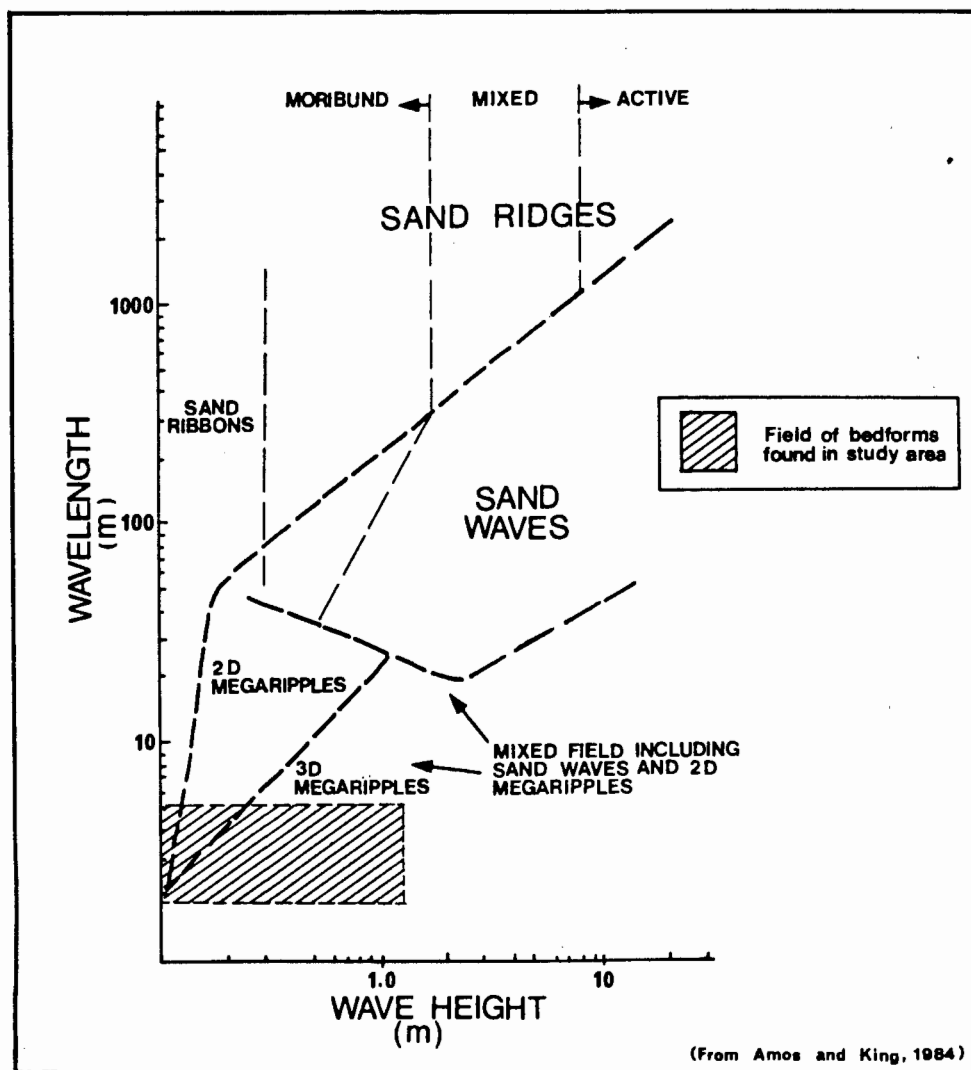


FIGURE 7.10

Table 7.5
Dimensions of bedforms in study area
from Eqn(8) (m)

Line	Fix	W_s	H_t	R_s	H_o	L
1/211	1200-1202	1	10	50	0,20	2
1/211	1208-1210	2	10	21	0,87	5
302	0932-0934	1,0	15	60	0,25	2-3
302	0934-0936	0,5	15	60	0,12	<1
405	1156-1158	8,0	13	58	1,58	-

Table 7.5 shows a sample of the measurements taken to calculate the amplitude and wavelength of well-defined bedforms from the sonographs. Following the morphometric classification of Amos and King (1984) the bedforms in the study area can be termed straight-crested (2-dimensional) and sinuous-crested (3-dimensional) megaripples (Fig.7.10). Other bedforms that are present are usually isolated, prominent features within the sediment and generally have an irregular outline.

7.3.1 Distribution

Sonographic features representing sedimentary bedforms on the seafloor occur across the inner shelf throughout the study area and can be categorized in the following manner:

- 1) Shallow-water and breaker-zone features.
- 2) Well-defined, easily recognizable megaripples, occurring in all water depths.
- 3) Diffuse, formless features with no rhythmic occurrence, usually found in water depths below 13 m and away from the proximity of bedrock outcrops.
- 4) Abrupt changes in sonographic "texture" of an otherwise featureless sediment-covered seafloor.

The common pattern on shoaling is from a smooth seafloor at -25 to -15 m with the large, diffuse bedforms present, through a zone of faint, poorly developed bedforms, into an area of regular, rhythmic bedforms, generally megaripples, at depths between -20 and -10 m. This is followed by a zone of large megaripples that have a confused pattern and are not clearly outlined on the sonographs. This pattern arises from the concurrent coarsening in sediment texture and the increased wave-induced bottom current activity on approaching the shore. This pattern is well developed in sediments of Long Beach, Agate and Gielie's Embayments.

Shallow-water and breaker-zone features.

Off the Orange River there are strong, diffuse reflectors with overlapping convex outlines, directed seaward (Map 5A); the water depth is about 10 m. The signal return within the area of the convex is usually darker and has a coarser "texture" than the surrounding seafloor (Plate 7.1). These features are present only off the Orange River mouth and southward to the first bedrock outcrop, an area bounded by a straight, sandy beach trending northwestward, with a gently seaward dipping sediment-covered seafloor, uninterrupted by bedrock outcrops (Map 5A and Fig.2.4A). The predominance of these features off the river mouth suggests that they arise from fluvial sediment input. At the time of the survey the mouth was open, but the river was not flowing strongly. Plate 7.1 also shows that the seafloor and sea-surface return signals are very much weaker within this zone, thereby inferring that the signal was somehow impeded, possibly by severe turbidity in the water. During the time that these lines were run the sea off the Orange River mouth was extremely

turbid, a foam-line on the sea-surface marking the boundary between the muddy, fresh river water and clear sea water (Plate 7.2). A change in acoustic character of the water could therefore also have given rise to these convex features. The sonographs were obtained from just seaward of the breaker-zone and air bubbles in the water, caused by the breaking waves, may also have affected the turbulence; the general seaward convexity of the outlines and reduced reflectivity of the seafloor and sea-surface lines support this.

Over the shoreface bedrock area north of Alexander Bay similar features are found. Here, at fairly regular intervals, the sonographs show a "washed-out" zone, where the seafloor reflectors are much reduced in intensity (Plate 7.3). These zones are situated alongside reefs that form coastal promontories. Aerial photographs indicate the presence of rip-current activity (inferred from the seaward deflection of the foam-line along the breaker-zone). The "washed out" zones also coincide with bathymetric depressions in the bedrock. These features have not been observed elsewhere in the study area.

Megaripples

The most commonly occurring sedimentary features are megaripples. These bedforms, which are readily recognized from the sonographs, occur in all water depths and are found throughout the study area. Close inshore, off the Orange River, narrow, coast-perpendicular fields of megaripples are observed (Plate 7.1). These fields are usually 20 m to 50 m wide, extend over 200 m in length and reach down to water depths of about 15 m. The crest spacing of the megaripples ranges from 1,0 m to 3,0 m in shallower water. Elsewhere, similarly elongated megaripple

fields are found contiguous with bedrock outcrops. At Tripp Shoal for example, narrow strips of megaripples run along the northern edge of the bedrock outcrop, in 15 m of water (Map 5A and Plate 7.4). The megaripples here have a wavelength of approximately 2 m, with crestlines running coast-parallel (i.e. northwestward). In places the megaripples have a double crestline (Plate 7.4) although this is not commonly found. All the embayments farther south have narrow megaripple fields along parts of their sediment-bedrock boundaries. These are particularly well developed in water depths shallower than -20 m and often continue for more than 200 m, varying in width between 20 m and 50 m. The wavelengths of these megaripples range from 1,0 m to 3,0 m.

The large channel north of Voltas Embayment (Map 5A) shows a correlation between sediment grain-size and presence of megaripples. The shoreward side of the channel at between -13 m and -17 m is covered by megaripples with wavelengths of about 1,5 m; Sample 22 has a mean phi value of 1,0 (medium-coarse sand) and 52,6% coarse sand with 1,6% gravel. Two hundred metres farther seaward sample 23, in an area of the channel that is without bedforms, has a mean grain size of 2,8 phi ("fine"-fine sand) and lacks a coarse sand fraction and a gravel fraction.

Megaripples are most widespread in Buchu Bay, where there are several separate fields strung along a north-south line between Agate and Klopper's Reefs (Map 5B). The terrace at -20 m on the seaward side of Agate Embayment has megaripples on three of its sides and extending southeastward to form a broad 250 m by 300 m area covered with bedforms, in water depths of between -18 m and -24 m. The wavelength of the megaripples varies from 1,0

to 1,5 m and the crests trend parallel to the shoreline. Sections of the megaripple-field farther southward have been traversed three times with side-scan sonar, during cruises in April 1980, May 1981 and February 1983 (Appendix). The mean position of the field remained the same, although the boundaries changed by about 100 m. These megaripple fields therefore appear to be relatively static, meta-stable features. The position of the megaripple fields appear to be controlled by the low, broad ridge in Buchu Bay (Map 4B). Closer to Peacock Bay another large megaripple field is situated (Map 5B). Wavelengths range up to 3 m and crestlines trend north-south, turning more northwest-southeast shoreward, i.e. generally parallel to the trend of the shoreface-bedrock outcrop.

Farther south, megaripples are present along the northern edges of Rietfontein and Giellie's Embayments, and also along the seaward edge of the shoreface-bedrock outcrop in Giellie's Embayment. The megaripple spacing varies between 1,0 m and 3,0 m, while crest orientation is generally coast-parallel. Locally, especially in Rietfontein Embayment, the bedform orientation varies, probably in response to the local hydrodynamics that is affected by the proximity of pronounced reefs. Whereas most of the megaripples are found in water depths of about -15 m and shallower, they do occur as deep as -25 m in Rietfontein Embayment (Map 5C) where the wavelengths measure as much as 2 m.

The channels extending seaward from the embayments (Map 5C) generally do not have any sedimentary bedforms, with the exception of a small area, at -30 to -32 m in one channel, where megaripples of about 1 m wavelength are found.

Diffuse, formless features.

These features are ill-defined and typically occur with a rounded, strongly reflective surface associated with an acoustic shadow zone (Plates 7.4 and 7.5). This type of bedform is generally found in water depths below -15 m and occurs isolated, with no rhythmic pattern as found with megaripples. They are generally found away from the proximity of bedrock outcrops, in the central part of the sediment embayments or seaward of the shoreface bedrock. In Buchu Bay such bedforms are present in water depths of -23 m to -25 m and measure 5 to 10 m long and about 5 m wide; their form is oblong and they trend northward. In the embayments off Rietfontein and Gielie's Bay this type of bedform is mostly found seaward of the -25 m isobath. However, occurrences in water depths as shallow as 10 m are also found, as is shown in Plate 7.5 which is from an area along the northeastern edge of Gielie's Embayment. In Collins Embayment large bedforms are found on the seaward side of the embayment, lying between -18 m and -23 m. Sediment samples recovered from areas where these bedforms occur are mostly fine sand (2 to 3 phi), with no gravel fraction and less than 5% mud content.

Changes in seafloor texture

Apart from the convex-shaped features found in shallow water, subtle changes in the sonographic "texture" of the seafloor, possibly indicative of a change in the sediment texture, are seen on the delta front and elsewhere in water depths below -20 m and in areas covered by very fine muddy sand and mud. The boundary between the textural zones is often sharp and distinct, but this could also be a function of the manner of recording, where the gain setting is automatically adjusted by

the Klein side-scan recorder. According to Flemming (pers. commun., 1984) any change in seafloor reflectivity, especially if it is a slight change, results in a momentary overreaction of the gain, before establishing a different "average" for the new surface being scanned. The overreaction is recorded as a stronger return signal, resulting in a darker line on the sonograph, which thus demarcates the two zones of sonograph texture.

The Orange prodelta muds seaward of the inner-shelf slope have a very homogeneous sonographic texture, with a light tone that is indicative of mud. Although sedimentary features such as mud lumps, mud volcanoes and slumps have been found on delta-front and prodelta deposits elsewhere (Coleman, 1976), none were recognized on the sonographs from the Orange Delta. Mud volcanoes, indicative of escaping gas, could be expected on the prodelta because of the presence of the ABL within these deposits.

Not all rhythmic features identified on the sonographs are the result of sedimentary bedforms. Reflections from surface waves and from physical boundaries within the water column (salinity, temperature, turbidity) may result in images on the sonograph record that appear to occur on the seafloor. The features described from the nearshore at the Orange River mouth may have arisen as a result of such changes as was mentioned earlier and shown on Plate 7.2. This is a difficult problem that may lead to errors in interpretation. A case in point is the paper by Morang and McMaster (1980) describing the occurrence of sandwaves inshore in shallow water depths. These so-called "bedforms" were subsequently shown to have resulted from the

interference pattern produced by reflections from surface waves (Werner, 1982; Cook, 1982). An example of this effect is shown in Plate 7.7. The sonograph shows a transition, from left to right, of a smooth-surfaced fine sand to subdued bedrock outcrop, covered by a sediment veneer with patches of megaripples. The prominent, undulatory pattern over the fine sand can be traced into the water column and is caused by the acoustic reflection of waves on the surface of the sea that is superimposed on the smooth, homogeneous reflection from the seafloor. The absence of this pattern over the rock outcrop area is due to the stronger signal from the rock surface masking the interference pattern from the surface of the sea. This particular problem obviously diminishes in calmer weather and over more irregular areas of sea floor.

7.4 Sediment transport on the inner shelf

The existence of bedforms on the seafloor implies sediment transport at certain times, depending on the energy of the incident waves and thus the resultant wave-induced bottom currents. To be able to estimate the amount of time sediment is actively transported at a particular depth, it is necessary to establish the wave conditions that would produce the threshold velocity to transport the sediment.

The median (50% exceedance) significant waveheight (H_s) on the inner shelf for all seasons except winter is 1,56 m and is 1,75 m for winter (Fig.7.6). The maximum-energy wave period (T_p) is between 10.5 sec and 12.5 sec for all seasons, being the highest in winter (Fig.7.4). Using these values as representing the average wave conditions the wave orbital velocity on the seafloor at water depths of 15 m, 20 m and 30 m are as follows:

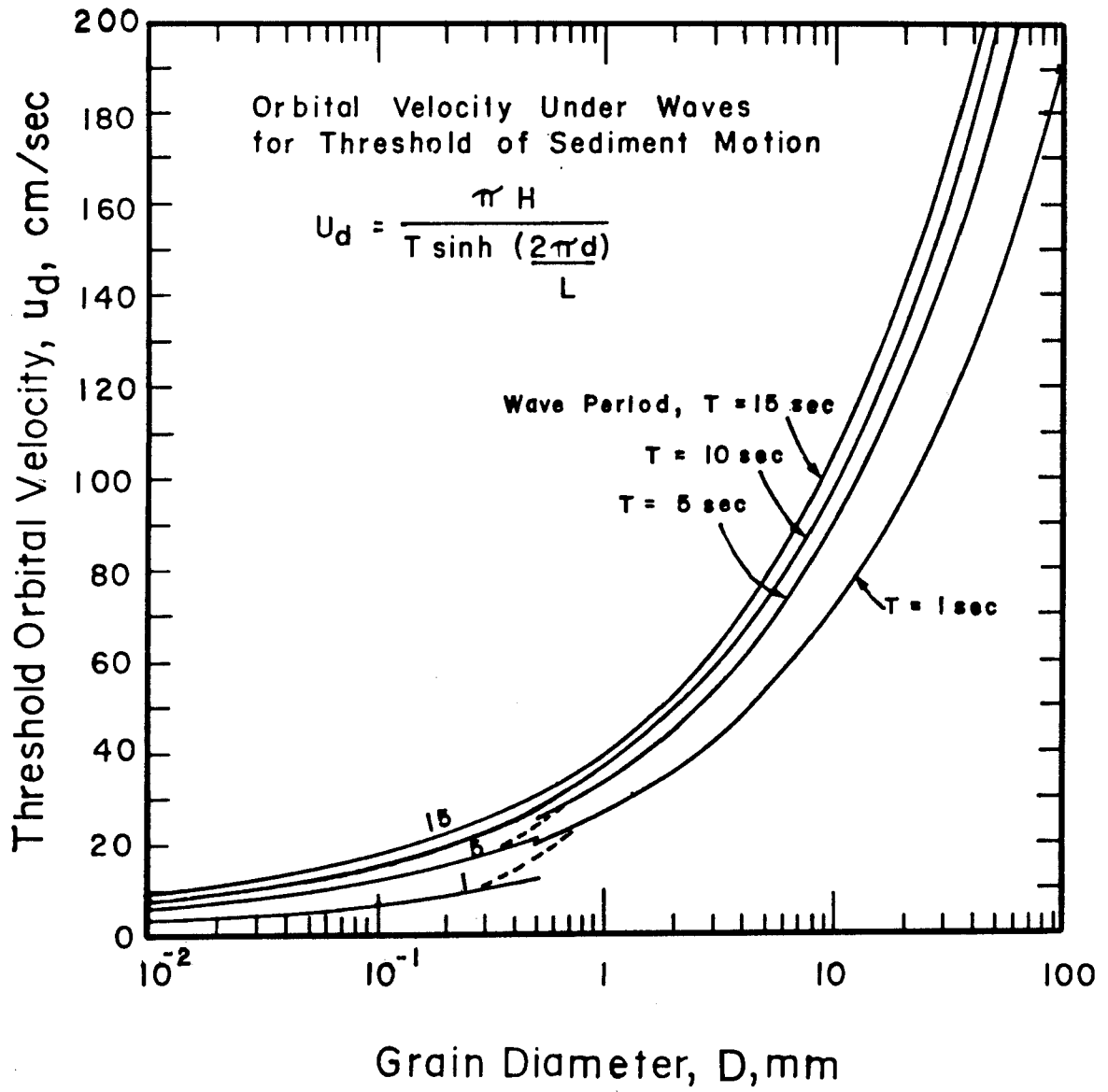
Table 7.6

Horizontal orbital velocity U_d for 50% exceedance wave conditions

H_s	T_p	d=15 m	d=20 m	d=30 m
(m)	(s)	cm/s	cm/s	cm/s
1,56	11,0	99	73	46
1,75	12,5	111	82	52

Komar and Miller (1975) produced a set of curves for various wave periods from which the orbital velocity that is required to transport sediment of a certain grain diameter may be derived (Fig.7.11). Having determined the value of U_d at various depths from equation 1 (Table 7.6), the grain diameter can be calculated for the sediment that will be transported, assuming a grain density of 2.65 g/cm^3 . The grain size that will be transported will vary from 1,5 mm (very coarse sand) at -30 m to 10,5 mm (gravel) at 15 m water depth (Fig.7.11). Megaripples can be expected to form under these average conditions (Table 7.4), and the extensive megaripple fields in Buchu Bay (Map 5B) indicate that these conditions prevail.

Davies (1964) classified the West Coast as a "storm dominated" coast line, which implies that the wave energy distribution is skewed towards the higher energy side of the spectrum. What is the maximum wave orbital velocity that may be expected on the inner shelf? Table 5 (Appendix) shows that wave periods of 20 sec and wave heights of 5.0 m have been recorded in all seasons. The percentage frequency curves for H_s and T_p (Figs.7.12A and B) show that these values occur only about 1% of the time. Although the effect that these wave conditions will



(From Komar and Miller, 1975)

FIGURE 7.11

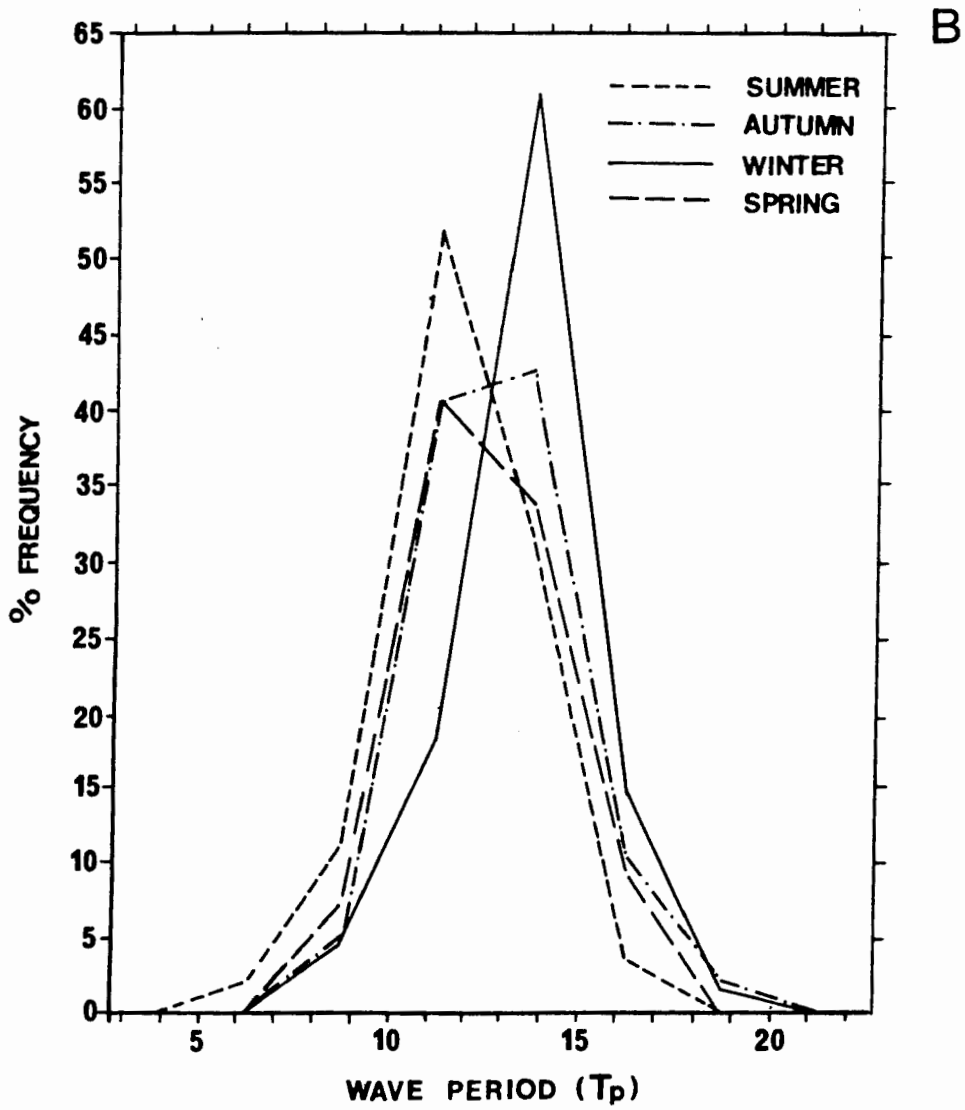
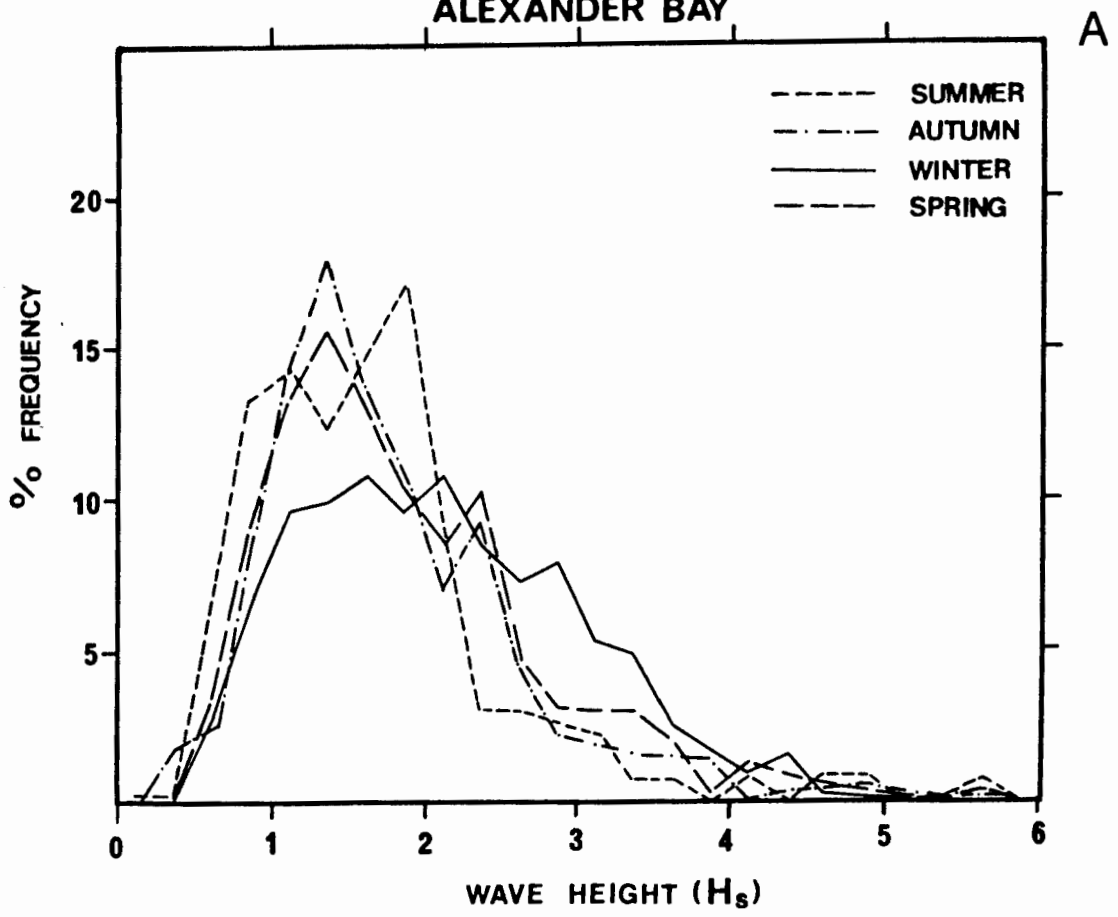


FIGURE 7.12

have on the sediment is severe, these conditions are very short-lived. No cumulative, lasting effect will remain as bedforms and sediment accumulations will probably be continuously altered by the milder conditions that prevail. More realistic would be to take the 5% exceedance value, i.e. those conditions that occur 5% of the time. That would give an average of 1,5 days per month that these conditions may be expected to be found. The corresponding value of U_d for these wave conditions is presented in Table 7.7.

Table 7.7

Horizontal orbital velocity U_d for 5% exceedance wave conditions

H_s (m)	T_p (s)	d=15 m cm/s	d=20 m cm/s	d=30 m cm/s
3,25	14,8	247	183	118

It is evident that during these storms all of the inner shelf will be subjected to very intense sediment transport. Figure 7.11 shows that quartzose sediment with grain diameters from 10,5 mm (medium pebbles) in -30 m water to over 10 cm (small cobbles) in -15 m water will be transported. The direction of transport can be determined indirectly, by considering whether the wave conditions were generated by a distant or local storm. Using Swart's (1983) range of waveheight over wavelength ratios, the 5% exceedance values of H_s and T_p give the following results:

Table 7.8

5% Exceedance wave-parameters for storm conditions

H/L =		Distant storm		Local storm			
		0,002		0,025		0,100	
5% exceedance		H_S (m)	T_P (s)	H_S (m)	T_P (s)	H_S (m)	T_P (s)
$H_S = 3,25$ (m)	$T_P = 14,8$ (s)	-	32,27	-	9,13	-	4,56
		0,68	-	8,54	-	34,17	-

Table 7.8 shows that for waveheights of 3,25 m (5% exceedance), the waves will mainly have been generated by distant storms as wave periods below 9 sec occur less than 10% of the time (Fig.7.12A) for all seasons except summer, which shows a 17% occurrence. (The modal wave period lies at approximately 14,5 s for winter, 12,5 s for autumn and spring and 11,25 s for summer.) Likewise the origin of waves with 14,8 s periods lies in distant storms as the wave heights corresponding to local storms (Table 7.8) have not been recorded (Fig.7.12A). Most of the waves that will cause maximum effect in sediment transport therefore originate from distant storms. This contradicts Van Ieperen's (1976) conclusion that most high-energy waves are generated by local storm conditions. Van Ieperen's data were derived from offshore (>50 m water depth) wave-recording stations that registered waves travelling offshore and alongshore and which would therefore not be incident on the coast. The distant storm waves originate in the low-pressure belt of the Southern Ocean (cf Chapter 1). With an incident direction from the south and south-southwest (Fig.7.3B). Longshore sediment transport under

these conditions will be towards the north.

Equally important are the minimum wave conditions that would transport gravel-size sediment, the size-fraction generally associated with diamondiferous deposits. The threshold orbital wave velocity at the seafloor required to transport granules (2-4 mm) will range from 45 cm/s to 52 cm/s (Fig.7.11) for wave periods between 5 s and 15 s (more than 95% of the recorded range). From equation 1 the equivalent wave height at various water depths can be determined. Table 7.9 gives the results:

Table 7.9

Minimum wave conditions to transport granule-size quartz grains

U _d (cm)	d = 15 m		d = 20 m		d = 30 m	
	H _s (m)	T _p (s)	H _s (m)	T _p (s)	H _s (m)	T _p (s)
45	4,0	5	9,0	5	45,0	5
52	0,7	15	0,9	15	1,4	15

Wave conditions capable of transporting granule-sized sediment over most of inner shelf depth-range (30 m, Table 7.9) falls close to the modal value of wave height and period (2,25 m and 14.5 sec in winter) (Figs.7.12A and B). The wave conditions on the inner shelf are therefore of more than sufficient energy to be able to transport granules (2 - 4 mm) of quartz on the inner shelf (Fig.7.8). By implication the hydrodynamically equivalent diamond will easily be transported as well.

As an approximation, the hydraulic equivalent grain diameter can be derived from the equation given by Middleton and Southard (1984):

$$\frac{D_H}{D_L} = \left(\frac{\rho_{SL}}{\rho_{SH}} \right)^{1/2} \text{-----(9)}$$

D_H and D_L are grain diameters of the heavy and light (quartz) minerals respectively.

ρ_{SL} and ρ_{SH} are the light and heavy mineral densities respectively.

If a quartz grain with a diameter of 2 mm is considered ($\rho_{SL} = 2,65 \text{ g/cm}^3$) then it would be hydrodynamically equivalent to a diamond ($\rho_{SH} = 3,5 \text{ g/cm}^3$) with grain diameter of 1,74 mm. The smaller diamond would be in hydraulic equivalence with the larger quartz particle, assuming that they have approximately the same shape.

7.5 Discussion

According to Reineck and Singh (1980) the morphology of megaripples is related to the process through which they formed. Symmetrical or slightly asymmetrical, straight-crested (2-dimensional), bifurcating ripples are formed by waves. Current ripples, conversely, are asymmetrical and the ripple crests do not bifurcate. Whereas it is generally difficult to establish bedform symmetry from sonographs in the study area, bifurcating crest lines are readily observed (Plate 7.4). Most of the megaripple fields in water depths greater than 15 m have bifurcating crestlines and appear to be symmetrical (i.e. the reflective surface and shadow zone have approximately the same widths), indicating that they formed through oscillatory water movement arising from wave action.

Morang and McMaster (1980), working on the east coast of north America, found strips of megaripples in the nearshore, orientated perpendicular to the shore. Between 200 and 400 m

offshore these strips coalesced and terminated. They found that within the strips, megaripples (wavelengths between 0,5 m and 1,0 m) trended parallel to the coastline. These strips were more numerous after a storm and the megaripples had an increased wavelength to up to 1,5 m. Morang and McMaster (1980) concluded that these bedforms may have formed as a result of rip-current activity.

McKenzie (1958) found on Australian coasts that there were fewer rip-currents during storm conditions, but that they tended to be more powerful. Cook (1970) working along the Californian coast, found that in the surf zone the rip currents formed distinct, shallow channels, the floors of which were covered by megaripples. The channels did not extend beyond the breaker zone. However, Reimnitz et.al. (1976) show evidence for rip-current activity down to water depths of -30 m and extending up to 1500 m from the beach. These megarippled strips were found along the moderate- to high-energy Pacific coast of Mexico. The megaripple strips ranged up to 100 m wide and the average wavelength of the megaripples was 1,25 m. The crest-lines of the bedforms ran coast-parallel. This conforms to the location and distribution of megaripples in the study area. The occurrence of megaripples is much more common inshore of the 15 m isobath than in deeper water. The crestlines of the megaripples appear to be symmetrical on the sonograph records and trend parallel to the shoreline. Where present, the megaripples are found in coast-perpendicular strips that are up to 50 m wide and continuous for more than a hundred metres, reaching over 500 m from the beach. These megaripples are formed when excess water flows away from a wave-setup area as longshore currents and is then transferred offshore by rip currents (Cook, 1970). Although megaripples

formed by rip currents would initially show strong seaward asymmetry, it is very likely that they will have been altered by persistent wave action to become more symmetrical (Cook, 1982). The image on the sonograph will reflect the altered condition, since the surveys could only be conducted in calm seas when rip-current activity would be reduced, particularly on the seaward edge of their influence. In the study area the strips of megaripples extending at right angles from the shore are commonly found contiguous to the bedrock outcrop, seldom within the sediment body. This suggests that the position of rip currents is strongly influenced by local bathymetry such as bedrock highs. Cook (1970) pointed out that rip currents are strongest off headlands, where they are often stationary. The position of the "washed-out" zones along the inner survey lines north of Alexander Bay suggested the presence of rip currents along the edges of the rocky reefs extending offshore. This would correspond with the position of the strips of megaripples, although the two features have not been found together on the sonographs. The more extensive influence of rip currents suggested by Reimnitz et al. (1976), could be a process for depositing the fine sand fraction beyond the surf zone. The sediment is transported offshore by currents to depths below the wave activity that is sufficient to remobilize the fine-sand fraction; finer fractions are carried even farther offshore.

7.6 Conclusions

The west coast is a storm-dominated, micro- to meso-tidal region, where wave-induced current activity on the inner shelf is predominantly responsible for sediment transport. An understanding of the nearshore wave climate along the coast is

therefore essential to determine the sediment dynamics on the inner shelf. Very few wave recorders have been deployed to date (Rossouw, 1984) so that only a rudimentary concept of the wave regime and attendant sediment movement along the coast exists.

The limited data-set obtained from a "Waverider" off Alexander Bay shows that active sediment transport takes place over the inner shelf. Average wave conditions (Table 7.6) are sufficient to transport very coarse sand (1-2 mm) down to a depth of 30 m below sea level; storm waves are able to move medium pebbles (1 cm) at -30 m and small cobbles (10 cm) in water depths of 15 m. The predominant south-southwesterly incidence direction of the waves results in a strong northward -directed littoral drift (Swart, 1983).

The conclusion in Chapter 6 that the surficial sediments on the inner shelf in the study area are in dynamic equilibrium with the wave regime is supported by the data presented here. The mean grain size of the sediment on the inner shelf lies in the fine-sand range and can therefore be expected to continually be transported by wave-induced currents. The result is the very well sorted sediment found in the study area (Fig.6.16).

It is evident that the present-day wave climate is capable of transporting diamonds on the inner shelf. Reworking of diamondiferous beach deposits and storm-lag deposits on wave-cut terraces at several depths on the inner shelf (cf Chapters 3 and 5) will result in a continual redistribution of diamonds, with a net transport direction northward. In the following chapter it will be argued that wave-induced currents have transported and deposited diamonds along the entire west coast of southern Africa for over 65 million years since the beginning of the Tertiary period.

PLATE 7.1

Sonograph showing convex reflectors and megaripple-strips perpendicular to the coastline.

Locality: Orange River mouth. (Map 5A).
Line 114: 1554-1556. (Map 1).

Explanation: a - strips of megaripples extending seaward; wavelength ± 2 m;
amplitude $\pm 0,5$ to 1 m.
b - convex reflectors. Note the obliteration of the sea-surface and seafloor reflectors within this area.

PLATE 7.2

Photograph showing sharp boundary between muddy water and clear seawater.

Locality: Off the Orange River mouth.

Note the pinger seismic unit being towed across the foam-lined boundary.

PLATE 7.3

Sonograph showing "washed-out" area arising from possible rip-current activity.

Locality: Alexander Bay. (Map 5A).
Line 1/223: 1632 - 1634. (Map 1).

Explanation: a - "washed-out" zone extending across the bedrock.
b - rugged, exposed bedrock with prominent reflective surfaces and broad shadow-zones, micro-topography 2 to 5 m.

PLATE 7.1

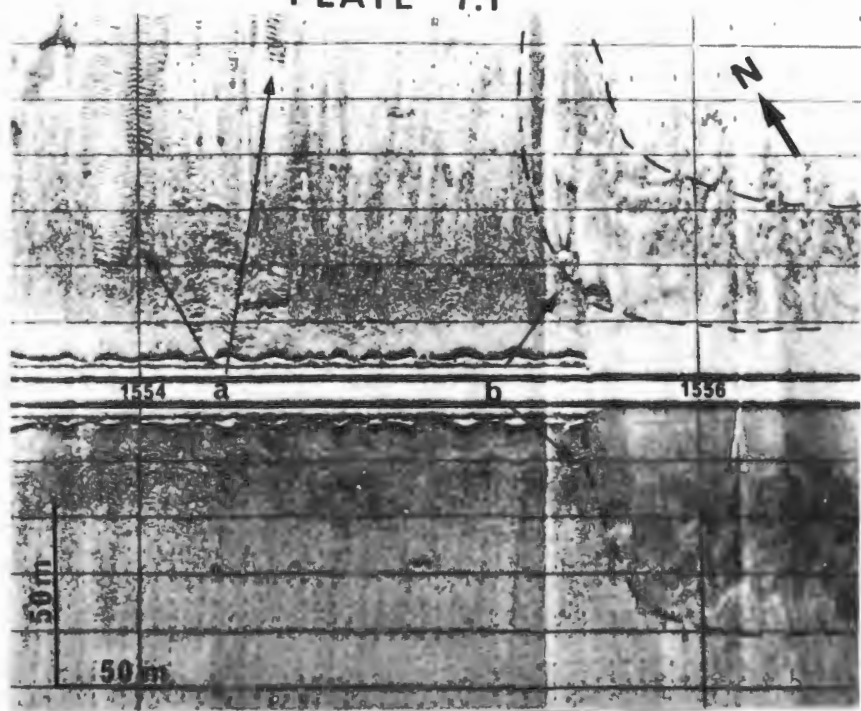


PLATE 7.2

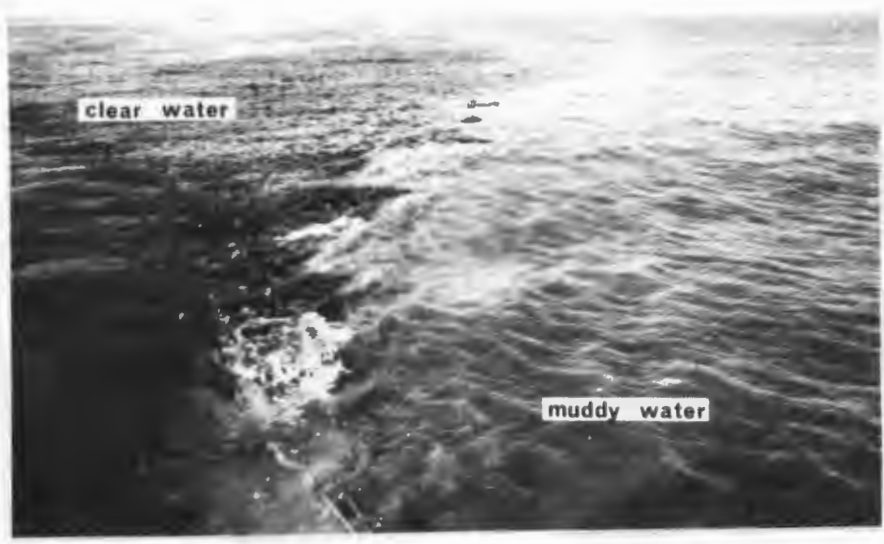


PLATE 7.3



PLATE 7.4

Sonograph showing megaripple-field.

Locality: Tripp Shoal. (Map 5A).
Line 1/213: 1228 - 1226. (Map 1).

Explanation: a - bifurcating, double-crested, two-dimensional megaripples; wavelength $\pm 1,5$ to 2 m.
amplitude $\pm 0,5$ m.
b - subdued bedrock (<2 m relief) with sediment veneer, forming ripples.

PLATE 7.5

Sonograph showing diffuse sedimentary structures.

Locality: Collins Embayment. (Map 5B).
Line 510: 1028-1030. (Map 1).

Explanation: a - diffuse sedimentary structures; probably shelly, gravelly, coarse sand.
b - fine-grained sand.

PLATE 7.6

Sonograph showing megaripples and diffuse sedimentary structures.

Locality: Gielie's Bay. (Map 5C).
Line 717: 1336-1338. (Map 1).

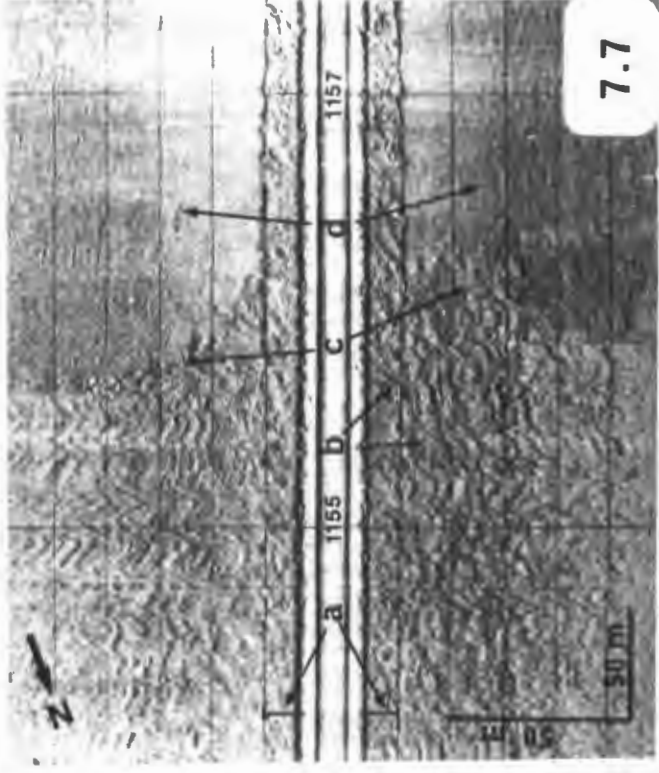
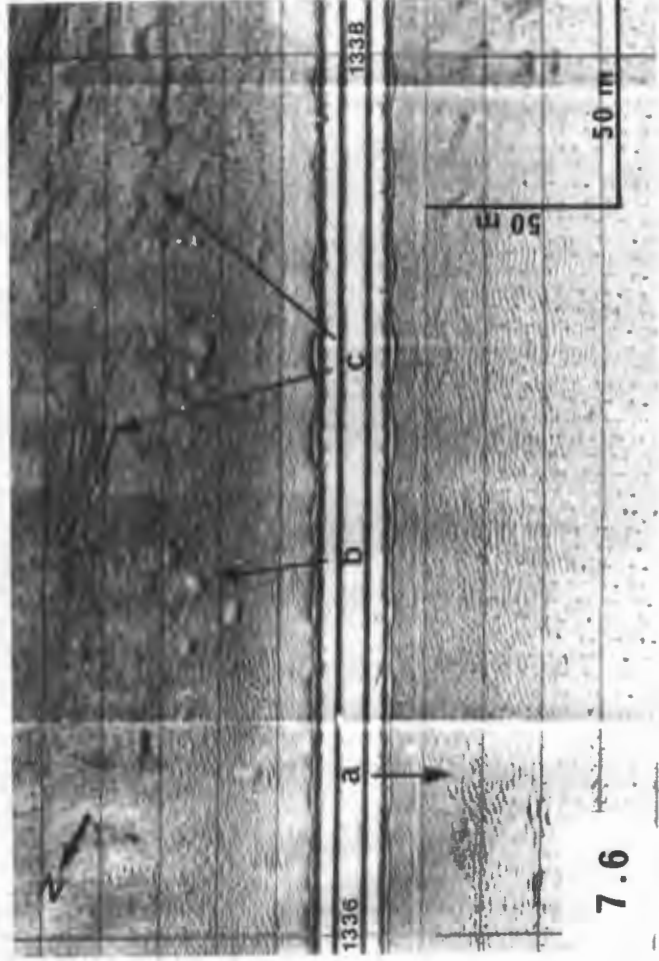
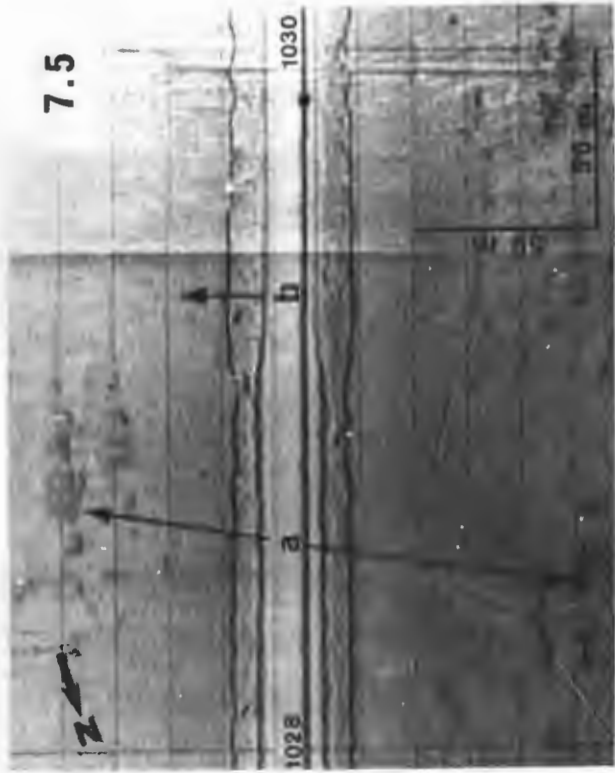
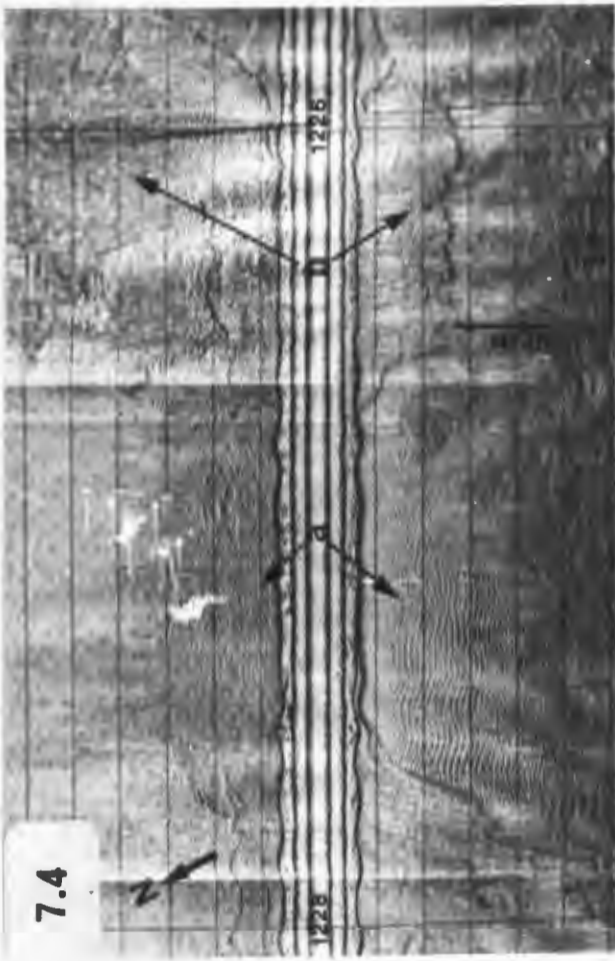
Explanation: a - bifurcating, three-dimensional megaripples; wavelength ± 1 to 1.5 m;
amplitude $\pm 0,5$ m.
b - rounded, diffuse sedimentary reflectors.
c - subdued ridge.

PLATE 7.7

Sonograph showing sea-surface interference patterns.

Locality: Collins Embayment. (Map 5B).
Line 507: 1155-1157. (Map 1).

Explanation: a - water-column.
b - interference pattern in the water-column and extending across the seafloor.
c - sediment - bedrock boundary.
d - very subdued bedrock relief with a thick sediment veneer, forming megaripples in places. Note absence of the interference pattern over the bedrock.



CHAPTER 8THE CAINOZOIC EVOLUTION OF THE DIAMONDIFEROUS DEPOSITS8.1 Introduction

The previous chapters have highlighted important aspects that need to be considered when determining the diamond potential of marine deposits on the inner shelf. Bedrock microtopography, manifested gullies, ridges, potholes and cliffs, as well as wave activity directly affect the distribution of diamonds. On the other hand, sediment texture and seismic stratigraphy may show the presence of potentially diamondiferous deposits in pebble horizons, storm-beaches and other deposits related to high-energy environments. However, to formulate a predictive model of marine diamond distribution, it is essential to understand the reasons for the present-day distribution of diamonds along the west coast.

8.1.1 Present-day distribution

The distribution of wave-transported diamonds on raised marine terraces and in the surf zone along the west coast shows a decrease in size and quantity away from river mouths that act as "point sources" (Keyser, 1976; Sutherland, 1982). The tailing off is much more gradual northward from the river mouth than southward (Stocken, 1962; Hallam, 1964) and is caused by the strong northward-directed longshore drift (Hoyt et al., 1969 and Swart, 1983). Infrequent storms from the west and northwest (Rossouw, 1984) generating high-energy waves, however, do result in an occasional southward mass transport lasting for a period of a few days (Keyser, 1972; Gurney et al., 1982).

Certain preferential localities for diamond-deposition exist. Hallam (1964), describing the diamond distribution onshore along the entire west coast, shows that heavy minerals will be concentrated on the northern side of south-facing bays and the southern side of ridges. Gurney et al. (1982), from their studies off the Olifants River, report that higher-than-average diamond concentrations occur at the seaward end of SSW-trending gullies, in potholes, and generally in depressions on terraces, where the diamonds are found close to the bedrock, associated with cobbles, boulders and pebbles. Keyser (1972), however, concludes from onshore work between Alexander Bay and Port Nolloth that diamonds are found throughout a deposit. However, he qualifies his conclusion by saying: "...with few exceptions, all zones of concentration occur in the vicinity of extinct rivers and drainage channels." (Keyser, 1972, p.15).

Early workers (Wagner and Merensky, 1928; De Villiers and Söhngé, 1959) did not attribute the presence of diamonds on the coast to fluvial transport from the interior, particularly the Orange River. Instead, they invoked a local source, either inland, but close to the coast, or situated offshore. Since it is now acknowledged that the diamonds were transported from the interior to the sea via the Orange River (Stocken, 1962; Hallam, 1964; Keyser, 1976 and Sutherland, 1982), their presence along the coast, far south of the Orange River, and their concentration at river mouths, need to be explained. This requires a review of the sea-level history of the west coast since the arrival of the first diamonds on the coast, as it was the interplay between sea-level fluctuations and longshore drift that produced the distribution of diamondiferous deposits found today.

8.2 The Tertiary Period

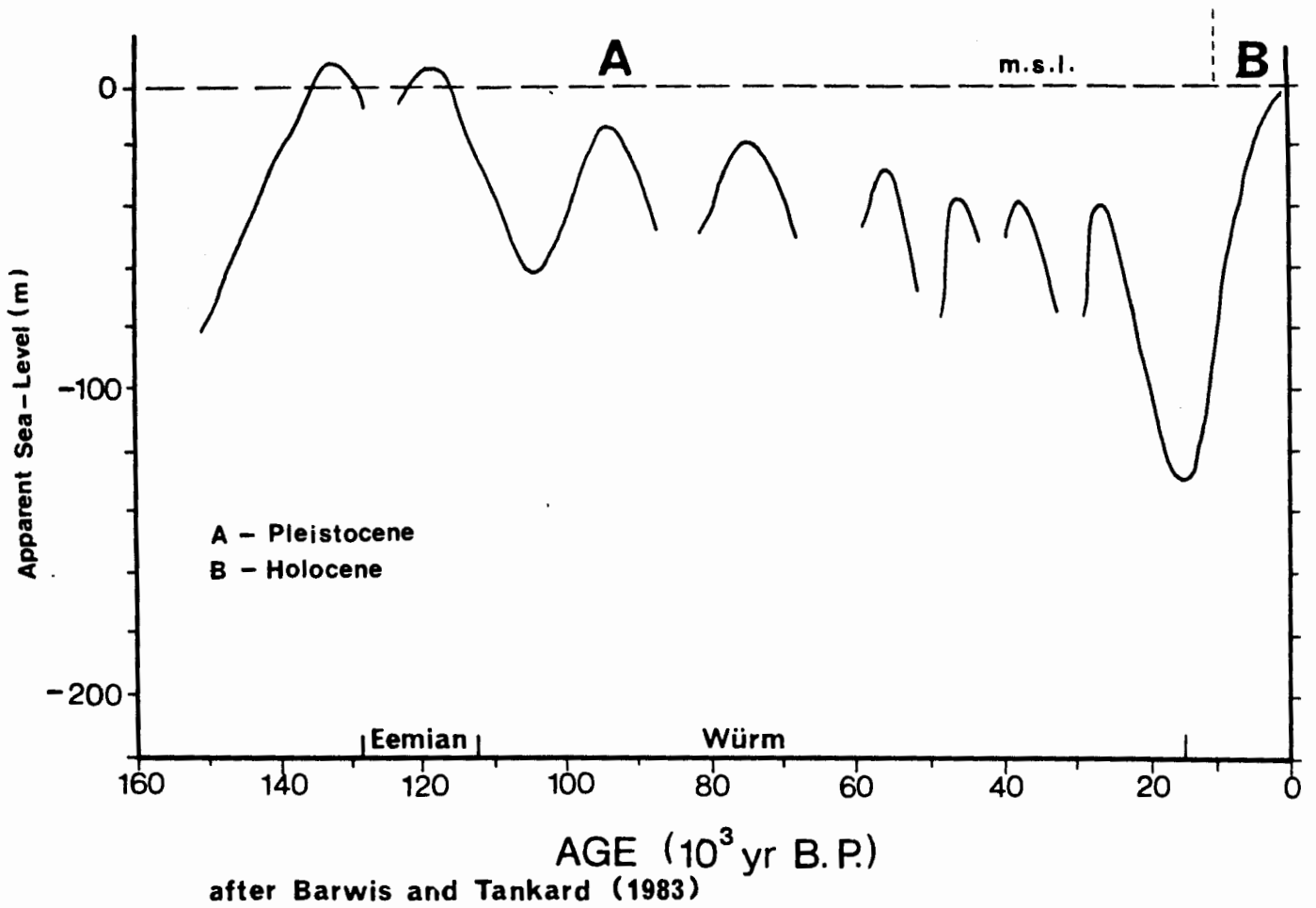
The continental margin had attained its present outline by the close of the Cretaceous Period, the Orange River maintaining a high sediment discharge into the Orange Basin (Dingle, 1973b). A major regression of over 600 m (Siesser and Dingle, 1981) in Late Cretaceous times (70 my to 65 my B.P.) affected the continental margin, causing an angular unconformity between the Upper Cretaceous and Lower Tertiary deposits (Dingle, 1973a).

Dingle and Hendey (1984) have suggested that due to differential uplift of the interior that accompanied the intrusion of diamond-bearing Cretaceous kimberlitic pipes, the Orange River changed its course at the close of the Cretaceous period, to flow into the sea during the Palaeogene via the present Olifants River about 400 km south of the present mouth. Diamonds arrived at the coast from the Cretaceous kimberlitic pipes that are concentrated in the Griqualand West region of the Orange River catchment area (Du Toit, 1954). The first diamondiferous marine deposits can therefore be expected to have accumulated on wave-cut terraces near the mouth of the palaeo-Olifants River.

The Palaeocene and Eocene epochs (65 my to 37 my B.P.) witnessed a sustained sea-level transgression that ranged up to 300 m above present-day sea-level (Siesser and Dingle, 1981). These conditions lasted approximately 25 my (Fig.8.1), except for about 5 my in Middle Eocene times (45 my B.P.), when the sea retreated to well below present sea-level. The Eocene closed with a transgression which reached as high as 100 m above present sea-level. A major Oligocene regression then ensued which

SEA-LEVEL CURVES

1. LATE QUATERNARY



2. LATE CRETACEOUS AND TERTIARY

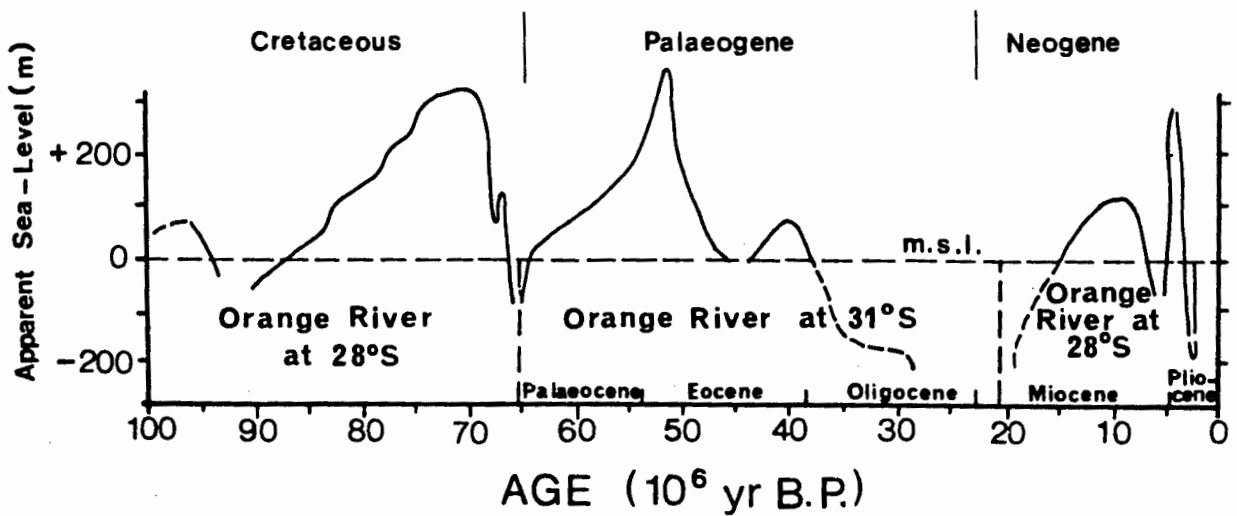


FIGURE 8.1

continued to Middle Miocene times and during which sea-level fell at least 500 m below its present position (Siesser and Dingle, 1981), exposing the entire continental shelf up to 230 km from the present shoreline to subaerial erosion. Lower Tertiary (Palaeogene) deposits attain thicknesses of between 500 and 600 m on the mid-shelf. The thickest succession is found north of the latitude of the Olifants River (Dingle, 1973a). Present-day outcrops occur only in a narrow zone on the shoreward side of the middle shelf (cf Fig.1.12).

From the Miocene onward, the Orange River again occupied its present course (Dingle and Hendey, 1984), originally occupied in the Cretaceous. These authors also note that this switch coincided with the major sea-level regression in the Oligocene-Miocene times. The Orange River would therefore have transported diamonds from the interior via the Olifants River for about 45 million years. Initially, during Palaeocene and Eocene times (65 my to 38 my B.P.), the diamondiferous deposits were developed on the wave-cut terraces now elevated above sea-level, but subsequently, over a period of about 20 my, deposition would have taken place on the continental shelf and the shelf-break. During regressions, exposed Palaeocene -Eocene marine placer deposits would then have been eroded by rivers, thus forming a secondary contribution to the deposits on the shelf. Fluvial erosion of these Palaeocene-Eocene deposits must have been extensive and severe (Hendey, 1983) since very few Early Tertiary marine deposits have been identified along the present-day west coast (cf Chapter 1). Erosion of the coastal plain would have been enhanced by tectonic uplift of the coastal hinterland (Hendey, 1983). The warm, tropical climate of the Early and Middle

Neogene (Shackleton and Kennett 1975; Deacon, 1983a and Coetzee, Scholtz and Deacon, 1983) was also conducive to the erosion process.

Two major transgressions during Mid-Miocene to Late Pliocene times inundated the present coastal plain (Dingle et al., 1983) but were interrupted by the "terminal Miocene event", when the sea retreated from its high position to below present sea-level (Fig.8.1). Diamonds were therefore once more transported to and deposited by wave action along what are now the raised wave-cut terraces of Namaqualand over a period of approximately 15 my, stretching from the Middle Miocene to the Late Pliocene, interrupted by a short but severe regression during late Miocene times. The Mid-Miocene transgression is indicated by the presence of estuarine worms at elevations between 27 and 63 m above sea-level in Middle Miocene deposits at Arrisdrift, 30 km upstream from the present Orange River mouth (Corvinus and Hendey, 1978). However, Hendey (1981b) placed these marine terraces (which are elevated up to 30 m above sea-level) in the Pliocene, corresponding with a transgression which deposited the Varswater Formation at Langebaanweg, 120 km north of Cape Town.

Dingle (1973a) concludes from stratigraphic work that Neogene deposits occur mostly seaward of the outer-shelf break. Lower Upper Tertiary (T_3 , Fig.1.12) deposits underlie most of the continental shelf, but only as a veneer approximately 30 m thick (Dingle, 1973a, Fig.10). Isolated outliers of Upper Upper Tertiary (possibly Miocene age) deposits are found on the shelf (Fig.1.12). Brain (1984) concludes from available evidence that intense upwelling had already occurred much earlier than the Middle Miocene, as was suggested by Siesser (1978). He quotes

Ward et al. (1983) who infer a major "... Early to Middle (possibly Late) Tertiary desert sand sea in the Southern and Central Namib ..." from fossil-dunes which were "... deposited by a dominant southerly palaeo-wind regime which was similar to the present wind system." By implication upwelling and northward-directed littoral drift would have been well established at the same time (cf Chapter 1). Dingle et al. (1983) attribute the scarcity of Neogene sediments on the continental shelf as indicating shallow water-depths over the shelf with the sediment being removed by longshore drift and blown back onshore by the prevailing southerly winds.

In a review on Late Tertiary sea-levels, Nunn (1984) emphasises the fact that, while Tertiary wave-cut terraces lie mostly at high elevations (>30 m) above present sea-level, it does not exclude the possibility of low-level Late Tertiary strandlines existing as well. These lower terraces would then have been reoccupied during subsequent Quaternary sea-level oscillations. Off the Orange River a buried terrace at -40 m reaches approximately 1 km in width (Fig.5.2) and may be the result of repeated sea-level occupations in both the Tertiary and Quaternary Periods (cf Chapter 3).

8.3 The Quaternary Period

Compared to the Tertiary, the Pleistocene saw more numerous cycles of relative sea-level changes. These ranged little over 100 m and mostly as regressions well below present sea-level with subsequent transgressions only extending a few metres above present sea-level. Based on erosion surfaces in the sediments on the continental shelf, Siesser and Dingle (1981) consider that

sea-level stood at least 200 m below present-day level at the start of the Pleistocene epoch. According to Hendey (1983) Quaternary interglacials resulted in sea-levels rising no more than 6 m above present datum level. There is, however, a lack of data on Early and Middle Pleistocene sea-level movements along the southern African continental margin which gives rise to disparate interpretations of possible sea-level trends. Tankard (1976) suggests that early Pleistocene sea-level was between 50 m and 60 m above datum, based on the assumption that there has been a regular regression from the Miocene sea-level high.

Pleistocene sea-level oscillations can be attributed to the growth and decay of high-latitude ice sheets (Deacon, 1983b), rather than tectonic activity as suggested for Tertiary sea-level changes (Nunn, 1984). Cycles of 100 000y duration characterised by colder and drier climates are interrupted by periods of warmer and wetter climates that lasted approximately 10 000y and of which the Holocene forms the most recent. These cycles have been attributed to oscillations in the Earth's orbital motion (Hoyle, 1984). However, little is known of the timing of glacial maxima between 30 000y B.P. and 1 my B.P., as this period falls between the ranges of reliability of the ^{14}C and K-Ar dating techniques (Mercer, 1983).

Hendey (1983) believes that sea-level changes were accompanied by changes in climatic conditions. Regressions were characterised by cooler temperatures, whereas transgressions, saw more temperate climates, because the greater expanse of seawater has a moderating effect on temperature changes. According to Deacon (1983b) there does not seem to be evidence of a change in the seasonal distribution of rainfall between the Pleistocene and

the present, but the total precipitation will have varied significantly with time. A reduction of between 30% and 50% in precipitation is suggested for the glacial maximum, because of reduced evaporation from the colder ocean waters (Deacon, 1983b). Erosion of marine deposits from the raised terraces is directly related to the volume of runoff from these terraces. Climatic changes therefore drastically affect the process of redistribution of diamondiferous marine deposits along the west coast.

Lancaster's (1981) suggestion that the Namib has been a desert throughout the Quaternary, implies that wind regimes were similar to those of today (Fig.1.5), although wind speeds were generally higher as a result of the increased pressure gradients and compression of latitudinal temperature gradients (Van Zinderen Bakker, 1982). The alignment of the southern dunes in the Namib suggests an increased persistence of the South Atlantic anticyclone during the Last Glacial and early Holocene (Lancaster, 1981). The resultant coast-parallel south-southeasterly winds brought about more severe local storm conditions and concomitant higher energy waves. The local storms would reinforce the swell incident from the south-southwest, resulting in an increased efficiency in littoral drift northward. Consequently wave-induced bottom currents were able to transport gravel-sized sediment (and diamonds) at greater depth than at present.

Barwis and Tankard (1983) indicate that during the upper Late Pleistocene sea level steadily receded in a series of recurrent transgressions that rose to a few metres above the present-day level at 135 000y and 125 000y B.P. (Eemian) and to

between -20 m and -40 m between 100 000y and 25 000y B.P. (Wurm) (Fig.8.1). Tankard (1976) shows that between 47 000y and 25 000y B.P. sea-level rose to about -20 m. He remarks that this long period of sea-level stillstand would be reflected in the bathymetry and cites the examples of Rocky Bank (Flemming, 1976a) and the prominent wave-cut cliff at -20 m along the West Coast (Murray et al., 1970; O'Shea, 1971) as evidence. Terraces at -30 m and -40 m that are found in the study area also point to periods when sea-level stood at about those levels, whereas the prominent wave-cut cliff at -20 to -24 m implies a palaeo-strandline at that depth. During the Wurm, sea level oscillated between -20 m and -130 m (Fig.8.1; Barwis and Tankard, 1983), retreating farthest during the Last Glacial maximum at 18 000y to 17 000y B.P. River rejuvenation and fluvial sedimentation on the continental shelf was extensive (Dingle and Rogers, 1972; Tankard and Rogers, 1978). Each successive transgression reworked the deposits from the previous regression, redistributing the sediment on new or re-activated terraces. Little evidence remains of marine deposits of Lower or Middle Pleistocene age on the continental shelf (Rogers, 1977; Birch, in prep). The deficit in Quaternary deposits on the shelf can to a large extent be accounted for in the deposits of the Namib Sand Sea (Rogers, 1977), having initially been transported northward by longshore drift and then blown onshore by the prevailing southerly winds. This only accounted for the removal of the sand-size fraction. The mud-fraction was transported offshore and, presumably, southward, to eventually form the Holocene terrigenous mudbelt. Gravels, pebbles and boulders were trapped on the shelf, to form a diamond-enriched lag deposit. The major Pleistocene deposit on

the shelf off the Orange River is a palaeo-delta lying below -120 m, and Rogers (1977) concludes that it formed during the Last Glacial regression.

After about 17 000y B.P. sea-level recovered rapidly during the Flandrian Transgression, exceeding the present-day sea-level by 5 to 6 m at 5 500y B.P. (Einsele et al., 1974; Flemming, 1977). The modern Orange Delta and terrigenous mudbelt (Fig.1.12) was formed during and since this transgression. The transgression occurred in a series of steps, with the rate decreasing or even temporarily stopping at different times (Fairbridge, 1961, Fig.14). It can be expected that most of the diamondiferous deposits will have accumulated during stillstands, when there was sufficient time to develop a sediment deposit on the wave-cut terraces.

8.4 Discussion

Hawthorne (1975) shows that Cainozoic erosion has removed the upper 1400 m of the kimberlite pipes that supplied the diamonds to the west coast. Because diamonds are concentrated towards the top of the kimberlite pipes in which they were formed (Gurney, pers. commun, 1986), it meant that the bulk of the diamonds available from these pipes would have been eroded and transported to the sea by the end of the Tertiary Period. Considering that sea-level was well below present-day datum for almost 50% of the Palaeogene Period (Fig.8.1), most of the diamonds would have been deposited on the Palaeogene outer-shelf break and the mid-shelf off the Olifants River. The Miocene return of the Orange River to its present-day course at 28°S, cut off the primary supply in the south in post Miocene times (Fig.8.1). Instead, diamonds were now deposited onto the

Namibian continental shelf and coastal zone. However, extensive erosion of onshore diamondiferous Palaeogene deposits supplied the Neogene deposits in the south with diamonds after the Orange River reverted back to its northern course. Furthermore, the thick Neogene deposits over the outer-shelf break are predominantly shallow-marine facies (Dingle, 1973a, Figs 10 and 11). Present-day diamondiferous deposits are typically shallow-marine and beach deposits (Keyser, 1972) so that the Neogene equivalent on the outer shelf is also likely to be diamond-bearing.

The diamonds in the Palaeogene and Neogene deposits on the middle and outer shelves must be regarded as permanently lost to exploitation because these deposits are indurated and out of reach of existing mining techniques. Nevertheless, it is suggested that it was mainly during the Palaeogene that the diamonds presently being mined between the Orange and the Olifants Rivers were brought to the sea. Lower Tertiary (T_1) and Lower Upper Tertiary (T_3) deposits (cf Fig.1.12 and Dingle, 1973a, Figs 10 and 11) were truncated on their landward ends during transgressions and regressions in the Neogene and Early Pleistocene. Erosion by wave-action would have released the diamonds from these deposits. Rogers (1977) reports that the Upper Upper Tertiary deposits (T_4) are foraminiferal limestones with no terrigenous component and he suggests a mid-shelf depositional environment (Fig.1.12). It is therefore unlikely that these deposits would be diamondiferous. The conclusion is that the diamonds eroded from the Tertiary deposits on the shelf are incorporated into the Miocene and Quaternary deposits onshore and the Quaternary deposits on the middle and inner shelves. It is from these deposits that the diamonds are being mined at present.

Crustal movement in the Tertiary and early Pleistocene resulted in the aggradation of river valleys (Rooseboom and Harmse, 1979) and the formation of playa lakes or deflation basins. This, coupled with the decreased runoff resulting from a general cooling of the climate towards the end of the Tertiary and in the Pleistocene (Mercer, 1983), would have resulted in the large-scale dumping of the sediment bedload in the aggrading valleys, only the finer sediment fractions reaching the sea. Diamonds, if still supplied through erosion at their source, would have been trapped in these alluvial deposits. This meant that Quaternary sea-level oscillations served only to redistribute pre-existing diamondiferous deposits along the coast, and over a vertical depth range of only about 130 m.

8.5 Conclusion

At the end of the Palaeogene Period the bulk of diamondiferous deposits was concentrated in the mid-shelf and outer-shelf break deposits off the Olifants River, and on the raised marine terraces in the vicinity. These deposits were essentially developed along palaeo-strandlines, concentrated with the heavy sediment fraction near the bedrock on wave-cut terraces. Each successive cycle of relative change in sea-level would erode the deposits, to be river-borne to new sea-levels and redistributed on new or reactivated wave-cut terraces through the agencies of longshore drift and wave-induced bottom currents. The net trend would have been northward, i.e. subsequent placer deposits formed mostly north of the original deposit so that with time a significant proportion of diamonds were transported a considerable distance up the coast.

It is evident from the foregoing that most of the exploitable diamondiferous deposits lie below present sea-level. The marine deposits will have been subjected to repeated sorting in the surf zone that would tend to concentrate the heavier sediment fractions closer to the bedrock. Constant reworking would trap the diamonds within the ever-thickening gravel-lag that was deposited in the gullies, potholes and fluvial channels eroded into the wave-cut terraces.

A systematic study of the seafloor, as is presented here, reveals those aspects of microtopography, bedrock structure, sediment texture, and stratigraphy that are essential in locating the diamondiferous deposits extant on the inner shelf today.

REFERENCES

- Ahmed, A.A-M. 1968. Geochemical and mineralogical studies of sediments from the southwest African shelf. Unpubl. MPhil thesis, Univ. London.
- Allen, J.R.L. 1970. Physical Processes of Sedimentation. Allen and Unwin, London. 248pp.
- Allsopp, H.L., Kostlin, E.O., Welke, H.J., Burger, A.J., Kroner, A. and Blignault, H.J. 1979. Rb-Sr and U-Pb Geochronology of late Precambrian-Early Palaeozoic igneous activity in the Richtersveld (South Africa) and southern South West Africa. Trans. geol. Soc. S.Afr., 82: 185-204.
- Amos, L.L. and King, E.L. 1984. Bedforms of the Canadian Eastern seaboard: A comparison with global occurrences. Mar. Geol., 57: 167-208.
- Anonymous. 1982. Some notes on the CDM raised beach complex. Geology Department, Consolidated Diamond Mines (CDM), Oranjemund, Excursion Guide, 4pp.
- Bailey, G.W. 1979. Physical and Chemical Aspects of the Benguela Current in the Luderitz Region. Unpubl. MSc. thesis, Oceanography Dept, Univ. of Cape Town, 225pp.
- Bang, N.D. 1971. The southern Benguela Current region in February, 1966: Part 2. Bathythermography and air-sea interactions. Deep-Sea Res., 18(2): 209-255.
- Bang, N.D. 1976. On estimating the oceanic flux budget of lateral and cross circulations of the southern Benguela upwelling system. First interdisciplinary Conf. mar. freshwater Res. S. Afr. (Port Elizabeth), Fiche S122. 6G4-7A11.
- Barwis, J.H. and Tankard, A.J. 1983. Pleistocene shoreline deposition and sealevel history at Swartklip, South Africa. J. sedim. Petrol., 53(4): 1281-1294.
- Birch, G.F. 1975. Sediments on the continental margin off the west coast of South Africa. Bull. jt geol. Surv./Univ. mar. Geosc. Gp, 6: 135pp.
- Birch, G.F. 1981. The Karbonat-Bombe: A precise, rapid and cheap instrument for determining CaCO_3 in sediments and rocks. Trans. geol. Soc. S. Afr., 84: 199-203.
- Birch, G.F. (in prep.) The Quaternary marine deposits on the continental shelf off the west coast of southern Africa. Bull. geol. Surv. S. Afr.
- Birch, G.F., Rogers, J., Bremner, J.M. and Moir, G. 1976. Sedimentation controls on the continental margin of Southern Africa. Proc. 1st. interdisc. Conf. mar. and freshwater Res. S. Afr. (Port Elizabeth), S122. Fiche 20A: C1-C12.

- Böhm, J. 1926. Über Tertiäre Versteinerungen vor der Bogenfelder Diamantfeldern. In: E. Kaiser (ed.), Die Diamantenwüste Südwestafrikas, Berlin, Dietrich Reimer (Ernst Vohsen) 2: 55-87.
- Boyd, A.J. 1983. Seasonal averages of sea surface temperature and some direct current measurements off south-western Africa. S. Afr. J. Sci., 79: 146.
- Brain, C.K. 1984. Comments on the Namib's past. S. Afr. J. Sci., 80: 158-159.
- Bremner, J.M. 1981. Geophysical investigations in the vicinity of Port Elizabeth Harbour. Rep. geol. Surv. S. Afr., 1981-0068: 10pp (unpubl.).
- Brink, V.D.S. and Rogers, J. 1978. Rapid granulometry of sand using a computer-linked settling tube. Proc. 18th Congr. geol. Soc. S. Afr. (Abstr.).
- Brundrit, G.B., De Cuevas, B. and Shipley, A.M. 1984. Significant sea-level variations along the West Coast of Southern Africa. 1979-83. S. Afr. J. Sci., 80: 80-82.
- Brundrit, G.B., Shipley, A.M., De Cuevas, B. and Brundrit, S. 1983. Low frequency sea level fluctuations off the West Coast 1957-75. Proc. 5th nat. oceanogr. Symp. S288, Grahamstown, S. Afr. (Abstr.).
- Bryan, G.M. and Simpson, E.S.W. 1971. Seismic refraction measurements on the continental shelf between the Orange River and Cape Town. In: Delany, F.M. (ed.). The Geology of the East Atlantic Continental Margin. Rep. Inst. geol. Sci., 70(16): 191-198.
- Carrington, A.J. and Kensley, B.F. 1969. Pleistocene molluscs from the Namaqualand coast. Ann. S. Afr. Mus., 52: 189-223.
- Coetzee, C.B. 1976. Diamonds: Namaqualand river deposits; marine (coastal deposits). Mineral Resources of the R.S.A., Pretoria. Government Printer, 25-30.
- Coetzee, J., Scholtz, A. and Deacon, H.J. 1983. Palynological studies and vegetation history of the fynbos. In: Deacon, H.J., Hendey, Q.B. and Lambrechts, J.J.N. (eds). Fynbos palaeocology: A preliminary synthesis. Rep. S. Afr. nat. sci. Prog., 75: 156-173.
- Coleman, J.M. 1976. Deltas: Processes of deposition and models for exploration. Champaign. Continuing Education Publication Company. 102pp.
- Coleman, J.M. and Prior, D.B. 1980. Deltaic sand bodies. Am. Ass. Petrol. Geol. Continuing Education course note series 15: 157pp.
- Cook, D.O. 1970. The occurrence and geologic work of rip currents off southern California. Mar. Geol., 9: 173-186.

- Cook, D.O. 1982. Nearshore bedform patterns along Rhode Island from side-scan sonar surveys - discussion. J. sedim. Petrol., 52(2): 677-680.
- Corvinus, G. 1983. The raised beaches of the west coast of South West Africa/ Namibia. Munich. C.H. Beck, Verlag, 97pp.
- Corvinus, G. and Hendey, Q.B. 1978. A new Miocene vertebrate locality at Arrisdrift in S.W.A. (Namibia). N. Jb Geol. Pal. Mh., 4: 193-205.
- Curry, J.R. 1965. Late Quaternary history, continental shelves of the United States. In: Wright, H.E. and Frey, D.G. (eds.). The Quaternary of the United States. Princeton Univ. Press, Princeton: 723-735.
- Davies, J.L. 1964. A morphogenic approach to world shorelines. Zeitschr. f. Geomorph., 8: 127-142.
- Davies, O. 1973. Pleistocene shorelines in the western Cape and South West Africa. Ann. Natal Mus., 21(3): 719-765.
- Deacon, H.J. 1983a. An introduction to the fynbos region, time scales and palaeoenvironments. In: Deacon, H.J., Hendey, Q.B. and Lambrechts, J.J.N. (eds.). Fynbos palaeoecology: A preliminary synthesis. Rep. S. Afr. nat. sci. Prog. 75: 1-20.
- Deacon, H.J. 1983b. Another look at the Pleistocene climates of South Africa. S. Afr. J. Sci., 79: 325-328.
- De Decker, A.H.B. 1970. Notes on an oxygen-depleted subsurface current off the west coast of South Africa. Investl. Rep. Div. Sea Fish. S. Afr., 84: 24pp.
- De Decker, R.H. 1982. Bathymetry of the inner shelf along the Cape west coast between the Orange River and Port Nolloth. Tech. Rep. jt geol. Surv./Univ. Cape Town mar. Geosc. Gp 13: 64-71.
- De Decker, R.H. 1983a. Report on the nearshore geophysical survey between the Orange River and Wreck point (Concession Area No.1) during May 1981. Rep. geol. Surv. S. Afr., 1983-0057: 6pp (Unpubl.).
- De Decker, R.H. 1983b. Report on the fieldwork in Concession Area no.1 during September 1982: Cruise 9/82. Rep. geol. Surv. S. Afr., 1983-0075: 6pp (Unpubl.).
- De Decker, R.H. 1983c. A proposed diver's sea prospecting form to be used at State Alluvial Diggings, Alexander Bay. Tech. Rep. jt geol. Surv./Univ. Cape Town mar. Geosc. Gp, 14: 244-254.
- De Decker, R.H. 1985a. Initial description of vibrocores from Diamond Concession Area No.1. Tech. Rep. jt geol. Surv./Univ. Cape Town mar. Geosc. Gp, 15: 46-54.

- De Decker, R.H. 1985b. Surficial sediments on the inner shelf between the Orange River and Wreck Point. Tech. Rep. jt geol. Surv./Univ. Cape Town mar. Geosc. Unit, 15: 135-156.
- De Decker, R.H. 1986. The wave regime on the inner shelf south of the Orange River and its implications for sediment transport. Tech. Rep. jt geol. Surv./Univ. Cape Town mar. Geosc. Unit, 15: 68-88.
- De la Cruz, M.A. 1978. Marine geophysical and geological investigations in Saldanha Bay. Bull. jt geol. Surv./Univ. mar. Geosc. Gp, 9: 115pp.
- De Villiers, J. and Söhnge, P.G. 1959. Geology of the Richtersveld. Mem. geol. Surv. S. Afr., 48: 295pp.
- Dietz, R.S. 1964. Wave base, marine profile of equilibrium, and wave-built terraces. A critical appraisal. Bull. geol. Soc. Am., 74: 971-991.
- Dingle, R.V. 1973a. The geology of the continental shelf between Luderitz and Cape Town (Southwest Africa), with special reference to Tertiary strata. J. geol. Soc. Lond., 129: 337-363.
- Dingle, R.V. 1973b. Regional distribution and thickness of post-Palaeozoic sediments on the continental margin of southern Africa. Geol. Mag., 110(3): 97-102.
- Dingle, R.V. 1973c. Preliminary stratigraphic classification of the Cainozoic succession on the South African continental shelf. Trans. roy. Soc. S. Afr., 40(5): 367-372.
- Dingle, R.V. 1977. South Africa. In: M. Moullade and A.E.M. Nairn (eds), Phanerozoic geology of the World I. The Mesozoic. Elsevier, Amsterdam.
- Dingle, R.V. and Hendey, Q.B. 1984. Late Mesozoic and Tertiary sediment supply to the eastern Cape basin (SE Atlantic) and palaeo-drainage systems in southwestern Africa. Mar. Geol., 56: 13-26.
- Dingle, R.V., Moir, G., Bremner, J.M., and Rogers, J. 1977. Bathymetry of the continental shelf off the Republic of South Africa and S.W.A. Map mar. Geosc. Ser. geol. Surv. S. Afr., 1.
- Dingle, R.V. and Rogers, J. 1972. Effects of sea-level changes on the Pleistocene palaeoecology of the Agulhas Bank. In: Van Zinderen Bakker, E.M. (ed). Palaeoecology of Africa, 4: 55-58. Cape Town, Balkema.
- Dingle, R.V. and Scrutton, R.A. 1974. Continental breakup and the development of post-Palaeozoic sedimentary basins around southern Africa. Bull. geol. Soc. Am., 85: 1467-1474.

- Dingle, R.V., Siesser, W.G. and Newton, A.R. 1983. Mesozoic and Tertiary Geology of Southern Africa. Rotterdam, Balkema. 375pp.
- D'Olier, B. 1979. Side-scan sonar and reflection seismic profiling. In: Dyer, K.R. (ed.). Estuarine hydrography and sedimentation. Cambridge, Cambridge Univ. Press, 57-86.
- Donovan, D.T. and Jones, E.J.W. 1979. Causes of world-wide changes in sealevel. J. geol. Soc. Lond., 136: 187-192.
- Drake, D.E., Kolpack, R.L. and Fischer, P.J. 1972. Sediment transport on the Santa Barbara-Oxnard Shelf, Santa Barbara Channel, California. In: Swift, D.J.P., Duane, D.B. and Pilkey, O.H. (eds). Shelf Sediment Transport. Stroudsburg. Dowden, Hutchinson and Ross, Inc. 307-331.
- Du Plessis, A. 1980. Cruise Report: T.B. Davie cruise 405. 29.4.80 to 7.5.80. Rep. geol. Surv. S. Afr., 1980-0716: 5pp (unpubl.).
- Du Plessis, A. and Glass, J.G.K. 1981. Geology of the seafloor in the vicinity of Jahleel and St. Croix islands - Algoa Bay. Rep. geol. Surv. S. Afr., 1981-0069: 20pp (unpubl.).
- Du Plessis, A., Scrutton, R.A., Barnaby, A.M. and Simpson, E.S.W. 1972. Shallow structure of the continental margin of southwestern Africa. Mar. Geol., 13: 77-90.
- Du Toit, A.L. 1954. The Geology of South Africa (3rd edn). Edinburgh, Oliver and Boyd. 611pp.
- Einsele, G., Herm, D. and Schwartz, H.U. 1974. Sea level fluctuation during the past 6000yr at the coast of Mauritania. Quatern. Res., 4: 282-289.
- Fairbridge, R.W. 1961. Eustatic changes in sea level. In: Ahrens, L.H. (ed). Physics and Chemistry of the Earth., 4: 99-185. London, Pergamon Press.
- Flemming, B.W. 1976a. Rocky Bank - Evidence for a relict wave-cut platform. Ann. S. Afr. Mus., 71: 33-48.
- Flemming, B.W. 1976b. Side-scan sonar: a practical guide. Int. hydrogr. Rev., 53: 65-92.
- Flemming, B.W. 1977. Depositional processes in Saldanha Bay and Langebaan Lagoon. Bull. Jt geol. Surv./Univ. Cape Town mar. Geosc. Gp., 8: 215pp.
- Flemming, B.W. 1978. Underwater sand dunes along the southeast African continental margin - observations and implications. Mar. Geol., 26: 177-198.
- Flemming, B.W. 1982. Causes and effects of sonograph distortion and some graphical methods for their manual correction. In: Russell-Cargill, W.G.A. (ed.). Recent Developments in Side Scan Sonar Techniques. Cape Town, ABC Press, 103-138.

- Flemming, N.C. 1965. Form and relation to present sea level of Pleistocene marine erosion features. J. Geol., 73: 799-811.
- Flemming, B.W. and Hay, E.R. 1983. On the bulk density of South African marine sands. Tech. Rep. jt geol. Surv./Univ. Cape Town mar. Geosci. Gp., 14: 171-176.
- Fowler, S.A. 1976. The Alluvial Geology of the Lower Orange River and Adjacent Coastal Deposits. Unpubl. M.Phil. thesis, Univ. London.
- Fowler, S.A. 1982. Sedimentology and Distribution of Heavy Minerals in the Lower Orange River Valley. Unpubl. D.Phil. thesis, Univ. London.
- Foster, R.W. 1974. Report on vibracore programme March 1972 to January 1974. Internal Rep. Mar. Diamond Corp. 1-35.
- Gurney, J.J., Walker, C.S.H., Prinsloo, K., Borchers, R. and Fleming, B.W. 1982. Diamond recoveries from the surf zone of the Namaqualand coast near the Olifants River. Abstr. 3rd Symp. Sedim. Div. geol. Soc. S. Afr., 13-14 Sept. 1982, Johannesburg, 84-87
- Hallam, C.D. 1964. The geology of the coastal diamond deposits of Southern Africa (1959). In: Haughton, S.H. (ed.). The Geology of some Ore Deposits in Southern Africa. Johannesburg, Geol. Soc. S. Afr., 671-728.
- Hamilton, E.L. 1979. Sound velocity and related properties of marine sediments, western Pacific. J. geophys. Res., 75(23): 4423-4431.
- Harris, T.F.W. 1978. Review of coastal currents in southern African waters. Rep. S. Afr. nat. sci Prog., 30: 103pp.
- Harris, T.F.W. and Shannon, L.V. 1979. Satellite-tracked drifter in the Benguela Current system. S. Afr. J. Sci., 75: 316-317.
- Hart, T.J. and Currie, R.I. 1960. The Benguela Current. Discovery Report, Univ. Cambridge, 31: 123-298.
- Haughton, S.H. 1931. The Late Tertiary and Recent deposits of the West Coast of South Africa. Trans. geol. Soc. S. Afr., 34: 19-58.
- Hawthorne, J.B. 1975. Model of a kimberlite pipe. In: Ahrens, L.H. (ed.). Physics and Chemistry of the Earth., 9:1-17. Oxford, Pergamon Press.
- Heine, K. 1982. The main stages of the Late Quaternary evolution of the Kalahari region, Southern Africa. In: Coetzee, J.A. and van Zinderen Bakker, E.M. (eds). Palaeoecology of Africa, 15: 53-76. Rotterdam, Balkema.

- Hendey, Q.H. 1981a. Palaeoecology of the late Tertiary fossil occurrences in 'E' Quarry, Langebaanweg, South Africa, and a reinterpretation of their geological context. Ann. S.Afr. Mus., 84(1): 104pp.
- Hendey, Q.B. 1981b. Geological succession at Langebaanweg, Cape Province, and global events of the Late Tertiary. S. Afr. J. Sci., 77: 33-38.
- Hendey, Q.B. 1983. Cenozoic geology and palaeo-geography of the fynbos region. In: Deacon, H.J., Hendey, Q.B. and Lambrechts, J.J.N. (eds.). Fynbos palaeoecology: A preliminary synthesis. Rep. S. Afr. nat. sci. Prog., 75: 35-60.
- Heydorn, A.E.F. and Tinley, K.L. 1980. Estuaries of the Cape. Part I. Synopsis of the Cape coast. Natural features, dynamics and utilization. S. Afr. Council. sci. ind. Res. Res. Rep., 380: 96pp. Stellenbosch: Nat. Res. Inst. Oceanol.
- Hoyle, F. 1984. On the causes of the ice ages. Earth, Moon and Planets, 31(3): 229-248.
- Hoyt, S.H., Smith, D.D., and Oostdam, B.L. 1965a. Sediment distribution on the inner continental shelf, west coast of southern Africa. Bull. Am. Assoc. Petrol. Geol., 49: 344-345 (Abstr.).
- Hoyt, S.H., Smith, D.D. and Oostdam, B.L. 1965b. Pleistocene low sea-level stands on the southwest African continental shelf. Abstr. 7th int. Ass. Quatern. Res., 227.
- Hoyt, S.H., Oostdam, B.L. and Smith, D.D. 1969. Offshore sediments and valleys of the Orange River (South and South West Africa). Mar. Geol., 7(1): 69-84.
- Ingram, R.L. 1965. Facies maps based on the megascopic examination of modern sediments. J. sedim. Petrol., 35(3): 619-625.
- Joubert, P. and Kroner, A. 1971. The Stinkfontein Formation south of the Richtersveld. Trans. geol. Soc. S. Afr., 75: 47-54.
- Jury, M. 1981. Coastal winds and upwelling. Trans. roy. Soc. S. Afr., 44(3): 299-302.
- Keyser, U. 1972. The occurrence of diamonds along the coast between the Orange River estuary and the Port Nolloth Reserve. Bull. geol. Surv. S. Afr., 54: 1-23.
- Keyser, U. 1976. Diamonds - Marine (coastal) deposits. In: Coetzee, C.B. (ed). Mineral Resources of the Republic of South Africa (5th edn.) Pretoria, Govt. Printer: 27-30.
- Kieser, J. 1984. Seafloor sediments and bedrock topography of State Alluvial Diggings Concession Area 3. Unpubl. Hons Proj., Geol. Dept., Univ. Cape Town. 32pp.

- Klinger, H. 1977. Cretaceous deposits near Bogenfels, S.W.A. Ann. S. Afr. Mus., 73: 81-92.
- Knebel, H.J., Needell, S.W. and O'Hara, C.J. 1982. Modern sedimentary environments on the Rhode Island inner shelf, off the eastern United States. Mar. Geol., 49: 241-256.
- Komar, P.D. 1976a. Beach Processes and Sedimentation. New Jersey., Prentice-Hall.
- Komar, P.D. 1976b. The transport of cohesionless sediments on continental shelves. In: Stanley, D.J. and Swift, D.J.P. (eds.). Marine Sediment Movement and Environmental Management. New York, John Wiley, 107-125.
- Komar, P.D. and Miller, M.C. 1975. On the comparison of the threshold of sediment movement under waves and unidirectional currents with a discussion of the practical evaluation of threshold. J. sedim. Petrol., 45: 362-367.
- Kröner, A. 1974. The Gariep Group. Part I. Late Precambrian Formations in the Western Richtersveld, Northern Cape Province. Bull. Precamb. Res. Unit, Geol. Dept, Univ. Cape Town 13: 115pp.
- Lamont, G.T. 1947. The Geology of Part of the Vanrhynsdorp Division, Cape Province. Unpubl. Ph.D. thesis, Dept Geol. Univ. Cape Town.
- Lancaster, N. 1979. Evidence for a widespread late Pleistocene humid period in the Kalahari. Nature, 279: 145-146.
- Lancaster, N. 1981. Palaeoenvironmental implications of fixed dune systems in Southern Africa. Palaeogeogr., Palaeoclim., Palaeoecol. 33: 327-346.
- Langhorne, D.W. 1973. A sandwave field in the outer Thames Estuary, Great Britain. Mar. Geol., 14: 129-143.
- Latun, V.S. 1962. The upwelling of deep water near the southwest coast of Africa. Bull. Acad. Sci. USSR geophys. Ser. (Translated by Am. Geophys. Union), USSR, 9: 770-775.
- Maree, B.D. 1966. Die voorkoms van diamante op land en onder die see langs die westkus van suidelike Afrika. Tegnikon, 15: 149-159.
- Martin, H. 1965. The Precambrian Geology of South West Africa and Namaqualand. Cape Town, Precamb. Res. Unit, Geol. Dept., Univ. Cape Town.
- Martin, R.A. 1981. Benthic foraminifera from the Orange-Luderitz shelf; southern African continental margin. Bull. jt geol. Surv./Univ. Cape Town mar. Geosci. Unit, 11: 75pp.
- Maud, R.R. 1968. Quaternary geomorphology and soil formation in coastal Natal. Ann. Geomorph., 7: 155-199.

- McCrae, G. 1983. Seafloor Sediments and Morphology in Blocks 2 and 3 of State Alluvial Diggings Concession Area 3, Offshore Namaqualand. Unpubl. Hons Proj., Geol. Dept., Univ. Cape Town. 27pp.
- McKenzie, P. 1958. Rip current systems. J. Geol., 66: 103-113.
- McKinney, R.F., Stubblefield, W.C. and Swift, D.T.P. 1974. Large scale current lineations on the central New Jersey shelf: investigations by side-scan sonar. Mar. Geol., 17: 79-102.
- Mercer, J.H. 1983. Cenozoic glaciation in the southern hemisphere. Ann. Rev. Earth Planet. Sci., 11:99-132.
- Merensky, H. 1909. The diamond deposits of Lüderitzland, German Southwest Africa. Trans. geol. Soc. S. Afr., 12: 13-23.
- Merensky, H. 1927. How I found the richest diamond field in the world. Min. ind. Mag. S. Afr., 4(6): 267pp.
- Meteorological Services of the Royal Navy and the South African Air Force 1944. Weather on the Coasts of Southern Africa. Vol.2. Local information. Cape Town: S. Afr. Govt.
- Middleton, G.V. and Southard, J.B. 1978. Mechanics of sediment movement. Soc. econ. Pal. Min. short Course Lecture Notes 3. (1st edn).
- Middleton, G.V. and Southard, J.B. 1984. Mechanics of sediment movement. Soc. econ. Pal. Min. short Course Lecture Notes 3. (2nd edn).
- Milliman, J.D. and Emery, K.O. 1968. Sea levels during the past 35 000 y. Science, 2: 1121-1123.
- Morang, A. and McMaster, R.L. 1980. Nearshore bedform patterns along Rhode Island from side-scan sonar surveys. J. sedim. Petrol., 50(3): 831-840.
- Morgans, J.F.S. 1956. Notes on the analysis of shallow-water soft substrata. J. Anim. Ecol., 25: 367-387.
- Mudie, J.D., Normak, W.R. and Cray, E.J. 1970. Direct mapping of the seafloor using side-scan sonar and trisponder navigation. Bull. geol. Soc. Am., 81: 1547-1554.
- Muller, G. and Gastner, M. 1971. The "Karbonat/Bombe", a simple device for the determination of the carbonate content in sediments, soils and other materials. N. Jb. Miner. Mh. 10: 466-469.
- Murray, L.G. 1969. Exploration and sampling methods employed in the offshore diamond industry. In: Proc. 9th Commonw. Min. metall. Congr. London. 71-124.

- Murray, L.G., Joynt, R.H., O'Shea, D.O'C., Foster, R.W. and Kleinjan, L. 1970. The geological environment of some diamond deposits off the coast of S.W.A. In: Delany, F.M (ed.). The Geology of the East Atlantic Continental Margin. Rep. Inst. geol. Sci., 70(16): 119-141.
- Nelson, G. and Hutchings, L. 1983. The Benguela upwelling area. Progr. Oceanogr., 12: 333-356.
- Newton, R.S., Seibold, E. and Werner, F. 1973. Facies distribution patterns on the Spanish Sahara continental shelf, mapped with side-scan sonar. "Meteor" Forsch-Ergebnisse; Reihe C, 15: 55-77.
- Nunn, P.D. 1984. Review of evidence for late Tertiary shorelines occurring on South Atlantic coasts. Earth-Sci. Rev., 20: 185-210.
- O'Shea, D.O'C. 1971. An Outline of the Inshore Submarine Geology of Southern S.W.A. and Namaqualand. Unpubl. MSc. thesis, Geol. Dept, Univ. Cape Town, 101pp.
- Petersen, N.D. 1983. Vibracore study of sediments on the inner and middle continental shelf between the Orange River and Chamais Bay - South West Africa. Unpubl. Hons. Proj. Geol. Dept, Univ. Cape Town, 36pp
- Pickerill, U.R.A. 1983. Wave built shelves on some low-energy coasts. Mar. Geol., 51: 193-216.
- Price, G.K. 1984. Lithofacies and biofacies in vibrocores from Quaternary sediments on the inner shelf north of the Orange River. Unpubl. Hons. proj. Geol. Dept Univ. Cape Town, 35pp.
- Reimnitz, E., Toimil, L.J., Shepard, F.P. and Gutierrez-Estrada, M. 1976. Possible rip current origin for bottom ripple zones to 30 m depth. Geology, 4: 395-400.
- Reineck, H-E. and Singh, I.B. 1980. Depositional Sedimentary Environments. (2nd edn). Berlin, Springer-Verlag, 542pp.
- Reuning, E. 1931. The Pomona-quartzite and Oyster-horizon on the west coast north of the mouth of the Oliphants R. Trans. roy. Soc. S. Afr., 19: 205-214.
- Rogers, A.W. 1915. The geology of part of Namaqualand. Trans. geol. Soc. S. Afr., 18: 72-101.
- Rogers, A.W. 1917. Namaqualand. S. Afr. geogr. J., 1: 23-33.
- Rogers, J. 1977. Sedimentation on the Continental Margin off the Orange River and the Namib Desert. Bull. jt geol. Surv./Univ. Cape Town mar. Geosc. Gp, 7: 162pp.
- Rooseboom, A. and Harmse, H.J. 1979. Changes in the sediment load of the Orange River during the period 1929-1969. Publ. int. Ass. hydrol. Sci., 128: 459-470.

- Rossouw, J. 1981. Wave conditions at Oranjemund: Summary of waverider data, March 1976 to April 1980. Rep. S. Afr. Coun. sci. ind. Res. T/SEA 8106: 4pp.
- Rossouw, J. 1984. Review of existing wave data, wave climate and design waves for South African and South West African (Namibian) coastal waters. Rep. S. Afr. Coun. sci. ind. Res. T/SEA 8401: 66pp.
- Rossouw, J., Coetzee, L.W. and Visser, C.J. 1982. A South African wave climate study. Proc. 18th coastal Eng. Conf. 1: 87-107.
- Sanders, J.E., Emery, K.O. and Uchupi, E. 1969. Microtopography of five small areas of the continental shelf by side-scanning sonar. Bull. geol. Soc. Am., 80: 561-572.
- Sargent, G.E.G. 1969. Further notes on the application of sonic techniques to submarine geological investigations, with special reference to continuous-reflection seismic profiling. Proc. 9th Commonw. Min. metall. Congr., 95-124.
- Schulze, B.R. 1965. Climate of South Africa. Part 8. General Survey. Weather Bur. Dept. Transport S. Afr., WB 28: 330pp.
- Shackleton, N.J. and Kennett, J.P. 1975. Palaeo-temperature history of the Cenozoic and the initiation of Antarctic glaciation: Oxygen and Carbon isotope analysis in DSDP sites 277, 279 and 281. In: Initial Repts Deep-Sea Drilling Project, 29: 743-755.
- Shannon, L.V. 1966. Hydrology of the south and west coasts of S.A. Investl. Rep. Div. Sea Fish. S. Afr., 58: 62pp.
- Shannon, L.V. 1985. The Benguela ecosystem Part 1. Evolution of the Benguela, physical features and processes. Oceanogr. Mar. Biol. Ann. Rev., 23: 105-182.
- Shannon, L.V. and Anderson, F.P. 1982. Applications of satellite ocean colour imagery in the study of the Benguela Current system. S. Afr. J. Photogrammetry, Remote Sensing and Cartography, 13(3): 153-169.
- Shepard, F.P. 1963. Submarine Geology. New York: Harper and Row, 555pp.
- Shepard, F.P. 1964. Nomenclature based on sand, silt and clay ratios. J. sedim. Petrol., 24: 151-158.
- Sheriff, R.E. 1976. Inferring stratigraphy from seismic data. Bull. Am. Ass. Petrol. Geol., 60(4): 528-542.
- Siesser, W.G. 1978. Aridification of the Namib desert. Evidence from oceanic cores. In: Van Zinderen Bakker, E.M. (ed.). Antarctic Glacial History and World Palaeoenvironments. Rotterdam, Balkema. 105-113.
- Siesser, W.G. and Dingle, R.V. 1981. Tertiary sea-level movements around southern Africa. J. Geol., 89: 83-96.

- Siesser, W.G. and Salmon, D. 1979. Eocene marine sediments in the Sperrgebiet, South West Africa. Ann. S. Afr. Mus., 79: 9-34.
- Simpson, E.S.W. 1971. The geology of the south-west African continental margin: a review. In: Delany, F.M. (ed.). The Geology of the East Atlantic Continental Margin. Rep. Inst. geol. Sci., 70(16): 157-170.
- Simpson, E.S.W. and Du Plessis, A. 1968. Bathymetric, magnetic and gravity data from the continental margin of southwestern Africa. Canad. J. Earth Sci., 5: 1119-1123.
- Simpson, E.S.W. and Needham, H.D. 1967. The floor of the southeast Atlantic: a review. In: UNESCO-IUGS Symposium Montevideo, Uruguay. Continental drift emphasizing the history of the South Atlantic area, 39-81.
- South African Committee for Stratigraphy. 1980. Stratigraphy of South Africa. Part I. Lithostratigraphy of the Republic of South Africa, South West Africa/Namibia, and the Republics of Bophuthatswana, Transkei and Venda. Handbook S. Afr. Geol. Surv. 8, 690pp.
- Stander, G.H. 1964. The Benguela Current off South West Africa. Investl. Rep. mar. Res. Lab. South West Africa, 12: 43pp.
- Stocken, C.G. 1962. The diamond deposits of the Sperrgebiet, SWA. Field Excursion guide, 5th ann. Congr. geol. Soc. S. Afr., 16pp.
- Sunamura, T. and Kraus, N.C. 1985. Prediction of average mixing depth of sediment in the surf zone. Mar. Geol., 62: 1-12.
- Sutherland, D.G. 1982. The transport and sorting of diamonds by fluvial and marine processes. Econ. Geol., 77(7): 1613-1620.
- Swart, D.H. 1981. Tables for the application of Vocoidal wave theory. Rep. S. Afr. Counc. sci. ind. Res., T/SEA 8010: 42pp.
- Swart, D.H. 1983. Physical aspects of sandy beaches - a review. In: McLachlan, A. and Erasmus, T. (eds). Sandy beaches as ecosystems. Amsterdam, Junk, 5-45.
- Taljaard, J.J. and Schumann, T.G.W. 1940. Upper air temperatures and humidities at Walvis Bay, South West Africa. Bull. Am. meteorol. Soc., 21: 293-296.
- Taljaard, J.J. 1972. Synoptic meteorology of the Southern Hemisphere. In: Newton, C.W. (ed.). Meteorology of the Southern Hemisphere. Meteorol. Monographs. Am. meteorol. Soc., 35 (13): 139-213.
- Taljaard, J.J., Schmidt, W. and Van Loon, H. 1961. Frontal analysis in the application to the Southern Hemisphere. Notos, (Weather Bureau) S. Afr. Dept Transport, 10: 25-58.

- Tankard, A.J. 1976. Cenozoic sea-level changes: a discussion. Ann. S. Afr. Mus., 71: 1-14.
- Tankard, A.J. and Rogers, J. 1978. Late Cenozoic palaeo- vironments on the west coast of South Africa. J. Biogeogr., 5: 319-337.
- Tankard, A.J., Jackson, M.P.A., Eriksson, K.A., Hobday, D.K., Hunter, D.R. and Minter, W.E.L. 1982. Crustal Evolution of Southern Africa. 3.8 Billion years of Earth History. New York, Springer-Verlag, 523pp.
- Terhorst, A. 1983. The Seafloor Character in Block 1 of State Alluvial Diggings Concession Area No.3. Unpubl. Hons Proj., Geol. Dept, Univ. Cape Town.
- Tripp, R.T. 1975. South African Sailing Directions. Vol.II. The coasts of South West Africa and the Republic of South Africa from the Kunene River to Cape Hangklip. Kenwyn: Hydrographer, S.Afr. Navy, 223pp.
- Twichell, D.C. 1983. Bedform distribution and inferred sand transport on Georges Bank. Sedimentology, 30(5): 695-710.
- Vail, P.R. and Hardenbol, J. 1979. Sea-level changes during the Tertiary. Oceanus, 22: 71-79.
- Van Ieperen, M.P. 1976. Characteristics of wave fields recorded along the western coast of Southern Africa. Proc. 1st interdisc. Conf. mar. freshwater Res. Port Elizabeth S. Afr., Fiche 8: G12-9B9.
- Van Zinderen Bakker, E.M. 1982. African palaeoenvironments 18000 yrs. B.P. In: Coetzee, J.A. and Van Zinderen Bakker, E.M. (eds). Palaeoecology of Africa, 15: 77-99. Rotterdam. Balkema.
- Wagner, P.A. 1914. The Diamond Fields of Southern Africa. Johannesburg, The Transvaal Leader.
- Wagner, P.A. and Merensky, H. 1928. The diamond deposits on the coast of Little Namaqualand. Trans. geol. Soc. S. Afr., 31: 1-41.
- Walcott, R.I. 1972. Past sea levels, eustacy, and the deformation of the Earth. Quatern. Res., 2: 1-14.
- Ward, J.D., Seely, M.K. and Lancaster, N. 1983. On the antiquity of the Namib. S. Afr. J. Sci., 79: 175-183.
- Werner, F. 1982. Nearshore bedform patterns along Rhode Island from side-scan sonar surveys - discussion. J. sedim. Petrol., 52(2): 674-677.

- Whelan, T., Coleman, J.M., Suhayda, J.N. and Roberts, H.H. 1977. Acoustical penetration and shear strength in gas-charged sediment. Mar. Geotech., 2: 147-159.
- Whitaker, A. 1984. Dust transport by bergwinds off the coast of South West Africa: direction, sources and flux to marine sediments. Unpubl. Hons. Proj., Geol. Dept., Univ. Cape Town. 31pp.
- Woodborne, M.W. 1982. Sediment distribution and the correlation between lithofacies and associated seismic reflection signatures in Table Bay. Unpubl. Hons. Proj., Geol. Dept., Univ. Cape Town, 34pp.
- Woodborne, M.W. 1984. Cruise Report SAD 2/83 - A nearshore geophysical survey between White Point and Stompneus Bay (Diamond Concession Areas 4a and 4b) - 14th February to 21st April 1983. Rep. geol. Surv. S. Afr., 1984-0085: 19pp.
- Woodborne, M.W. 1985. Some preliminary notes on the bathymetry of the inner shelf between White Point and Stompneus Bay, Cape West Coast. Tech. Rep. jt geol. Surv./Univ. Cape Town mar. Geosc. Unit, 15: 157-172.
- Woodborne, M.W. 1986. The seafloor geology of the Namaqualand inner shelf between White Point and Stompneus bay - an interpretation based on side-scan-sonar, sampling and underwater photography. Tech. Rep. jt geol. Surv./Univ. Cape Town mar. Geosc. Unit, 16: 187-207.
- Wright, J.A. 1964. Gully pattern and development in wave-cut bedrock shelves north of the Orange River mouth, South West Africa. Trans. geol. Soc. S. Afr., 67: 163-171.

APPENDIXA. METHODSA.1. Fieldwork

Four cruises were undertaken to the study area between 1980 and 1983 during which side-scan sonar, high-resolution seismics and sediment sampling were done.

The initial cruise TBD 405 (Du Plessis, 1980), on the R.V. Thomas B. Davie, took place from April 29 to May 7 1980. The survey area extended between 1km and 9 km from the shore and consisted of sets of coast-parallel and coast-perpendicular lines (Maps 1A to C). The coast-parallel lines, run between 200 m and 400 m apart, covered a zone between 1km and 2.5 km offshore, the lines totalling a distance of 165 km. Sixteen lines were run perpendicular to the coast, and with four additional lines across Peacock Bank, totalled 145 km of ground covered. These lines extended between 2 km and 9 km from the shore.

Most of the data were recovered during a cruise that was undertaken between the 4th and 25th of May 1981 (De Decker, 1983a). The vessel used was a converted 12 m tunny boat, the Seedelwer I, used by State Alluvial Diggings for their marine diamond exploration. Lines were run either 100 m or 200 m apart, covering the area between the breaker zone and the inner line of cruise TBD 405, an area about 1,0 km to 1,5 km wide and extending from the Orange River to Wreck Point. A total of 380 km of coast-parallel lines were run in an area of approximately 65 km² (Maps 1A to C).

During a survey undertaken in Diamond Concession Area 4, in

February 1983, (Woodborne, 1984), several tielines were run in the study area from the breaker zone to the seaward edge of the previously run coast-parallel lines. Altogether 6 lines (Lines D3 to D8, Map 1) totalling 19 km, were run between Cape Voltas and Gielie's Bay, mostly across the sediment-filled embayments.

Forty-five grab samples of surficial sediment were recovered during a cruise in September 1982 (De Decker, 1983b). The remaining fifty-four grab-samples were collected by the personnel at State Alluvial Diggings during October and November 1982 (Fig.6.3). In Chapter 6 the reasons for the non-uniform sampling distribution are given. The samples were principally recovered to verify the sonographic interpretation previously made of the seafloor.

The geophysical data were collected during late summer and autumn, in the hope that the south and southeasterly winds which are prevalent in summer (cf. Figs.1.5 and 1.6) would have abated by then. Calm seas are essential if good quality side-scan sonar and seismic records are to be obtained as a choppy sea will cause the transducers to trail erratically through the water.

A.2 Equipment

A.2.1 Navigational

Position fixes were made using an MRD-1 Tellurometer system. It employs 3 shore-based remote stations in line of sight which receive and re-emit a radio signal transmitted via the master antenna on the survey vessel. Three intersecting ranges are thus received by the master unit on the boat. The computer integrates these ranges and gives a position fix that is usually accurate to within 1 m. Fixes were recorded every 2 minutes on cruise TBD

405 and every minute on the other cruises. To ensure that the ranges from the remote stations intersect at high angles and thus give an acceptable fix, the units had to be repositioned at intervals as the survey progressed along the coast.

A.2.2 Seismics

A 3,5 kHz EDO-WESTERN "pinger" subbottom profiler was used for all the seismic lines, except for TBD 405 lines 27 to 34 and 20c. These lines were recorded using a 500J multi-electrode sparker unit, using frequencies between 0.7 and 1.5kHz. An EPC 4100 recorder was used with a sweep range of 125 msec, except for two lines across Peacock Bank, when the recorder was set to 250 msec. The records were annotated every five minutes for the TBD 405 lines and every two minutes for the other lines.

The EDO-WESTERN transducer was mounted on a catamaran which was towed 5 to 10 m astern of the boat, floating about 0,5 m below the sea surface. It was used in this fashion for the inshore lines run during cruises SAD 5/81 and SAD 2/83. On the TBD 405 cruise in deeper water a midwater towing system was able to be employed to reduce the effect of surface swell.

A.2.3 Side-scan sonar

Cruise TBD 405: An EG&G Mark IB side-scan sonar recorder, owned by the Geological Survey was used with a 272 Saf-T Model 100kHz transducer in the tow-fish. The scanning range was set at 200 m, to obtain at least 100% coverage for the lines spaced between 200 m and 400 m apart, except for Lines 3C, 4R, 5C and 6 between Alexander Bay and Homewood Harbour, when the 100 m range setting was used. The best resolution in the records lies between the 25 m and 100 m scan lines.

Cruises SAD 5/81 and 2/83: During these surveys a rented

Klein Hydroskan two-channel recorder, Model 521, linked to a 100kHz tow fish Model 422S-001A was used because of its taping capabilities. The range setting was kept at 100 m to maintain a constant resolution, even when running lines 200 m apart.

Peripherals to the recorder that were tried during the SAD 5/81 survey included:

- a) An eight-track Hewlett Packard magnetic tape recorder to place the uncorrected side-scan record on tape for later manipulation in the laboratory. Lines 201A to 210A between Cape Voltas and Alexander Bay and Lines 510 to 520 between Rietfontein and Geeldoring (Map 1) were recorded on tape;
- b) A towed speed-sensor unit that uses the speed of the boat through the water as a reference to control the paper-feed rate automatically, thereby producing an isometric record;
- c) A K-MAPS signal-processing box for speed correction. It is manually set, enabling one to relate paper-feed rate to the true speed of the boat over the ground - either in metres per second or in knots. The speed of the vessel over the ground is continually supplied by the navigational system as a digital readout in m/s. In this way approximately scale-corrected (isometric) records were obtained.

The records were annotated every 5 minutes during Cruise TBD 405, and every 2 mins on the SAD cruises. No attempt was made to obtain isometric records during the initial TBD 405 cruise in 1980. On the SAD 5/81 cruise the various peripherals described above were tried. Most of the lines were, however, run using the manual speed-corrector since this gave a better result than the towed speed-sensor. This method can only approach the required isometry in scale, as it is not possible to adjust the paper

feed-rate for every change in ship's speed. The best results are achieved if the navigational system is interfaced with the K-MAPS system, allowing continuous and instantaneous corrections to changes in speed.

No peripherals were used for the 6 tielines run during cruise SAD 2/83.

A.2.4 Sediment sampling

Ninety-nine sediment samples were retrieved using a modified Van Veen grab capable of penetrating about 10 cm and taking about 10 kg of surficial sediment. Approximately 3 kg of subsample taken from the centre of the sample ensured that the effects of winnowing of fines while raising the grab were reduced to a minimum. The samples were placed into plastic tubs for further analysis in the laboratory.

A.2.5 Wave-measurements

A "Waverider" buoy system, deployed by the Fisheries Development Corporation, was used to collect wave data as part of a feasibility study for a harbour at Alexander Bay. The buoy was stationed about 500 m west of Alexander Bay, in 14 m of water (Fig.7.2). The available records extend from March 1 1982 to September 30 1983, thus covering the autumn (March, April and May) and winter seasons (June, July and August) twice, whereas, except for September, spring (September, October, November) and summer were covered once only. Readings were collected every 6 hours (at 02h00, 08h00, 04h00 and 20h00) with the recording period lasting 20 min. The maximum number of readings per month was thus 120 or 124, depending on the number of days in the month. However, technical problems reduced this figure so that an average of 86% (2005 out of a possible 2316) readings were recorded (Table 5).

A.3 Data reduction

The shallow-water nature of the project necessitated that, for reasons of safety and towfish-stability, the lines had to be run coast-parallel. This caused a conflict in interests, since the optimal scanning direction for the side-scan sonar would have been achieved along coast-perpendicular lines, in order to scan perpendicular to NNE-trending bedrock features such as gullies and ridges. The nature of the bedrock morphology would likewise have been better displayed had the seismic lines traversed across coast-parallel wave-cut cliffs and terraces.

A.3.1 Track Chart

Base maps were drawn at two scales. The data from Cruise TBD 405 were plotted at 5-minute-fix intervals at a scale of 1:10 000, whereas the lines run during SAD 5/81 were plotted at 2-minute-fix intervals and at a scale of 1:2 000. The MRD-1 was programmed to print a position fix every minute, using the LO17 coordinate system, for Cruise TBD 405, SAD 9/82 and SAD 2/83. For Cruise SAD 5/81 the local SAD-grid coordinate system was used, but the coordinate values were subsequently converted to LO17 (Map 1). LO coordinates are practical for local surveys, because they use the metre as a unit length and because the X- and Y- axis scales are equal (orthogonal) making it easy to measure distances and to calculate scales.

For the 1:10 000-scale track chart, the area was divided into 3 parts and the data plotted onto separate base maps each covering about 10 km of the coast and an area between 6 and 9 km seaward. Map A extends from the Orange River to Cape Voltas, Map B covers Cape Voltas to Rietfontein, and Map C runs from Rietfontein to Wreck Point.

Originally, the SAD 5/81 data were plotted onto 1:2 000 base-maps corresponding to the survey blocks into which the coast-parallel lines were subdivided (Map 1). In this way 9 base-maps were produced, with the local SAD-grid as a coordinate system. Subsequently standardized 1:2 000 LO17-grid sheets were produced by SAD and the track lines were then transferred onto them (Map 1). These sheets were then reduced to 1:10 000 and the data added to the existing data from the TBD 405 cruise. Map 1 is presented at a scale of 1:40 000.

A.3.2 Seismic data:

For the bedrock isobath and internal-reflector data depths were read from the pinger records assuming the velocity of sound through water and unconsolidated sediments to be 1500 m/sec. (D'Olier, 1979). The resolution of the pinger system depends on a variety of factors. For the 3.5 kHz pinger, assuming a sound velocity of 1500 m/sec through unconsolidated sediment, the best resolution would be 10 cm. This is based on the relation: $\text{wavelength} = \text{velocity}/\text{frequency}$ and the limiting value of a quarter wavelength for an horizon to be resolved (Sheriff, 1976). In the study area the resolution was approximately 1 to 2 m, the average for normal working conditions and within the range given by D'Olier (1979). Poor sea conditions, particularly high swell and surface chop adversely affected the resolution occasionally, whereas recorder setting, sediment type (fine sand would give better resolution than gravel) and to a much lesser extent, turbidity and water temperature, would also have influenced the quality of the resolution.

Good quality, high-resolution seismic data can be obtained from the inner shelf if the data are tape-recorded and replayed

using a swell-filter unit, thereby eliminating the adverse effect of surface swell on the records.

TBD 405 data: The data for the bathymetry map were taken from records obtained with the hull-mounted 12kHz ELAC echosounder on the R.V. Thomas B. Davie. The recorder was set to compensate for the depth of the transducer beneath the waterline.

Because the pinger was towed mid-water, depths below sealevel to bedrock and to subbottom reflectors, were obtained by first measuring the depth below the seafloor from the seismic record, then adding the water depth from the echosounder recorder at that point to the value obtained from the seismic record. No corrections were made to account for the displacement between the echosounder and the seismic profiler being towed 10 to 15 m behind the boat. Readings were taken at every event mark (i.e. 5 min) and at inflexion points in the topography and plotted onto the 1:10 000 scale maps. This gave an average of 40 data points per square kilometre for the coast-parallel lines.

SAD 5/81 and 2/83 data: Depths were read directly from the seismic profiles, assuming the same velocity of sound as above. Readings were taken every minute and at changes in the topography. The data density was about 100 data points per square kilometre.

Seafloor isobath data from the SAD cruises were plotted onto the 1:2 000-scale worksheets, whereas the other data, from all the cruises, were plotted onto 1:10 000-scale basemaps. The 1:2 000-scale bathymetry maps were reduced to 1:10 000 scale after which the TBD 405 data were added. If a discrepancy in depth occurred where two lines coincided (generally over rugged topography) the value from the SAD records was considered correct

because there was more control over these data than over the TBD 405 data; the difference never exceeded 3 m. All values from the coast-parallel lines were contoured at 1 m intervals. The data from the tielines extending over the inner-shelf slope were represented by means of "fence diagrams". These give a more accurate representation of the seafloor and subbottom for these widely-spaced lines than contouring would have given.

No corrections for tide were made because the west coast is a microtidal region with a spring-tide range of only 1.8 m (Heydorn & Tinley, 1981). This is within the resolution of the seismic system, considering the general wave conditions along the west coast.

A.3.3 Side-scan sonar

In order to facilitate the interpretation of side-scan sonar records, it is essential to know the inherent distortions in the sonographs and where possible to correct them. Flemming (1982) gives a detailed analysis of the causes and effects of distortions in sonographs. He lists distortions for which corrections (at present) are not possible. Some distortions, such as yawing, rolling, pitching and crabbing result from tow-fish instability. A decrease in resolution along the range direction is a function of the spreading out of the scanning beam with distance from the transducer. Further scale-distortions are introduced with rapid change in the height of the transducer above the seafloor - such as when rugged topography is traversed - and in scanning a seafloor with an appreciable gradient. Variations in the velocity of sound, resulting from changes in temperature, salinity and turbidity of the water also contribute to distortions of the image on the sonograph. However, all these

distortions are comparatively minor when compared with the distortions produced by variable ship's speed, paper-feed rate and the height of the transducer above the seabed.

The resolution of the side-scan sonar system will depend on various factors. Two resolutions are involved:

1) The transverse resolution (T_r) is "the minimum distance between two objects parallel to the line of travel that will be recorded on paper as separate objects" (Flemming, 1976b, p.68). T_r is a function of the beam width at the point of measurement on the seafloor through the relation:

$$T_r = \sin A \times D_s$$

where A is the beam width (1° for the Klein and $1,2^\circ$ for the EG and G system) and D_s is the horizontal distance between transducer and object.

2) The range resolution (R_r) according to Fleming (1976b, p.68) is "the minimum distance between two objects perpendicular to the line of travel that will be recorded on paper as separate objects." If the minimum spacing for plotting features separately is 1 mm, then the resolution is 1/ the paper width per channel (203 mm for the Klein and 125 mm for the EG and G records) times the scan range. The range resolution at 200 m scan range for the EG and G records (TBD 405) is $1/125 \times 200 \text{ m} = 1,60 \text{ m}$ and for the Klein records, at 100 m range, (SAD cruises) is then $1/203 \times 100 \text{ m} = 0.49 \text{ m}$. This range resolution does not change along the scan line, whereas the transverse resolution deteriorates with distance. The T_r for the EG and G records (TBD 405) will be 4,19 m at 200 m improving to 52 cm at the 25 m scan line, whereas the Klein records (SAD cruises) at 100 m will have a transverse resolution of 1,25 m, and 0,26 m at the 15 m scan line.

Scale corrections: When interpreting a side-scan record (Fig.4.1) the scale distortions in the record need to be removed to allow the accurate positioning and orientation of the interpreted features. Flemming (1982) lists several means by which scale distortions due to ship's speed, paper-feed rate and transducer height from seafloor can be corrected. To remove compressional distortions along the record a graphical method using a "distortion ellipse" was devised by Newton et al. (1973) and developed by Flemming (1976). It is a simple and effective way to calculate the true orientation of lineaments from the record baseline, if the relation between the ship's speed over the ground and paper-feed rate is known. The degree of lateral slant-range distortion will vary depending on the obliquity of the sonar beam. Usually the transducer is towed about 10% of the range scale above the seafloor, eg. 10 m for the 100 m range. To produce an isometric record, it is necessary to eliminate the range distortion which compresses the short ranges and extends the far ranges (D'Olier, 1979; Flemming, 1982). The true range (R_t) can be calculated from Pythagoras' equation (Fig.4.1):

$$R_t = (R_s^2 - H_t^2)^{1/2}$$

where R_s = slant range

H_t = transducer height above seafloor.

Flemming (1982) has produced a series of nomograms for scanning ranges between 50 m and 500 m which can be used to correct the range distortion. Using the relevant distortion ellipse and the applicable nomogram, one could arrive at a scale-corrected interpretation of the distorted record. It is a tedious task which produces a corrected interpretation only; the original records remain anisometric. In modern systems these corrections

are automatically incorporated and the records have no scale distortions at all i.e. they are isometric.

The records produced during cruises TBD 405, SAD 5/81 and SAD 2/83 are not isometric. (Although the second cruise had the necessary peripherals linked to the recorder, technical problems prevented their effective use). Two methods were used in the laboratory to obtain the scale corrections: For TBD-405 records a closed-circuit television system was used. A transfer scope was utilized to obtain isometric records from the SAD data. By these methods the orthogonal axes of the records could be corrected, but the slant-range correction remains a manual operation.

The TV-system uses a camera to display the original record onto a monitor. The axes of the image on the monitor can be changed by electronic means, i.e. the record is "stretched" or "compressed". Knowing the ratio between the orthogonal axes that would produce an isometric record the image can be manipulated until this is achieved. The image on the monitor is then photographed and one has a photograph of an isometric record. Unfortunately, the resolution of the TV image is poor, but the technique does permit direct tracing of features which would have the correct relative orientation. The photographs can also be used to produce quasi-corrected sonograph mosaics. Records from the TBD-405 cruise that show seafloor features were corrected in this fashion, and postcard-size prints of the photographs were made. These were then enlarged (using a planvariograph) to 1:10 000 scale to match the base-maps, and the sonograph features traced onto the map. This system was previously used by De la Cruz (1978) in his detailed study of Saldanha Bay.

The records from the SAD cruises were manipulated by means of a Bausch and Lomb Stereo Zoom Transfer Scope belonging to the Estuarine and Coastal Research Unit of the CSIR at Stellenbosch. This optical instrument, commonly used in cartographic offices, can produce an apparent scale-distortion in one direction up to twice the original scale (termed "anamorphic stretching"). The distortion direction, in which the anamorphic stretching is done, can be rotated through 360° . In addition the transfer scope has a zoom lens that can enlarge the image up to seven times. Combining these two functions, one can manipulate the image of the sonograph to obtain an isomorphic scale for the orthogonal axes. The image is then photographed and prints can then be produced at a suitable scale. (For the study they were printed at a scale of 1:2 000).

The method used with the transfer-scope was firstly to produce postcard-size photographs of the original, scale-distorted record between consecutive time-fixes. These photographs were then placed singly onto the photo-stage of the transfer scope, with strips of the track chart, drawn at 1:2 000 scale, placed on the map stage. These strips consisted of a base-line, representing the transducer trace on the record, with each time-fix marked by a perpendicular line. Looking through the oculars of the transfer scope the two images were then superimposed (i.e. the base-line of the track-chart strips and the transducer trace on the record were aligned). Because the scanning range on all the SAD-cruise side-scan records was kept at 100 m, the distance along the time lines corresponding to 100 m could be marked off on all the strips of the track chart beforehand.

Using the zoom facility, the original 100 m-scan line was matched to that marked on the track-line strip by superimposing the images. This scale will change only if the fish height above the seafloor has changed. So for any one line this setting will remain approximately the same. The anamorphic stretching mode is used to expand or contract the record image to match exactly the time-fixes drawn on the track-line strips. This configuration gives the correct isometric scale for the sonograph. This isometric image is then photographed and the next section of record processed.

A 35 mm Ricoh 500 G camera with a fixed 40-mm lens was loaded with a medium-speed (125 ASA) film to ensure a fine-grained image. The camera was placed with its lens flush against one ocular of the transfer scope, the aperture was set wide at f4, shutter speed at automatic and focus at infinity. (In addition to the standard lighting of the transfer scope, two 500-watt bulbs were placed close to the photo stage to illuminate the photograph that was to be corrected.)

The photographs of the corrected isometric record, printed at 1:2 000 scale, lost some of the original detail, but were adequate to be able to trace seafloor features and prominent reflectors. The prints could then be cut to exclude the water column and pasted onto a basemap of similar scale to produce a mosaic. For this study a mosaic was not constructed, but instead a detailed interpretation of the sonographic features (Maps 5A to C) was made using the scale-corrected photographs.

This elaborate procedure of scale-correcting the sonographs will be obviated in future if the data are placed on magnetic tape and rerun in the laboratory, e.g. using Klein's K-Maps system.

A.3.4 Sediments

A flow chart of the laboratory procedures followed is presented in Figure A.1

In the laboratory approximately 500 g of the sediment was subsampled, placed in dialysis tubing and left overnight in fresh water to remove interstitial salt. The sample was then wet split to obtain subsamples for textural and compositional analyses. For the textural analysis the sub-sample was then wet-sieved through 2 mm and 63 μ m sieves to remove the gravel and mud from the sand fraction. The mud-fraction was collected in a plastic tub and allowed to settle. The gravel and sand fractions were oven-dried at 100°C and then weighed. The mud fraction was retrieved from the tub by decanting the excess water, placing the settled mud in a glass beaker and then oven drying. The weights of the three fractions were determined to obtain weight percentages of gravel, sand and mud for the sample.

The sand fraction of the sub-sample was mechanically split until approximately 5 g of the sediment was retained. A computer-linked settling tube housed in the Geological Survey offices in Bellville was then used to do the size analysis of this sub-sample (Brink and Rogers, 1978).

The frequency percentages for the mud, gravel and 5 one-phi sand-fractions are presented in Table 3. Cumulative and frequency curves for the sand-fraction are plotted, and the sand-fraction's mean, skewness, and sorting values are presented (Table 4).

To determine the carbonate and organic carbon content of the sediment, the subsamples were dried, mechanically split and then crushed. Only samples with more than 10% mud content were

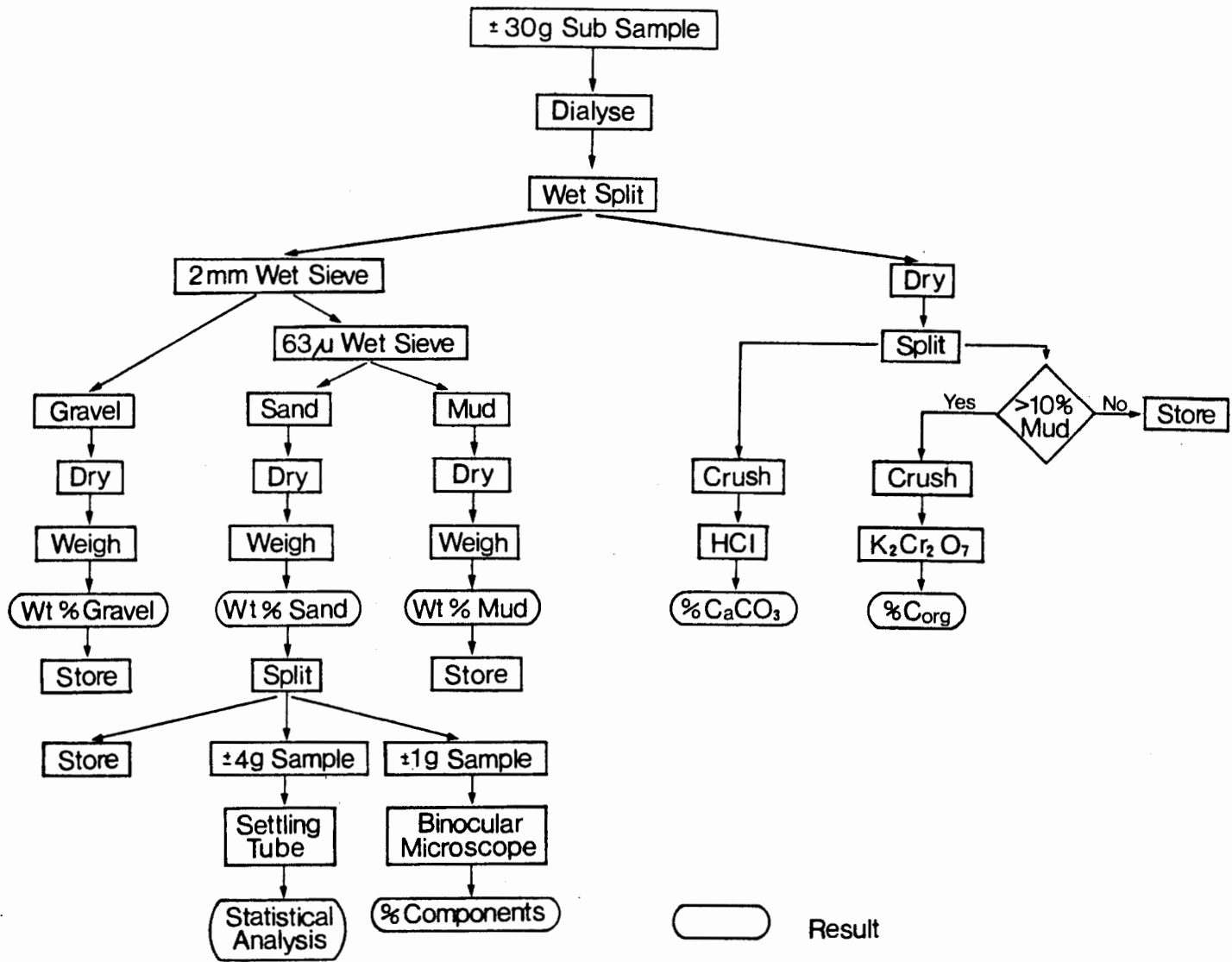


FIGURE A.1

analysed for organic carbon, using a wet-chemical method developed by Morgans (1956). The technique consists of oxidising the organic carbon using potassium dichromate and then back-titrating with ferrous sulphate. All the samples were analysed for carbonate by the "Karbonat-Bombe" method (Muller and Gastner, 1971; Birch, 1981). In this method 1g of sample is added to 5ml conc. HCl in a container fitted with a pressure gauge. The pressure of the released gases is converted to percentage carbonate, having normalized the value against a standard of pure CaCO_3 .

A.3.5 Wave Data

The parameters most commonly used in wave dynamics are (Rossouw, 1984):

T_p - the maximum-energy wave period at which the maximum energy occurs.

T_z - the mean wave period, determined by dividing the duration of the record by the number of times the record crosses the zero line in an upward direction.

H_s - the significant wave height, calculated as the average one-third of the highest waves in the record.

Using the "Waverider" data, values for T_p , T_z and H_s are determined for each 20-minute recording period. The mean values for the four daily recording periods are calculated and these are then summed to obtain an average value for each parameter. The frequency occurrence is then expressed as a percentage for each month, and an average value for each season (3-month period) is calculated. Table 5 gives the percentage occurrence of T_p , T_z and H_s per season.

B. TABLESB.1 Explanation of column headings.

TABLE B1. SAMPLE LOCATIONS

Loc.No. - Location number of the sediment sample.
 Sample No. - Number allocated to samples in the tubs.
 Water Depth - Sediment sampling depth, from bathymetry map.
 L.O.17 Coords - Orthogonal Coordinate system used in study.

TABLE B2. PERCENTAGE COMPONENT DISTRIBUTION

Loc. No. - Location number of the sediment sample.
 Qtz - quartz and feldspar particle fraction.
 Hf - Rock fragments and heavy minerals fraction.
 Sh - Biogenic particle fraction, other than sponge spicules and foraminifera.
 Mi - Biotite and Muscovite particle fraction.
 Sp - Sponge spicules
 Fo - Foraminifera and ostracoda fraction.

Percentage rangeGrain-size codes

A+	>90%	S+	1-5%	0 - Very coarse sand (1-2 mm)
A-	75-90%	S-	1%	1 - Coarse sand (0,5-1,0 mm)
P+	50-75%	S=	<<1%	2 - Medium sand (0,25-0,5 mm)
P-	25-50%			3 - Fine sand (0,125-0,25 mm)
C+	10-25%			4 - Very fine sand (0,062-0,125 mm)
C-	5-10%			

TABLE B3. PERCENTAGE DISTRIBUTION OF SIZE-FRACTIONS, CARBONATE
AND ORGANIC CARBON

Loc. No.	- Location number of the sediment sample.
Mud	- The size fraction above 4 phi.
VFS	- Very fine sand size fraction (3 to 4 phi).
FS	- Fine sand size fraction (2 to 3 phi)
MS	- Medium sand size fraction (1 to 2 phi).
CS	- Coarse sand size fraction (0 to 1 phi).
VCS	- Very coarse sand size fraction (-1 to 0 phi).
GRAVEL	- Gravel size fraction (less than -1 phi).
CaCO ₃	- Percentage Calcium Carbonate.
C _{org}	- Percentage Organic Carbon.

TABLE B4. STATISTICAL SUMMARY

Loc. No.	- Location number of sediment sample.
MEAN	- Mean grain size (phi).
SORT	- Standard sorting value.
Sk	- Skewness.
1%	- First percentile value.

TABLE B5. PERCENTAGE OCCURRENCE T_p, T_z and H_s PER SEASON

T _p	- Peak wave period.
T _z	- Wave period at zero-moment crossing.
H _s	- Significant wave height.

TABLE B1
SAMPLE LOCATIONS

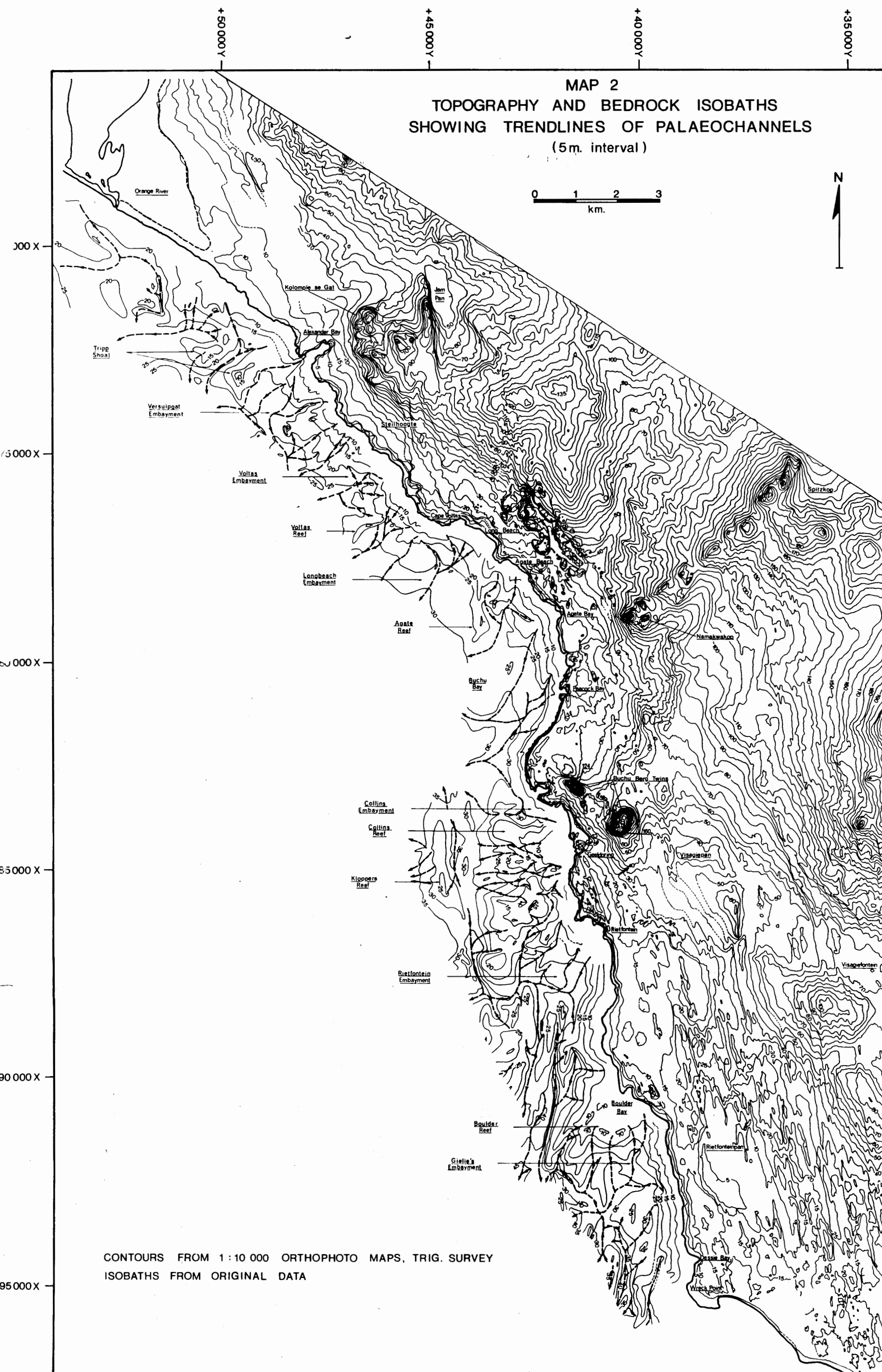
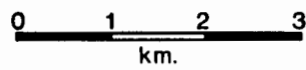
LOC. No.	SAMPLE No.	WATER DEPTH(m)	L.O.17. X	COORDS Y
1	0002	12.5	3169520	53536
2	0003	15.0	3170067	54112
3	0004	18.0	3170458	54990
4	0007	16.5	3172414	50360
5	0008	19.5	3173186	51063
6	0009	14.0	3173190	48195
7	0138	14.5	3173268	48233
8	0137	15.0	3173380	48303
9	0010	17.0	3173479	48670
10	0011	20.0	3174122	49441
11	0143	15.0	3173520	48110
12	0142	14.5	3173688	47885
13	0013	17.0	3174045	48088
14	0014	20.0	3174427	48468
15	0015	21.0	3174779	49040
16	0144	15.0	3173886	47786
17	0012	14.0	3173828	47631
18	0145	16.0	3174053	47784
19	0146	15.5	3174296	47703
20	0147	18.0	3174451	47860
21	0148	20.0	3174669	48077
22	0016	17.0	3174857	47116
23	0149	18.0	3174912	47205
24	0017	19.0	3175093	47358
25	0018	21.0	3175487	47696
26	0019	23.0	3176005	48080
27	0152	16.0	3175254	46526
28	0154	18.5	3175390	46857
29	0020	17.0	3175585	46269
30	0021	20.0	3175931	46688
31	0022	23.5	3176847	47327
32	0158	15.0	3175700	46116
33	0159	19.5	3176064	46282
34	0160	22.0	3176242	46446
35	0161	23.0	3176567	46532
36	0023	23.5	3176952	46383
37	0024	27.0	3177482	46889
38	0027	26.5	3177588	45090
39	0028	28.0	3177825	46722
40	0029	27.5	3178385	45918
41	0165	10.0	3172049	44346
42	0026	19.5	3177346	44769
43	0166	12.0	3177299	44101
44	0167	17.0	3177375	44393
45	0168	20.0	3177697	44495
46	0030	14.5	3177628	43831
47	0031	21.0	3177913	44103
48	0174	16.5	3177830	43780
49	0032	23.0	3178344	44071

LOC. No.	SAMPLE No.	WATER DEPTH(m)	L.O.17. X	COORDS Y
50	0033	26.5	3179088	44337
51	0176	9.5	3177820	43377
52	0173	18.5	3178144	43553
53	0171	20.5	3178362	43743
54	0178	14.0	3178133	43250
55	0172	20.0	3178504	43440
56	0036	24.5	3178786	43730
57	0034	14.5	3178301	43086
58	0035	20.5	3178688	43274
59	0179	11.0	3178416	42814
60	0180	16.0	3178670	42828
61	0181	21.0	3179126	43077
62	0183	13.0	3178860	42343
63	0037	13.5	3179020	42263
64	0188	20.5	3180008	42474
65	0039	20.0	3180287	42414
66	0040	21.5	3180468	42482
67	0038	20.5	3180442	42414
68	0190	9.0	3180903	42054
69	0191	21.0	3180872	42433
70	0041	23.5	3180501	42678
71	0044	20.5	3181366	42561
72	0042	25.0	3180696	43239
73	0192	10.0	3181880	42694
74	0045	19.0	3181462	42981
75	0193	17.5	3182048	42983
76	0046	18.0	3182611	42852
77	0047	27.5	3182844	43281
78	0053	29.0	3182819	43469
79	0076	20.0	3183232	42470
80	0075	23.0	3183423	42931
81	0074	23.5	3183266	43120
82	0048	14.0	3183861	42148
83	0083	23.0	3183783	42687
84	0049	24.5	3183780	42903
85	0085	27.5	3183747	43303
86	0050	11.5	3184930	42124
87	0056	10.0	3186594	41286
88	0057	19.0	3186860	41836
89	0097	28.5	3187382	42716
90	0060	18.0	3187314	41201
91	0061	23.0	3187654	41710
92	0063	30.0	3188097	42384
93	0062	27.0	3188240	41650
94	0065	27.0	3189796	41571
95	0122	15.0	3191498	41053
96	0131	18.0	3192304	39916
97	0133	11.0	3193958	39314
98	0072	32.0	3194133	40728
99	0073	37.0	3194751	40464

TABLE B2
PERCENTAGE COMPONENT DISTRIBUTION

Loc.No.	Qtz	Hf	Sh	Mi	Sp	Fo
1	3A-	4C+	3S+	3S+	-	-
2	3A-	4C-	3S+	2S+	S=	-
3	4A-	4C-	3S+	3S+	-	-
4	4A-	4C+	3S+	3S+	-	-
5	2A-	3C+	2S+	3S+	-	-
6	2A-	3C+	2S+	3S+	-	4=
7	3A-	3C+	3C-	3S+	S=	S=
8	3P+	2P-	2C-	3S+	S=	S=
9	4P+	4P-	3S+	3S+	S=	S=
10	3A-	4C+	2S+	3S+	S=	-
11	3A-	4C+	2C-	3S+	S=	-
12	2A-	2C-	1C+	-	S=	-
13	3P+	3P-	3C=	3S+	-	S=
14	2A-	3C+	2C-	3S-	-	-
15	3P+	4P-	3S+	3S+	-	S=
16	3A-	4C+	3S+	3S+	S=	S=
17	4A-	4C+	3C+	4S+	S-	-
18	4A-	4C+	3S+	4S+	S-	-
19	4A-	4C-	3C-	4S+	S-	S=
20	4P+	4P-	3C-	4S+	S-	S=
21	3A-	3C-	3C-	4S+	S-	S+
22	2A-	3C-	1C+	3S-	-	-
23	4P+	4P-	3C-	4S+	S-	S-
24	4P+	4P-	3C-	4S+	S-	S-
25	4A-	4C+	2C-	3S+	S-	S-
26	4A-	4C+	2C-	3S+	S-	S-
27	4A-	4C+	3C-	4S+	S-	S+
28	4P+	4P-	3C-	3S+	S-	S=
29	2A-	3C+	2C+	3S+	S-	S-
30	4P+	4P-	3C-	3S+	S-	-
31	4P+	4P-	3C-	3S;	S=	S=
32	2A-	3C-	1C+	3S+	-	-
33	3P+	3P-	3C-	3S+	S-	S+
34	3P+	3P-	3S+	3S-	S-	-
35	2A-	3C+	1C-	4S+	S-	S+
36	4P+	4P-	3C-	3S+	S-	-
37	4P+	4P-	3C-	3S+	S-	S+
38	4A-	4C+	3C-	4S+	S-	S-
39	3P+	4P-	3C-	4S+	S-	-
40	4A-	4C+	3C+	4S+	S-	S+
41	3A-	3C+	2C+	3S+	S+	S+
42	3A-	4C+	2C+	3S+	S-	S+
43	3A-	3C-	2C+	3S-	S-	S+
44	4A-	4C+	3C+	4S-	S-	S;
45	4A-	4C+	2C+	3S-	S-	S+
46	3A-	4C-	2C+	3S-	S-	S+
47	3A-	4C+	2C+	3S-	S-	S+
48	3A-	3C-	2C+	3S-	S-	S+
49	3A-	4C+	2C-	3S-	S-	S+

MAP 2
 TOPOGRAPHY AND BEDROCK ISOBATHS
 SHOWING TRENDLINES OF PALAEOCHANNELS
 (5 m. interval)



300 X
 35 000 X
 40 000 X
 45 000 X
 50 000 X
 55 000 X
 60 000 X
 65 000 X
 70 000 X
 75 000 X

CONTOURS FROM 1:10 000 ORTHOPHOTO MAPS, TRIG. SURVEY
 ISOBATHS FROM ORIGINAL DATA

Loc. No.	Qtz	Hf	Sh	Mi	Sp	Fo
50	3A-	3C-	2C+	3S-	S+	S-
51	3A-	4C-	2C+	3S-	S-	S+
52	3A-	4C-	2C+	3S-	S-	S+
53	3A-	3C+	3C+	3S+	S-	S+
54	3A-	3C-	2C+	3S-	S-	S-
55	3A-	3C+	2C+	3S-	S-	S+
56	3A-	3C+	2C+	3S-	S-	S+
57	3A-	4C-	3C+	4S-	S-	S+
58	3A-	3C+	2C+	3S-	S-	S-
59	3A-	4C-	3C+	3S-	S-	S+
60	3A-	4C-	3C+	3S-	S-	S+
61	3A-	4C-	2C+	3S-	S-	S+
62	3A-	4C-	3C+	3S-	S-	S+
63	3A-	4C-	2C+	3S-	S-	S+
64	3A-	3C-	2C+	3S-	S-	S+
65	3A-	4C-	3C+	3S-	S-	S+
66	1A-	3C-	0C+	-	S-	S-
67	2A-	3C-	1C+	-	-	S-
68	3A-	4C-	3C+	-	-	S-
69	3A-	3C-	2C+	S-	S-	S+
70	3A-	4C-	2C+	S-	S-	S+
71	3A-	4C-	3C+	S-	S-	S+
72	2P+	2C-	0P+	-	S-	S=
73	3A-	3C-	2C+	-	S-	C-
74	3A-	3C-	2C+	-	S-	C-
75	3A-	4C-	3C+	-	S=	S+
76	3A-	4C-	3C+	-	S-	C-
77	2P+	4C-	1P-	-	S=	S+
78	3A-	4C+	2C+	-	S-	S+
79	4A-	4C-	3C+	S-	-	S+
80	4A-	4C-	3C+	S=	S-	C-
81	4A-	4C-	3C-	S=	S-	S+
82	4A-	4C-	3C+	S=	S-	S+
83	4A-	4C-	3C+	S=	S-	C-
84	4P-	4S+	3P+	S=	S+	C-
85	4P-	4S+	3P+	S=	S+	C-
86	3P+	4S+	3P-	-	S-	S-
87	3P+	3S+	3P-	-	-	C-
88	2A-	3C-	1C+	-	-	S+
89	2A-	3C-	1C+	-	-	C-
90	3P-	4S+	3P+	-	-	C-
91	4P+	4C-	3P-	-	-	S+
92	4P-	4S+	3P+	-	S+	C-
93	4P+	4S+	3P-	-	S+	C-
94	4P-	4S+	3P+	S-	S+	C-
95	3A-	4C-	3C+	3S+	S-	S+
96	3P+	4C-	3P-	-	-	S+
97	4A-	4C-	3C+	-	-	S+
98	4A-	4C-	3C+	-	S-	S+
99	2P+	4S+	1P-	-	-	S+

TABLE B3
PERCENTAGE DISTRIBUTION

LOC. No.	MUD	VFS	FS	MS	CS	VCS	GRAVEL	CaCO ₃	C _{org}
1	2.71	17.67	71.72	5.75	2.11	0.00	0.05	7.8	-
2	4.83	28.98	66.94	0.13	0.00	0.00	0.00	11.3	-
3	4.51	32.74	61.86	0.88	0.00	0.00	0.00	13.2	-
4	1.74	11.14	86.79	0.33	0.00	0.00	0.00	9.9	-
5	3.67	23.28	65.65	5.76	1.60	0.00	0.04	10.3	-
6	4.01	5.55	38.08	46.67	5.70	0.00	0.00	18.0	0.5
7	2.71	24.37	72.92	0.00	0.00	0.00	0.00	18.3	-
8	5.55	9.92	42.24	14.96	18.44	0.92	7.97	13.6	-
9	6.95	22.86	67.96	2.06	0.17	0.00	0.00	12.3	-
10	7.81	21.37	65.29	4.21	1.32	0.00	0.01	17.1	0.7
11	3.54	30.66	65.46	0.34	0.00	0.00	0.00	18.3	-
12	0.00	0.10	4.69	53.64	40.92	0.00	0.64	14.7	-
13	5.92	21.70	72.38	0.00	0.00	0.00	0.00	11.5	-
14	6.80	21.84	2.78	0.55	0.00	0.18	0.18	17.1	-
15	7.12	14.77	77.86	0.24	0.00	0.00	0.01	6.7	4.4
16	1.41	23.25	75.34	0.00	0.00	0.00	0.00	10.7	-
17	7.69	25.36	66.95	0.00	0.00	0.00	0.00	14.8	-
18	0.00	31.47	68.54	0.00	0.00	0.00	0.00	18.5	-
19	9.72	9.76	42.97	17.19	6.79	0.00	13.57	9.2	-
20	2.55	27.39	70.06	0.00	0.00	0.00	0.00	5.2	-
21	10.76	17.47	52.21	11.44	1.96	0.00	6.17	7.9	-
22	0.00	0.23	5.81	39.77	52.62	0.00	1.57	24.0	-
23	1.00	25.05	72.86	1.09	0.00	0.00	0.00	13.6	-
24	7.24	27.41	65.35	0.00	0.00	0.00	0.00	10.5	-
25	19.01	24.82	56.17	0.00	0.00	0.00	0.00	11.5	0.7
26	10.24	21.86	67.90	0.00	0.00	0.00	0.00	10.3	1.2
27	0.91	11.35	82.42	4.76	0.55	0.00	0.00	15.8	-
28	10.21	17.59	72.20	0.00	0.00	0.00	0.00	11.8	-
29	1.13	4.65	27.81	59.00	7.42	0.00	0.00	32.1	-
30	7.81	20.86	70.86	0.47	0.00	0.00	0.00	7.8	-
31	7.05	21.29	71.64	0.00	0.00	0.00	0.02	5.3	-
32	0.70	1.63	5.96	68.64	22.94	0.00	0.13	14.7	-
33	12.25	24.12	63.63	0.00	0.00	0.00	0.00	6.9	0.6
34	6.24	28.15	65.61	0.00	0.00	0.00	0.00	14.8	-
35	15.50	9.18	29.84	5.55	16.77	0.00	23.15	14.8	-
36	6.08	27.77	65.33	0.39	0.00	0.00	0.43	6.6	-
37	12.04	25.82	61.78	0.00	0.00	0.00	0.36	9.2	0.4
38	21.23	41.89	36.42	0.43	0.00	0.00	0.03	13.3	-
39	21.21	34.69	44.10	0.00	0.00	0.00	0.00	10.5	-
40	32.86	33.75	33.37	0.00	0.00	0.00	0.02	11.1	0.82
41	0.00	0.91	54.73	43.49	0.87	0.00	0.00	32.9	-
42	2.53	15.88	80.51	0.96	0.00	0.00	0.12	18.4	-
43	0.00	1.49	71.81	26.70	0.00	0.00	0.00	30.3	-
44	0.70	14.02	82.39	2.88	0.00	0.00	0.00	29.6	-
45	9.62	30.89	58.42	1.05	0.00	0.00	0.03	14.7	-
46	0.00	1.38	74.36	23.79	0.00	0.00	0.47	37.8	-
47	10.02	18.64	53.44	14.98	3.46	0.00	0.47	16.9	-
48	1.53	8.93	81.80	6.85	0.21	0.00	0.69	18.7	-
49	32.82	40.87	24.34	1.96	0.00	0.00	0.00	16.0	-

LOC. No.	MUD	VFS	FS	MS	CS	VCS	GRAVEL	CaCO ₃	C _{org}
50	34.59	40.90	22.96	1.15	0.00	0.00	0.40	15.4	1.4
51	0.00	0.00	18.95	72.25	5.80	0.00	0.00	21.8	-
52	2.85	25.12	68.13	3.61	0.00	0.00	0.29	23.5	-
53	18.92	40.42	38.35	2.32	0.00	0.00	0.00	23.1	1.22
54	0.18	2.50	82.23	14.88	0.19	0.00	0.02	22.4	-
55	4.80	37.01	55.94	2.03	0.21	0.00	0.01	22.7	-
56	19.34	37.72	39.91	2.81	0.00	0.00	0.22	17.1	-
57	0.00	1.84	89.35	8.81	0.00	0.00	0.00	28.2	-
58	3.95	21.89	51.90	15.15	6.06	0.00	1.05	23.4	-
59	0.00	1.87	86.70	11.43	0.00	0.00	0.00	29.6	-
60	0.00	1.55	84.26	14.19	0.00	0.00	0.00	34.6	-
61	9.15	26.70	49.85	13.93	0.35	0.00	0.02	27.3	-
62	0.00	5.99	86.30	7.71	0.00	0.00	0.00	19.7	-
63	0.14	0.87	48.86	49.66	0.46	0.00	0.00	25.3	-
64	2.49	13.14	77.20	7.15	0.00	0.00	0.02	23.4	-
65	1.09	8.24	78.67	12.00	0.00	0.00	0.00	31.7	-
66	0.14	0.00	2.15	31.38	45.03	3.46	17.83	25.9	-
67	1.29	6.12	78.76	13.53	0.30	0.00	0.00	24.4	-
68	0.60	0.70	93.77	4.40	0.42	0.00	0.10	32.9	-
69	0.75	5.01	83.77	10.00	0.47	0.00	0.00	29.3	-
70	4.98	10.77	83.14	1.12	0.00	0.00	0.00	27.6	-
71	0.78	6.32	89.32	3.58	0.00	0.00	0.00	21.3	-
72	0.40	0.00	0.91	37.10	57.96	0.00	3.63	32.0	-
73	0.34	1.09	88.84	9.72	0.00	0.00	0.00	26.9	-
74	4.02	14.11	78.29	3.56	0.00	0.00	0.02	23.7	-
75	0.86	6.49	92.65	0.00	0.00	0.00	0.00	20.8	-
76	0.47	1.91	86.79	10.82	0.00	0.00	0.00	11.8	-
77	0.34	0.49	10.61	51.99	4.42	0.00	32.15	49.3	-
78	3.34	14.47	54.73	22.11	3.10	0.00	2.25	32.1	-
79	3.29	13.79	80.86	2.05	0.00	0.00	0.01	27.6	-
80	18.69	16.84	62.73	1.74	0.00	0.00	0.00	30.3	0.6
81	12.93	22.14	57.33	6.44	0.78	0.00	0.38	32.1	-
82	1.66	12.90	80.45	4.99	0.00	0.00	0.00	32.1	-
83	12.15	27.66	59.13	1.06	0.00	0.00	0.00	40.1	-
84	100.00	0.00	0.00	0.00	0.00	0.00	0.00	-	-
85	33.26	13.32	16.83	12.97	7.62	0.00	16.00	38.5	0.5
86	0.00	0.04	8.49	84.86	6.60	0.00	0.01	25.0	-
87	0.00	0.20	42.30	56.10	1.40	0.00	0.00	54.7	-
88	0.70	0.31	5.20	50.32	33.47	0.00	0.00	23.1	-
89	0.81	2.66	10.10	58.16	25.27	0.00	3.00	17.0	-
90	1.92	9.50	87.01	1.57	0.00	0.00	0.00	38.9	-
91	4.10	12.18	75.47	8.25	0.00	0.00	0.00	31.6	-
92	61.96	32.30	5.37	0.00	0.00	0.00	0.37	84.2	0.9
93	25.00	35.37	40.62	0.00	0.00	0.00	0.01	38.2	-
94	40.67	22.42	31.94	4.13	0.00	0.00	0.84	35.5	1.3
95	3.12	13.73	80.62	1.58	0.00	0.00	0.95	34.2	-
96	1.00	4.84	94.16	0.00	0.00	0.00	0.00	32.1	-
97	0.73	6.56	90.22	2.20	0.29	0.00	0.00	25.6	-
98	1.00	6.39	91.56	0.00	0.00	0.00	1.05	31.7	-
99	1.00	0.49	7.58	41.21	46.42	0.00	3.30	61.5	-

Table B4
STATISTICAL SUMMARY

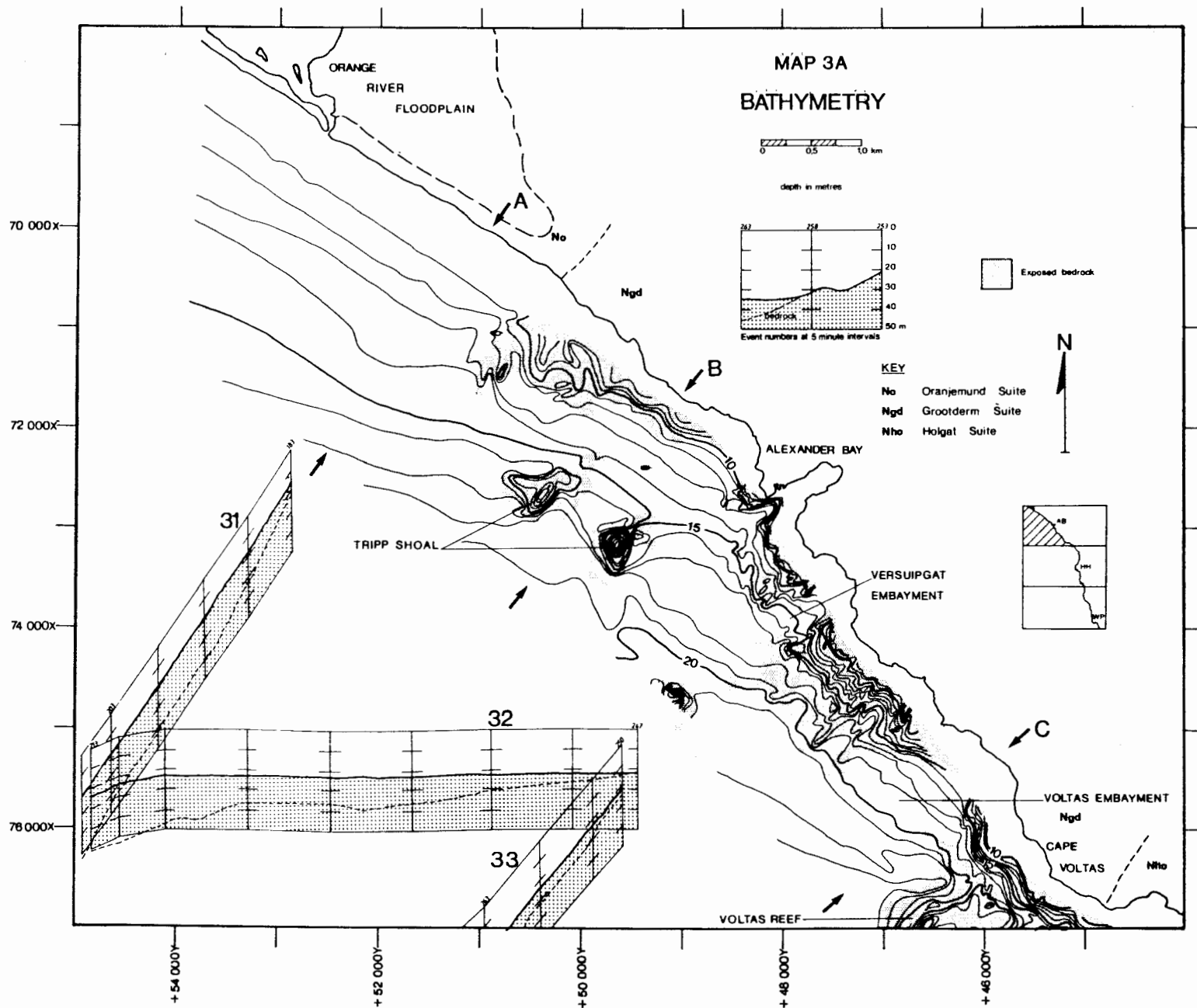
LOC. No.	MEAN (phi)	SORT	SK	1% (phi)
1	2.62	0.50	-0.68	0.80
2	2.88	0.28	0.21	2.30
3	2.90	0.32	-0.06	2.00
4	1.66	0.27	0.19	2.10
5	2.70	0.50	-0.78	0.80
6	1.90	0.72	0.11	0.50
7	2.83	0.26	0.35	2.40
8	2.01	0.99	-0.31	-1.00
9	2.78	0.36	-0.40	1.40
10	2.70	0.49	-0.47	0.90
11	2.87	0.31	0.10	2.30
12	1.13	0.40	0.96	0.50
13	2.83	0.25	0.31	2.30
14	2.78	0.39	-0.75	1.10
15	2.78	0.23	0.23	2.35
16	2.80	0.28	0.33	2.30
17	2.85	0.28	0.31	2.30
18	2.90	0.24	0.35	0.08
19	2.21	0.76	-0.32	0.30
20	2.86	0.26	0.31	2.40
21	2.53	0.61	-0.42	0.60
22	1.09	0.42	1.17	0.50
23	2.79	0.33	0.06	1.90
24	2.91	0.22	0.39	2.50
25	2.90	0.26	0.41	2.40
26	2.82	0.28	0.36	2.30
27	2.55	0.41	-0.38	1.00
28	2.78	0.26	0.30	2.30
29	1.76	0.68	0.35	0.70
30	2.79	0.28	0.17	2.20
31	2.82	0.25	0.27	2.35
32	1.30	0.48	1.09	0.60
33	2.89	0.22	0.42	2.50
34	2.87	0.27	0.32	2.40
35	1.97	1.04	-0.29	-0.10
36	2.86	0.31	0.05	2.30
37	2.89	0.23	0.37	2.50
38	3.06	0.38	0.06	2.20
39	2.98	0.27	0.29	2.50
40	3.02	0.32	0.18	2.40
41	2.07	0.35	-0.06	1.00
42	2.68	0.33	0.38	2.00
43	2.23	0.31	0.31	1.60
44	2.59	0.36	0.25	1.80
45	2.86	0.38	0.06	1.90
46	2.22	0.32	0.08	1.40
47	2.44	0.67	-0.34	0.40
48	2.45	0.38	0.16	1.50
49	3.10	0.47	-0.32	1.70

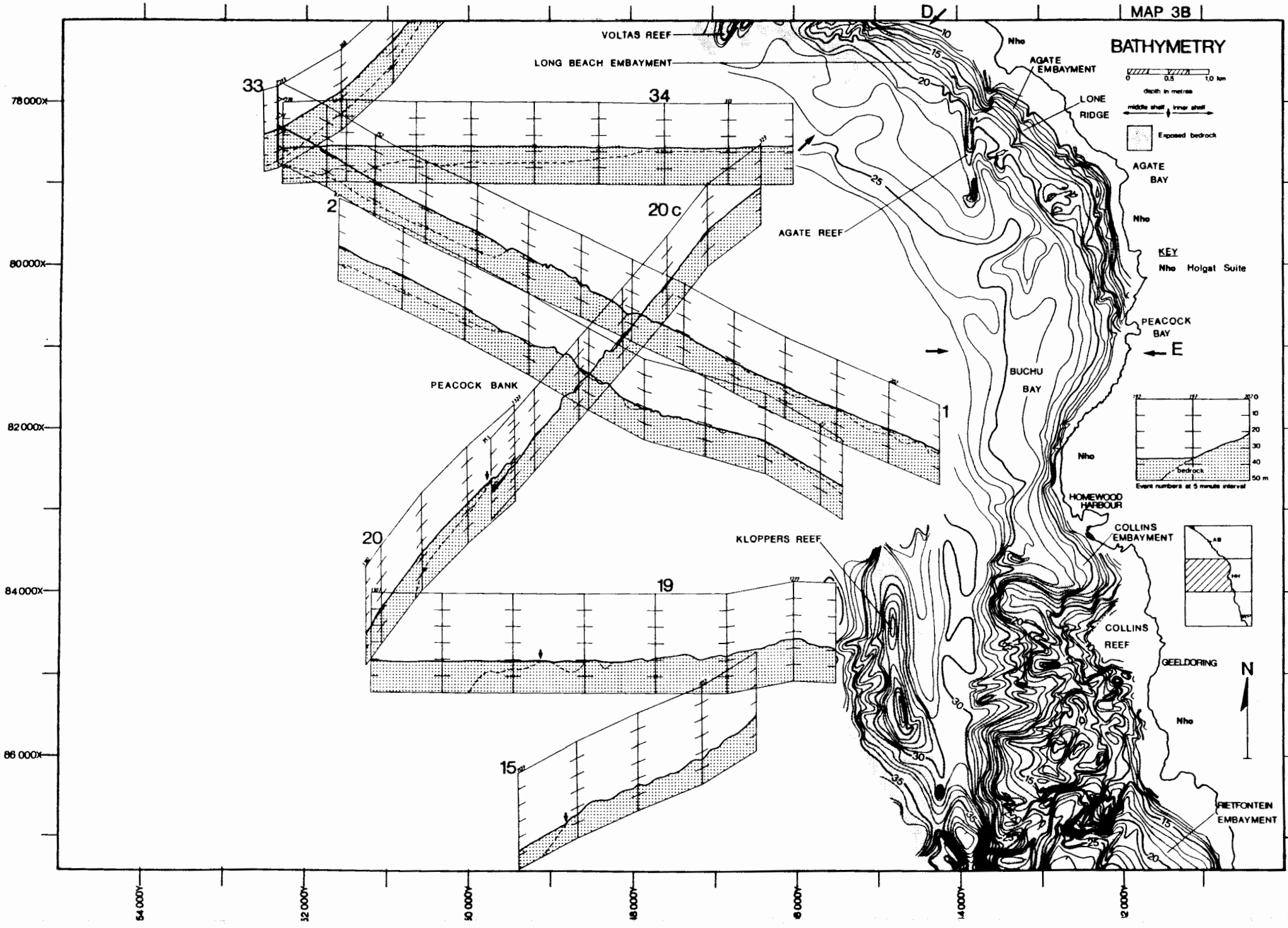
LOC. No.	MEAN (phi)	SORT	SK	1% (phi)
50	3.11	0.39	-0.35	1.80
51	1.69	0.40	-0.25	0.50
52	2.70	0.42	0.09	1.70
53	3.01	0.42	-0.09	1.90
54	2.29	0.34	-0.06	1.30
55	2.88	0.43	-0.35	1.30
56	2.97	0.47	-0.29	1.50
57	2.33	0.29	0.24	1.60
58	2.46	0.76	-0.39	0.70
59	2.34	0.28	0.16	1.70
60	2.31	0.32	-0.20	1.40
61	2.65	0.60	-0.29	1.10
62	2.43	0.34	0.15	1.60
63	2.02	0.38	0.06	1.10
64	2.66	0.38	-0.39	1.50
65	2.43	0.41	0.04	1.30
66	0.92	0.51	0.10	-0.50
67	2.43	0.43	-0.31	1.10
68	2.38	0.27	-0.67	1.30
69	2.46	0.40	-0.62	1.10
70	2.59	0.33	0.35	1.90
71	2.52	0.29	0.29	1.90
72	0.96	0.35	0.37	0.20
73	2.33	0.28	-0.22	1.40
74	2.59	0.39	0.15	1.50
75	2.47	0.30	0.53	2.00
76	2.33	0.28	0.28	1.70
77	1.56	0.46	0.47	0.70
78	2.34	0.66	-0.17	0.80
79	2.61	0.36	0.37	1.80
80	2.75	0.38	0.23	1.70
81	2.67	0.53	-0.22	1.05
82	2.56	0.39	0.13	1.50
83	2.85	0.37	0.18	1.90
84		NO	DATA	
85	2.22	0.97	-0.12	0.50
86	1.46	0.39	0.65	0.60
87	1.91	0.43	-0.03	0.90
88	1.20	0.44	0.63	0.30
89	1.35	0.60	0.68	0.30
90	2.54	0.32	0.29	1.90
91	2.50	0.40	0.26	1.80
92	3.32	0.30	0.09	2.70
93	3.03	0.43	0.17	2.30
94	2.83	0.52	-0.34	1.30
95	2.62	0.37	0.29	1.80
96	2.55	0.24	0.51	1.40
97	2.46	0.34	0.08	1.30
98	2.55	0.26	0.50	2.10
99	1.13	0.49	0.89	0.40

TABLE B5
 PERCENTAGE OCCURRENCE T_p , T_z and H_s PER SEASON

T_p (sec)	AUTUMN	WINTER	SPRING	SUMMER
2.5 - 5.0	0	0	0	0
5.0 - 7.5	0	0	0	2.15
7.5 - 10.0	4.91	4.83	7.18	10.97
10.0 - 12.5	40.40	18.49	40.43	51.76
12.5 - 15.0	42.13	60.63	42.82	31.62
15.0 - 17.5	10.37	14.58	9.57	3.49
17.5 - 20.0	2.19	1.48	0	0
20.0 - 22.5	0	0	0	0
<hr/>				
T_z (sec)				
2.0 - 4.0	0	0	0	0
4.0 - 6.0	10.04	5.44	16.41	31.45
6.0 - 8.0	57.51	36.37	58.28	64.69
8.0 - 10.0	28.58	49.52	24.18	13.85
10.0 - 12.0	3.85	8.24	1.11	0
<hr/>				
H_s (m)				
0 - 0.25	0	0	0.21	0
0.25 - 0.50	1.77	0	0.23	0
0.50 - 0.75	2.48	2.73	3.63	6.93
0.75 - 1.0	8.52	6.75	8.93	13.20
1.0 - 1.25	14.67	9.58	13.35	14.30
1.25 - 1.50	17.83	9.89	15.55	12.27
1.50 - 1.75	13.05	10.68	12.78	14.83
1.75 - 2.0	11.13	9.63	10.43	17.17
2.0 - 2.25	7.07	10.75	8.70	8.73
2.25 - 2.50	9.28	8.67	7.75	3.13
2.50 - 2.75	4.30	7.36	4.38	2.93
2.75 - 3.0	2.20	7.87	3.08	2.60
3.0 - 3.25	1.82	5.23	3.05	2.07
3.25 - 3.50	1.50	4.93	3.05	0.30
3.50 - 3.75	1.50	2.58	1.95	0.30
3.75 - 4.0	1.48	0.83	0.20	0
4.0 - 4.25	0	0.98	1.25	0.30
4.25 - 4.50	0.13	1.18	0.63	0
4.50 - 4.75	0.34	0.21	0.43	0.30
4.75 - 5.0	0.40	0.17	0.20	0.30
5.0 - 5.25	0.27	0	0	0
5.25 - 5.50	0.20	0	0	0
5.50 - 5.75	0	0	0.20	0.30
<hr/>				
No of readings	623	572	453	357

7 JUL 1986





BATHYMETRY

0 0.5 1.0 km

Depth in metres
middle shelf inner shelf

Exposed bedrock

AGATE BAY

Nho

KEY

Nho Holgat Suite

PEACOCK BAY

Nho

BUCHU BAY

Nho

HOMWOOD HARBOUR

COLLINS EMBAYMENT

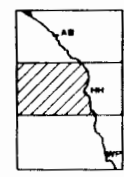
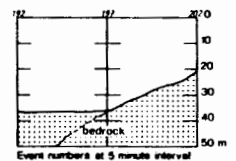
COLLINS REEF

GEELDORING

Nho

FRETFontein EMBAYMENT

Nho



78 000x

80 000x

82 000x

84 000x

86 000x

54 000y

52 000y

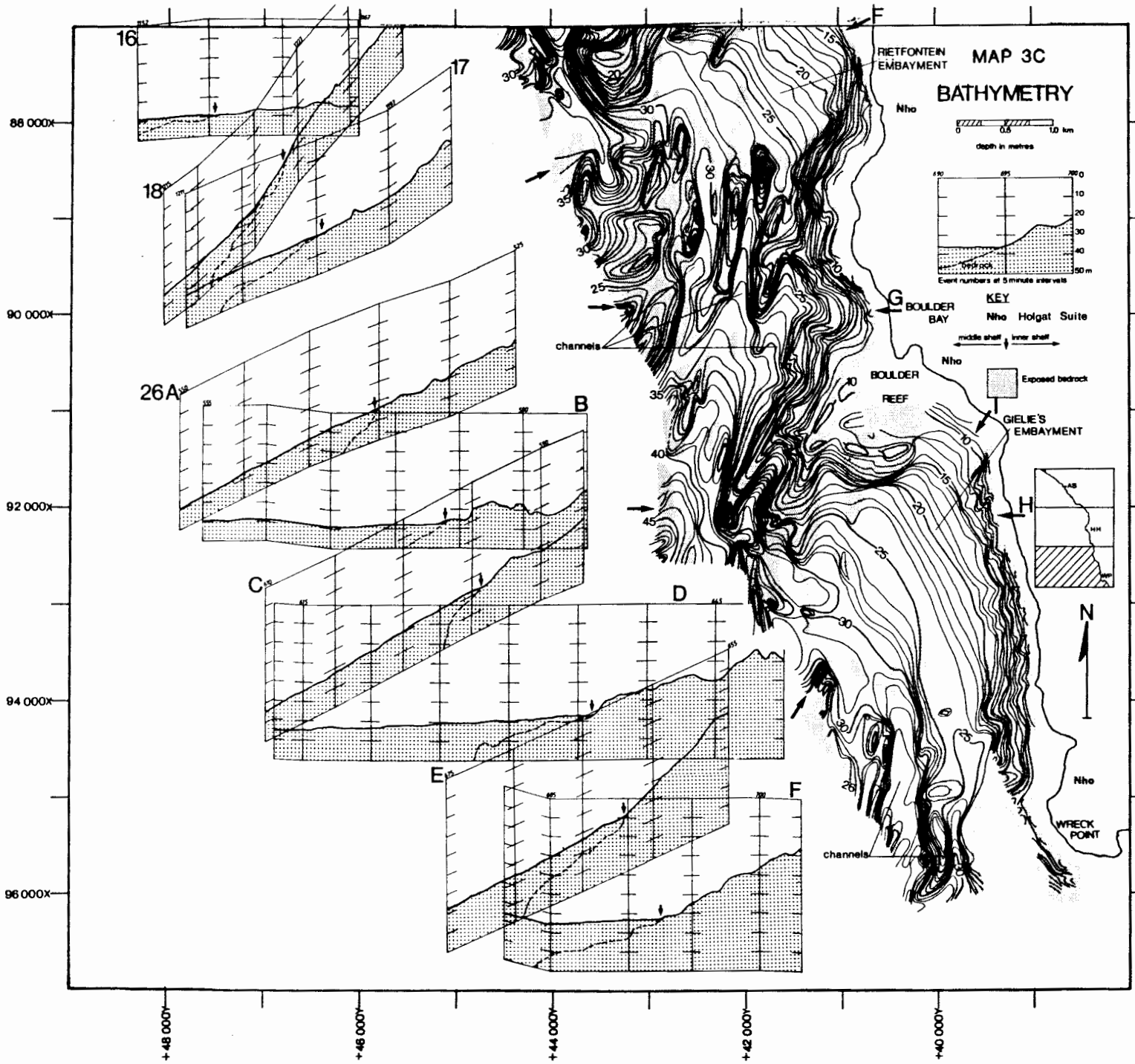
50 000y

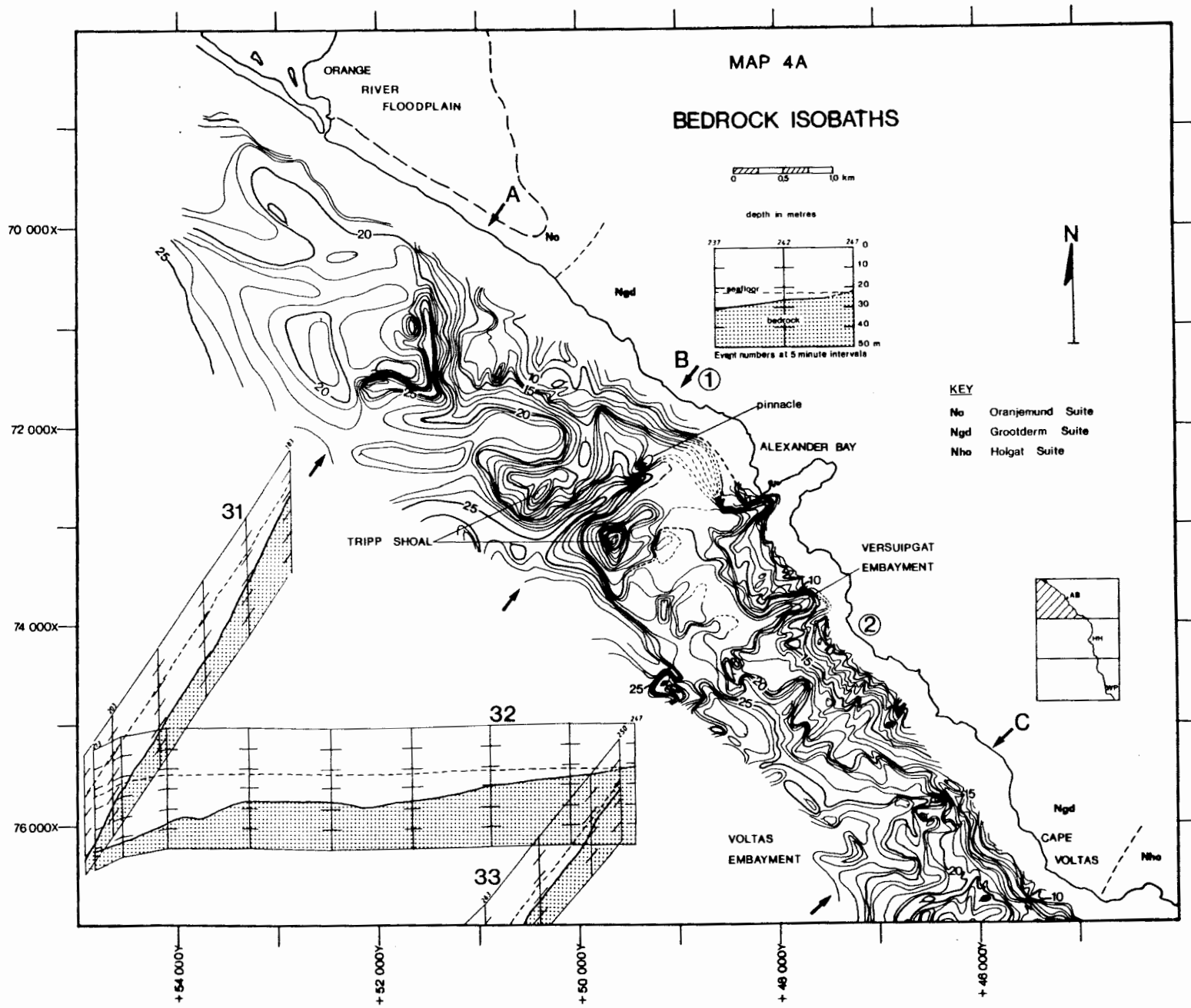
48 000y

46 000y

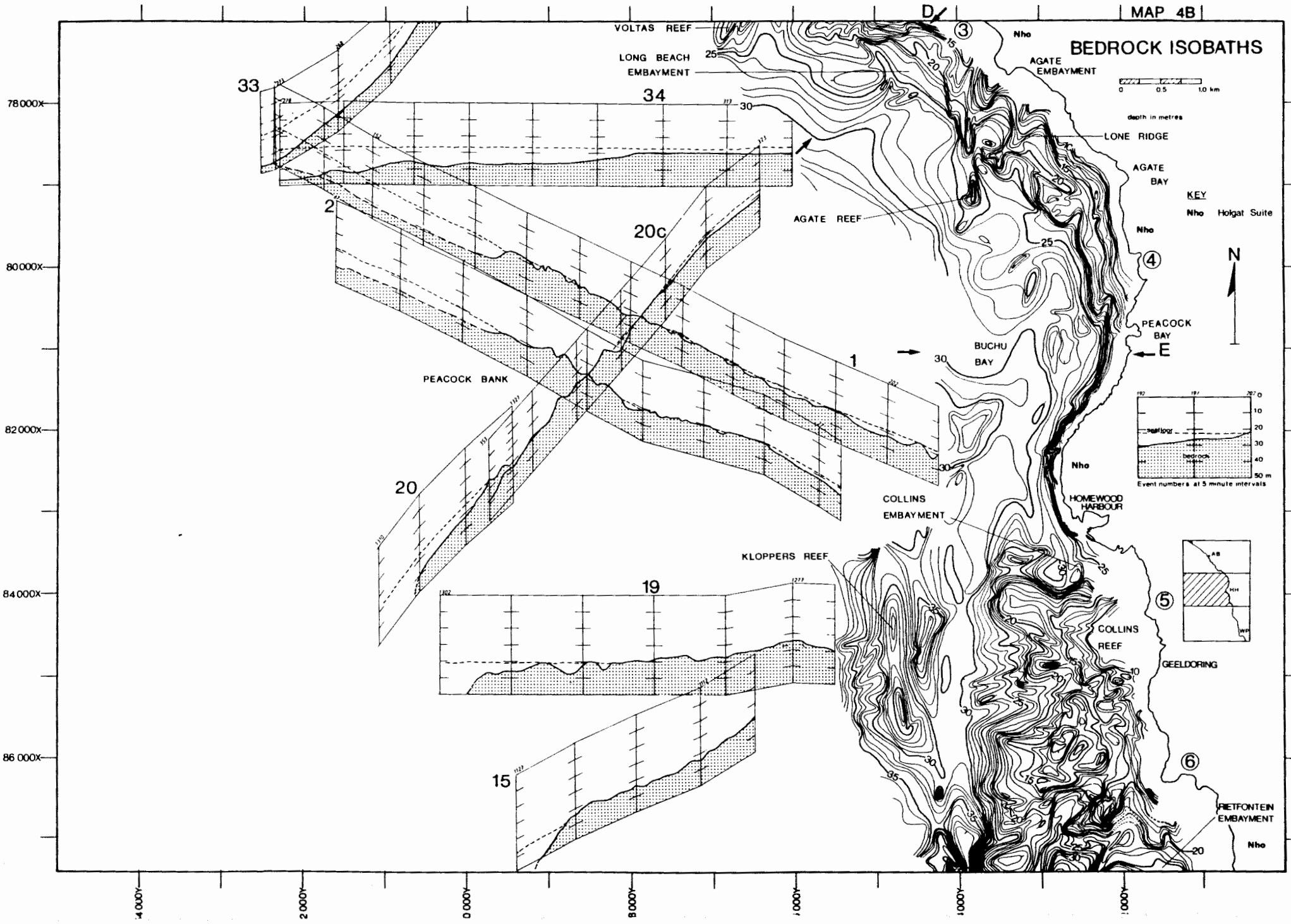
44 000y

42 000y

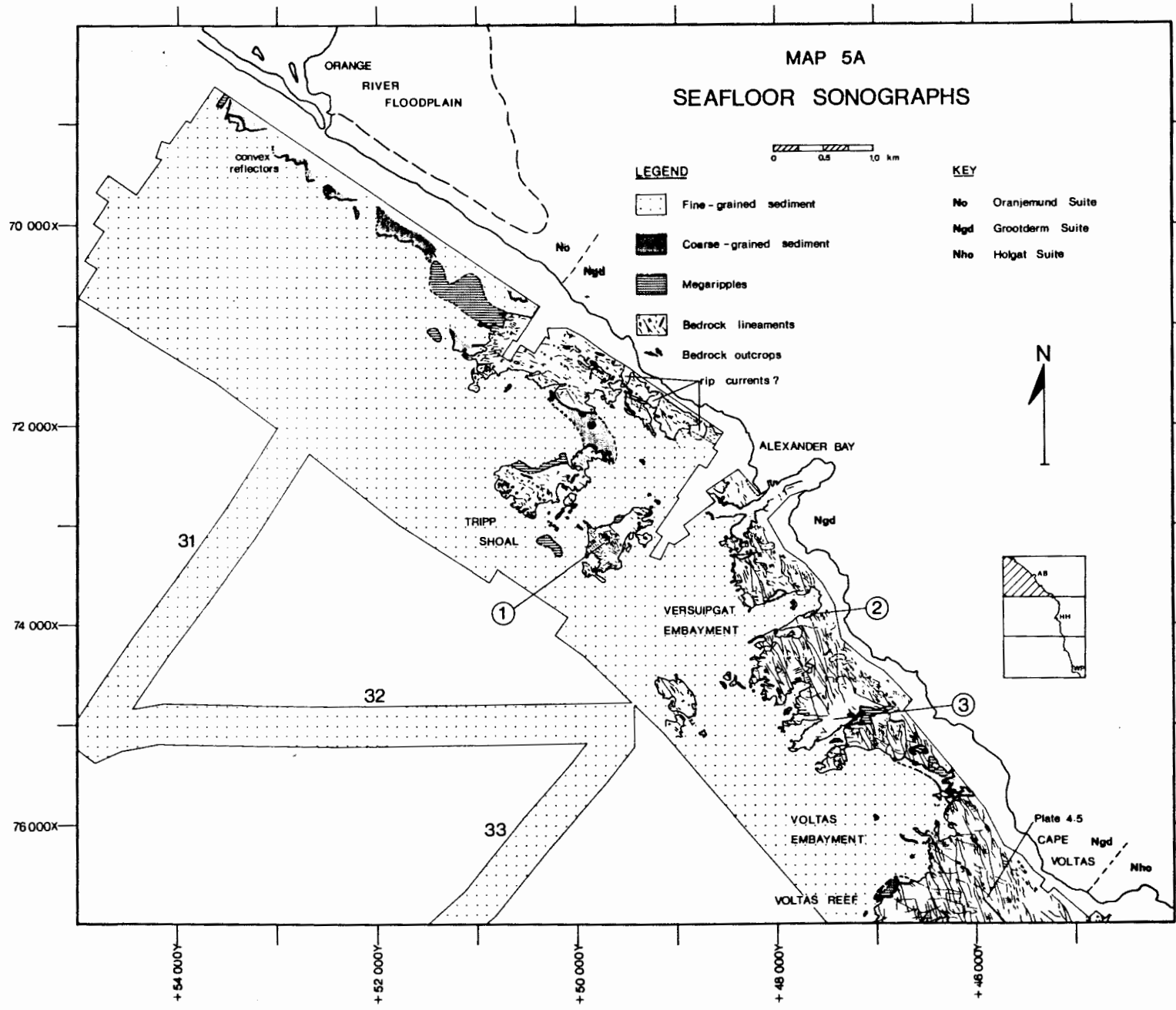









BEDROCK ISOBATHS



MAP 5A
SEAFLOOR SONOGRAPHS

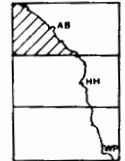


LEGEND

-  Fine-grained sediment
-  Coarse-grained sediment
-  Megaripples
-  Bedrock lineaments
-  Bedrock outcrops

KEY

- No Oranjemund Suite
- Ngd Grootderm Suite
- Nho Holgat Suite



+54 000X
+52 000X
+50 000X
+48 000X
+46 000X

70 000X
72 000X
74 000X
76 000X

31

32

33

1

2

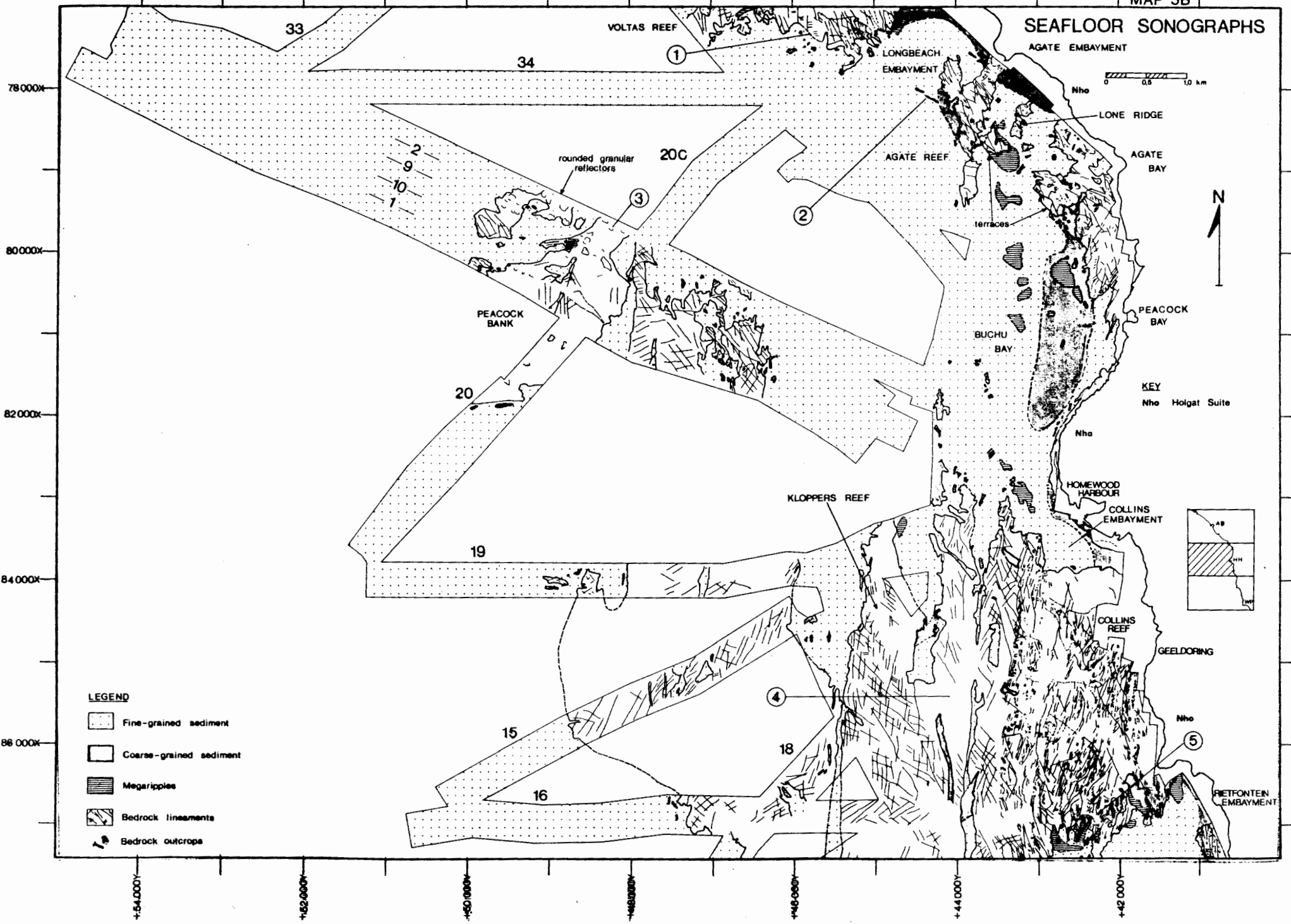
3

Plate 4.5




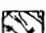

CAPE

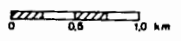
VOLTAS

SEAFLOOR SONOGRAPHS

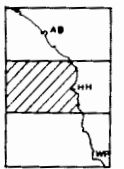


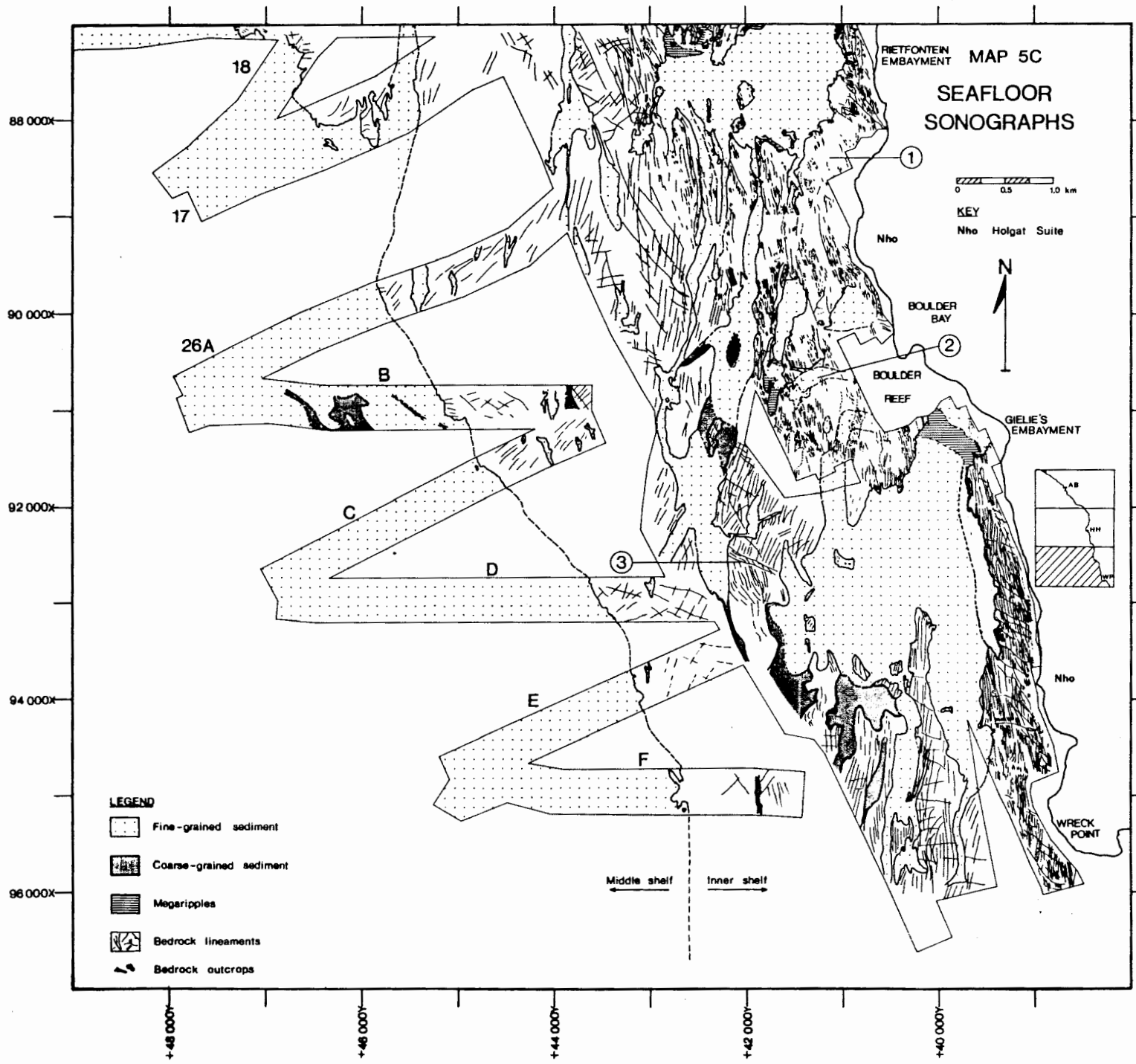
LEGEND

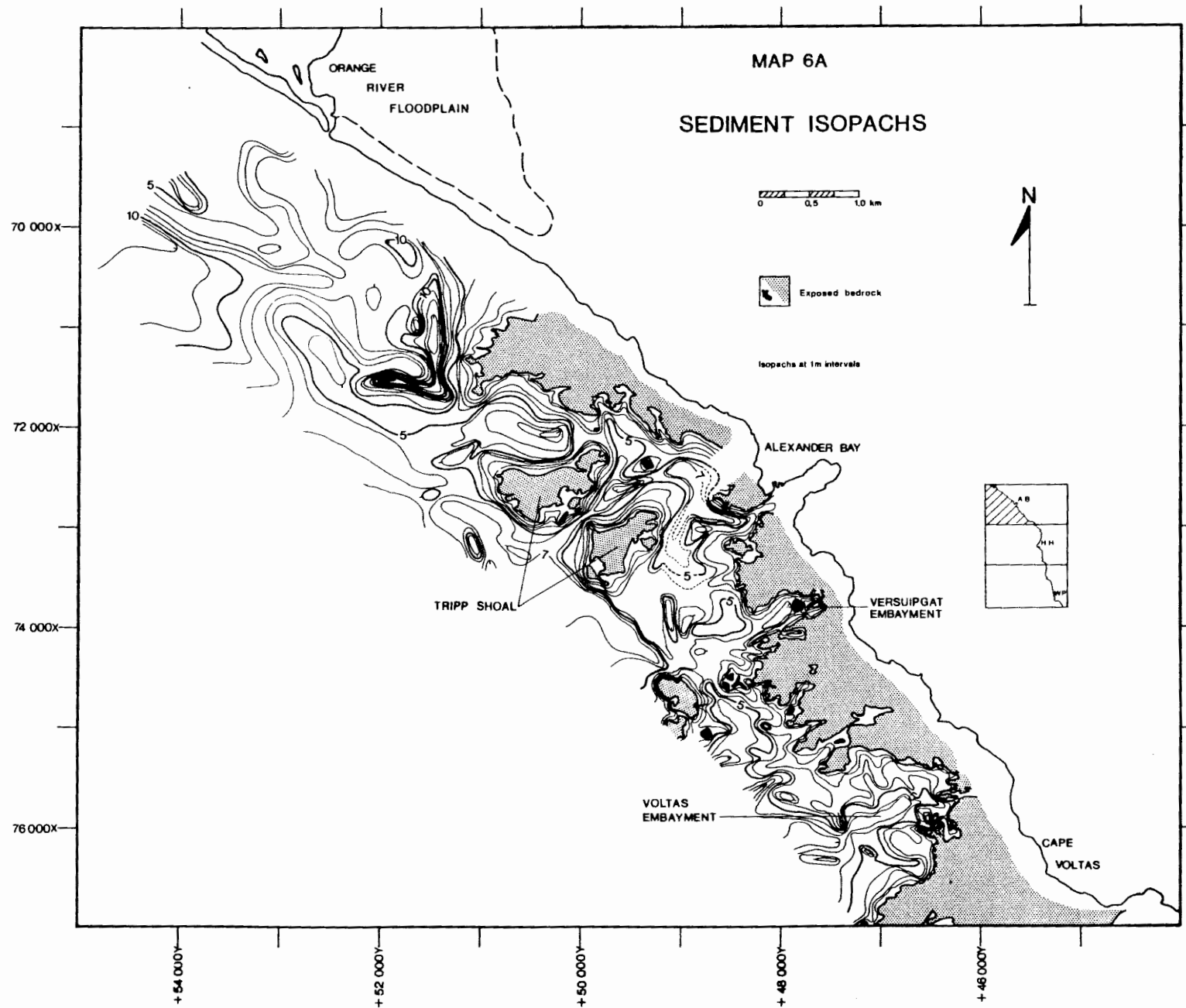
-  Fine-grained sediment
-  Coarse-grained sediment
-  Megaripples
-  Bedrock lineaments
-  Bedrock outcrops



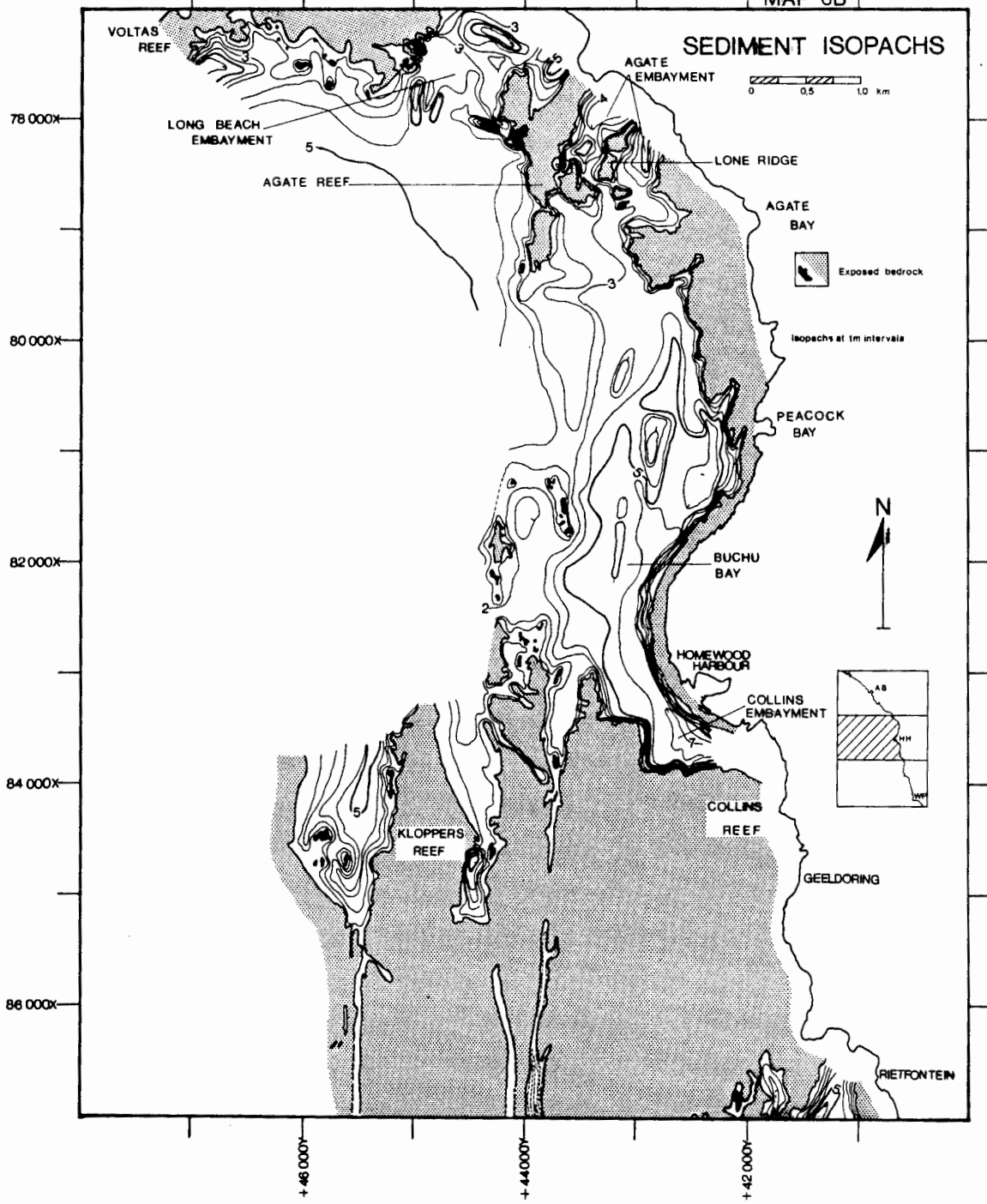
KEY
Nho Holgat Suite



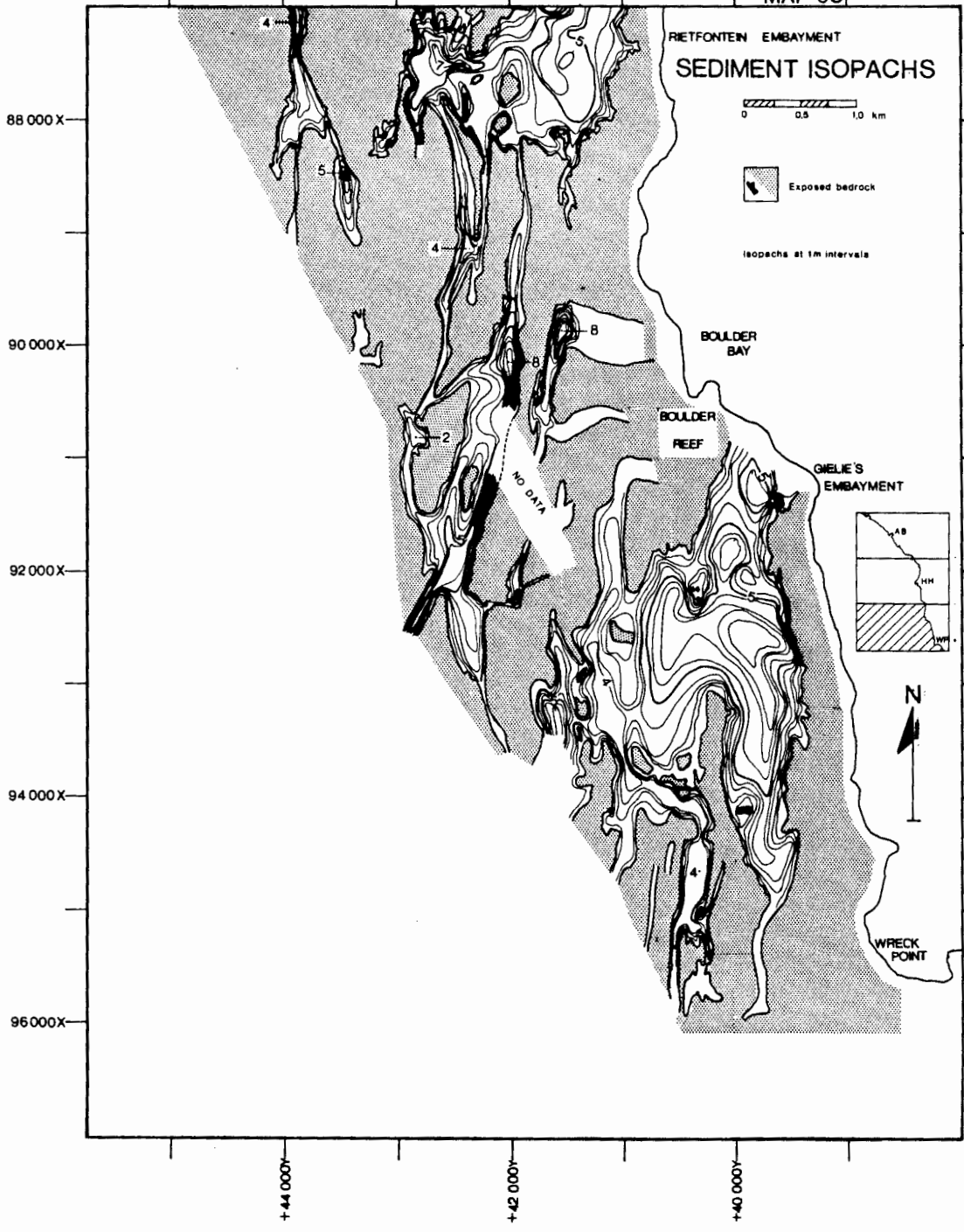




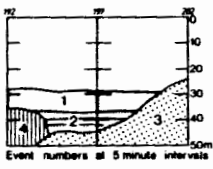
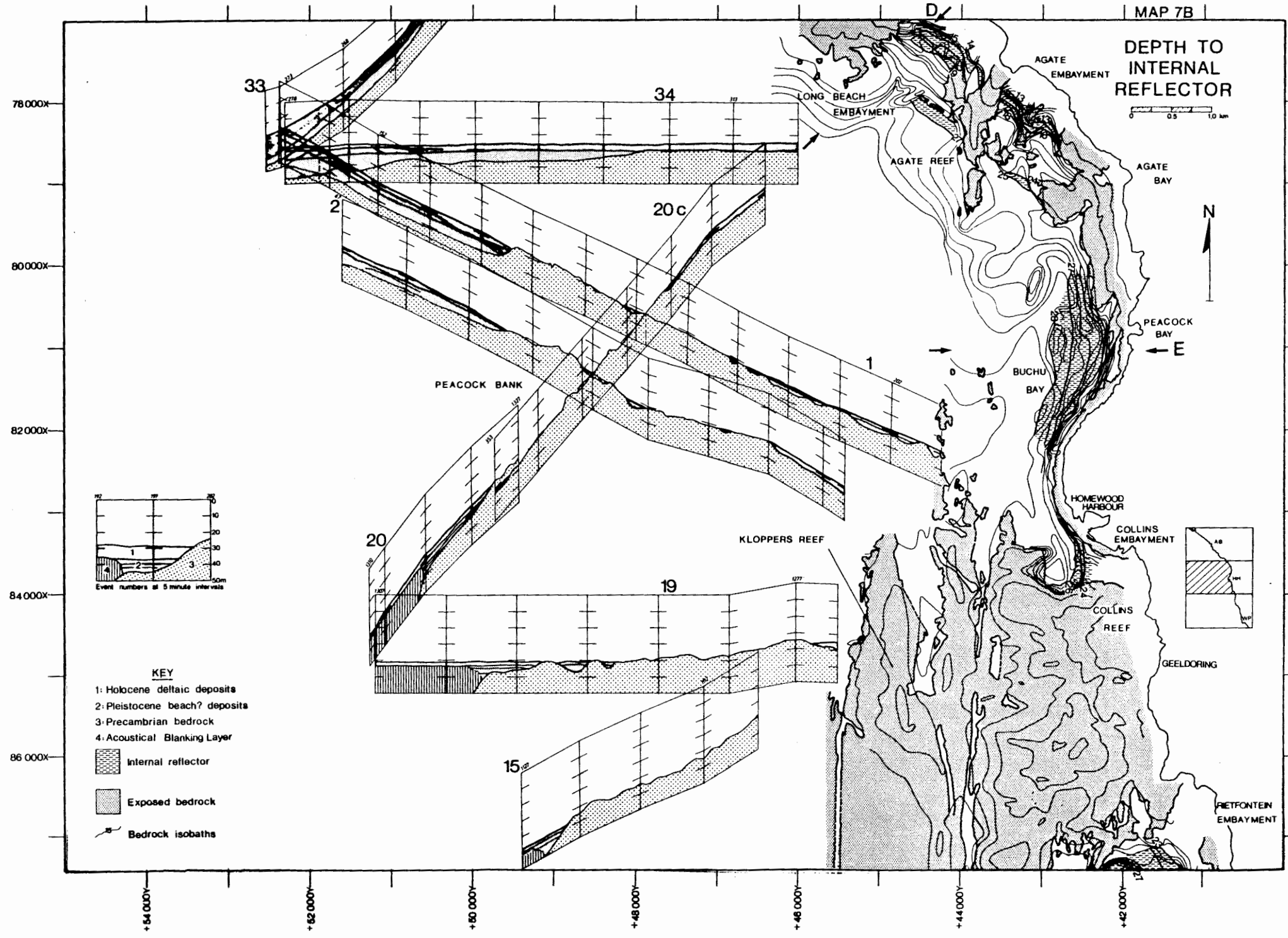
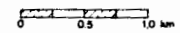
MAP 6B



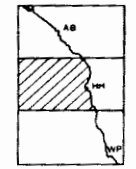
MAP 6C



DEPTH TO INTERNAL REFLECTOR

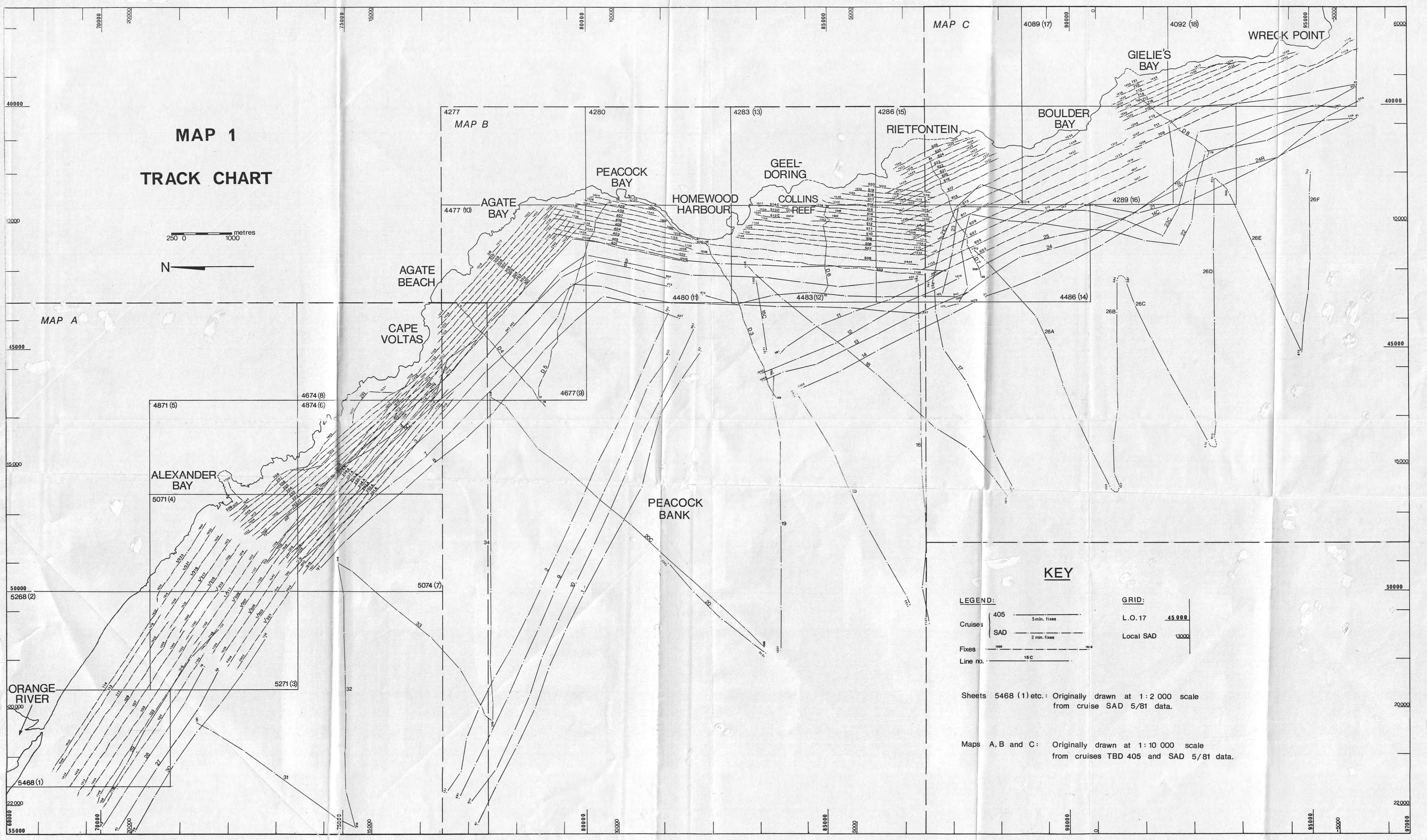


- KEY**
- 1: Holocene deltaic deposits
 - 2: Pleistocene beach? deposits
 - 3: Precambrian bedrock
 - 4: Acoustical Blanking Layer
 - Internal reflector
 - Exposed bedrock
 - Bedrock isobaths



MAP 1 TRACK CHART

250 0 1000 metres



KEY

LEGEND:

- Cruises 405 5 min. fixes
- SAD 2 min. fixes
- Fixes
- Line no. 16 C

GRID:

- L. O. 17 45 000
- Local SAD 13000

Sheets 5468 (1) etc.: Originally drawn at 1:2 000 scale from cruise SAD 5/81 data.

Maps A, B and C: Originally drawn at 1:10 000 scale from cruises TBD 405 and SAD 5/81 data.

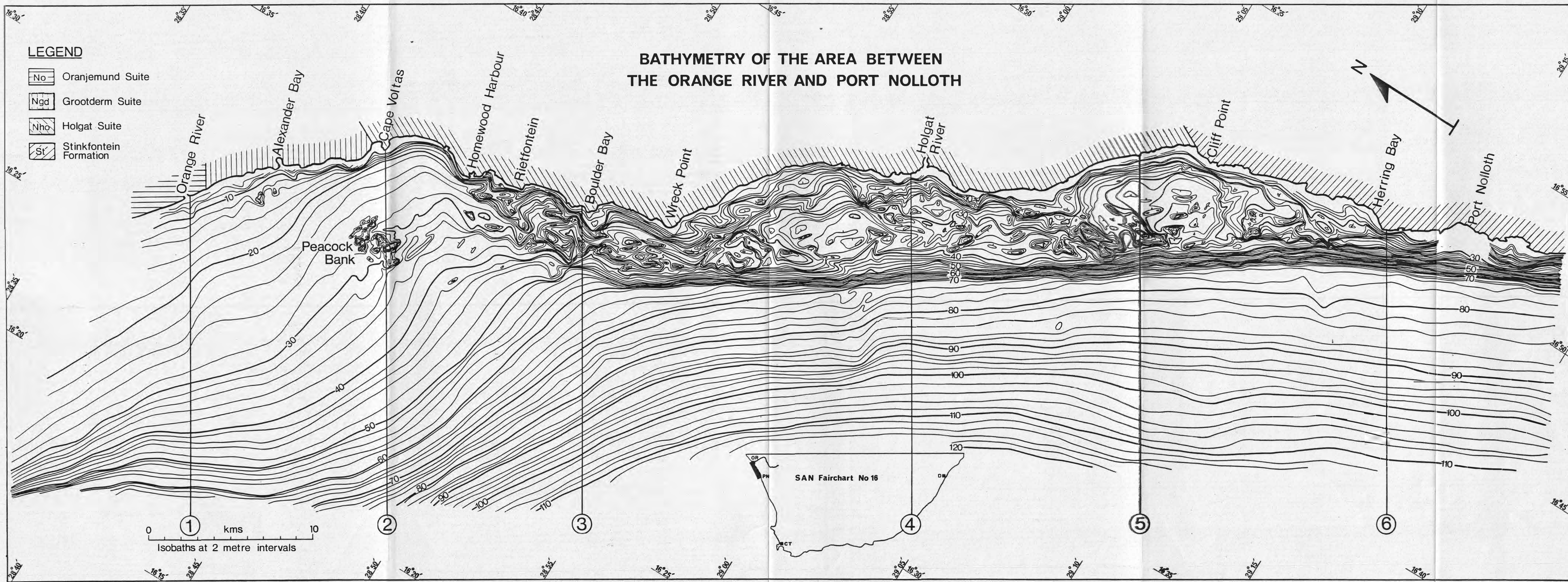
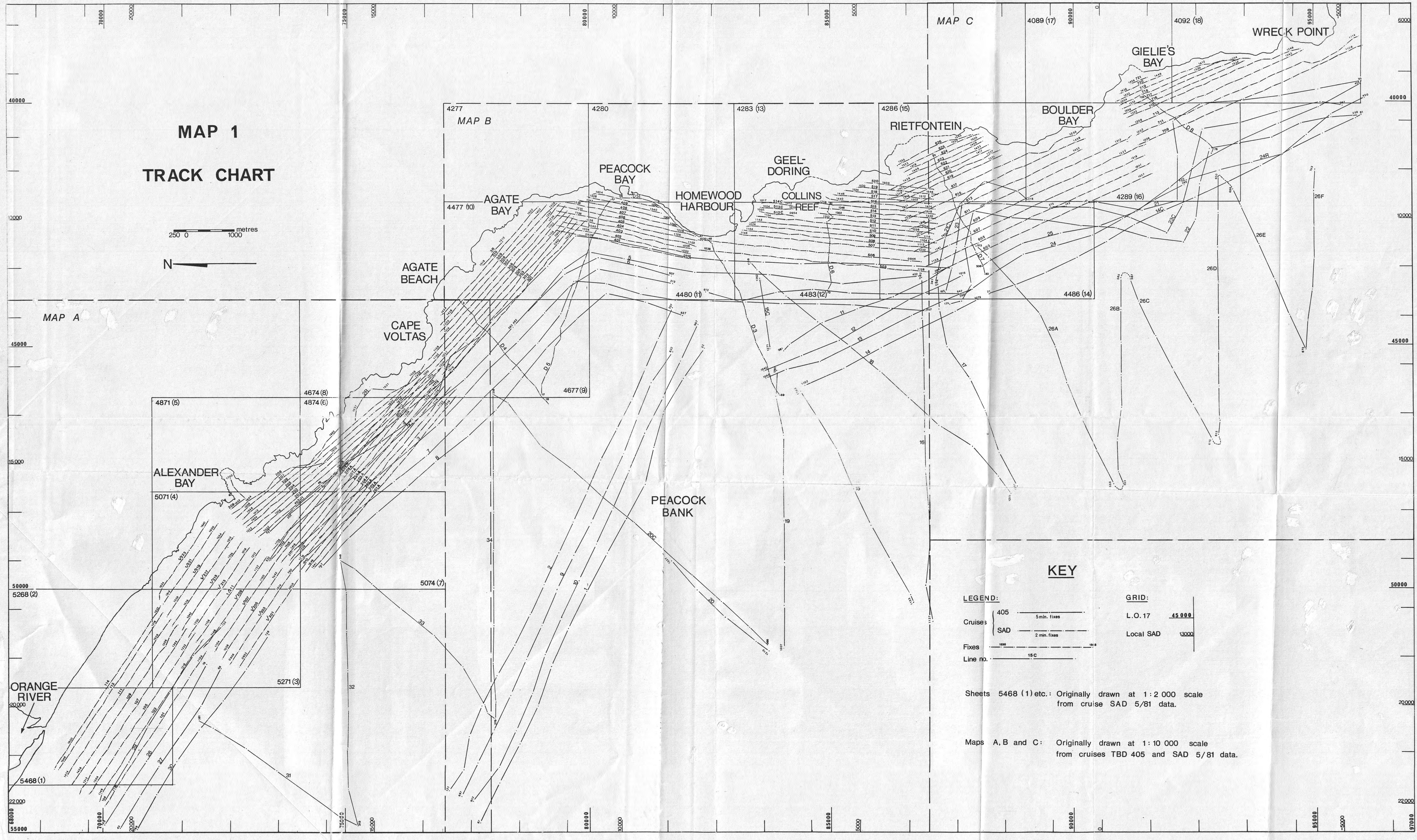


FIGURE 2.2

MAP 1 TRACK CHART

250 0 1000 metres



KEY

LEGEND:

- Cruises 405 5 min. fixes
- SAD 2 min. fixes
- Fixes 15 C
- Line no.

GRID:

L. O. 17 45 000
Local SAD 13000

Sheets 5468 (1) etc.: Originally drawn at 1:2 000 scale from cruise SAD 5/81 data.

Maps A, B and C: Originally drawn at 1:10 000 scale from cruises TBD 405 and SAD 5/81 data.